ZooKeys 759: 1–27 (2018)
doi: 10.3897/zookeys.759.24584
http://zookeys.pensoft.net

RESEARCH ARTICLE

A peer-reviewed open-access journal
ZooKeys
Launched to accelerate biodiversity research

An automated device for the digitization and 3D modelling of insects, combining extended-depth-of-field and all-side multi-view imaging

Bernhard Ströbel[1], Sebastian Schmelzle[2], Nico Blüthgen[2], Michael Heethoff[2]

1 *Department of Mathematics and Natural Sciences, University of Applied Sciences Darmstadt, Schöfferstr. 3, 64295 Darmstadt, Germany* **2** *Ecological Networks, Technische Universität Darmstadt, Schnittspahnstr. 3, 64287 Darmstadt, Germany*

Corresponding author: *Michael Heethoff* (heethoff@bio.tu-darmstadt.de)

Academic editor: *N. Akkari* | Received 20 February 2018 | Accepted 16 April 2018 | Published 17 May 2018

http://zoobank.org/80808C1A-79CC-46BE-AD95-151F2EADC51F

Citation: Ströbel B, Schmelzle S, Blüthgen N, Heethoff M (2018) An automated device for the digitization and 3D modelling of insects, combining extended-depth-of-field and all-side multi-view imaging. ZooKeys 759: 1–27. https://doi.org/10.3897/zookeys.759.24584

Abstract

Digitization of natural history collections is a major challenge in archiving biodiversity. In recent years, several approaches have emerged, allowing either automated digitization, extended depth of field (EDOF) or multi-view imaging of insects. Here, we present DISC3D: a new digitization device for pinned insects and other small objects that combines all these aspects. A PC and a microcontroller board control the device. It features a sample holder on a motorized two-axis gimbal, allowing the specimens to be imaged from virtually any view. Ambient, mostly reflection-free illumination is ascertained by two LED-stripes circularly installed in two hemispherical white-coated domes (front-light and back-light). The device is equipped with an industrial camera and a compact macro lens, mounted on a motorized macro rail. EDOF images are calculated from an image stack using a novel calibrated scaling algorithm that meets the requirements of the pinhole camera model (a unique central perspective). The images can be used to generate a calibrated and real color texturized 3Dmodel by 'structure from motion' with a visibility consistent mesh generation. Such models are ideal for obtaining morphometric measurement data in 1D, 2D and 3D, thereby opening new opportunities for trait-based research in taxonomy, phylogeny, eco-physiology, and functional ecology.

Keywords

Focus stacking, morphometry, structure from motion, photogrammetry, 3D modelling, DISC3D

Introduction

Digitization has become a major challenge in the curation of natural history collections (Beaman and Cellinese 2012; Berents et al. 2010; Hudson et al. 2015; Mantle et al. 2012; Mathys et al. 2015; Mertens et al. 2017; Moore 2011; Vollmar et al. 2010). Among zoological collections, insects are unparalleled in their number of species and specimens. Hence, automatization of image acquisition and processing seems mandatory for large-scale digitization projects. Whole-drawer imaging (Mantle et al. 2012) allows high-throughput digitization of multiple specimens in one image. The available resolution of approximately 30 µm/pixel, however, seems insufficient for the inspection of delicate morphological details. Furthermore, only the dorsal view is imaged, making lateral and ventral characters inaccessible from the digital data. Hence, this system seems to be well-suited for an online inspection of available specimens in a collection but does not replace physical handling of the specimens for many taxonomical / morphological studies. Images with higher resolution require the specimens to be imaged individually. Due to the small size of many insects, however, images need to be taken with an extended depth of field (EDOF) technique (Brecko et al. 2014). A number of commercially available software solutions allow EDOF image calculation from focus stacks by post-processing (Brecko et al. 2014), and some cameras also have suitable built-in EDOF options (Mertens et al. 2017). In the case of multi-view EDOF imaging, however, time-consuming manual processing is necessary (Nguyen et al. 2014) and available commercial software does not provide well-defined perspectives due to the inability to include information on camera position into EDOF calculation. Hence, large-scale digitization projects use multi-view imaging only when specimens are large enough to keep them in focus as a whole, and use only one or two viewing directions if EDOF images should be needed (Mathys et al. 2015). Sets of images from multiple views do not only provide digital access to more morphological characters, they can also be used to generate colored and textured 3D models of the specimens (Mathys et al. 2013; Mathys et al. 2015; Nguyen et al. 2014; Ströbel et al. 2017). Measurements taken on the virtual 3D models instead of the physical samples protect the delicate specimens and can be easily repeated at any time. Due to the above-mentioned restrictions in combining EDOF and multi-view imaging, however, 3D modelling of higher numbers of small insects seemed impractical (Nguyen et al. 2014).

Traditionally, species descriptions and other scientific or popular documentations focus on 1-D characters, e.g., body length, the length of single body parts or relative length ratios between body parts. However, since organisms have 3D shapes, 2D or 3D traits are meaningful complementary information to characterize body shape and variation more completely (Tatsuta et al. 2017). Hence, phylogenetic analyses should consider morphometrics of shapes and relative landmark positions (Tobias et al. 2010; Wiens 2000). Moreover, many relevant functional morphological traits are in fact 2D or 3D. A 'functional trait' represents any kind of phenotypic (morphological, physiological or life-history) characteristic of an organism assumed to influence its performance (McGill et al. 2006). Biodiversity research increasingly focuses on the composi-

tion of species' traits rather than considering only species identities and numbers alone (Loreau et al. 2001; Mouillot et al. 2013; Petchey and Gaston 2002). In the concept of 'environmental filters', changes in the environment cause a shift in the distribution of functional traits in species communities (Diaz et al. 1998; Gámez-Virués et al. 2015; Mouillot et al. 2013). Reported changes in morphological trait compositions of insect communities include an increasing relative abundance of species with larger eyes (relative to head width) with increasing land-use intensity (Simons et al. 2016), or decreased forewing length with higher habitat fragmentation (Gámez-Virués et al. 2015). More subtle variation in size and shape across individuals within a species can provide additional insights into environmental responses or resource limitation (Emlen 1997; Peat et al. 2005). Finally, developmental stress in a growing organism may cause asymmetries, e.g., differences between left and right legs, wings, or horns of insects, potentially associated with lower reproductive success or other fitness deficits (Hendrickx et al. 2003; Møller and Thornhill 1998). Hence, many of these functional traits relate to 3D structures, but have been characterized only in 1D or 2D, largely constrained by the availability of methods. In particular, surfaces and volumes are important characteristics that are relevant in a functional eco-physiological context but can only be measured in 3D (Brückner et al. 2017; Kühsel et al. 2017). Therefore, besides archiving and digitizing museum collections, trait-based research areas in functional ecology, eco-physiology, and evolutionary biology would greatly benefit from easily available 3D scanning techniques.

Established tomographic 3D techniques have some shortcomings when it comes to pinned insects. Although delivering landmark data with a high precision (e.g., Betz et al. 2007; Heethoff and Norton 2009; Schmelzle et al. 2009), X-ray microtomography requires costly equipment or access to very limited beamtime at suitable synchrotron facilities. Furthermore, high X-ray attenuation of the needle compared to the insect body results in distracting artifacts. Finally, as pinned insects are dried without preserving their inner organization, tomography seems of limited value, also since it does not recover color/texture of the specimen. Hence, the use of visible light in combination with real color imaging seems the most adequate technique for digitizing insect collections.

Visible light is to some extent reflected or remitted at or near the surface of the insect. Light returning from the specimen bears information about position, reflectivity, and color, and forms the basis for optical 3D surface scanning. Triangulation techniques determine the spatial position of surface points by the intersection of light rays. In the case of passive triangulation, ambient illumination is applied, and all rays used for measuring are viewing rays of different cameras or of a camera in different positions. Two such techniques, 'Structure from Motion' (SfM) and 'Shape from Silhouette' (SfS), are suitable for 3D insect scanning (Mathys et al. 2013; Nguyen et al. 2014).

SfS (Cheung et al. 2005; Furukawa and Ponce 2009; Gallo et al. 2014) is based on viewing rays tangential to the object (see Suppl. material 1: Fig. S1). These enclose visual cones with respect to the projection centers of the cameras. The object surface is approximated by the 'visual hull', the common intersection of all visual

cones. Resulting 3D models need to be calibrated by scaled markers included in the images. Moreover, since there are no silhouette rays from concave parts of an object, it is not possible to reconstruct indentations on insect bodies. Until now, the only published device for capturing natural-color 3D models of pinned insects is based on SfS (Nguyen et al. 2014). Estimated as a 'proof of concept' by the authors, this pioneering system used a DSLR camera and a two-axis rotating table. The camera calibration was carried out with the aid of a mat with printed markers, imaged together with the insect pinned on this marker mat. In consequence, only a part of the sensor area was available for the specimen. Moreover, the arrangement of specimen and mat precludes imaging the underside of the insects. The authors propose to either mount the specimens with an auxiliary second pin or to re-pin the insects. This is a major shortcoming of the SfS setup since re-pinning bears an ultimate risk of damaging the specimen, and probably no museum would agree to re-pin any type specimens from their collection.

SfM (Seitz et al. 2006; Szeliski 2011; Ullmann 1979; Westoby et al. 2012) is a photogrammetric technique that uses images from different viewing directions (i.e., different camera positions with respect to the specimen or different specimen poses with respect to the camera) and identifies corresponding feature points on these images (see Suppl. material 1: Fig. S1). Unlike traditional photogrammetry, SfM does not need a previous calibration of camera positions and orientations, since these are determined together with the object structure (simultaneous calibration). This becomes possible by the high number of corresponding feature points that can be detected in overlapping images of well-textured objects such as insect specimens - an approach that has been boosted by the emergence of efficient new algorithms for feature detection and matching (e.g., SIFT, Lowe 2004), powerful graphics processor units, and user-friendly software (Agisoft PhotoScan), including generation of 3D-models with visibility-consistent meshing (VCM) techniques (see also: Aroudj et al. 2017; Vu et al. 2012).

Here, a new imaging device (the Darmstadt Insect SCanner: DISC3D) is presented that overcomes the restrictions of the above-mentioned EDOF multi-view imaging, and provides data suitable for both, digitally archiving insects (and other small objects) and generating 3D models. We developed DISC3D with the aim of affordability, clonability, and minimization of manual processing steps. DISC3D allows specific configurations for different requirements (e.g., high resolution for archiving, high number of views for 3D modelling of complex structures, or fast imaging for mass digitalization).

Materials and methods

DISC3D is published under the Creative Commons license CC BY-SA (https://creativecommons.org). The total costs of the device range between 4,000€ and 8,000€ (depending on the camera and availability of computers and educational software licenses). In the following an overview is given of the components of

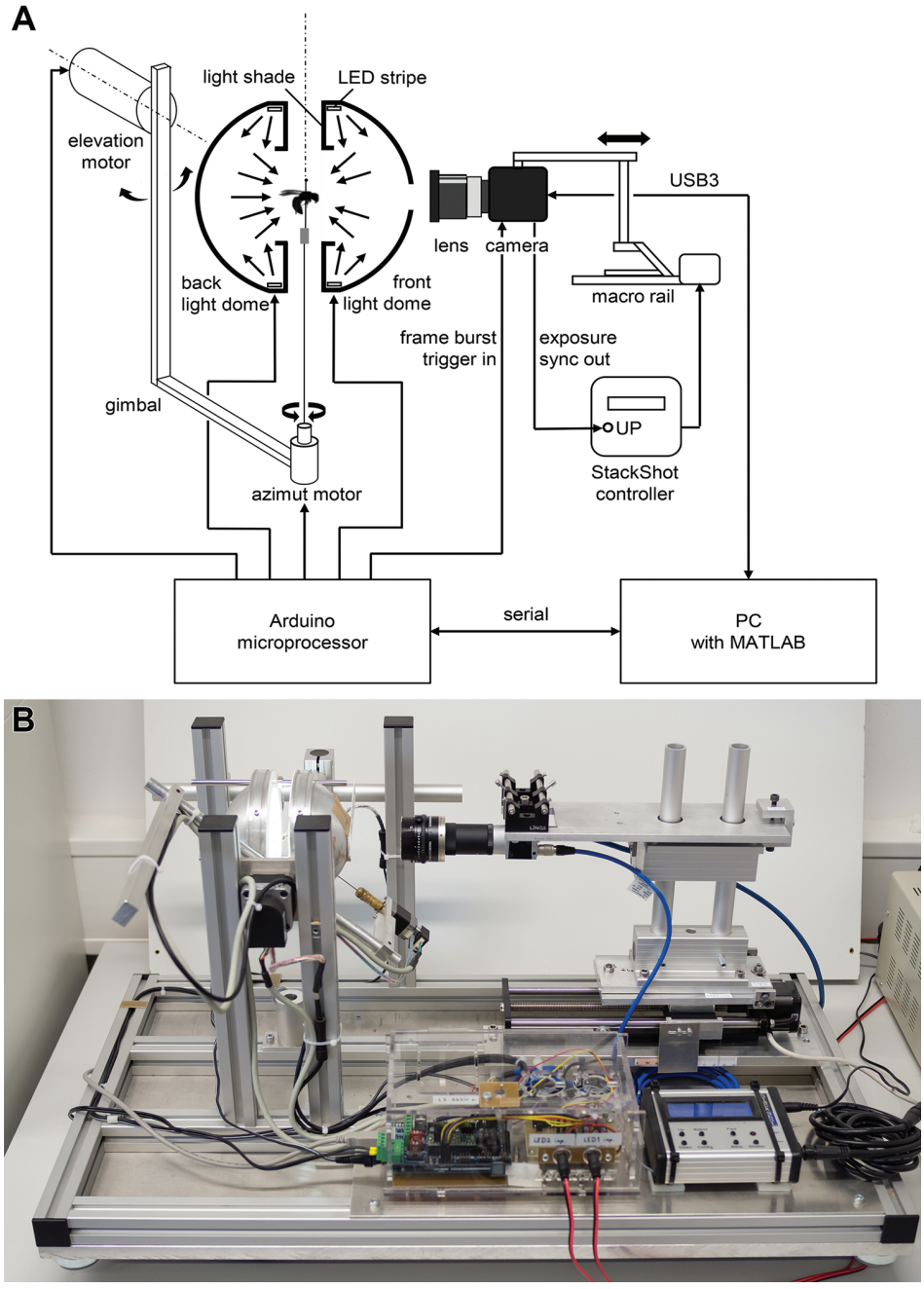

Figure 1. Schematic setup (**A**) and image (**B**) of the Darmstadt Insect Scanner DISC3D.

DISC3D (Fig. 1) and the measuring process. Detailed technical information and calculations can be found in the supplement. Visit also www.econetlab.net/disc3d for current developments.

Animals used in the study

For demonstration of DISC3D, a set of pinned insects and snail shells from our collection with a representative shape range and sizes between 1.5–30 mm were chosen. The following species were included:

Coleoptera:
Prosopocoilus savagei Hope (23 mm)
Anoplotrupes stercorosus Scriba (21 mm)
Stenocorus meridianus L. (19 mm)
Typhaeus typhoeus L. (18 mm)
Rutpela maculata Poda (17 mm)
Valgus hemipterus L. (8 mm)
Cryptocephalus sericeus L. (7 mm)
Pogonocherus hispidus L. (6 mm)
Phyllobius pyri L. (6 mm)
Tytthaspis sedecimpunctata L. (3 mm)

Lepidoptera:
Zygaena filipendulae L. (15 mm body size, 30 mm wingspan)

Hymenoptera:
Paraponera clavata Fabricus (20 mm)
Osmia adunca Panzer (12 mm)
Sphecodes ephippius L. (8 mm)

Diptera:
Thricops sp. Róndani (8 mm)
Culex pipiens L. (5 mm)
Oscinella frit L. (1.5 mm)

Gastropoda:
Helicodonta obvoluta O.F. Müller (9 mm)
Aegopinella nitens Michaud (8 mm)
Discus rotundatus O.F. Müller (5 mm)

Specimen mounting and orientation

A black foam plastic adapter is used to connect the insect pin to a ca. 100 mm long and 1 mm thick supporting steel pin. The mounting is adjusted to the center of rotation of a two-axis motorized gimbal and allows a free view on the specimen from virtually all sides. During an insect scan, the specimen undergoes a preassigned 'pose program' with

an approximately constant angular distance between neighboring poses. Pose programs can be adjusted for specific needs (e.g., shape and complexity of the object). In this study, we mostly used a standard pose program with a mean angular distance of 10° of two neighboring poses, and a total number of 412 poses, 14 of which are not accessible due to geometric and optical constraints of the sample holder (see Suppl. material 1: Fig. S2). For repeatability of the poses, the stepper motors of the gimbal are reinitialized before every insect scan.

Illumination

Many insect surfaces are glossy and show bright reflections ('hotspots') when illuminated directly by a point-shaped light source. For that reason, we use two separately addressable hemispherical illumination domes: a 'front-light dome' that is adjacent to the camera but averted, and a 'back-light dome' on the far side facing the camera (Fig. 2). Each dome is equipped with a dimmable white LED strip attached to its inner circumference and a light shade extending into the dome that prevents direct illumination of the samples. Through backscattering by the white coated inner surface of the dome, illumination of the samples is indirect and nearly homogeneous. Both the front-light and the back-light dome feature a slot to accommodate the supporting pin when tilted by the gimbal. The front-light dome additionally features an opening with an exchangeable aperture for the camera, whereas the back-light dome can be completely removed to easily switch samples between scans.

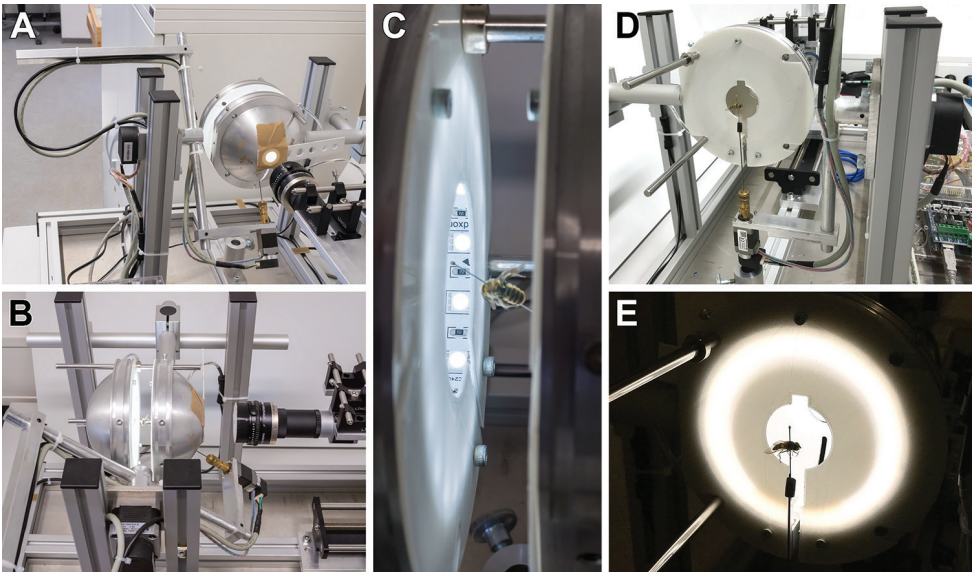

Figure 2. Illumination by two hemispherical white-coated domes (**A–C**). The back-light-dome can be removed for specimen mounting (**D, E**). No direct light from the LED-stripes hits the specimens (**C, E**).

The indirect front-light illumination of the sample is optimal for curved or bumpy glossy insect surfaces. The back-light dome produces an even background illumination, and with the front-light switched off, a silhouette image of the insect can be captured. This silhouette image can be used to mask the background in the images taken with front-light illumination.

Optics and focus stacking

DISC3D is equipped with an industrial camera and a compact macro lens (Fig. 3). The main advantages of this configuration over a DSLR camera system are the excellent angular accessibility to the specimen, the absence of a mechanic shutter, and full computer control of both image acquisition and processing. The detailed criteria for the choice of the optics and further technical data can be found in the Suppl. material 1. To extend the shallow depth-of-field of the insect images, a video stream of images is captured under front-light condition as the camera moves forward (towards the specimen), with the focal plane crossing the whole insect body. The result is a stack of images which are later merged for a front-light EDOF-image, a technique known as 'focus stacking' or 'z-stacking' (see Suppl. material 2). As the camera moves back to the starting point, another video stream is taken under back-light condition,. The resulting back-light EDOF image serves for the segmentation of the background. The motion of the camera along its axis is accomplished by a motorized macro rail system (Cognisys StackShot™, Cognisys Inc., Traverse City, USA; see Suppl. material 1: S3).

Image acquisition and processing

The complete process of image acquisition and processing is controlled with MATLAB (Mathworks, Natick, USA). Camera configuration and start, as well as the readout of the images are accomplished via the USB3 Vision interface standard. An Arduino Mega 2560 microcontroller board, connected to the PC via a serial interface controls the motion of the gimbal motors, switches the LEDs, and triggers the video stream of the camera. To synchronize the macro rail controller with the video stream, the StackShot motion is triggered by the 'exposure active' camera output signal of the first video frame.

For the calculation of the EDOF image from the focus stack, several proven software products are available (Brecko et al. 2014). Nevertheless, we decided to develop our own MATLAB code for the following reasons: (i) the incurring raw images can be processed in parallel to the scan, avoiding the transfer of a large amount of data to a different software; (ii) the high repeatability of the macro rail motion allows calibrating the focus stack acquisition, an option which considerably accelerates the later EDOF image calculations but is not supported by standard focus stacking software; (iii) to ensure that EDOF images can be used for photogrammetry, they must comply with

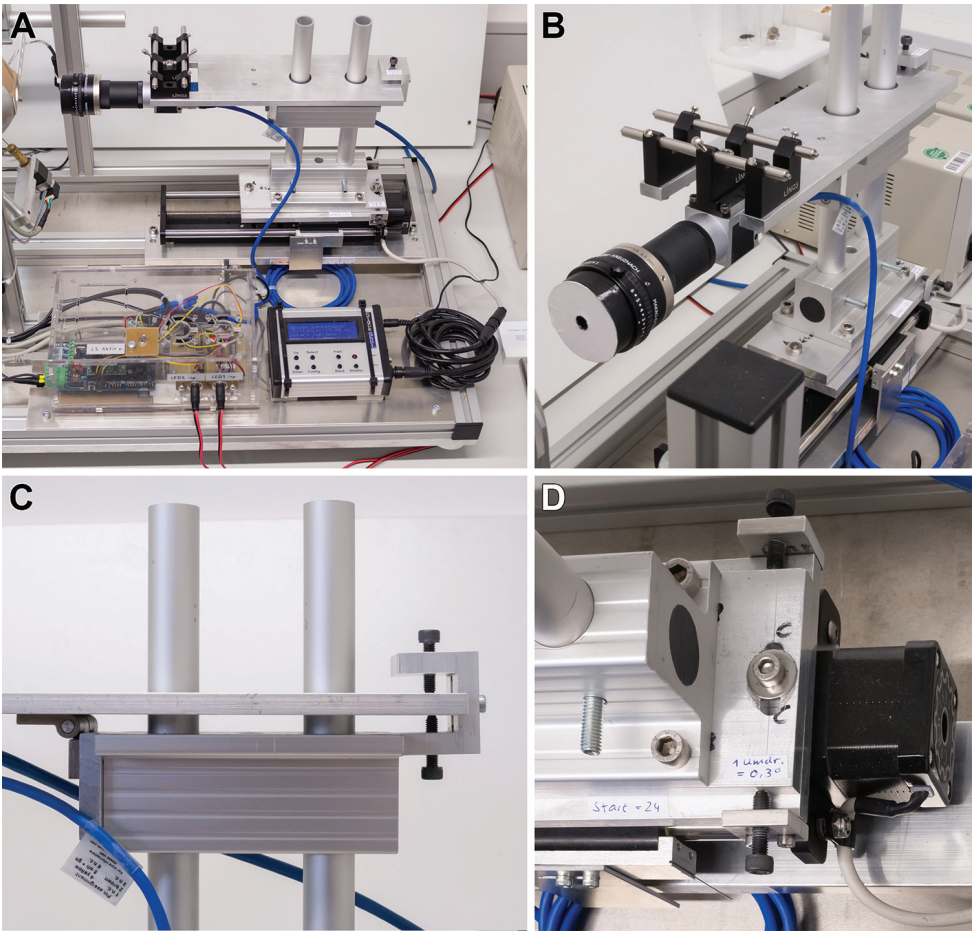

Figure 3. The camera is mounted on a macro-rail (**A**). The camera position and orientation can be fine-tuned in all directions (**B–D**). The camera lens is covered by a pinhole-cap (**B**).

the pinhole camera model, i.e., all parts of the images must be consistent with a unique perspective (Luhmann et al. 2013). The EDOF images produced by standard focus stacking software usually do not meet this condition. The process of EDOF image calculation on the base of the calibration of the focus stack acquisition is illustrated in Fig. 4 and fully described in the Suppl. material 1: S4, see also Suppl. material 2: SV1.

After focus stack processing of the front-light and back-light images, a binary mask for the segmentation of the background is calculated and saved in the alpha-channel of the front-light image (Fig. 5; see also Suppl. material 1: S5). Up to half a terabyte of raw image data are acquired during an insect scan with 10° mean angular distance between the poses. Processing results in storage of 398 masked images in the lossless PNG file format with a total of 300–600 MB. Depending on the size of the insects, the total scanning time including stack processing ranges from two to five hours. Because only about 40–100 min are needed for the actual measurement (image acquisition),

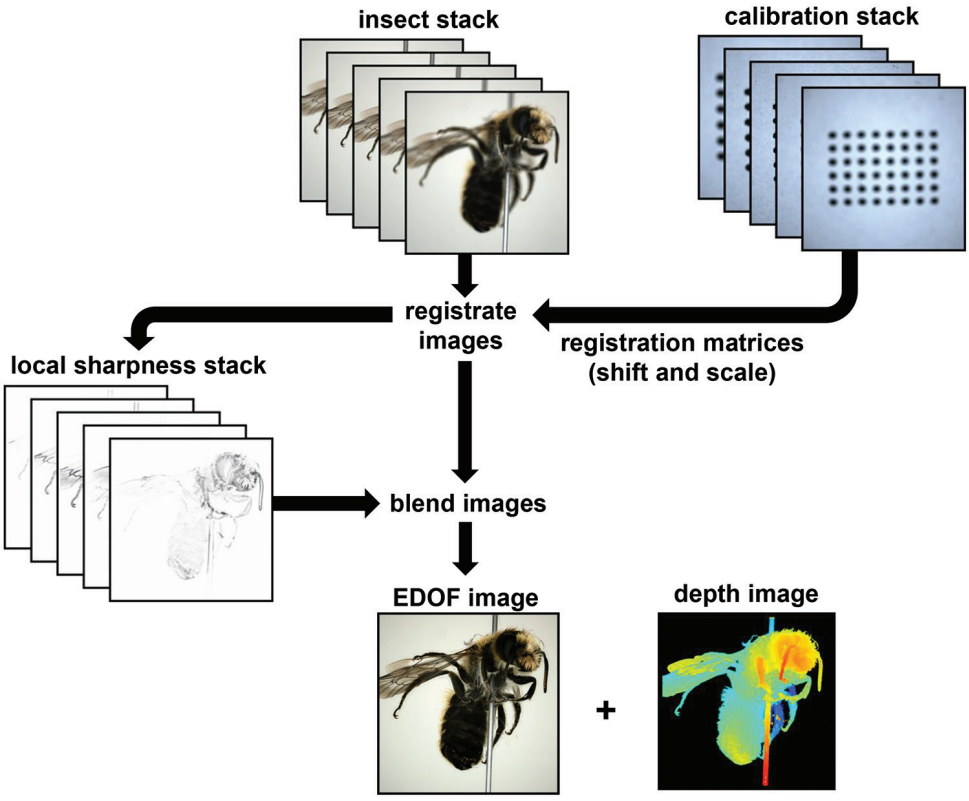

Figure 4. Workflow of EDOF-calculation. For a detailed description, see Suppl. material 1: S2.

faster image processing could considerably accelerate the scans. Other options to reduce the scan time are discussed in the Suppl. material 1: S6.

The MATLAB code is menu-based and includes (i) several calibration functions, (ii) the control of insect positioning, front- and backlight illumination, camera exposure and gain parameters, (iii) the interactive adjustment of several EDOF calculation and masking parameters on the base of the quality of obtained images, and (iv) the start of the scan with the chosen pose program and evaluation range of the image stacks. The interactive adjustment allows customizing all parameters to the specific characteristics of the particular specimen. Alternatively, proven parameter sets from earlier scans of the same or similar specimens can be used. The scan itself is completely automatic.

3D modelling

After the scan, the masked EDOF images of all poses are transferred to the SfM software PhotoScan Pro 1.4 (Agisoft LLC, St. Petersburg, Russia). Depending on shape and surface texture of the insects, images of some poses may not contain a sufficient number of matching feature points to allow the simultaneous calibration of the respec-

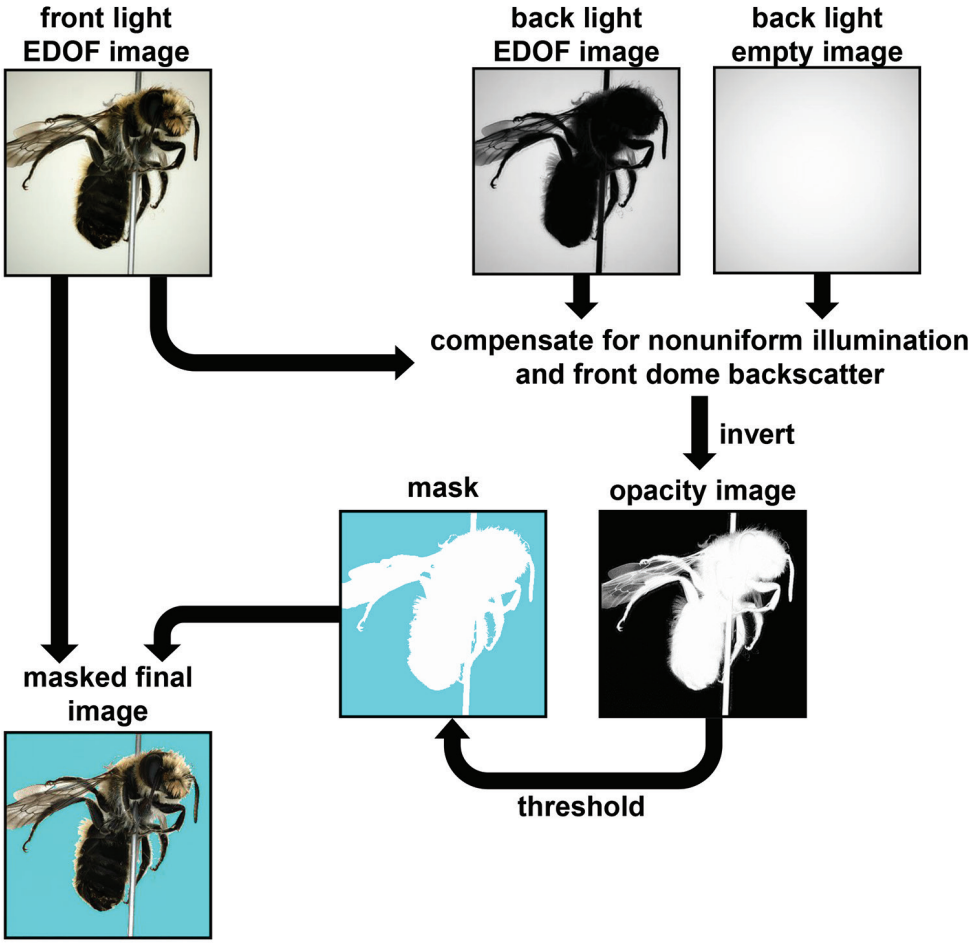

Figure 5. Workflow of image masking using front- and back-light information.

tive camera positions. Such weak poses are discarded by PhotoScan Pro, which impairs the quality of the resulting model. To cope with this problem, and to accelerate the SfM calculation, a special 3D target with a high number of features (textured sphere, see Fig. 6) is used for a "pose calibration". Thanks to the high repeatability of the motorized gimbal, the camera data (internal parameters, positions, and orientations) found with this sphere target can be used as an approximation in later insect scans with the same pose program. Additionally, the known diameter of the sphere can be compared to the resulting 3D model to verify the correct scaling of the model (see Suppl. material 1: S7). PhotoScan Pro allows further optimization of these camera data, thus considerably improving the quality of the resulting 3D point cloud. Our standard workflow with PhotoScan Pro is: (i) add images; (ii) import masks; (iii) import camera positions from the pose calibration and calculate point cloud (sparse cloud); (iv) optimize camera positions; (v) build (and refine) mesh; (vi) build texture; (vii) export

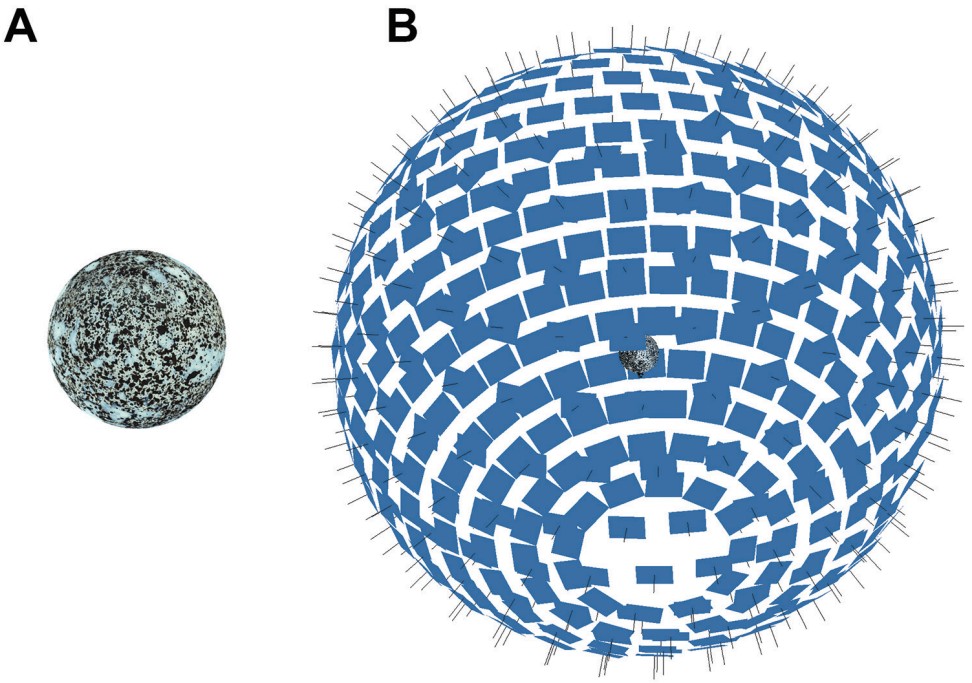

Figure 6. Calibration sphere (**A**) and camera positions estimated in PhotoScan Pro (**B**).

3D-model in desired format. Further automatization could be achieved by a python script including most if not all steps.

For animation (see Suppl. material 3: SV2), 3D-models (meshes) and textures of scanned specimens were exported in the Wavefront OBJ format, imported into Blender (www.blender.org) and rendered with a lighting model suitable to mimic a semi-natural appearance of surface structure and reflections. Resulting animated videos were edited with the free software Shotcut (Meltytech, LLC.). PhotoScan Pro can also export 3D-models directly into 3D-PDFs and several other 3D formats.

Morphometry

Some of our 3D models were used to demonstrate the ease of obtaining 3D morphometric data of the scanned specimens in PhotoScan Pro. Surface area and volume were measured and plotted against each other.

Additionally, the reliability of measurements taken on 3D models was tested by comparing morphometric data obtained from the model and on the specimen itself using the statistical analysis software PAST (Hammer et al. 2001). The width of the scutellum (*sc*) and the length of the tibia (*ti*) of the left hind leg were measured on a specimen of the dung beetle *Anoplotrupes stercorosus,* using both, a Keyence VHX-5000 digital microscope equipped with a Z20 lens, and on a 3D-model of the same specimen taken with DISC3D, using the measuring tools in PhotoScan Pro.

Results and discussion

The quality of the images and the 3D models of DISC3D is demonstrated here by some illustrative examples of insects and snail shells. We present some models as animated videos and some as textured or non-textured polygon-models, implemented as interactive 3D content.

Archiving multi-angle EDOF images

DISC3D allows automatic acquisition of multi-view EDOF images for digitization and digital archiving of pinned insects. There is a trade-off between the digital resolution (size of the pixels on the side of the insects), and the number of views on the one hand, and the scanning time on the other hand. The quality and digital resolution of the EDOF images created by our stacking algorithm is well suitable for the inspection of many relevant morphological features and avoids artifacts of other approaches (Nguyen et al. 2017). Industrial cameras with higher resolution could also be used (e.g., Basler acA4600-10uc with 14 MP), but would lead to larger file sizes, longer image processing times (see Suppl. material 1: S2), and longer times for 3D reconstruction. Hence, we think that the 4 MP camera we used is a good compromise of image quality, resolution, and processing time for many needs in insect imaging (see Figs 7, 8). The absence of spot-like specular reflections ('highlights', cf. Fig. 8C, D) is unusual in macro photography and gives our EDOF images a somehow 'flat' appearance. However, this effect results from the ambient dome illumination and prevents lighting artifacts from being misinterpreted as insect features.

SfM workflow

All 3D models shown here have been generated with Agisoft PhotoScan Pro with visibility-consistent mesh generation enabled. We show the results of the main steps, exemplified by a scan of a 6 mm long specimen of the Lesser Thorn-tipped Longhorn Beetle *Pogonocherus hispidus* (Fig. 8). Image data were taken with a magnification of 1.26 (resulting in a digital resolution of 4.37 μm). After importing the 398 EDOF images, the masks from the alpha channel, and the external camera parameters from the pose calibration with the textured sphere, the sparse cloud was generated with highest accuracy settings, and finally the camera externals were optimized with respect to the actual data (Fig. 9B). The optimized alignment can either be used for the generation of a dense cloud to be meshed into a closed surface model (Fig. 9C) or for VCM generation (Fig. 9D). VCM is a new (and experimental) feature of PhotoScan Pro 1.4. However, since the time needed to generate a meshed model was considerably shorter (0.5–2 h for VCM vs 4–8 h for dense cloud calculation), and delicate structures (e.g., setae, wings) turned out to be modelled much better (Figs 9, 10), we exclusively used this option. Finally, meshes were smoothed, reduced to 75.000 faces (polygons) and textured, using the 'mosaic' option

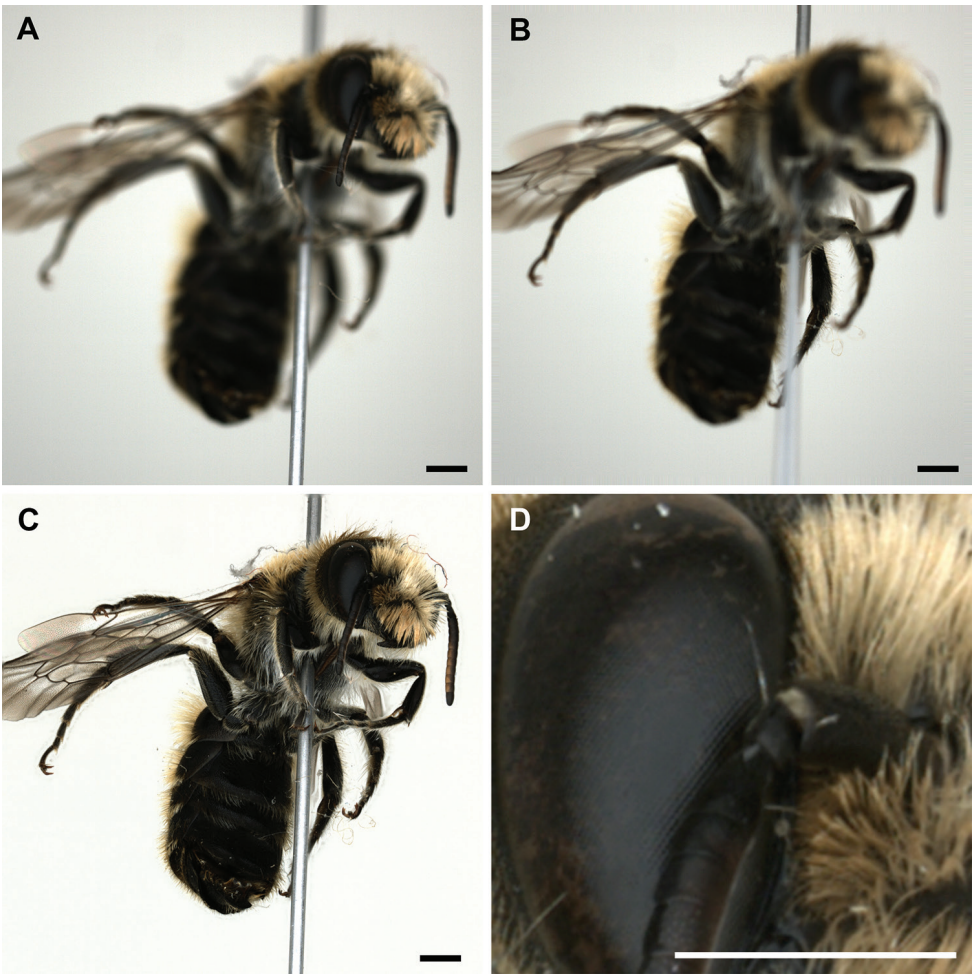

Figure 7. *Osmia adunca*, two exemplary raw images of the front-light stack, with the focal plane going through the proximal (**A**) and the distal part (**B**) of the sample, the EDOF image (**C**), and a detail of the latter (**D**) demonstrate the resolution. Scale bars: 1 mm.

and a 2500*2500 pixel texture atlas. Most models initially had several hundred thousand (up to a few million) faces, with a higher spatial resolution of the models, but also larger files. The reduction to 75.000 faces causes an acceptable loss of detail in most cases while keeping the file size of the model small. The difference is illustrated for the shell structure of the snail *Discus rotundatus* O.F. Müller (5 mm shell diameter, Fig. 11).

Illustrative examples

A set of insect and snail specimens were chosen with a representative shape and size range of 1.5–30 mm for visualization (Fig. 12 and Suppl. material 3: SV2).

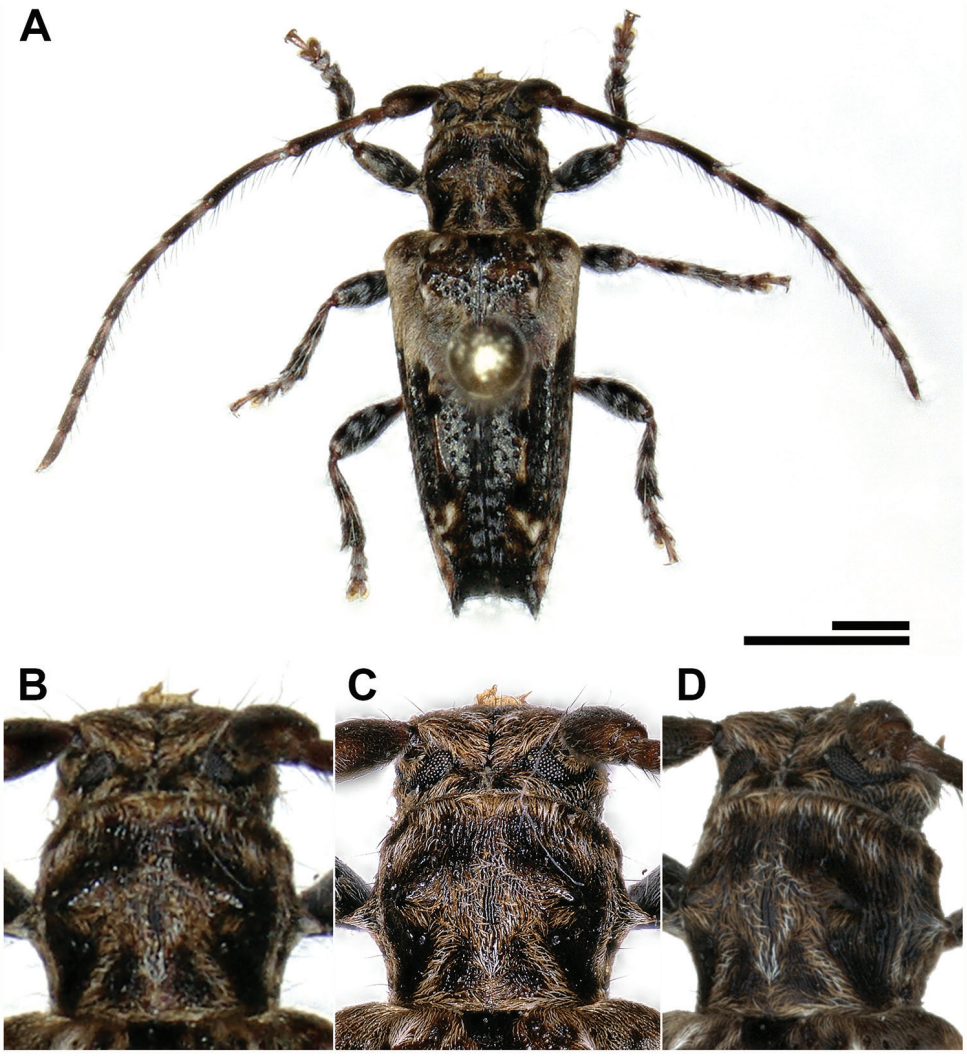

Figure 8. Comparison of images taken with a Keyence VHX 5000 digital microscope (lens: Z20, **A–C**) and DISC3D (**D**). The whole specimen of *Pogonocherus hispidus* can be imaged at once with the VHX 5000 with a X30-magnification (**A**). To compare the digital resolution, we focus on the pronotum of the beetle (**B**: VHX 5000, ×30; **C**: VHX 5000, ×100, **D**: DISC3D, ×1.26). Scale bars: 1 mm.

With 1.5 mm, *Oscinella frit* is probably the smallest object that has ever been 3D modeled by SfM techniques (Fig. 13). A thin insect pin of size 000 with a diameter of 0.25 mm has been used for preparation, and it becomes obvious that smaller insects could hardly be pinned, even with the thinnest pins with a diameter of 0.1 mm, without strongly distorting the shape of the specimen. This could to some extend be circumvented by carefully gluing samples onto the needles, as demonstrated here for the snail shells. Since our sample holder is designed for pinned samples, the device seems well suitable for even the smallest specimens that can be prepared by pinning.

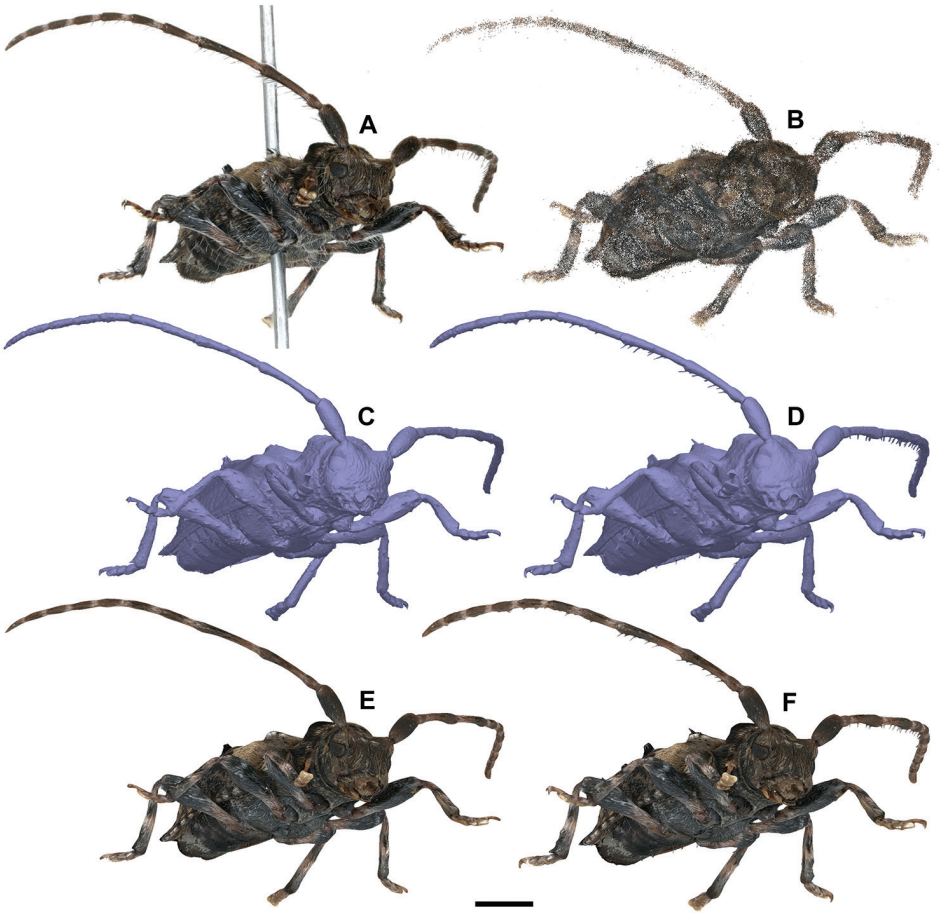

Figure 9. Workflow of model generation of *Pogonocherus hispidus* with PhotoScan Pro. In total, 398 EDOF-images are taken with DISC3D (one example is shown in **A**). Using the image data, masks and camera positions estimated with the calibration sphere (see Fig. 6), a sparse cloud with optimized camera positions is generated (**B**). Two options for model generation are available: direct mesh calculation based on a dense point cloud (**C**) or meshing with visual consistency (**D**). Resulting meshes can be textured (**E, F**). Scale bar: 1mm.

We further provide interactive 3D-models of a mid-sized (*Pogonocherus hispidus*, 6 mm, Fig. 14) and a large beetle specimen (*Prosopocoilus savagei*, 23 mm, Fig. 15). The interactive 3D figures allow measuring certain morphometric parameters with the measuring toolbox.

The models generated with EDOF images obtained by DISC3D have several advantages when compared to the models published by (Nguyen et al. 2014): (i) specimens can be scanned without being re-pinned; (ii) the synchronous process of image acquisition and EDOF calculation allows full automatization; (iii) SfM enables modelling of even deep indentations, which could be demonstrated with the umbilici and apertures of the snail shells (Fig. 16; see Suppl. material 3: SV2).

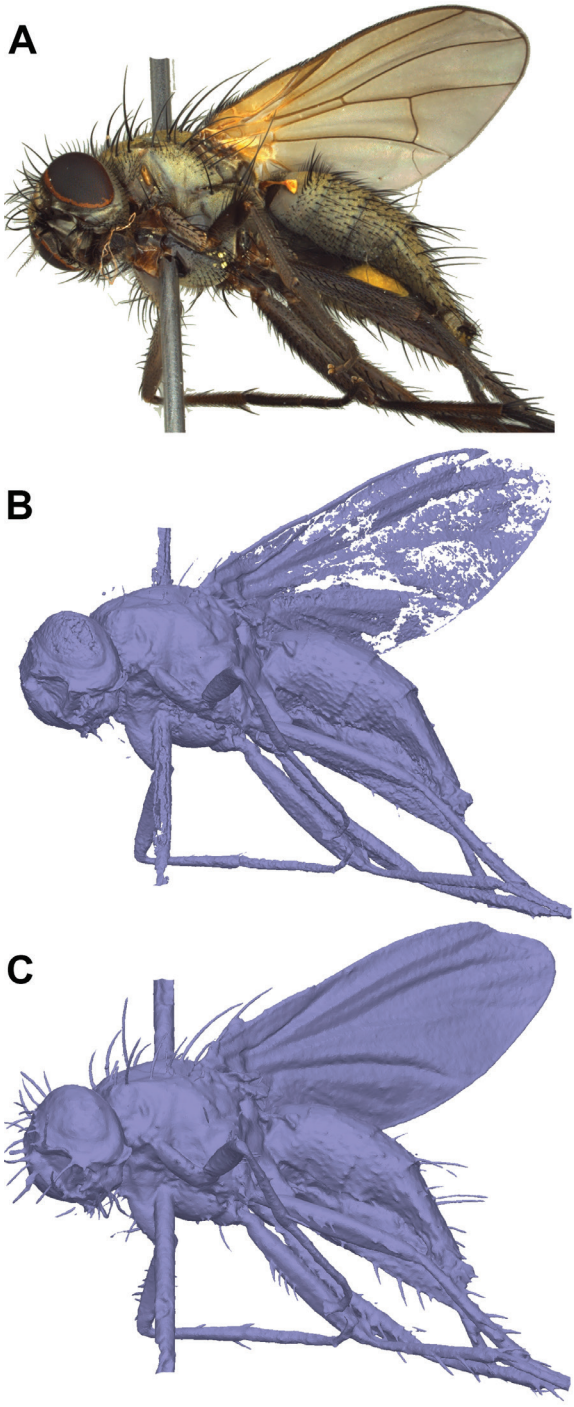

Figure 10. Comparison of dense-cloud-based mesh generation and visual consistency meshing of *Thricops* sp. (**A** EDOF image). Thin and delicate structure like wings and setae are not well modelled from the dense cloud (**B**) but well preserved by visual consistency meshing (**C**).

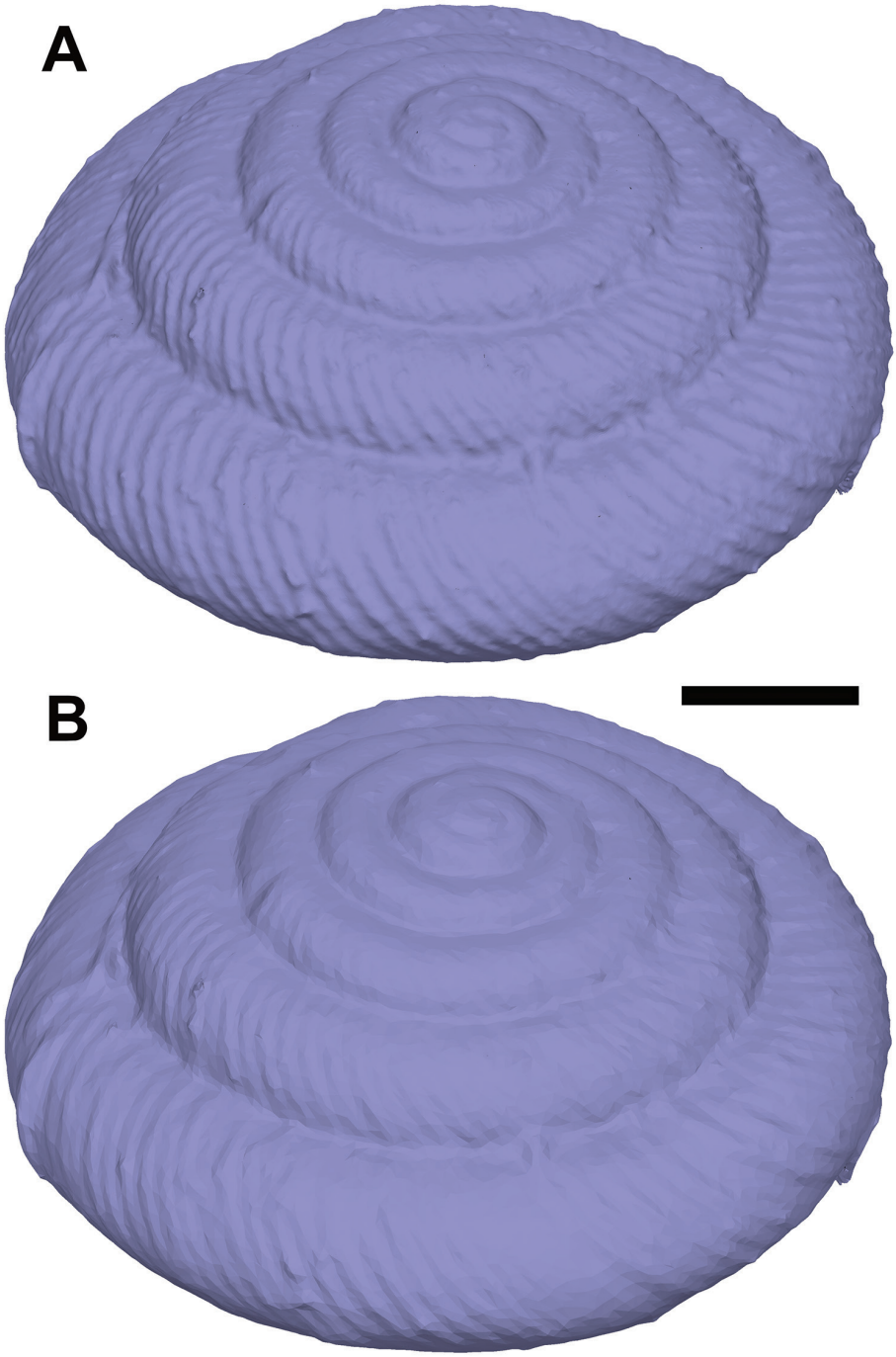

Figure 11. Comparison of mesh quality and number of polygons, exemplified by a model of the shell of *Discus rotundatus*. The model with 1 million faces (**A**) has a file size (3D-PDF) of 35 MB and shows more detail, but the reduced model with 75.000 faces (**B**) still well resembles the structure with a file size (3D-PDF) of only 3 MB.

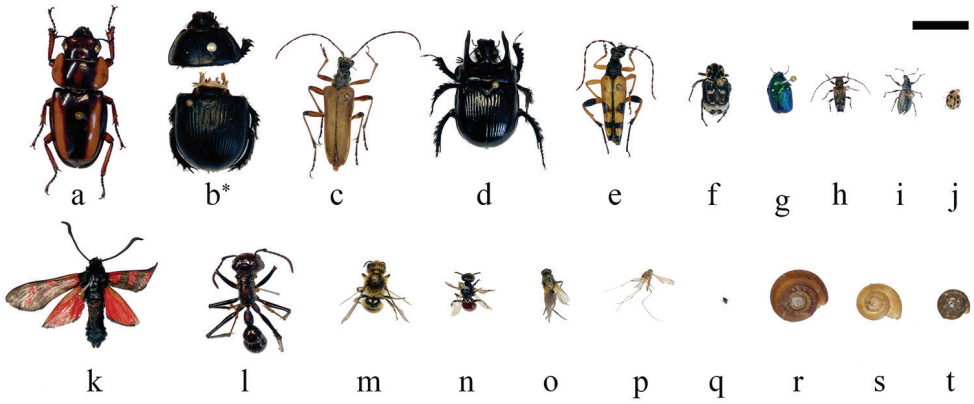

Figure 12. Overview and size comparison of the specimens used in this study. Coleoptera: **a** *Prosopocoilus savagei* **b** *Anoplotrupes stercorosus*, *: specimen was broken during comparative measurements **c** *Stenocorus meridianus* **d** *Typhaeus typhoeus* **e** *Rutpela maculata* **f** *Valgus hemipterus* **g** *Cryptocephalus sericeus* **h** *Pogonocherus hispidus* **i** *Phyllobius pyri* **j** *Tytthaspis sedecimpunctata*; Lepidoptera: **k** *Zygaena filipendulae*; Hymenoptera: **l** *Paraponera clavata* **m** *Osmia adunca* **n** *Sphecodes ephippius*; Diptera: **o** *Thricops* sp., **p** *Culex pipiens* **q** *Oscinella frit*; Gastropoda: **r** *Helicodonta obvoluta* **s** *Aegopinella nitens* **t** *Discus rotundatus*.; Scale bar: 1 cm (keep in mind that not all specimens are equidistant to the lens; i.e., at the same height of the needle).

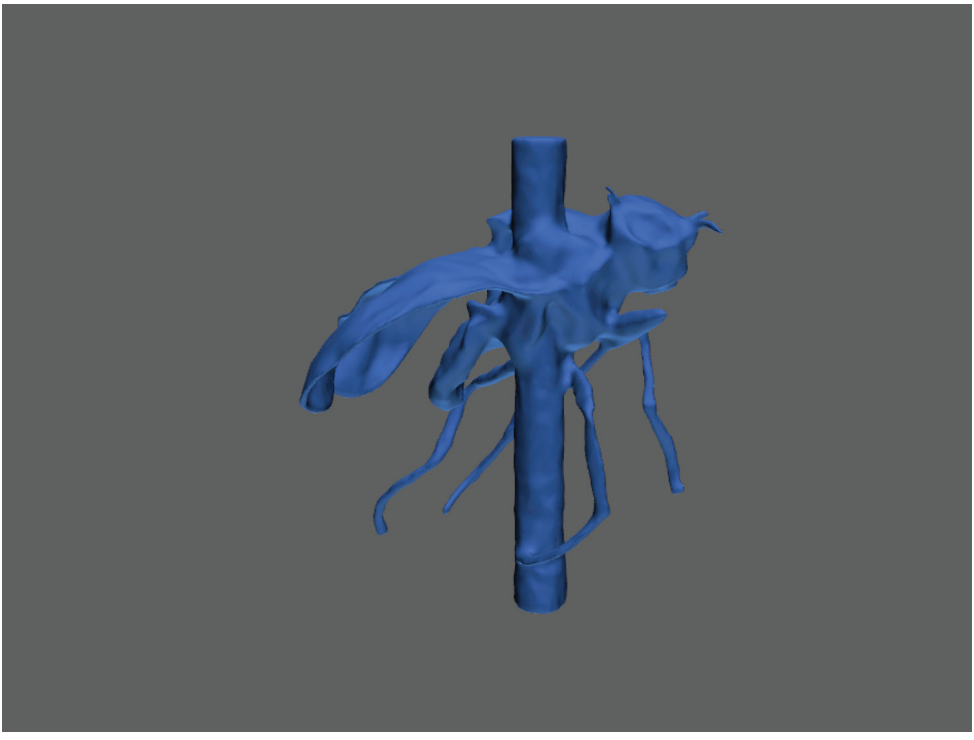

Figure 13. Interactive 3D-model of *Oscinella frit* (1.5 mm body size).

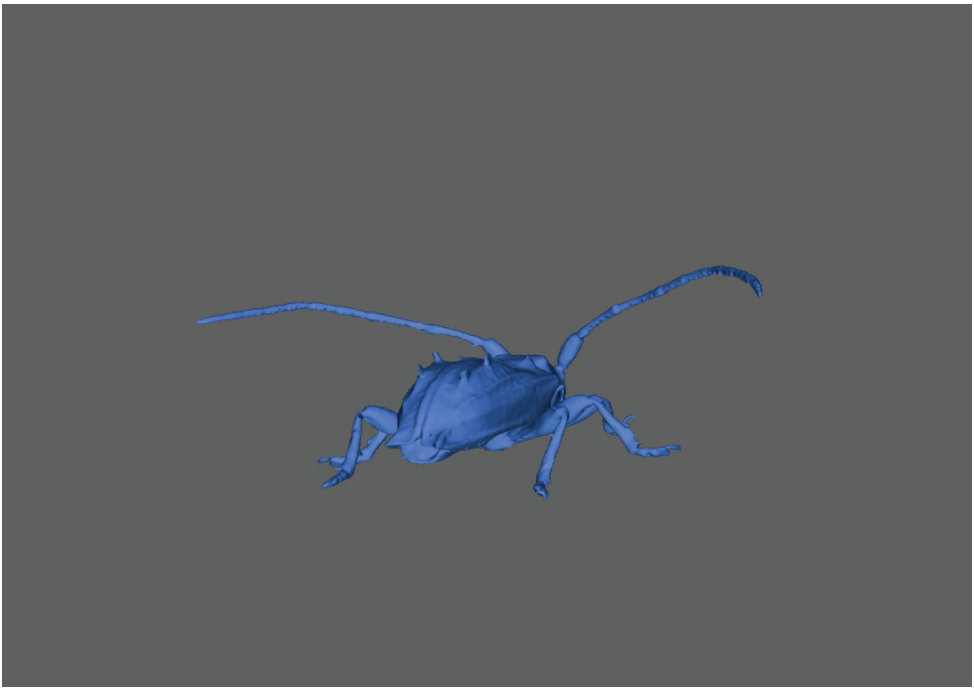

Figure 14. Interactive 3D-model of *Pogonocherus hispidus* (6 mm body size).

Figure 15. Interactive 3D-model of *Prosopocoilus savagei* (23 mm body size).

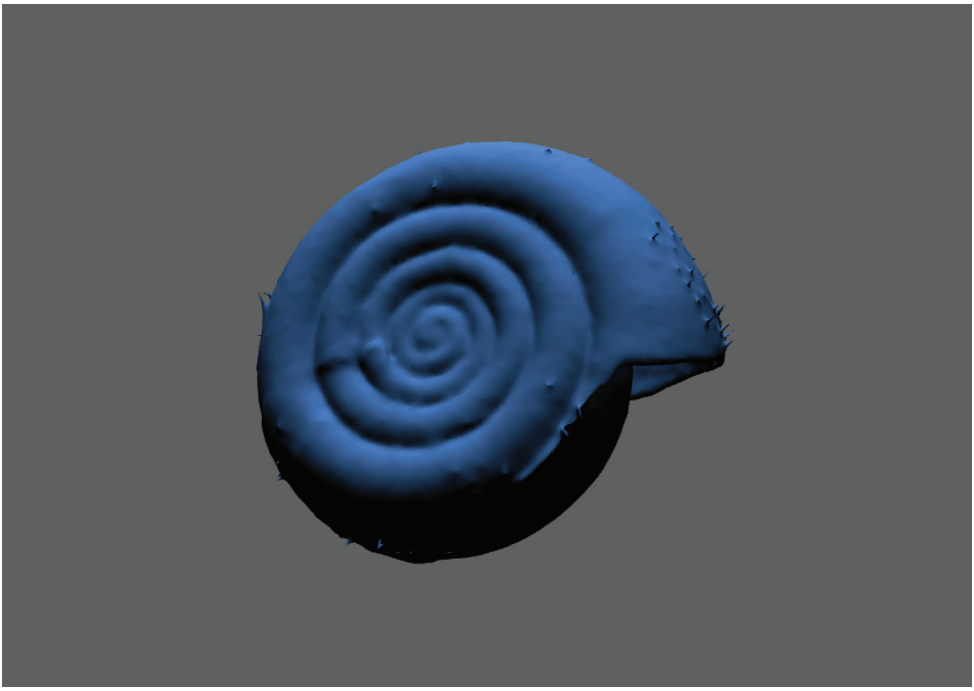

Figure 16. Interactive 3D-model of *Helicodonta obvoluta* (9 mm shell diameter).

Morphometry using 3D models

Surface area and volume of the 3D models were measured in PhotoScan Pro and plotted against each other (Fig. 17). The surface areas and volumes range from 0.072 cm^2 and 0.00031 cm^3 (*Oscinella frit*) to 9.99 cm^2 and 1.0986 cm^3 (*Anoplotrupes stercorosus*), respectively. Some specimens had unfolded wings, generally leading to higher surface areas. The biological consequences of SA/V ratios will not be discussed here (we just aimed at demonstrating the ease of measuring), but they affect physiological processes and can influence performance and distribution of species (Kühsel et al. 2017).

3D models are not only helpful to obtain data which are impossible to be measured on the specimen itself (like surface area), they may also help to obtain more reliable data even of 1D measurements by avoiding parallax errors. We asked 22 people (laypersons, students and skilled entomologists) to measure two simple distances between easily observable landmarks that differed in their susceptibility to parallax errors (width of scutellum (*sc*) and length of the tibia (*ti*) of the left hind leg) on a specimen of the dung beetle *Anoplotrupes stercorosus,* using both, a Keyence VHX-5000 digital microscope (=2D), and a 3D-model (=3D) of the same specimen (Fig. 18). Even with the 'easy' measurement of *sc*, we found remarkable differences in the measurements (in mm: 2D: mean 2.63, SD: 0.21, range: 2.32–3.11; 3D: mean 2.72, SD: 0.07, range: 2.58–2.87) which were even greater regarding *ti* (in mm: 2D: mean 6.11, SD: 0.51, range: 5.24–6.88; 3D: mean 6.61, SD: 0.07, range: 6.45–6.73). There was a strong person-effect for measurements taken with the microscope (Friedmann-

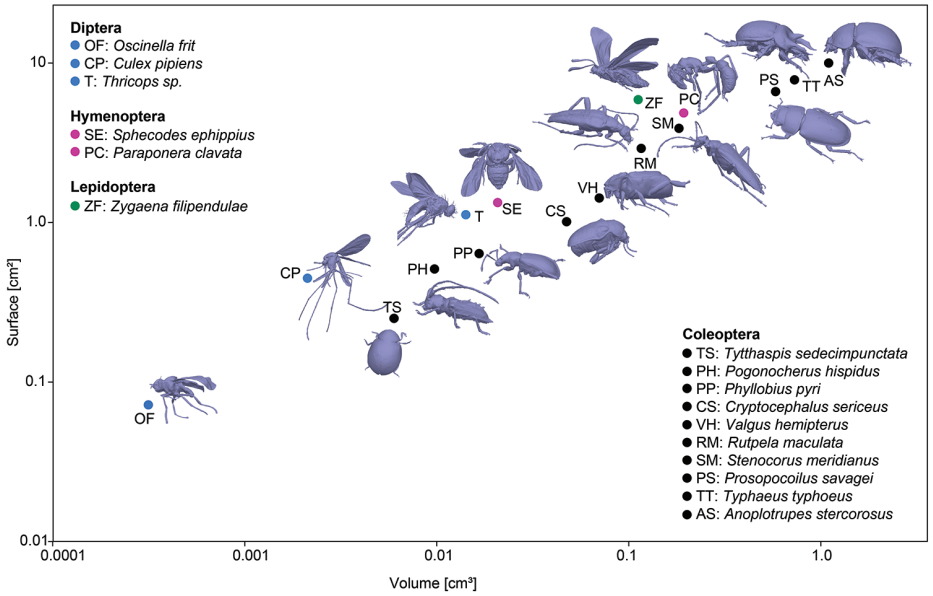

Figure 17. Relation of surface area and volume for all insect species presented here. While the dipteran, hymenopteran and lepidopteran species had their wings unfolded, all beetles had the wings folded underneath their elytra. Models are not to scale.

test; 2D: $\chi^2 = 75$, $p < 0.001$, $df = 21$), but not for measuring on the 3D model (Friedmann-test; 3D: $\chi^2 = 27$, $p = 0.14$, $df = 21$), indicating that less training and care are necessary when measuring on the 3D model. Moreover, morphometric data measured on the 3D model were more reliable: the coefficient of variance (CV) of individual 2D microscopic measurements was more than three times higher for *sc*, and more than seven times higher for *ti* , as compared to 3D model measurements (*sc*: CV(2D) = 8.0%, CV(3D) = 2.5%, F-test: $F = 9.87$, $p < 0.0001$; *ti*: CV(2D) = 8.3%, CV(3D) = 1.1%, $F = 49.69$, $p < 0.0001$).

Due to observer errors, morphometric data can vary by more than 14% of the mean measured value (Viscardi et al. 2010), leading to the introduction of noise and potential bias when compiling composite datasets. We also observed a maximum deviation of 14% from the mean value of both, *sc* and *ti* when using the microscope. This error was strongly reduced to 5.5% (*sc*) and 2.4% (*ti*) when using the 3D model. Hence, morphometric measurements taken on 3D models do not only allow access to 'new' data (e.g., surface areas), they also provide more reliable and less error-prone data.

Conclusions

To the best of our knowledge, DISC3D is the first and only system for automated multi-view EDOF imaging. The system allows the digitization of natural history col-

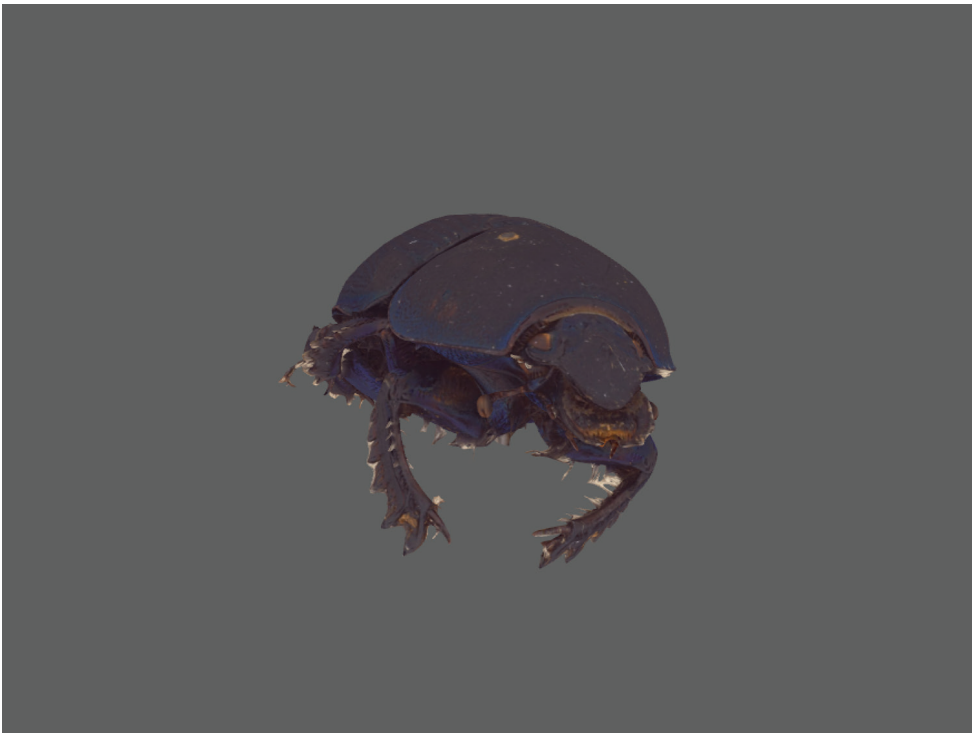

Figure 18. Interactive, textured 3D-model of *Anoplotrupes stercorosus* (21 mm body size).

lections and effective exchange of information about a specimen, avoiding physical handling or transfer of the specimen itself. The 3D-models facilitate accurate reproducible 1D, 2D, and 3D measurements to characterize the specimen, including functionally relevant traits such as surfaces or volumes, a promising perspective for functional ecology, comparative zoology, and physiology. For large scale digitization projects, several scanners could be used simultaneously. Due to the high degree of automatization, one person should be able to operate up to five devices in parallel for scanning and 3D-modelling. We encourage the community to copy our device and to join us in further developing DISC3D for archiving and 3D-modelling purposes. We will be happy to provide relevant information and share our experience.

Acknowledgements

We would like to thank Ken Justice and Stephan Neser (HDA) for providing ideas and technical support. The workshop team (Faculty of Biology, TUDA) is acknowledged for technical support. Numerous students from both institutions (HDA and TUDA) assisted in developing DISC3D.

References

Aroudj S, Seemann P, Langguth F, Guthe S, Goesele M (2017) Visibility-consistent thin surface reconstruction using multi-scale kernels. ACM Transactions on Graphics 36: 187. https://doi.org/10.1145/3130800.3130851

Beaman RS, Cellinese N (2012) Mass digitization of scientific collections: New opportunities to transform the use of biological specimens and underwrite biodiversity science. ZooKeys 209: 7–17. https://doi.org/10.3897/zookeys.209.3313

Berents P, Hamer M, Chavan V (2010) Towards demand-driven publishing: Approaches to the priotization of digitization of natural hstory collection data. Biodiversity Informatics 7: 113–119.

Betz O, Wegst U, Weide D, Heethoff M, Helfen L, Lee W-K, Cloetens P (2007) Imaging applications of synchrotron X-ray phase-contrast microtomography in biological morphology and biomaterials science. I. General aspects of the technique and its advantages in the analysis of millimetre-sized arthropod structure. Journal of Microscopy 227: 51–71. https://doi.org/10.1111/j.1365-2818.2007.01785.x

Brecko J, Mathys A, Dekoninck W, Leponce M, VandenSpiegel D, Semal P (2014) Focus stacking: Comparing commercial top-end set-ups with a semi-automatic low budget approach. A possible solution for mass digitization of type specimens. ZooKeys 464: 1–23. https://doi.org/10.3897/zookeys.464.8615

Brückner A, Heethoff M, Blüthgen N (2017) The relationship between epicuticular long-chained hydrocarbons and surface area - volume ratios in insects (Diptera, Hymenoptera, Lepidoptera). PLoS one 12: e0175001. https://doi.org/10.1371/journal.pone.0175001

Cheung KM, Baker S, Kanade T (2005) Shape-from-silhouette across time part I: Theory and algorithms. International Journal of Computer Vision 62: 221–247. https://doi.org/10.1007/s11263-005-4881-5

Diaz S, Cabido M, Casanoves F (1998) Plant functional traits and environmental filters at a regional scale. Journal of Vegetation Science 9: 113–122. https://doi.org/10.2307/3237229

Emlen DJ (1997) Diet alters male horn allometry in the beetle *Onthophagus acuminatus* (Coleoptera: Scarabaeidae). Proceedings of the Royal Society of London B: Biological Sciences 264: 567–574. https://doi.org/10.1098/rspb.1997.0081

Furukawa Y, Ponce J (2009) Carved Visual Hulls for Image-Based Modeling. International Journal of Computer Vision 81: 53–67. https://doi.org/10.1007/s11263-008-0134-8

Gallo A, Muzzupappa M, Bruno F (2014) 3D reconstruction of small sized objects from a sequence of multi-focused images. Journal of Cultural Heritage 15: 173–182. https://doi.org/10.1016/j.culher.2013.04.009

Gámez-Virués S, Perović DJ, Gossner MM, Börschig C, Blüthgen N, de Jong H, Simons NK, Klein AM, Krauss J, Maier G, Scherber C, Steckel J, Rothenwöhrer C, Steffan-Dewenter I, Weiner CN, Weisser W, Werner M, Tscharntke T, Westphal C (2015) Landscape simplification filters species traits and drives biotic homogenization. Nature Communications 6: 8568. https://doi.org/10.1038/ncomms9568

Hammer Ø, Harper DAT, Ryan PD (2001) PAST: Paleontological statistics software package for education and data analysis. Palaeontologia Electronica 4: art. 4.

Heethoff M, Norton RA (2009) A new use for synchrotron X-ray microtomography: three-dimensional biomechanical modeling of chelicerate mouthparts and calculation of theoretical bite forces. Invertebrate Biology 128: 332–339. https://doi.org/10.1111/j.1744-7410.2009.00183.x

Hendrickx F, Maelfait JP, Lens L (2003) Relationship between fluctuating asymmetry and fitness within and between stressed and unstressed populations of the wolf spider *Pirata piraticus*. Journal of Evolutionary Biology 16: 1270–1279. https://doi.org/10.1046/j.1420-9101.2003.00633.x

Hudson LN, Blagoderov V, Heaton A, Holtzhausen P, Livermore L, Price BW, van der Walt S, Smith VS (2015) Inselect: Automating the Digitization of Natural History Collections. PLoS one 10: e0143402. https://doi.org/10.1371/journal.pone.0143402

Kühsel S, Brückner A, Schmelzle S, Heethoff M, Blüthgen N (2017) Surface area-volume ratios in insects. Insect Science 24: 829–841. https://doi.org/10.1111/1744-7917.12362

Loreau M, Naeem S, Inchausti P, Bengtsson J, Grime JP, Hector A, Hooper DU, Huston MA, Raffaelli D, Schmid B, Tilman D, Wardle DA (2001) Biodiversity and ecosystem functioning: current knowledge and future challenges. Science 294: 804–808. https://doi.org/10.1126/science.1064088

Lowe DG (2004) Distinctive image features from scale-invariant keypoints. International Journal of Computer Vision 60: 91–110. https://doi.org/10.1023/B:Visi.0000029664.99615.94

Luhmann T, Robson S, Kyle S, Boehm J (2013) Close Range Photogrammetry and 3D Imaging. Walter de Gruyter, Berlin, 702 pp. https://doi.org/10.1515/9783110302783

Mantle BL, Salle JL, Fisher N (2012) Whole-drawer imaging for digital management and curation of a large entomological collection. ZooKeys 209: 147–163. https://doi.org/10.3897/zookeys.209.3169

Mathys A, Brecko J, Semal P (2013) Comparing 3D digitizing technologies: What are the differences? Digital Heritage International Congress. Marseille, 201–204. https://doi.org/10.1109/DigitalHeritage.2013.6743733

Mathys A, Brecko J, Vandenspiegel D, Cammaert L, Semal P (2015) Bringing collections to the digital era. Digital Heritage 2015. Granada, 155–158. https://doi.org/10.1109/DigitalHeritage.2015.7413858

McGill BJ, Enquist BJ, Weiher E, Westoby M (2006) Rebuilding community ecology from functional traits. Trends in Ecology & Evolution 21: 178–185. https://doi.org/10.1016/j.tree.2006.02.002

Mertens JEJ, Roie MV, Merckx J, Dekoninck W (2017) The use of low cost compact cameras with focus stacking functionality in entomological digitization projects. ZooKeys 712: 141–154. https://doi.org/10.3897/zookeys.712.20505

Møller AP, Thornhill R (1998) Bilateral symmetry and sexual selection: a meta-analysis. The American Naturalist 151: 174–192. https://doi.org/10.1086/286110

Moore W (2011) Biology needs cyber infrastructure to facilitate specimen-level data acquisition for insects and other hyperdiverse groups. ZooKeys 147: 479–486. https://doi.org/10.3897/zookeys.147.1944

Mouillot D, Graham NA, Villéger S, Mason NW, Bellwood DR (2013) A functional approach reveals community responses to disturbances. Trends in Ecology & Evolution 28: 167–177. https://doi.org/10.1016/j.tree.2012.10.004

Nguyen C, Adock M, Anderson S, Lovell DR, Fisher N, La Salle J (2017) Towards high-throughput 3D insect capture for species discovery and diagnostics. arXiv:1709.02033v02031. https://doi.org/10.1109/eScience.2017.90

Nguyen CV, Lovell DR, Adcock M, La Salle J (2014) Capturing Natural-Colour 3D Models of Insects for Species Discovery and Diagnostics. PLoS ONE 9: e94346. https://doi.org/10.1371/journal.pone.0094346

Peat J, Darvill B, Ellis J, Goulson D (2005) Effects of climate on intra-and interspecific size .variation in bumble-bees. Functional Ecology 19: 145–151. https://doi.org/10.1111/j.0269-8463.2005.00946.x

Petchey OL, Gaston KJ (2002) Functional diversity (FD), species richness and community composition. Ecology Letters 5: 402–411. https://doi.org/10.1046/j.1461-0248.2002.00339.x

Schmelzle S, Helfen L, Norton RA, Heethoff M (2009) The ptychoid defensive mechanism in Euphthiracaroidea (Acari: Oribatida): A comparison of muscular elements with functional considerations. Arthropod Structure & Development 38: 461–472. https://doi.org/10.1016/j.asd.2009.07.001

Seitz SM, Curless B, Diebel J, Scharstein D, Szeliski R (2006) A comparison and evaluation of multi-view stereo reconstruction algorithms. Proceedings of the IEEE Computer Society Conference on Computer Vision and Pattern Recognition. IEEE Computer Society, New York, 519–526. https://doi.org/10.1109/CVPR.2006.19

Simons NK, Weisser WW, Gossner MM (2016) Multi-taxa approach shows consistent shifts in arthropod functional traits along grassland land-use intensity gradient. Ecology 97: 754–764.

Ströbel B, Justice K, Heethoff M (2017) Mikrophotogrammetrie präparierter Insekten. In: Luhmann T, Schumacher C (Eds) Photogrammetrie, Laserscanning, Optische 3D-Messung Beiträge der Oldenburger 3D-Tage 2017. Wichmann Verlag, Berlin, 344–356.

Szeliski R (2011) Computer Vision: Algorithms and Applications. Springer, London, 812 pp. https://doi.org/10.1007/978-1-84882-935-0

Tatsuta H, Takahashi KH, Sakamaki Y (2017) Geometric morphometrics in entomology: Basics and applications. Entomological Science 21: 164–184. https://doi.org/10.1111/ens.12293

Tobias JA, Seddon N, Spottiswoode CN, Pilgrim JD, Fishpool LD, Collar NJ (2010) Quantitative criteria for species delimitation. Ibis 152: 724–746. https://doi.org/10.1111/j.1474-919X.2010.01051.x

Ullmann S (1979) The interpretation of Structure from Motion. Proceedings of the Royal Society B 203: 405–426. https://doi.org/10.1098/rspb.1979.0006

Viscardi P, Sakamoto M, Sigwart JD (2010) How long is a piece of Strix? Methods in measuring and measuring the measurers. Zoomorphology 129: 185–194. https://doi.org/10.1007/s00435-010-0111-y

Vollmar A, Macklin JA, Ford LS (2010) Natural history specimen digitization: Challenges and concerns. Biodiversity Informatics 7: 93–113. https://doi.org/10.17161/bi.v7i2.3992

Vu H-H, Labatut P, Pons J-P, Keriven R (2012) High accuracy and visibility-consistent dense multiview stereo. IEEE Transactions on Pattern Analysis and Machine Intelligence 34: 889–901. https://doi.org/10.1109/TPAMI.2011.172

Westoby MJ, Brasington J, Glasser NF, Hambrey MJ, Reynolds JM (2012) 'Structure-from-Motion' photogrammetry: A low-cost, effective tool for geoscience applications. Geomorphology 179: 300–314. https://doi.org/10.1016/j.geomorph.2012.08.021

Wiens JJ (2000) Phylogenetic analysis of morphological data. Smithsonian Institution Press, 232 pp.

Supplementary material 1

Technical information

Authors: Ströbel B, Schmelzle S, Blüthgen N, Heethoff M

Data type: text, figures and tables

Explanation note: Detailed technical information and additional theoretical background.

Link: https://doi.org/10.3897/zookeys.759.24584.suppl1

Supplementary material 2

SV1: EDOF imaging

Authors: Ströbel B, Schmelzle S, Blüthgen N, Heethoff M

Data type: video

Explanation note: This video demonstrates the effect of the registered EDOF-calculation.

Link: https://doi.org/10.3897/zookeys.759.24584.suppl2

Supplementary material 3

SV2: Illustrative examples

Authors: Ströbel B, Schmelzle S, Blüthgen N, Heethoff M

Data type: video

Explanation note: Illustrative examples of insects and snail shell models generated with DISC3D.

Link: https://doi.org/10.3897/zookeys.759.24584.suppl3

ZooKeys 759: 29–56 (2018)
doi: 10.3897/zookeys.759.22981
http://zookeys.pensoft.net

RESEARCH ARTICLE

A peer-reviewed open-access journal
ZooKeys
Launched to accelerate biodiversity research

Three new species of *Thelepus* Leuckart, 1849 from Europe and a re-description of *T. cincinnatus* (Fabricius, 1780) (Annelida, Terebellidae)

Igor Jirkov[1]

1 *Department of Hydrobiology, Biological Faculty, Moscow Lomonosov State University, Moscow, Russia*

Corresponding author: *Igor Jirkov* (ampharete@yandex.ru)

Academic editor: *C. Glasby* | Received 13 December 2017 | Accepted 4 April 2018 | Published 17 May 2018

http://zoobank.org/A7645CBD-F29D-4F99-A2C5-709197B95F28

Citation: Jirkov I (2018) Three new species of *Thelepus* Leuckart, 1849 from Europe and a re-description of *T. cincinnatus* (Fabricius, 1780) (Annelida, Terebellidae). ZooKeys 759: 29–56. https://doi.org/10.3897/zookeys.759.22981

Abstract

The review of a large amount of material previously identified as the terebellid annelid, *Thelepus cincinnatus* (Fabricius, 1780) shows that, within European waters from the Mediterranean to the North Pole, this species should be split into four species, three of which (*T. davehalli* **sp. n.**, *T. marthae* **sp. n.**, and *T. parapari* **sp. n.**) are newly described here and *T. cincinnatus* s. str. is re-described. These four species each show distinct distribution ranges. *Thelepus cincinnatus* has notopodia on almost all segments and numerous eyespots; it inhabits the high boreal and arctic shelf and the North Atlantic slope, and probably also occurs on the North Pacific shelf and slope. *Thelepus marthae* **sp. n.** has no eyespots and inhabits deep waters of the high Arctic. *Thelepus davehalli* **sp. n.** has no eyespots and has notopodia on 1/2 to 2/3 of the anterior of the body; it inhabits boreal shelf waters (from Iceland to the Mediterranean) below the tidal front. *Thelepus parapari* **sp. n.** differs from the previous three species in that the uncini of the first uncinigerous segment has two teeth above the main fang; it inhabits shallow, coastal waters of the Mediterranean, inshore from the tidal front.

Keywords

cosmopolitan species, generic characteristic, identification key, morphological characters, Polychaeta, taxonomic revision, taxonomy

Introduction

Thirty years ago, Hutchings and Glasby stated "Many species of *Thelepus* have been described, but many inadequately, and type material in most cases needs to be re-examined" (Hutchings and Glasby 1987: 226). Unfortunately, this situation has persisted and led to the appearance of another "cosmopolitan species", which is, in reality, a complex of pseudocryptic species. The type species of *Thelepus*, *T. cincinnatus*, was reported as cosmopolitan by Hartmann-Schröder (1996). Despite being absent from the tropics (thus not truly cosmopolitan), its reported range is very wide: from the eastern North Atlantic, from Cape Verde in the south, through the Mediterranean to the western North Atlantic and the Caribbean, the North Polar Basin and the North Pacific: Japan and Washington (Uschakov 1955; Imajima and Hartman 1964; Hobson and Banse 1981; Holthe 1986; Jirkov 2001). Hartman (1966) also reported *T. cincinnatus* amongst Antarctic polychaetes. Existing records indicate a vertical distribution from the eulittoral zone to a depth of ca. 4000 m (Holthe 1986). However, recent investigations indicate the species' true range is not as extensive, with the Caribbean for example already excluded from its range (Londoño-Mesa 2009). The extensive range and habitat preferences of *T. cincinnatus* were investigated during the examination of European material for the Fauna Ibérica Project. As a result, instead of the single species *T. cincinnatus,* these records indicate four species: *T. cincinnatus* s. str. and three new species described here. The previously reported range of *T. cincinnatus* within the Arctic and North Atlantic is thus divided between these four species. It should be noted that *T. cincinnatus* also has a long list of subjective synonyms: 12 according to Bellan (2008); Fauvel (1927) also accepted *T. nucleolata* (valid according to Hsueh and Li 2016) as a synonym of *T. cincinnatus*. Unfortunately, all these synonymized taxa were described at least a century ago, and have poor original descriptions and an absence of type material; it is not possible to confirm their taxonomic status.

Materials and methods

The higher taxonomy used in this paper follows Read and Fauchald (2018). Morphological terms used in this paper follow Nogueira et al. (2010) and are explained in Fig. 1A. Taxonomic abbreviations used are as follows:

BS	branchiferous segment;	**C**	chaetiger;	**T**	thoracic;
		S	segment;	**U**	unciniger.

The number following the abbreviation refers to the number of the segment (e.g. BS1 means branchiferous segment 1). Institutional abbreviations used are as follows:

APEM APEM Ltd., UK;
Aveiro Biology Department of the Universidade de Aveiro, Portugal;
KGB Department of Hydrobiology Moscow Lomonosov State University, Russia;

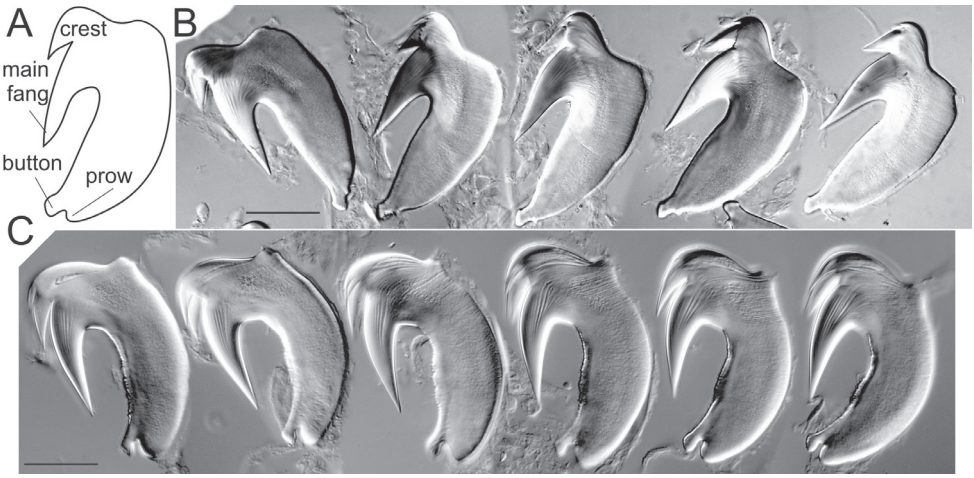

Figure 1. Uncinial parts and uncini of *T. triserialis* and *T. setosus*. **A** uncinial parts according to Nogueira et al. (2010) **B** uncini U1 *T. setosus* APEM 413169 **C** uncini U1 *T. triserialis* MNCN 2508. Scale bars: 20 μm.

MNCN Museo Nacional de Ciencias Naturales, Madrid, Spain;
ZIN Zoological Institute of Russian Academy of Science, St. Petersburg, Russia.

This study was based almost exclusively on collections from the KGB. Mediterranean specimens were examined from the collection at the MNCN; specimens from UK waters were examined from the APEM collection. All material, if not stated otherwise, is deposited at KGB. Sampling data are given in Table 1.

Photographs were produced at the PP Shirshov Institute of Oceanology, at the Russian Academy of Science, Moscow using a Leica DFC490 camera mounted on either a Leica M165C stereomicroscope or a Leica DMI 4000B compound microscope; at the Department of Invertebrate Zoology, Biological Faculty, Moscow State University using a Leica DFC425C camera mounted on a Leica DMI 5000B compound microscope; and at the MNCN by a Leica DFC550 camera mounted on a Leica MZ16A stereomicroscope. In order to increase contrast, specimens were stained with methylene blue (water solution).

Some external morphological characters are not always and/or easily visible. Eyespots are located on back of upper lip, which is usually curved backward, so it is necessary to unbend the lip forwards to observe this feature (Fig. 2C–F). Additionally, sometimes eyespots do not form an entire band; instead, a dorsally interrupted band is present, so careful examination is required. Nephridial papillae are often poorly visible, so it is necessary to investigate several specimens, preferably well preserved and mature to get a clear picture. Counting the number of branchial filaments requires careful examination as it will appear that more rows are present due to the presence of numerous obscuring filaments. Some characters develop ontogenetically. Unfortunately usually specimens are incomplete, so it is not possible to assess age of specimen using its length. Further, length greatly depends on the degree of retraction

Table 1. Collection data and institutional repository for all investigated material. Abbreviations (in addition to those in Material & methods): SP-22 – drifting ice station Severniy Polus 22; VNIRO – Russian Federal Research Institute of Fisheries and Oceanography, n/a – not applied, - – no data.

Species	Ship or expedition	Cruise. station or collection number	Latitude N	Longitude	Depth, m	T °C	S‰	Day	Month	Year	Number of specimens	Collection
T. cincinnatus	Alaid	30.6	74°14'	19°20'E	64	0.91	34.8	1	7	1980	73	KGB
T. cincinnatus	Alaid	30.7	74°30'	28°00'E	388	0.86	34.9	4	7	1980	1	KGB
T. cincinnatus	Alaid	30.8	74°30'	32°30'E	190	-1.53	34.8	4	7	1980	136	KGB
T. cincinnatus	Alaid	30.13	68°51'	37°20'E	75	2.68	34.0	11	7	1980	15	KGB
T. cincinnatus	Molchanov	14.9303	69°53'	41°39'E	95	-	-	18	4	1986	2	KGB
T. cincinnatus	Otkupshikov	181.19	69°15'	35°48'E	145	1.70	34.6	9	7	1978	7	KGB
T. cincinnatus	Persey	5.183	76°33'	41°12'E	230	-	-	1	9	1924	5	KGB
T. cincinnatus	Persey	5.220	75°09'	18°47'E	35	-	-	30	9	1924	1	KGB
T. cincinnatus	Persey	12.650	74°36'	32°34'E	172	-1.35	-	7	6	1927	11	KGB
T. cincinnatus	Persey-3	14.3024	47°20'	49°00'W	115	-	-	8	9	1975	3	KGB
T. cincinnatus	Persey-3	15.3341	44°43'	49°02'W	217	-	-	6	5	1976	1	KGB
T. cincinnatus	Persey-3	15.3521	48°20'	52°06'W	185	-1.00	-	19	6	1976	2	KGB
T. cincinnatus	Persey-3	15.3529	47°58'	49°45'W	185	-	-	20	6	1976	20	KGB
T. cincinnatus	Persey-3	14.2724	47°00'	47°30'W	215	2.00	-	25	6	1975	3	KGB
T. cincinnatus	Saratov	16.1374	69°10'	36°00'E	47	7.04	34.0	26	8	1947	2	KGB
T. cincinnatus	Sevastopol	5.1078	63°55'	13°03'W	650	3.38	35.0	15	7	1957	5	KGB
T. cincinnatus	Sevastopol	9.1580	62°00'	24°56'W	1350	-	-	26	6	1958	10	KGB
T. cincinnatus	Sevastopol	10.1768	65°47'	11°02'W	173	2.86	34.9	16	10	1958	1	KGB
T. cincinnatus	Sevastopol	8.1427	64°45'	12°31'W	157	1.34	34.8	9	4	1958	26	KGB
T. cincinnatus	Sevastopol	8.1411	61°50'	1°45'E	185	7.37	35.3	6	4	1958	4	KGB
T. cincinnatus	Shmidt	26.2301	79°20'	45°53'E	65	-	-	11	8	1986	2	KGB
T. cincinnatus	Tunetz	105.22	74°30'	20°10'E	94	-0.12	34.7	7	7	1978	45	KGB
T. cincinnatus	Tunetz	105.23	74°30'	31°20'E	245	-0.76	34.9	8	7	1978	3	KGB
T. cincinnatus	VNIRO	2003.223808	67°07'	41°24'E	20	-	-	-	-	2003	18	KGB
T. cincinnatus	VNIRO	2003.223820	68°08'	39°46'E	8	-	-	-	-	2003	2	KGB
T. cincinnatus	VNIRO	2003.223900	69°29'	32°39'E	12	-	-	-	-	2003	2	KGB
T. cincinnatus	VNIRO	2003.223984	69°28'	32°35'E	9	-	-	-	-	2003	2	KGB

Species	Ship or expedition	Cruise. station or collection number	Latitude N	Longitude	Depth, m	T °C	S‰	Day	Month	Year	Number of specimens	Collection
T. cincinnatus	VNIRO	2003.2231011	67°14'	41°16'E	15	-	-	-	-	2003	2	KGB
T. cincinnatus	n/a	129/33188	75°05'	113°25'E	36	-	-	27	8	1912	2	ZIN
T. cincinnatus	n/a	132/33190	77°21'	107°E	37	-1.2	-	26	8	1913	3	ZIN
T. cincinnatus	n/a	139/33197	75°17'	113°50'E	43	1.5	-	9	9	1912	1	ZIN
T. cincinnatus	n/a	208/33265	71°08'	175°52'W	41	-	-	7	9	1929	1	ZIN
T. cincinnatus	n/a	212/33268	80°47'	89°50'E	52	-	-	31	8	1930	2	ZIN
T. davehalli	Sevastopol	5.1089	62°30'	7°48'W	150	8.78	35.2	16	7	1957	2	KGB
T. davehalli	Sevastopol	5.1091	61°59'	6°07'W	130	8.73	35.3	17	7	1957	5	KGB
T. davehalli	Sevastopol	5.1102	60°35'	0°36'W	135	9.24	35.4	18	7	1957	36	KGB
T. davehalli	Sevastopol	5.1104	60°35'	0°45'E	130	8.16	35.4	18	7	1957	6	KGB
T. davehalli	Sevastopol	5.1105	60°35'	1°21'E	130	7.72	35.4	19	7	1957	1	KGB
T. davehalli	Sevastopol	5.1157	64°56'	24°25'W	155	8.17	35.1	31	7	1957	1	KGB
T. davehalli	Sevastopol	8.1443	62°30'	7°12'W	94	6.38	35.3	11	4	1958	1	KGB
T. davehalli	Sevastopol	8.1453	62°00'	6°14'W	112	6.34	35.2	16	4	1958	207	KGB, MNCN
T. davehalli	Sevastopol	8.1464	60°34'	0°36'W	145	6.2	35.3	17	4	1958	25	KGB
T. davehalli	Sevastopol	8.1465	60°35'	0°01'W	110	6.18	35.3	17	4	1958	1	KGB
T. davehalli	Sevastopol	8.1466	60°35'	0°47'E	128	5.89	35.4	18	4	1958	8	KGB
T. davehalli	Sevastopol	8.1468	60°35'	2°05'E	127	5.91	35.3	18	4	1958	1	KGB
T. davehalli	Sevastopol	8.1490	73°40'	20°34'E	495	1.73	35.1	28	4	1958	1	KGB
T. davehalli	Sevastopol	10.1790	62°32'	7°00'W	100	9.42	35.2	22	10	1958	2	KGB
T. davehalli	Sevastopol	10.1792	62°00'	6°14'W	115	9.47	35.1	24	10	1958	32	KGB
T. davehalli	Sevastopol	10.1801	60°56'	1°34'W	134	10.3	35.4	25	10	1958	1	KGB
T. davehalli	Sevastopol	10.1803	60°35'	0°34'W	140	11.3	35.3	25	10	1958	16	KGB
T. davehalli	Sevastopol	10.1804	60°35'	0°02'E	110	11.1	35.3	26	10	1958	4	KGB
T. davehalli	Sevastopol	10.1805	60°35'	0°35'E	138	9.18	35.4	26	10	1958	13	KGB
T. davehalli	Sevastopol	15.2548	62°30'	7°15'W	95	9.01	35.2	28	11	1959	15	KGB
T. davehalli	Sevastopol	15.2574	60°36'	0°45'E	130	9.22	35.3	10	12	1959	2	KGB
T. davehalli	Sevastopol	15.2587	62°00'	6°12'W	120	8.4	35.2	12	12	1959	43	KGB

Species	Ship or expedition	Cruise. station or collection number	Latitude N	Longitude	Depth, m	T °C	S‰	Day	Month	Year	Number of specimens	Collection
T. davehalli	n/a	DBUA-0000389.01.	40°30'–40°50'	8°40'–9°30'W	101	-	-		7–8	1994	2	Aveiro
T. davehalli	n/a	APEM AD-DGT09	55°49'	0°07'E	79	-	-	17	3	2014	2	KGB
T. davehalli	n/a	16.01/488	Naples		-	-	-	-	-	-	3	MNCN
T. marthae	Sevastopol	15.2512	65°45'	5°00'E	1000	-0.64	34.9	17	11	1959	6	KGB
T. marthae	Alaid	30.3	68°00'	10°00'E	958	-0.79	34.9	13	6	1980	501	KGB, MNCN
T. marthae	Persey	14.860	73°33'	59°53'E	380	-1.64	-	21	9	1927	2	KGB
T. marthae	Sevastopol	5.1068	65°45'	8°01'W	1230	-0.9	-	12	7	1957	2	KGB
T. marthae	Sevastopol	5.1097	61°21'	3°12'W	1275	-0.9	34.9	18	7	1957	6	KGB
T. marthae	Sevastopol	5.1114	63°00'	4°27'E	860	2.8	34.9	20	7	1957	1	KGB
T. marthae	Sevastopol	5.1212	67°39'	22°36'W	650	-0.47	35.0	7	8	1957	44	KGB
T. marthae	Sevastopol	5.1214	67°54'	21°57'W	805	-0.52	34.9	7	8	1957	1	KGB
T. marthae	Sevastopol	5.1216	67°53'	20°15'W	970	-0.32	35.0	7	8	1957	2	KGB
T. marthae	Sevastopol	8.1358	66°27'	6°02'E	770	-0.89	34.9	25	3	1958	2	KGB
T. marthae	Sevastopol	8.1372	69°40'	8°00'W	960	-0.88	34.9	29	3	1958	1	KGB
T. marthae	Sevastopol	8.1383	66°30'	12°40'W	920	-0.9	34.9	31	3	1958	2	KGB
T. marthae	Sevastopol	10.1702	66°38'	4°59'E	1125	-0.94	34.9	27	9	1958	2	KGB
T. marthae	Sevastopol	10.1723	68°34'	14°04'W	1280	-0.81	34.9	2	10	1958	2	KGB
T. marthae	Sevastopol	10.1758	62°44'	2°41'W	890	-0.64	34.9	13	10	1958	1	KGB
T. marthae	Sevastopol	10.1770	67°18'	23°33'W	511	-0.4	35.0	17	10	1958	47	KGB
T. marthae	Sevastopol	10.1772	67°49'	24°40'W	1510	-0.74	35.1	18	10	1958	13	KGB
T. marthae	Sevastopol	15.2457	71°06'	10°21'W	1360	-0.79	34.9	6	11	1959	4	KGB
T. marthae	Sevastopol	15.2549	63°00'	7°30'W	710	-0.2	34.9	4	12	1959	40	KGB
T. marthae	Shmidt	26.2002	80°06'	29°50'E	305	-	-	8	8	1986	1	KGB
T. marthae	SP-22	78.60	73°43'	161°50'W	300	-	-	-	12	1978	26	KGB
T. marthae	SP-22	79.69	74°25'	164°08'W	445	-	-	4	1	1979	10	KGB
T. marthae	SP-22	79.72	74°35'	164°00'W	795	-	-	7	1	1979	5	KGB
T. marthae	SP-22	79.74	74°38'	164°30'W	465	-	-	9	1	1979	11	KGB

Species	Ship or expedition	Cruise. station or collection number	Latitude N	Longitude	Depth, m	T °C	S‰	Day	Month	Year	Number of specimens	Collection
T. marthae	SP-22	79.105	75°11'	170°05'W	315	-	-	27	2	1979	6	KGB
T. marthae	SP-22	79.108	75°13'	170°30'W	370	-	-	4	3	1979	4	KGB
T. marthae	SP-22	79.112	75°14'	171°10'W	455	-	-	10	3	1979	42	KGB
T. marthae	SP-22	79.115	75°02'	171°30'W	382	-	-	16	3	1979	11	KGB
T. marthae	SP-22	79.120	74°54'	171°37'W	330	-	-	24	3	1979	8	KGB
T. marthae	SP-22	79.122	74°55'	171°40'W	345	-	-	26	3	1979	5	KGB
T. marthae	SP-22	79.124	74°55'	171°55'W	355	-	-	1	4	1979	2	KGB
T. marthae	SP-22	79.128	74°53'	172°15'W	332	-	-	10	4	1979	2	KGB
T. marthae	Tunetz	105.6	68°00'	10°00'E	970	-0.96	34.9	15	6	1978	75	KGB
T. marthae	Tunetz	105.16	72°50'	14°00'E	960	-0.96	34.9	30	6	1978	1	KGB
T. marthae	Tunetz	105.21	74°30'	15°55'E	930	-0.3	34.9	6	7	1978	4	KGB
T. marthae	Vichegda	2.22	72°47'	58°51'E	380	-1.84	34.9	12	9	1975	12	KGB
T. marthae	Vichegda	2.30	72°00'	57°00'E	330	-1.8	34.8	16	9	1975	10	KGB
T. marthae	n/a	1/33266	79°08'	78°10'E	95	-	-	18	8	1930	7	ZIN
T. parapari	n/a	16.01/5689	Roquetas de Mar Almería, Andalucía, Spain		2	-	-	-	3	1986	31	MNCN
T. parapari	n/a	16.01/5700			2	-	-	-	7	1986	37	MNCN
T. parapari	n/a	16.01/5704	Cala Uruguay, Almería, Andalucía, Spain		15	-	-	-	7	1986	25	MNCN
T. parapari	n/a	16.01/5706	Playa de los Genoveses, cabo de Gata, Almería, Andalucía, Spain		2	-	-	26	3	1986	57	MNCN
T. parapari	n/a	16.01/5709	Nerja, Málaga, Andalucía, Spain		-	-	-	19	1	1983	1	MNCN
T. parapari	n/a	16.01/5711			-	-	-	28	12	1982	1	MNCN
T. parapari	n/a	16.01/5712			-	-	-	29	12	1983	1	MNCN
T. parapari	n/a	16.01/5713			-	-	-	14	6	1983	1	MNCN
T. parapari	n/a	16.01/5714			-	-	-	27	10	1983	3	MNCN
T. parapari	n/a	16.01/5716	Los Escullos, Almería, Andalucía, Spain		-	-	-	-	10	1984	9	MNCN
T. parapari	n/a	16.01/5717			-	-	-	-	10	1983	11	MNCN
T. triserialis	n/a	2508	39°48'	0°11'30"E	-	-	-	29	04	1996	1	MNCN

of the worm during fixation. I recommend using relative size (assessed by eye), as length depends on muscle retraction during fixation and furthermore worms often are incomplete posteriorly. Maximum size of the largest specimen was estimated for each sample or set of nearby samples as maximum size varies between distant samples, over a species range.

Systematics

Terebellidae Johnston, 1846

Read and Fauchald (2018) is followed in using the family rank Terebellidae rather than Thelepodidae.

Thelepodinae Hessle, 1917

Thelepus Leuckart, 1849

Type species. *Amphitrite cincinnata* Fabricius, 1780.

Diagnosis. Branchiae formed of numerous simple filaments arranged in more or less distinct parallel transverse rows arising from S2–S4; notochaetae from S3 (= BS2), uncini from C3 (= S5); lateral lobes absent.

Remarks. The genus includes 48 species (Hsueh and Li 2016), distributed from the Arctic to the Antarctic and from the littoral to abyssal zones. The most important taxonomic characters used for species separation based on Day (1955), Hutchings and Glasby (1987), and this study are:

The number of branchial segments. The number of BS varies from zero to three; most species have three BS. Only six species currently accepted as valid have two BS. Very little variation in the number of BS was observed; only one specimen amongst more than a thousand of all four species had a third branchia, on one side only. Of course, juveniles may have fewer BS, and some of the very small worms in the examined material had only one BS, or branchiae were absent. The final number of BS seems to appear when the size of the worm is approximately 1% of maximum.

The branchial fields from which the filaments arise. A distinct median gap and lateral extension of the filaments appears to be constant within a species, but in species with numerous filaments both tend to change with size: as the gap becomes narrower, the extension goes further laterally.

The number of branchial filaments. Some species have very few filaments in total, while others have many (10–40 or more). The number of filaments tends to increase with increasing size of the animal. Once adulthood is achieved, there is little variation in the number of filaments, independent of the size of the worms. According to our data, the maximum size of worms varies between localities for the same species, but

the maximum number of filaments is relatively constant within a species. Hutchings and Glasby (1987) suggested that the relative number of branchial filaments between BS2, BS3, and BS4 is more important than the actual number of filaments. However, if there are only a few filaments, variation in their number leads to significant changes in the relative number of branchial filaments and this feature becomes unreliable.

The number of segments with notopodia and notochaetae. There are two groups of species within *Thelepus*: (1) notochaetae present only on the anterior half of the body; there are numerous fully-developed segments without notopodia that differ from notopodial segments only by the absence of notopodia, and (2) species with notochaetae present for most of the body, absent only in the segments clustered near the pygidium. This difference seems to be diagnostic.

The number of rows of uncini. Uncini can be in a single row or form a loop; all of the species investigated have a single row, but *T. nucleolata* Claparède, 1870, described from the Mediterranean (Gulf of Naples) has uncini forming a loop after S14. The species is poorly known and has not been recorded since the original description. The presence or absence of the loop seems to have high taxonomic value.

The shape of the uncinus. The most important features seem to be the shape of the prow, the position of the attachment button, and the arrangement of teeth above the main fang-forming crest. The last character is better seen in SEM photographs, whilst the first two are better observed using a compound microscope. Three of the four investigated species with two BS have very similar U1 uncini, but other species inhabiting European waters, *T. setosus* (Quatrefages, 1866) and *T. triserialis* (Grube, 1855), have very different uncini (Fig. 1B, C). The shape of the uncini may vary along the body; they usually decrease in size but, in *T. parapari* sp. n., the shape also changes. Therefore it is best to examine and compare uncini from a specified unciniger, such as U1; comparison of previously described uncini without detail of the segment of origin has limited value.

Presence/absence of eyespots. Hutchings and Glasby (1987) reported that, in some specimens of *T. plagiostoma* Schmarda, 1861 and *T. robustus* (Grube, 1878), eyespots may be absent. The species examined for this paper either have eyespots or not. Eyespots are sub-epithelial and disappear if the epithelium is macerated due to poor fixation.

Comparative size of notopodia. In some species, the first notopodia are distinctly underdeveloped (for example Fig. 4D), whilst other species have all anterior notopodia of almost equal size. However, this difference may only be apparent in large worms.

Notochaetae. The notochaetae of the four investigated species look very similar. The shape of the notochaetae is of limited taxonomic value, at least for the species examined here.

Tubes. The tubes of all the investigated species are constructed using local material (shell fragments, small stones, spicules etc.) without specificity. Tubes are also attached to larger substrata, usually stones, if possible. Some tubes have a branched crown very similar to that reported for *Axionice conchilega* (Pallas, 1766) by Holthe (1986); this was observed in material examined in this study from the Norwegian Sea.

Key to European *Thelepus*

1	Two BS	**2**
–	Three BS	**6**
2	Uncini in a single row throughout	**3**
–	Uncini after S14 form loop	***T. nucleolata*** **(Claparède, 1870)**
3	Notopodial segments present on 50–66% of body length	***T. davehalli*** **sp. n.**
–	Notopodial segments present on at least 90% of body length	**4**
4	Uncini of TU1 with one tooth above main fang	**5**
–	Uncini of TU1 with two teeth above main fang	***T. parapari*** **sp. n.**
5	Eyespots numerous (may disappear if epithelium is macerated due to poor fixation)	***T. cincinnatus*** **(Fabricius, 1780)**
–	Eyespots absent	***T. marthae*** **sp. n.**
6	Prow of uncinus well developed with a button above (Fig. 1B). Few branchial filaments	***T. triserialis*** **(Grube, 1855)**
–	Prow of uncinus poorly developed (Fig. 1C). Numerous branchial filaments	***T. setosus*** **(Quatrefages, 1866)**

Taxonomic remarks on European species

Species identification is straightforward when examining a series of well preserved, complete specimens. However, single and incomplete specimens (posterior absent) are often encountered. For such specimens, the researcher should initially examine the presence/absence of eyespots and then the sample locality/habitat. This information is usually sufficient for precise identification for comparatively well preserved (fresh) material. A synopsis for all known species of *Thelepus* with two branchiferous segments is given in Table 2.

Thelepus cincinnatus **(Fabricius, 1780), s. str.**
Figs 2, 3, 11, 12

Thelepus cincinnatus: type locality Greenland (probably Frederikshâb), type material probably never designated (Holthe 1986): ? Fauvel 1927: 271–272, fig. 95 i–m; Pettibone 1954: 327–328, fig. 37e, f; Zatsepin 1948: 154, table XXXVIII, 7 (partim); ?Hartmann-Schröder 1996: 528–530, Abb. 258; Holthe 1986: 140–142, fig. 63, map 62 (partim); Jirkov 2001: 526–527 (partim).

Material (Table 1): 413 specimens from 33 stations collected at 8–1350 m, bottom temperature -1.53–7.37 °C. Ten specimens from Alaid station 6 deposited at MNCN: 16.01/17777.

Additional material. *Thelepus antarcticus* ZIN IV.1.2 (5 specimens)

Table 2. Synoptic character data for all known species of the genus *Thelepus* with two branchiferous segments. Abbreviations: n.d. – absence of data.

Species	eyes-pots	Filaments		number of		% body length with notopodia	loop	type locality	source
		BS1	BS2	segments	pairs of notopodia				
T. antarcticus Kinberg, 1866	yes	15	12	ca.100	ca.100	ca.100%	no	Antarctica	Benham (1921); present study
T. cincinnatus (Fabricius, 1780)	yes	<30	<22	ca.100	70–106	ca.100%	no	West Greenland	Pettibone 1954; present study
T. crassibranchiatus Treadwell, 1901	yes	4	2	n.d.	>38	n.d.	n.d.	Puerto Rico	Treadwell (1901); Londoño-Mesa (2009)
T. davehalli sp. n.	no	<20	<10	ca. 100	30–40	1/2–2/3	no	N-E Atlantic shelf	present study
T. hamatus Moore, 1905	yes	5	5	60	32	50%	?	Pacific Alaska	Hilbig (2000)
T. marthae sp. n.	no	<10	<5	ca.100	<65	90%	no	deep Arctic ocean	present study
T. nucleolata (Claparède, 1870)	yes	6	4	n.d.	n.d.	n.d.	yes	Gulf of Naples, Italy	Claparède (1870)
T. pascua (Fauchald, 1977)	no	1	1	n.d.	>=32	n.d.	no	Atlantic Panama	Fauchald (1977); Londoño-Mesa (2009)
T. parapari sp. n.	yes	<11	<8	ca. 70	<56	95%	no	Mediterranean	present study

Description. Largest specimen 140 mm in length and 5 mm in width, although some fragments distinctly larger (up to 7 mm width); maximum size estimated at over 200 mm; larger specimens had been collected at shallow depths, less than 100 m. Number of segments increased with body size; number in investigated specimens: 113.

Buccal tentacles numerous, equal to body length, grooved. Eyespots rounded subepithelial spots, black or dark brown, numerous, usually in several transverse rows on back of upper lip (Fig. 2A, B). Even smallest specimens (<0.5 mm width R/V Sevastopol st. 1769) with numerous eyespots. Specimens from deepest sample (R/V Sevastopol, st. 1580, 1350 m) also with numerous eyespots.

Branchial filaments numerous, long and tangled (Fig. 2A, C–G). Due to tangling it was impossible to count number of branchial filaments in large worms (>5–6 mm width) without removing them one by one. Maximum number of BS1 filaments ca. 20–30, extending laterally to a point level with midpoint or lower edge of row of U1 uncini; outermost filaments usually 2–3 times shorter than those most developed. BS2 with a maximum of 15–20 filaments. One specimen (from Alaid 30.13) had four filaments on BS3 on right hand side of body; length of these was equal to notopodia of same segment. Filaments attached to a transverse elevated stump in 1–2 irregular rows depending on number of filaments. Number of filaments increases with body size;

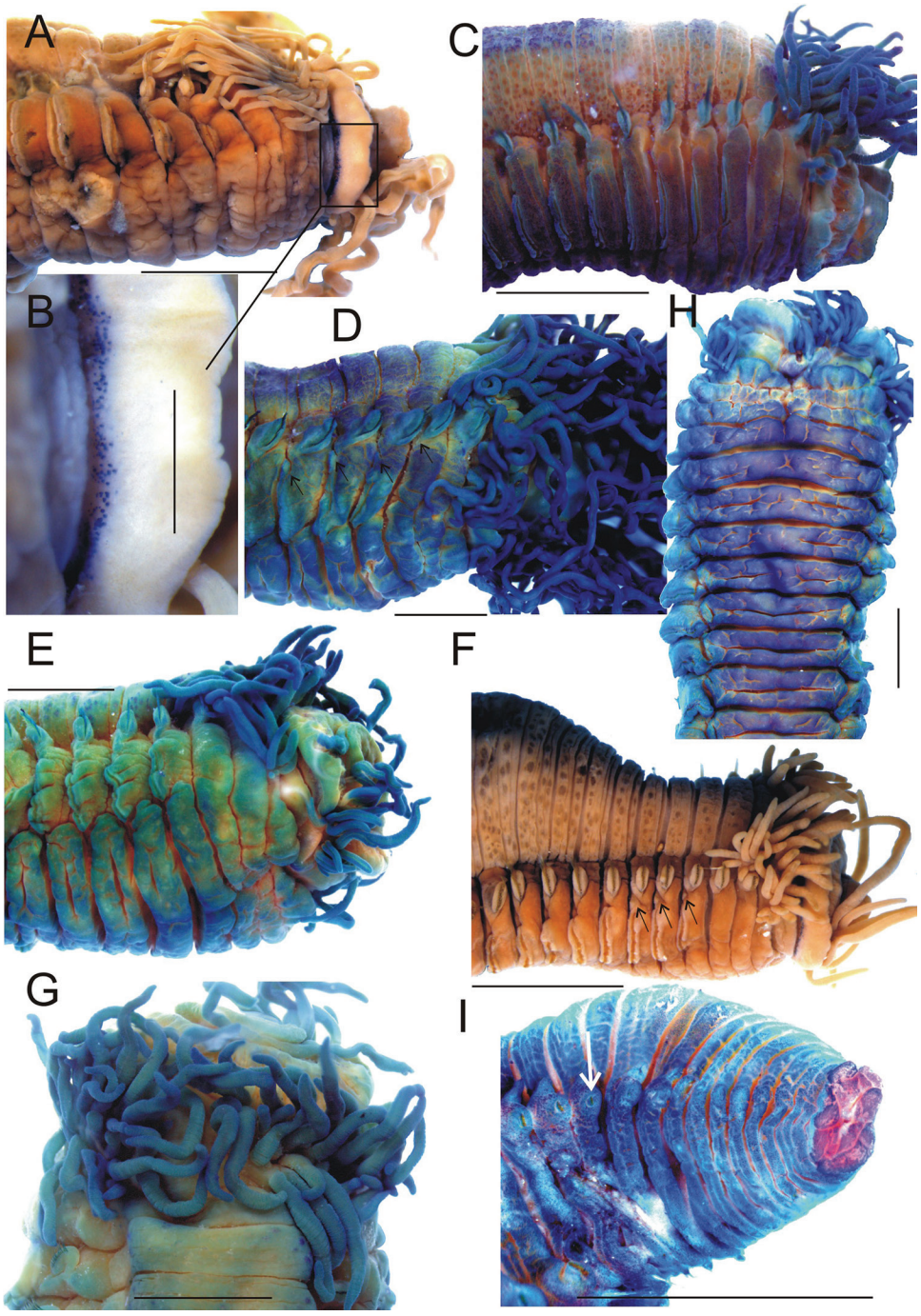

Figure 2. *Thelepus cincinnatus* external morphology. **A, C–I** lateral view of anterior end **B** detail, showing eyespots **G** dorsal view of anterior end **H** ventral view of anterior end **I** lateral view of posterior end (arrow indicates last segment with notochaetae). **A, B, F, I** Alaid st. 30.13 **C** Alaid st. 8 **D, E, H, G** Alaid st. 6. All worms except **A, B, F** stained with methylene blue **D, F** arrow indicates nephridial papillae. Scale bars: 2 mm except **B** 0.5 mm.

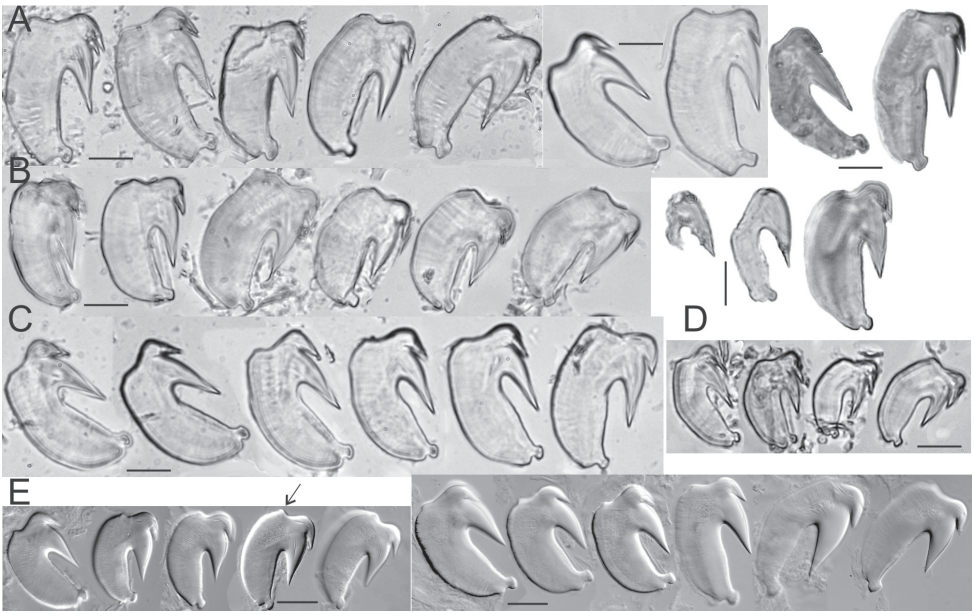

Figure 3. *Thelepus cincinnatus* and *Thelepus antarcticus* uncini. **A** Alaid 30.6 **B** Alaid 30.8 **C, D** Alaid 30.13 **A–C** uncini from U1 **D** uncini from posterior body **E** *Thelepus antarcticus* ZIN IV.1.2, arrow indicating hump, which is different from that in *T. cincinnatus*. Each block from one specimen, all uncini from TU1. Third block of **A** and second block of **B** shows stage of development of uncini. Scale bars: 20 μm.

small worms (1–2 mm width) have fewer than 10 filaments on BS1. Smallest specimen (Sevastopol 1769, width <0.5 mm) with no filaments. Extension of filaments laterally depends upon worm size, with filaments extending only to level of upper margin of uncinal row in small worms. Wide medial gap separating left and right groups of filaments. Lateral lobes absent. Dorsum with warts or subepithelial honeycomb, forming more or less regular rows (Fig. 2C, F); number of rows increases with size of segments and worm. Segmentation distinct. Ventrum glandular, more so with increased "wrinkling" (Fig. 2H). Poorly visible, small nephridial papillae on S4–S7 above neuropodia; those on S5–S7 largest and usually only ones visible (Fig. 2D, F, arrowed).

Notopodia commence from BS2, with anterior notopodia large and transverse. Notopodia raised on body surface or flattened, depending on whether fixation occurs whilst within or outside of tube. Notopodia of BS2 equal to or only slightly smaller than those most developed. Notopodia numerous and present on almost all segments except 10–20 posteriormost developing segments; in investigated material present on up to 106 segments. Last notopodia poorly developed, several times shorter than those most developed and almost without rami, with only a few notochaetae; last neuropodia also reduced (Fig. 2I). Part of worm without notopodia not exceeding 10% of whole body length. Notochaetae in few (ca.10) anterior segments in two transverse rows: posterior row with long chaetae, distal half (winged part) becomes stained with methylene blue, anterior row with short chaetae; other notopodia with a single row of notochaetae. Notochaetae with narrow brims (Fig. 11B).

Neuropodia from C3, tori increasing in size to U10, then becoming progressively shorter. Uncini in a single row with well-developed prow and crest and one tooth in profile (Fig. 3); within a neuropodium main fang develops first, crest develops later (Fig. 3D).

Pygidium with crenulated margin, without cirri or papillae.

Differential diagnosis. Morphologically, *T. cincinnatus* is closest to *T. antarcticus* Kinberg, 1866. The original description of *T. antarcticus* is very brief. The most complete re-description is by Benham (1921). It looks very similar to *T. cincinnatus*; however, I do not believe that it is the same species, since direct comparison of material from the northern and southern hemispheres is necessary to find differences. For the present time it can be stated that, although both species are of equal size (up to 200 mm length and 7 mm in diameter), *T. cincinnatus* has at least twice as many branchial filaments as *T. antarcticus.* The five specimens investigated (length up to 5 cm) have no more than 15 branchial filaments on BS1, distinctly fewer eyespots and slightly different uncini, with a hump (Fig. 3E).

Thelepus cincinnatus differs from other new species described herein as indicated: from *T. davehalli* sp. n. by the presence of eyespots and the absence of numerous completely developed posterior segments without notopodia; from *T. marthae* sp. n. by the absence of eyespots and by the higher number of branchial filaments and segments with notopodia*;* and *T. parapari* sp. n. has a crest of uncini on TU1 with two rows in profile, while *T. cincinnatus* has only one. Other species of *Thelepus* with two pairs of branchiae and eyespots have at least three times fewer branchial filaments and all but *T. parapari* sp. n. have half the number of segments with notopodia (Table 2).

Remarks. The investigated material included almost 2000 specimens (from more than 100 stations) from the high Arctic to the Mediterranean, from depths between 2 m and almost 2 km. The type locality of *T. cincinnatus* is outside the ranges of all investigated species, but *T. cincinnatus* s. str. investigated specimens perfectly agree with the description of topotypes (Pettibone 1954). It is supposed that Pettibone's description is that of the true *T. cincinnatus.*

In some samples, specimens lacked eyespots; however, this is likely to be due to fading because specimens in same samples (with several specimens present) have eyespots, but they are paler, smaller and less numerous than is typical. This fading seems to depend on preservation method: all material with faded eyespots had been stored in formalin for over ten years. The age of samples does not influence fading significantly; although all specimens without eyespots were collected over 50 years ago, other specimens collected a century ago and kept in alcohol had retained eyespots. So absence of eyespots should not be considered to be a characteristic of this species.

Three subspecies (varieties according to original descriptions) of *T. cincinnatus* have been described (Bellan 2008) and, based on the discussion below, none are considered valid.

Thelepus cincinnatus var. *andreanae* McIntosh, 1922. McIntosh wrote "dorsal cephalic collar with eye-specks"; as all other *Thelepus* with two pairs of branchiae from the area near the type locality also lack eyespots, this name should be accepted as a junior synonym of *T. cincinnatus* s. str. as believed by Bellan (2008).

Thelepus cincinnatus var. *canadensis* McIntosh, 1885; has eyespots according to the original description. Type locality: 43°04'N, 64°05'W, 51 fms. Specimens collected near the type locality of this subspecies (R/V "Persey-3" see Table 1) did not show differences from other specimens, confirming Hartman's (1959) acceptance of *T. cincinnatus* var. *canadensis* as a junior synonym of the stem subspecies.

Thelepus cincinnatus var. *profundus* Roule, 1896. The description is too short to be informative: 'Un seul individu, différant du type par sa taille e plus petite, par son tube plus mince et couvert extérieurement d'un enduit peu épais formé de vase grise, et par la forme de ses plaques onciales; ces dernières sont plus étroites, et leurs trois dents plus espacées'. No figures are given so it is impossible to determine which species he was describing and as no type material was deposited in Paris (Solís-Weiss et al. 2004) this subspecies should be treated as a *nomen dubium*.

Other literature reports of *Thelepus cincinnatus* include:

Fauvel (1927) reported for *T. cincinnatus*; "nombreux points oculiformes"; however, most or all the area covered by the "Faune de France" seems to lie outside the range of *T. cincinnatus*, but includes the range of *T. parapari* sp. n. with eyespots, so he probably observed *T. parapari* sp. n.

Zatsepin (1948) and Holthe (1986); despite their descriptions agreeing well with *T. cincinnatus* s. str., they probably observed the other species described here, because these species' ranges fall within those covered by their papers. The same is true for our papers (Jirkov 2001; Jirkov and Leontovich 2013), where we overlooked *T. marthae* sp. n., *T. davehalli* sp. n., and *T. parapari* sp. n. but, in this case, it is supported by re-investigation of the material.

Hartmann-Schröder (1996) reported eyespots for *T. cincinnatus* (Abb. 258), but her figures showed too few branchial filaments and no visible eyespots (they cannot be confirmed or observed in the figure shown). Either the specimen in the figure is too young (there is no scale) or she was studying a different species.

Thelepus davehalli sp. n.

http://zoobank.org/7F969CCC-1770-4B35-9373-2271D9876ACC
Figs 4, 11

Material (Table 1): 444 specimens from 27 stations, collected at depths from 94–495 m, 1.73 °C–11.3 °C. Holotype st. Sevastopol 2587. Material is deposited at the KGB, three paratypes from Sevastopol st.1453 are deposited at the MNCN 16.01/17772. Material from Aveiro (DBUA0000389.01) and Naples (MNCN 16.01/488) is not included in the type series as it was collected too far away from the type locality, despite seeming to be morphologically identical.

Description (based on holotype and paratypes). Holotype with 97 segments, 32 segments with notopodia, 95 mm length. Paratypes up to 100 mm long and 5 mm wide; number of segments increased with body size, up to 91.

Several tens of grooved buccal tentacles as long as half body length. Eyespots absent. Branchial filaments numerous, long and tangled (Fig. 4A, C). Due to tangling,

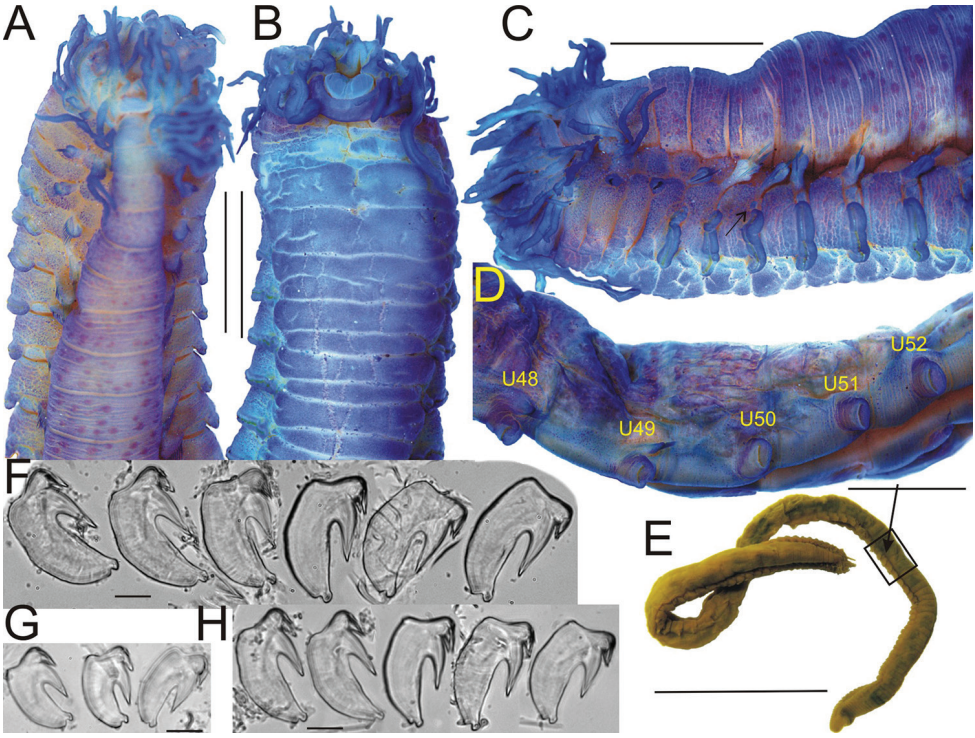

Figure 4. *Thelepus davehalli* sp. n. **A–C** anterior end: **A** dorsal view **B** ventral view **C** lateral view (arrowed nephridial papilla) **D** U48–U52 lateral view **E** – total view, rectangle shows position of **D** (arrow indicates last segment with notochaetae) **F–H** uncini: **F, G** U1 **H** U48, **A–F, H** Sevastopol st. 2587: **A–E** holotype **F, H** paratype **G** APEM 232335. All worms but **E** stained with methylene blue. Scale bars: 2 mm (**A–E**); 20 μm (**F–H**).

it was impossible to count number of branchial filaments in large worms (>5–6 mm width) without removing them one by one. Maximum number of BS1 filaments ca. 20 (13 in holotype), extending laterally to a point level with upper edge of row of U1 uncini. BS2 with ca. ten filaments (nine in holotype). Filaments attached to a transverse elevated stump in 1–2 irregular rows but, due to numerous filaments, there appear to be more rows. Number of filaments increases with body size; small worms (1–2 mm width) with ca. 5 filaments on BS1. Lateral extension of filaments depends upon worm size: in small worms, filaments extend only to a point level with notopodia. Lateral lobes absent. Dorsum with warts or subepithelial honeycomb, forming more or less regular rows (Fig. 4A, C); number of rows increases with size of segments and worms. Segmentation distinct. Nephridial papillae on S5–S7 above neuropodia (Fig. 4C, arrowed), usually poorly visible or not visible; papillae on S4 apparently absent. Ventrum glandular, with "wrinkling" (Fig. 4B) increasing with worm size.

Notopodia from BS2. In small worms, more or less similar, almost cylindrical; in large worms, anterior notopodia transversely flattened, those in first few anterior segments several times smaller than those that are most developed (Fig. 4). Largest speci-

mens in each sample with about 30–40 segments with notopodia, the smallest with fewer, but even specimens ten or more times smaller than largest (by size) with over 30; the next 40–60 segments without notopodia, i.e. about 1/3–1/2 of body length without notopodial segments. Notochaetae with narrow brims (Fig. 11A).

Neuropodia from C3; tori increasing in size to U10, then becoming progressively smaller. Uncini in a single row, uncini of U1 with well-developed prow and crest with one tooth in profile (Fig. 4F, G); posterior uncini (U48) very similar (Fig. 4H).

Pygidium with crenulated margin, without cirri or papillae.

Differential diagnosis. Only one previously known species, *T. pascua* (Fauchald, 1977) from the Atlantic coast of Panama, has two pairs of branchiae and no eyespots. It differs from *T. davehalli* sp. n. in its lower number of branchial filaments: single filament in BS1 and BS2 in *T. pascua*; up to 20 filaments in BS1 and up to 10 filaments in *T. davehalli.* Only one previously known species, *T. hamatus* Moore, 1905 from Pacific Alaska, has two pairs of branchiae and segments of the posterior half of the body without notopodia. It differs from *T. davehalli* in the presence of eyespots and a lower number of branchial filaments: five in BS1 and BS2 in *T. hamatus*; up to 20 filaments in BS1 and up to 10 filaments in *T. davehalli. Thelepus davehalli* differs from the other species described in this paper and other known species with two pairs of branchiae in the presence of fully developed segments without notopodia in the posterior 1/3–1/2 of the body.

The last biramous parapodia of *Thelepus davehalli* is well developed (not reduced), following uniramous parapodia with well-developed neuropodia, contrary to other species described in this study (Fig. 4D, E). Anterior segments lack well-developed notopodia, contrary to those in *T. cincinnatus* and *T. marthae*.

Remark. *Thelepus cincinnatus* var. *andreanae* McIntosh, 1922 was described from within the range of *T. davehalli*. However, McIntosh clearly stated "Dorsal cephalic collar with eye-specks" while this new species has no eyespots.

Etymology. The species is named after my friend Mr. David Hall, Head of Marine and Freshwater Laboratories, Associate Director APEM Ltd., UK (Fig. 5).

Thelepus marthae sp. n.

http://zoobank.org/10A8FCD4-3C8D-4B71-B5C6-341403C7F10E
Figs 6, 7, 11C

Thelepus cincinnatus: Zatsepin 1948: 154, table XXXVIII, 7 (partim); Jirkov 2001: 526–527 (partim) – non Fabricius 1780.

Material (Table 1): 921 specimens from 38 stations collected from depths between 95–1,510 m, bottom temperature -1.84–2.8 °C. Holotype: R/V Tunetz cruise 105 station 6. Material is deposited at the KGB, fifteen paratypes from Alaid st. 6 are deposited at MNCN 16.01/17773, seven paratypes are deposited at ZIN 1/33266.

Description (based on holotype and paratypes)**.** Holotype with 81 segments, 55 segments with notopodia, 55 mm length. Paratypes up to 80 mm in length, 6–7 mm in

Figure 5. David Hall. The photograph was taken by his eldest daughter, Tara Hall.

width, 100 segments, last segments still in formation and clustered, not fully developed, with poorly-developed neuropodia, so not possible to count total number of segments.

Several tens of buccal tentacles, their length in fixed specimens equal to half of body length. Eyespots absent (Fig. 6A–C). BS1 with up to ten filaments (seven in holotype); BS2 with up to five (four in holotype) (Fig. 6F, H). Number of filaments increases with worm size; smallest worms, width <1 mm, with either no branchiae or with 1–2 filaments on BS1 and none on BS2. However, maximum number of filaments constant in different samples (containing sufficient worms) despite a range of maximum worm sizes across the samples. For example, largest worms from sample SP-22 st. 60 are at least three times larger than those from sample Alaid st. 3, but maximum number of filaments observed is same. Branchial filaments of BS1 extend laterally from level of notopodia of C1, to a maximum level with upper margin of uncinal row of U1. Filaments attached in a single row on an elevated stump. A wide medial gap separates left and right groups of filaments. Lateral lobes absent. Barely visible nephridial papillae on S4–S7 above neuropodia (Fig. 6A, B arrowed), in most specimens, few papillae visible, usually none. Ventrum glandular, with "wrinkling" (Fig. 4B) increasing with worm size (Fig. 6G).

Notopodia from S3, anterior notopodia almost cylindrical. Notopodia on C1, often C2, and sometimes C3 two to three times smaller than most developed notopodia (app. C10), sometimes one notopodium on C1 absent (Sevastopol 1358). Most developed notopodia transversally flattened, then reduced in size and become cylindrical again. In the most posterior segments notopodia very small; notochaetae present but several times shorter than most developed ones with no more than 10 per ramus; neuropodia also reduced to small pinnuli with few uncini. Notochaetae absent in 20–40 developing segments near pygidium (Fig. 6E); exact number difficult to determine as both annulation and neuropodia poorly developed. Some specimens also without

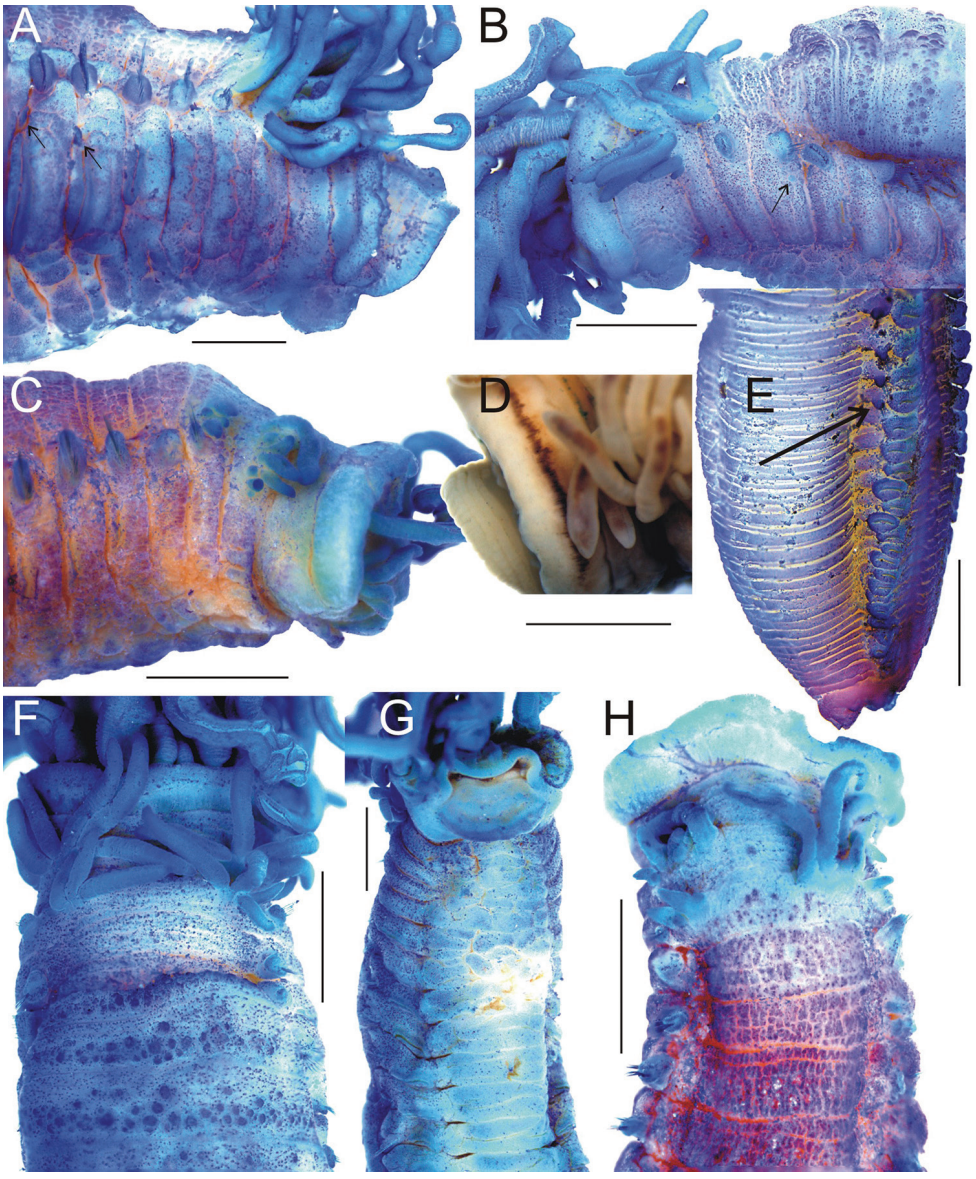

Figure 6. *Thelepus marthae* sp. n. external morphology. **A–C** lateral view of anterior end (arrowed nephridial papillae) **D** detail of anterior end, showing pigmented eyespots **E** lateral view of posterior end (arrowed last segment with notochaetae) **F, H** dorsal view of anterior end **G** ventral view of anterior end. **A** SP-22 st.60 **B, F, G** holotype **C, H** Alaid 30.3 **D, E** SP-22 st. 72. Scale bars: 1 mm. All worms but **D** stained with methylene blue.

notopodia on the 10–20 preceding reasonably well-developed segments. Number of segments with notopodia around 60 (in few complete worms available for this species), with several posterior segments lacking notopodia. However, segments without notopodia form only ca. 10% of the total worm length. Notochaetae of anterior segments

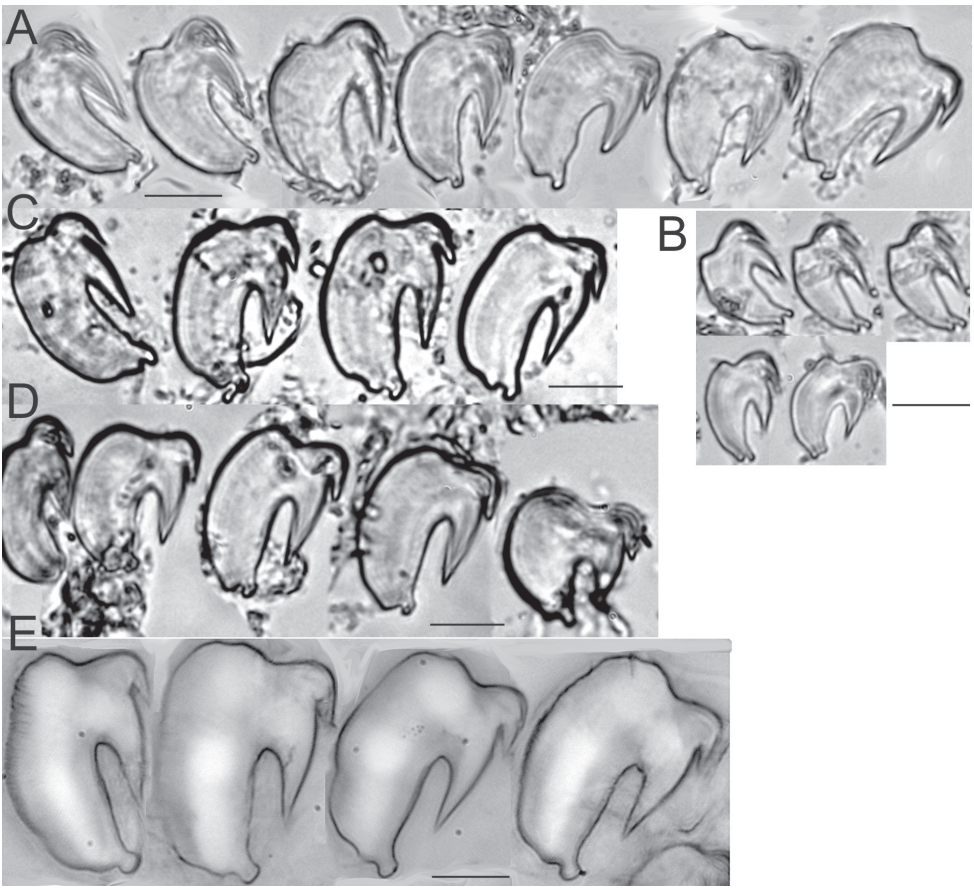

Figure 7. *Thelepus marthae* sp. n. uncini. **A, B** – Tunetz 105.6 **C, D** Alaid 30.3 **E** SP-22 60. **A, C–E** uncini of U1 **B** uncini of U20 from the pygidium. Each block from one specimen. Scale bars: 20 μm.

two to three times longer than notochaetae of posterior segments. Notochaetae in two transverse rows: anterior row with short chaetae, distal half (winged part) becomes stained with methylene blue, posterior row with long chaetae. Notochaetae with narrow brims (Fig. 11C).

Neuropodia from C3; tori increasing in size to U10, then becoming progressively slightly shorter. Uncini in single row. Uncini of U1 with well-developed prow and crest with one tooth in profile (Fig. 7A, C–E), posterior uncini (U20 from pygidium) very similar (Fig. 7B).

Pygidium with crenulated margin without cirri or papillae (Fig. 6E).

Differential diagnosis. Only one previously known species, *T. pascua* (Fauchald, 1977) from the Caribbean coast of Panama, has two pairs of branchiae and no eyespots. It differs from *T. marthae* in the lower number of branchial filaments: single filament in BS1 and BS2 in *T. pascua*; up to 20 filaments in BS1 and up to 10 filaments in *T. marthae. Thelepus marthae* differs from *T. davehalli* (described above) in the

typically observed absence of fully developed segments without notopodia; if present, they form no more than 10% of the body length. *Thelepus marthae* differs from *T. crassibranchiatus* Treadwell, 1901, *T. hamatus* Moore, 1905 and *T. pascua* (Fauchald, 1977) (which have eyespots) in the higher number of branchial filaments and segments with notopodia. *Thelepus marthae* differs from *T. cincinnatus* and *T. antarcticus* in the lower number of branchial filaments and segments with notopodia. *Thelepus marthae* differs from *T. parapari* in the shape of its uncini.

Remark. One specimen (SP-22 st. 72) has numerous spots (Fig. 6D); together forming a transverse row, as with typical eyespots but, in this case, each individual spot is longitudinal instead of rounded as in *T. cincinnatus* (Fig. 2B) and other Terebellidae. These spots are in the same place as eyespots, but their very unusual shape makes their interpretation as eyespots doubtful; other interpretations are possible.

Etymology. Species is named after my friend Dr. Martha K. Leontovich (Fig. 8); she has described several new terebellid species.

Thelepus parapari sp. n.

http://zoobank.org/8B263E58-716A-4994-B773-E360665853B8
Figs 9, 11D

Material (Table 1): 177 specimens from 11 stations collected 26.03.1986 between rhizomes of *Posidonia*, coralligenous formations, calcareous concretions and under stones, 2–15 m, Andalusia, Spain. Holotype MNCN 16.01/17774 (previously part of MNCN 16.01/5706), 5 paratypes previously deposited in MNCN 16.01/5706 now deposited in KGB.

Description (based on holotype and paratypes)**.** Holotype with 58 segments, 50 of them with notopodia, 50 mm length. Paratypes up to 60 mm in length, 2 mm in width, 60–70 segments, posterior segments clustered and developing with poorly-developed neuropodia, so not possible to count total number of segments.

Several tens of buccal tentacles, their length in fixed specimens equal to half of body. Eyespots absent in most specimens (Fig. 9A), only some with reddish eyespots forming a band without dorsal gap (Fig. 9B). Eyespots probably fade during preservation or variation in this character. Preserved body uniformly beige to yellowish, without distinct patterns of pigmentation; one specimen with eyespots with reddish spots around branchiae. BS1 with up to 12 filaments (11 in holotype); BS2 with slightly fewer filaments (eight in holotype; generally, >70% number on BS1). Filaments thin and very long, reaching more than half of corresponding segment's width (Fig. 9A, C). Number of filaments increases as worm grows; smallest observed worms (width <0.5 mm) with 1–2 filaments on BS1 and one on BS2. Branchial filaments of BS1 attach in an irregular row on a slightly elevated stump and extend laterally to a point level with notopodia of C1 or sometimes level with upper margin of uncinal row of C3. Filaments of BS2 do not reach notopodia and usually form two rows. A wide medial gap separates left and right groups of filaments. Lateral lobes absent.

Figure 8. Dr. Martha K. Leontovich. The photograph was taken by the author.

Notopodia commence from S3, almost cylindrical anteriorly; those from C1 onwards of equal size. Posterior notopodia poorly developed (almost no rami), with few notochaetae that are several times shorter than most developed notochaetae; neuropodia also reduced. Notochaetae absent only in developing segments near pygidium, approximately ten such segments, exact number difficult to determine as both annulation and neuropodia poorly developed (Fig. 9D). Characteristic number of segments with notopodia less than 60 (based on few available complete worms). Segments without notopodia from only ca. 5% of total worm length. Relatively distinct (in comparison with species described above), small nephridial papillae on S4–S7, above neuropodia (Fig. 9A). Ventrum glandular, without distinct pads (Fig. 9A, E).

Notochaetae sometimes form two distinct transverse rows: anterior row with short chaetae, posterior row with longer chaetae, distal half (winged part) becomes stained with methylene blue, but usually in one row with mixed short and long chaetae; flanges appear to be wider than in species described above (Fig. 11D).

Neuropodia from C3, tori. Uncini in a single row. Uncini of U1 with two teeth in profile above main fang, unlike three species described above (Fig. 9F). However, posteriorly, uncini have only one tooth in profile, in common with species described above (Fig. 9G).

Pygidium with crenulated margin, without cirri or papillae.

Differential diagnosis. Only one previously known species, *T. pascua* (Fauchald, 1977), from the Caribbean coast of Panama has two pairs of branchiae and no eyespots. It differs from *T. parapari* in the lower number of branchial filaments: single

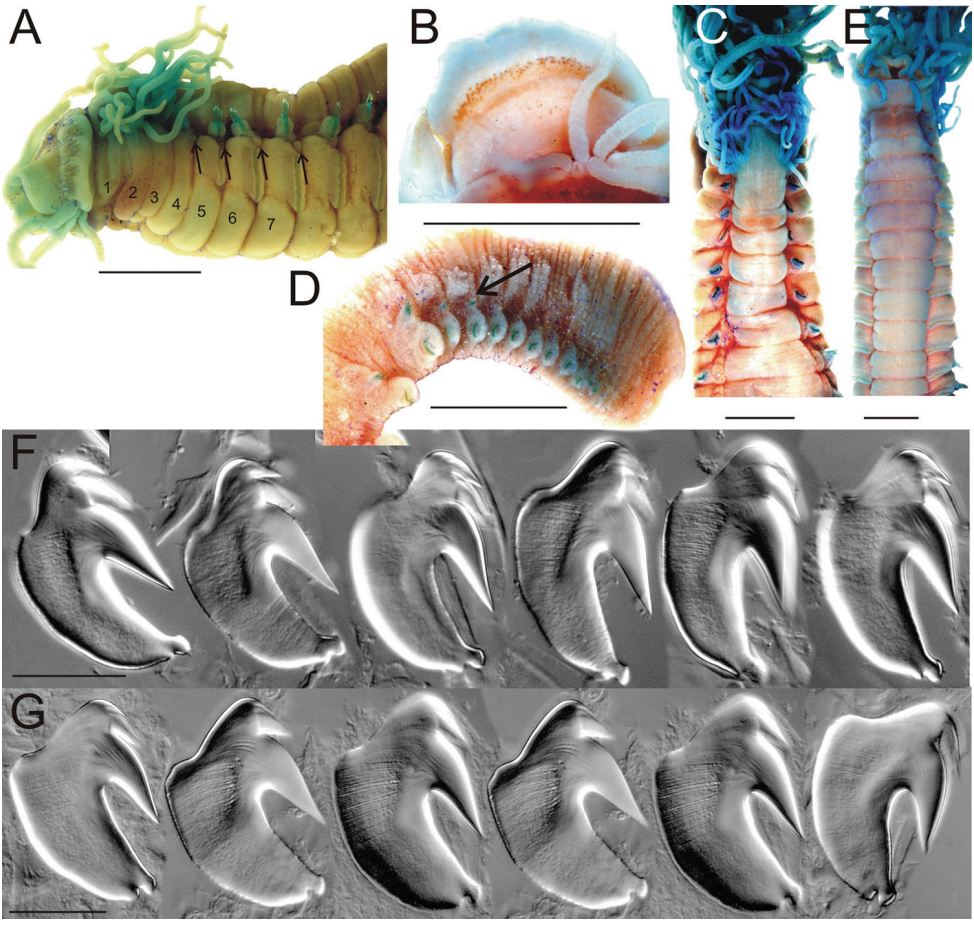

Figure 9. *Thelepus parapari* sp. n. **A** lateral view of anterior end (numbers of S are shown, nephridial papillae arrowed) **B** detail of anterior end, showing pigmented spots **C** dorsal view **D** view of posterior end (arrowed last segment with notochaetae) **E** ventral view **F** U1 uncini **G** U25 uncini. **A, C–E** holotype **B** MNCN 5700 **F–H** MNCN 5706. All worms stained with methylene blue. Scale bars: 1 mm (**A–E**); 20 μm (**F, G**).

filament in BS1 and BS2 in *T. pascua*; up to 11 filaments in BS1 and up to 8 filaments in *T. parapari. Thelepus parapari* differs from *T. davehalli* (described above) in the absence of fully-developed segments without notopodia. *Thelepus parapari* differs from *T. crassibranchiatus* Treadwell, 1901, *T. hamatus* Moore, 1905 and *T. pascua* (Fauchald, 1977) (all of which have eyespots) in the higher number of branchial filaments and segments with notopodia. *Thelepus parapari* differs from *T. cincinnatus* and *T. antarcticus* in the lower number of branchial filaments and segments with notopodia. *Thelepus parapari* differs from *T. cincinnatus* and *T. marthae* (described above) in the shape of the uncini of U1. *Thelepus nucleolata* (Claparède, 1870), as *Heterophenacia nucleolata,* was described from nearby (Gulf of Naples), but *T. parapari* has uncini in a single row, whilst in *T. nucleolata* they form two rows.

Etymology. Species is named after my friend Dr. Julio Parapar, Universidade da Coruña, Spain (Fig. 10).

Figure 10. Dr. Julio Parapar. The photograph was taken by Dr. Juan Moreira.

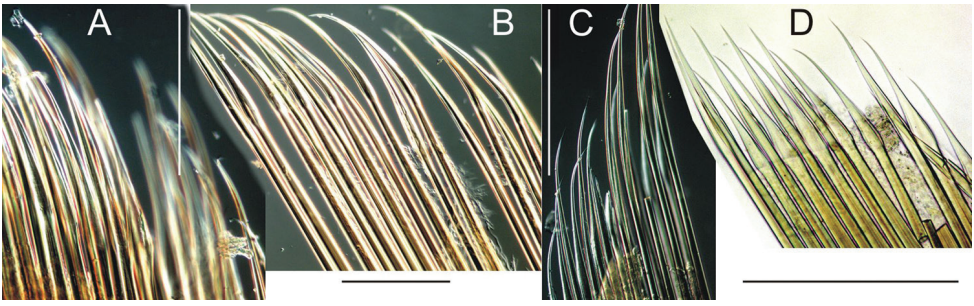

Figure 11. Notochaetae of *Thelepus*. **A** *T. davehalli* **B** *T. cincinnatus* **C** *T. marthae* **D** *T. parapari*. Scale bars: 0.25 mm. **A** Sevastopol 15.2587 C7 **B** Alaid 30.6 C4 **C** Tunetz 105.6 C9 **D** MNCN 5706 C10.

Discussion of species ranges

Species range is a good character to assist with identification. Taxonomically similar species may have different, usually complimentary, ranges and, in this instance, the number of differing ranges is few. Usually, a species' range lies within a limited suite of ecological characters; for example, it is unlikely that the same species inhabits both intertidal and abyssal zones. On first impression, it seems that the ranges of the four species described here overlap (Fig. 12); however, in reality they are complimentary. Obviously *T. cincinnatus* s. str. is not a cosmopolitan species and it is even less widely distributed than previously supposed. Its range is limited to northern boreal and Arctic regions at least to the Chukchi Sea. In the Norwegian and Barents Seas and near Newfoundland, it was found at shelf depths from 8 to 200–400 m; in the North Atlantic south of Iceland, it occurs deeper at least up to 1300 m, so it can be expected south

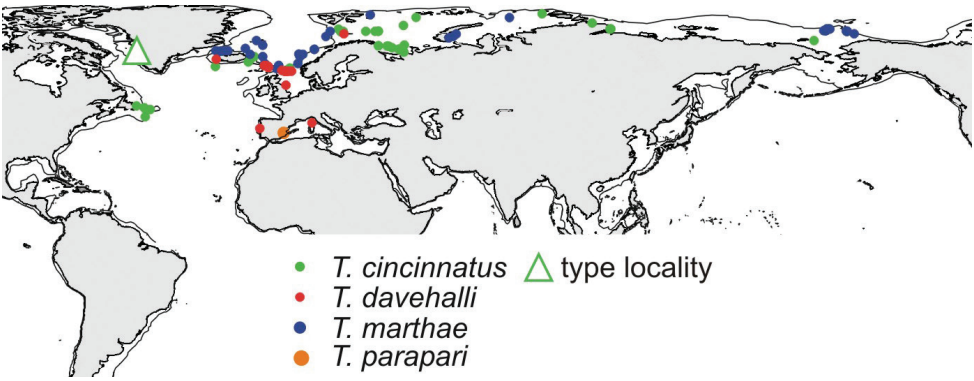

Figure 12. Map showing records of *Thelepus.* 500-m isobath is shown**.**

of Newfoundland at similar depths, in the high Arctic it is limited to shelf. I have not yet studied material from the Pacific Ocean, but as it was found in the Chukchi Sea, *T. cincinnatus* s. str. would be expected to occur in the North Pacific and it was reported by Uschakov (1955), Imajima and Hartman (1964) and Hobson and Banse (1981). Such a range (pers. obs.) is very usual in polychaetes and other benthic taxa. According to this study, at shelf depths to the south, *T. cincinnatus* is replaced by *T. davehalli* and, to the north, by *T. marthae*. *Thelepus marthae* also inhabits the Arctic slope from the Norwegian Sea to the slope of the Chukchi Sea but depth itself is not the limiting factor for the range: *T. marthae* can be found as shallow as 95 m in parts of the shelf nearby the slope. So ranges of *T. cincinnatus* and *T. marthae* are overlapping by depth limits, but not overlapping spatially. The fourth species previously identified as *T. cincinnatus*, *T. parapari,* inhabits upper sublittoral habitats in the Mediterranean (between the tidal front and the shore); in deeper water, below the tidal front, it is replaced by *T. davehalli.*

Of the other *Thelepus* species with two pairs of branchiae, *T. antarcticus* is limited to the Southern Ocean, *T. crassibranchiatus* and *T. pascua* are tropical west Atlantic species; the ranges of these species are significantly geographically removed from those of the species described here. *Thelepus nucleolata* (Claparède, 1870) is described from the shallow Mediterranean and thus is sympatric with *T. parapari. Thelepus hamatus* is reported from Alaska to California (Moore 1906; Hartman 1969; Hilbig 2000) and is sympatric with *T. cincinnatus* at least in British Columbia: *T. cincinnatus* was reported from this province by Berkeley (1968) and it is the type locality of *T. hamatus*, despite not having been listed by Berkeley (1968).

Acknowledgements

The author thanks Prof. V. V. Malachov (Moscow State University) and Dr A. Sazhin (PP Shirshov Institute) for the use of equipment for preparing photographs. Mr D.

J. Hall and Dr. T. M. Worsfold (APEM) for the loan of specimens and access to the APEM collection. Dr Marián Ramos, Principal Researcher of the "Fauna Ibérica XI" project and Dr Javier Sánchez Almazán, Collection Manager at the MNCN, for providing access and assistance in the study of the MNCN collection. Mr D. J. Hall and Dr T. M. Worsfold made edits to the English. Thanks also to The Centre for Environment, Fisheries and Aquaculture Science (Cefas), especially Mr Paul McIlwaine, for providing material and data on *T. davehalli*. Dr. Christopher J. Glasby for his valuable and friendly comments on the manuscript and careful editing.

Financial support

This work was supported by the Russian Science Foundation (grant number 14-50-00029) for studies in Russia and by Fauna Ibérica XI – Polychaeta VI" (Reference: MICINN CGL2010-22267-C07-01) outside of Russia.

References

Bellan G (2008) *Thelepus cincinnatus*. In: Read G, Fauchald K (Eds) (2017) World Polychaeta database. Accessed through: World Register of Marine Species at http://www.marinespecies.org/aphia.php?p=taxdetails&id=131543 [Accessed on 2018-02-08]

Benham WB (1921) *Polychaeta.* Australian Antarctic Expedition 1911–1914, Scientific Reports, Series C - Zoology and Botany 6(3). William Applegate Gullick, government Printer, Sydney, 128 pp.

Berkeley C (1968) A checklist of Polychaeta recorded from British Columbia since 1923, with references to name changes, descriptions, and synonymies. II. Sedentaria. Canadian Journal of Zoology 46: 557–567. https://doi.org/10.1139/z68-073

Claparède E (1870) Les Annélides Chétopodes du Golfe De Naples. Genève et Bale H. Georg, Libraire, 10, Corraterie, Pt. 2, 225 pp.

Day JH (1955) The Polychaeta of South Africa. Part 3. Sedentary species from Cape shores and estuaries. Journal of the Linnean Society of London, Zoology 42(287): 407–452 http://dx.doi.org/10.1111/j.1096-3642.1955.tb02216.x

Fabricius O (1780) Fauna Groenlandica, systematice sistens, Animalia Groenlandiae occidentalis hactenus indagata, quoad nomen specificum, triviale, vernaculumque synonyma auctorum plurium, descriptionem, locum, victum, generationem, mores, usum, capturamque singuli prout detegendi occasio fuit, maximaque parte secundum proprias observationes: Hafniae [Copenhagen] et Lipsiae., Polychaeta & Annelida data, 266–315; 374–384. http://dx.doi.org/10.5962/bhl.title.13489

Fauchald K (1977) Polychaetes from intertidal areas in Panama, with a review of previous shallow-water records. Smithsonian Contributions to Zoology 221: 1–81. https://doi.org/10.5479/si.00810282.221

Fauvel P (1927) Polychètes sédentaires. Addenda aux Errantes. Archiannélides, Myzostomaires. Faune de France 16: 1–404.

Grube AE (1878) Annulata Semperiana. Beiträge zur Kenntniss der Annelidenfauna der Philippinen. Memoires de L'Academie Imperiale des Sciences de St. Petersbourg, Ser. 7, 25(8): 1–300.

Hartman O (1959) Catalogue of the Polychaetous Annelids of the World. Parts 1 and 2. Allan Hancock Foundation Occasional Paper 23: 1–628.

Hartman O (1966) Polychaeta Myzostomidae and Sedentaria of Antarctica. Antarctic Research Series. Vol.7: 1–158. https://doi.org/10.1029/AR007

Hartman O (1969) Atlas of the sedentariate polychaetous annelids from California. Allan Hancock Foundation, University of Southern California, Los Angeles, 812 pp.

Hartmann-Schröder G (1996) Annelida, Borstenwürmer, Polychaeta. 2nd revised ed. The fauna of Germany and adjacent seas with their characteristics and ecology. Vol. 58. Gustav Fischer, Jena, Germany, 648 pp.

Hilbig B (2000) Family Terebellidae Malmgren, 1867. In: Blake JA., Hilbig B, Scott PV (Eds) Taxonomic Atlas of the Benthic Fauna of the Santa Maria Basin and Western Santa Barbara Channel. 7 - The Annelida Part 4. Polychaeta: Flabelligeridae to Sternaspidae. Santa Barbara Museum of Natural History 30: 231–293.

Hobson KD, Banse K (1981) Sedentariate and archiannelid polychaetes of British Columbia and Washington. Canadian Bulletin of Fisheries and Aquatic Sciences, 209, Ottawa, 144 pp.

Holthe T (1986) Polychaeta Terebellomorpha. Marine Invertebrates of Scandinavia 7, Norwegian University Press, 194 pp.

Hsueh P-W, Li K-R (2016) New species of Thelepodidae (Terebelliformia, Polychaeta) from Taiwan. Zootaxa 4170(3): 510–524 http://doi.org/10.11646/zootaxa.4170.3.5

Hutchings PA, Glasby CJ (1987) The Thelepinae (Terebellidae) from Australia, with a discussion of the generic and specific characters of the subfamily. Bulletin of the Biological Society of Washington 7: 217–250.

Imajima M, Hartman O (1964) The Polychaetous Annelids of Japan. Part II. Allan Hancock Foundation Publications Occasional Paper. University of Southern California Press Los Angeles, California. Vol 26: 239–452.

Jirkov IA (2001) [Polychaeta of the Arctic Ocean]. Yanus-K, Moskva, 632 pp. [in Russian]

Jirkov IA, Leontovich MK (2013) Identification keys for Terebellomorpha (Polychaeta) of the Eastern Atlantic and the North Polar Basin. Invertebrate Zoology 10(2): 217–243.

Leuckart R (1849) Zur Kenntnis der Fauna von Island. Erster Beitrag (Würmer). Archiv für Naturgeschichte, Berlin. 15(1): 149–208, plate 3.

Londoño-Mesa MH (2009) Terebellidae (Polychaeta: Terebellida) from the Grand Caribbean region. Zootaxa 2320: 1–93.

McIntosh WC (1885) Report on the Annelida Polychaeta collected by H.M.S. Challenger during the years 1873–1876. Report on the Scientific Results of the Voyage of H.M.S. Challenger during the years 1872–76, Ser. Zoology 12: 1–554.

McIntosh WC (1922) A monograph of the British marine annelids. Polychaeta: Hermellidae to Sabellidae. London, Ray Society 4(1): 1–250.

Moore JP (1906) New species of Ampharetidae and Terebellidae from the North Pacific. Proceedings of the Academy of Natural Sciences of Philadelphia 57: 846–860, plate XLVI.

Nogueira JMM, Hutchings PA, Fukuda MV (2010) Morphology of terebelliform polychaetes (Annelida: Polychaeta: Terebelliformia), with a focus on Terebellidae. Zootaxa 2460: 1–185.

Pettibone MH (1954) Marine polychaete worms from Point Barrow, Alaska, with additional records from the North Atlantic and North Pacific. Proceedings of the United States National Museum 103(3324): 203–356. https://doi.org/10.5479/si.00963801.103-3324.203

Read G, Fauchald K (Eds) (2018) World Polychaeta database. Terebellidae Johnston, 1846. Accessed through: World Register of Marine Species at: http://www.marinespecies.org/aphia.php?p=taxdetails&id=982 [Accessed on 2018-03-01]

Roule L (1896) Annélides. Résultats scientifiques de la campagne du CAUDAN dans le Golfe de Gascogne. Annales de l'Université de Lyon 26: 439–471.

Schmarda LK (1861) Neue Wirbellose Thiere: Beobachted und Gesammelt auf einer Reise um die Erdr 1853 bis 1857. Turbellarien, Rotatorien und Anneliden. Leipzig, Verlag von Wilhelm Engelmann 1(2): 1–164.

Solís-Weiss V, Bertrand Y, Helléouet M-N, Pleijel F (2004) Types of polychaetous annelids at the Muséum national d'Histoire naturelle, Paris. Zoosystema 26(3): 377–384.

Treadwell AL (1901) The Polychaetous annelids of Porto Rico. Bulletin of the United States Fish Commission 20(2): 181–210.

Uschakov PV (1955) Monogoshchetinkovye chervi dal'nevostochnykh morei U.S.S.R. [Polychaeta of the Far Eastern Seas of the USSR]. Izdatel'stvo Akademii Nauk SSSR. Moscow & Leningrad, 445 pp. [in Russian]

Zatsepin VI (1948) [Class Polychaeta]. In: Gayevskaja NS (Ed.) Identification keys for fauna and flora of the USSR northern seas Sovetskaya Nauka, 94–167. [in Russian]

ZooKeys 759: 57–80 (2018)
doi: 10.3897/zookeys.759.24129
http://zookeys.pensoft.net

RESEARCH ARTICLE

A peer-reviewed open-access journal
ZooKeys
Launched to accelerate biodiversity research

A DNA barcode library for ground beetles of Germany: the genus *Amara* Bonelli, 1810 (Insecta, Coleoptera, Carabidae)

Michael J. Raupach[1], Karsten Hannig[2], Jérôme Morinière[3], Lars Hendrich[4]

1 *Institute for Biology and Environmental Sciences, Carl von Ossietzky University Oldenburg, Carl von Ossietzky Straße 9-11, 26111 Oldenburg, Germany* **2** *Bismarckstraße 5, 45731 Waltrop, Germany* **3** *Taxonomic coordinator – German Barcode of Life (GBOL), Bavarian State Collection of Zoology (SNSB – ZSM), Münchhausenstraße 21, 81247 München, Germany* **4** *Sektion Insecta varia, Bavarian State Collection of Zoology (SNSB – ZSM), Münchhausenstraße 21, 81247 München, Germany*

Corresponding author: *Michael J. Raupach* (michael.raupach@rub.de)

Academic editor: *B. Guéorguiev* | Received 31 January 2018 | Accepted 27 March 2018 | Published 17 May 2018

http://zoobank.org/24EFCAD0-DDD7-49DC-9B1C-73860B521108

Citation: Raupach MJ, Hannig K, Morinière J, Hendrich L (2018) A DNA barcode library for ground beetles of Germany: the genus *Amara* Bonelli, 1810 (Insecta, Coleoptera, Carabidae). ZooKeys 759: 57–80. https://doi.org/10.3897/zookeys.759.24129

Abstract

The genus *Amara* Bonelli, 1810 is a very speciose and taxonomically difficult genus of the Carabidae. The identification of many of the species is accomplished with considerable difficulty, in particular for females and immature stages. In this study the effectiveness of DNA barcoding, the most popular method for molecular species identification, was examined to discriminate various species of this genus from Central Europe. DNA barcodes from 690 individuals and 47 species were analysed, including sequences from previous studies and more than 350 newly generated DNA barcodes. Our analysis revealed unique BINs for 38 species (81%). Interspecific K2P distances below 2.2% were found for three species pairs and one species trio, including haplotype sharing between *Amara alpina*/*Amara torrida* and *Amara communis*/*Amara convexior*/*Amara makolskii*. This study represents another step in generating an extensive reference library of DNA barcodes for carabids, highly valuable bioindicators for characterizing disturbances in various habitats.

Keywords

Central Europe, cytochrome *c* oxidase subunit I, German Barcode of Life, mitochondrial DNA, molecular specimen identification, *Zabrus*

Introduction

With the rise of modern sequencing technologies in the early 1990s, DNA sequences have been increasingly used as supplementary markers for species description, identification, and classification (Raupach et al. 2016). In this context, DNA barcoding has become the most popular approach for the assignment of specimens throughout all life stages to described and classified species following the Linnean guidelines (Hebert et al. 2003a, 2003b). In the case of animals, an app. 660 base pair (bp) fragment of the mitochondrial cytochrome *c* oxidase subunit I (COI) gene has been chosen as standardized barcode marker (Hebert et al. 2003a, 2003b). The concept of DNA barcoding is based on a simple assumption: every species will most likely have unique DNA barcodes with low intraspecific variation and interspecific variation that exceeds the variability within species, generating a so-called DNA barcoding gap that highly depends on the studied taxonomic groups (Hebert et al. 2003a, 2003b, Čandek and Kuntner 2015, Koroiva and Kvist 2017). In spite of the fact that various effects can limit the usefulness of DNA barcodes and mitochondrial DNA in general, e.g., the presence of pseudogenes or numts (e.g., Bensasson et al. 2001, Leite 2012, Jordal and Kambestad 2014, Haran et al. 2015), heteroplasmy (e.g., Magnacca and Brown 2010, Robinson et al. 2015), effects of *Wolbachia* infections within terrestrial arthropods (e.g., Hurst and Jiggins 2005, Werren et al. 2008, Smith et al. 2012), or general critics on the concept (e.g., Will and Rubinoff 2004, Collins and Cruickshank 2013), numerous studies have demonstrated that DNA barcoding yields excellent results across a broad range of various animal taxa (e.g., Costa et al. 2007, Aliabadian et al. 2013, Knebelsberger et al. 2014, Lobo et al. 2015, Raupach et al. 2015, Barco et al. 2016). Today, barcode data can be easily managed and analysed using the public Barcode of Life data base (BOLD; www.boldsystems.org; Ratnasingham and Hebert 2007). This core data retrieval interface offers various analytical tools, including the Barcode Index Number (BIN) system (Ratnasingham and Hebert 2013).

In term of arthropods, most DNA barcoding studies focus on insects (Raupach and Radulovici 2015), e.g., the Ephemeroptera, Plecoptera and/or Trichoptera (Zhou et al. 2009, Zhou et al. 2011, Ruiter et al. 2013, Moriniére et al. 2017), Heteroptera (Jung et al. 2011, Park et al. 2011, Raupach et al. 2014), Hymenoptera (Smith and Fisher 2009, Smith et al. 2013, Schmidt et al. 2015), Lepidoptera (e.g., Hajibabaei et al. 2006, Hausmann et al. 2011, Hausmann et al. 2013, Kekkonen et al. 2015), and others (e.g., Glover et al. 2010, Morinière et al. 2014, Hawlitschek et al. 2017). In comparison to the high number of described species, however, the number of studies analysing the Coleoptera (e.g., Greenstone et al. 2011, Woodcock et al. 2013, Pentinsaari et al. 2014, Hendrich et al. 2015, Oba et al. 2015, Rougerie et al. 2015, Han et al. 2016), and in particular the Carabidae or ground beetles (Greenstone et al. 2005, Raupach et al. 2010, 2011, 2016b), is still low.

Ground beetles represent highly valuable and frequently used bioindicators for the characterization of disturbances in various habitats such as forests, meadows, fens, or river banks (e.g., Lövei and Sunderland 1996, Rainio and Niemelä 2003, Koivula 2011, Kotze et al. 2011). Within the Carabidae, *Amara* Bonelli, 1810 is a large genus in the

tribe Zabrini Bonelli, 1810. Many species are Holarctic, but a few are Neotropical or occur in Eastern Asia. About 150 European species are known (Luff 2007), with 52 recorded for Germany (Trautner et al. 2014). Beetles of this genus are typically characterized by their rather oval and parallel-sided form, with females that are often somewhat duller than the males and may even differ in body shape (Luff 2007) (Fig. 1). While ground beetles are mostly carnivorous, numerous *Amara* species feed on plant seeds as both larvae and adults (e.g., Hůrka 1996, Jørgensen and Toft 1997, Holland 2002, Klimeš and Saska 2010), although some species consume seeds only as a supplement to their predominantly predatory diet (e.g., Goldschmid and Toft 1997, Holland 2002, Koprdova et al. 2008). They typically require dry habitats, uncultivated areas and open vegetation on light soils, such as sand, gravel, or chalk (e.g., Kromp 1989, Thomas et al. 2001). As a consequence of their more or less homogenous habitus and very subtle morphological differences between species (e.g., the shape of the pronotum or coloration of antennomeres), *Amara* is known as the most challenging genus of ground beetles in terms of species identification in Central Europe. Nevertheless, Fritz Hieke (1930–2015) devoted his scientific career to this genus and thoroughly cleared up the difficult taxonomic assessment of this genus at all levels (e.g., Hieke 1984, 1988, 2005). In this context he published a list of valid names and their synonyms, with over 560 specific and subspecific, and 47 subgeneric names (Hieke 1995, 2011).

Here we present the next step in building-up a comprehensive DNA barcode library of Central European species of ground beetles as part of the German Barcode of Life project (GBOL), focusing on the genus *Amara*. The analysed barcode library included 46 *Amara* species as well as one species of *Zabrus* Clairville, 1806 which represents the second genus of the tribe Zabrini known from Central Europe. Four species (*Amara littorea* Thomson, 1857, *Amara makolskii* Roubal, 1923, *Amara sabulosa* Audinet-Serville, 1821, and *Amara spectabilis* Schaum, 1858) were not covered by previous studies so far. (Raupach et al. 2010, Pentinsaari et al. 2014, Hendrich et al. 2015). In summary, 358 new barcodes were generated and a total number of 690 DNA barcodes examined.

Material and methods

Sampling of specimens

All new studied beetles were collected between 1997 and 2017 using various sampling methods (e.g., hand collecting, pitfall traps). Beetles were stored in ethanol (96%) and determined by two of the authors (KH, MJR), K.-H. Kielhorn (Berlin, Germany) and F. Köhler (Bonn, Germany) using the keys in Hieke (2006) or Paill (2016). In total, 358 new DNA barcodes of 37 species were generated. Furthermore, 332 DNA barcodes of three previous studies (Raupach et al. 2010: 17 specimens, 5 species; Pentinsaari et al. 2014: 113 specimens, 34 species; Hendrich et al. 2015: 202 specimens, 32 species) were included, generating a data set of 690 DNA barcodes from 47 species in total. Five

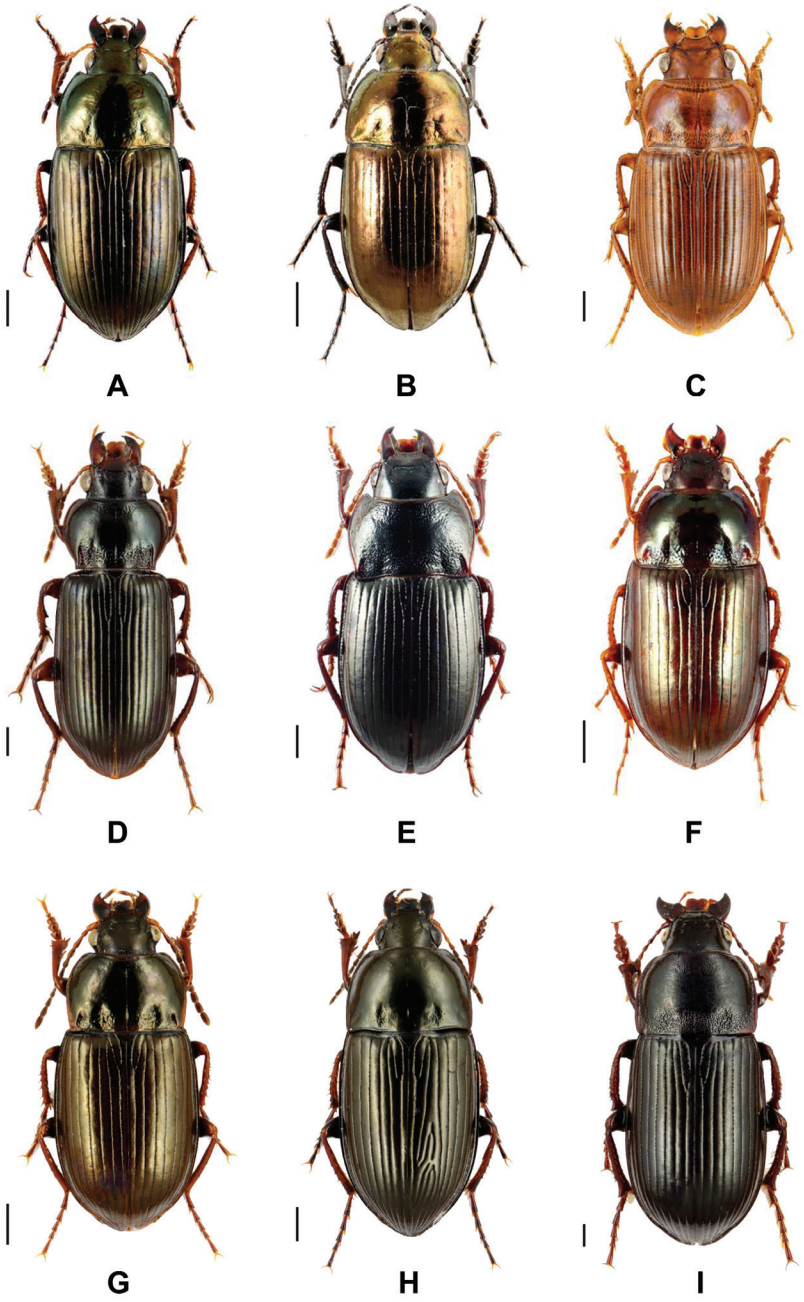

Figure 1. An image collection of some representative species of the analysed ground beetles. **A** *Amara (Amara) similata* (Gyllenhal, 1810) **B** *Amara (Amarocelia) erratica* (Duftschmid, 1812) **C** *Amara (Bradytus) fulva* (Müller, 1776) **D** *Amara (Curtonotus) convexiuscula* (Marsham, 1802) **E** *Amara (Leirides) spectabilis* Schaum, 1858 **F** *Amara (Paracelia) quenseli* (Schönherr, 1806) **G** *Amara (Xenocelia) cursitans* Zimmermann, 1931 **H** *Amara (Zezea) kulti* Fassati, 1947, and **I** *Zabrus tenebrioides* Goeze, 1777. Scale bars 1 mm. All images were obtained from www.eurocarabidae.de.

of the studied species are not known from Germany, including *Amara alpina* (Paykull, 1790) (*n* = 3; collected in Finland, see Pentinsaari et al. 2014), *Amara hyperborea* Dejean, 1831 (*n* = 1; collected in Finland, see Pentinsaari et al. 2014), *Amara interstitialis* Dejean, 1828 (*n* = 1; collected in Finland, see Pentinsaari et al. 2014), *Amara spectabilis* Schaum, 1858 (*n* = 3, collected in Austria), and *Amara torrida* Panzer, 1796 (*n* = 4; collected in Finland, see Pentinsaari et al. 2014). The number of specimens per species ranged from one (6 species) to a maximum of 55 for *Amara aenea* (De Geer, 1774). Most beetles were collected in Germany (*n* = 513, 74.4%), whereas various specimens from other countries were included for comparison: Finland (99, 14.4%), Austria (41, 5.9%), Italy (12, 1.7%), Sweden (7, 1%), Estonia (4, 0.6%), France (4, 0.6%), Czech Republic (3, 0.4%), Denmark (3, 0.4%), Belgium (2, 0.3%), and Slovenia (2, 0.3%).

DNA barcode amplification, sequencing, and data depository

All laboratory operations were carried out, following standardized protocols for COI amplification and sequencing (Ivanova et al. 2006, deWaard et al. 2008), at the Canadian Center for DNA Barcoding (CCDB), University of Guelph, the molecular labs of the Zoologisches Forschungsmuseum Alexander Koenig in Bonn, the German Centre of Marine Biodiversity Research, Senckenberg am Meer, in Wilhelmshaven, or the working group Systematics and Evolutionary Biology at the Carl von Ossietzky University Oldenburg, all in Germany. Photos were taken from each studied beetle before molecular work was performed. One or two legs of one body side were removed for the subsequent DNA extraction which was performed using the QIAmp Tissue Kit (Qiagen GmbH, Hilden, Germany) or NucleoSpin Tissue Kit (Macherey-Nagel, Düren, Germany), following the extraction protocol.

Detailed information about primers used, PCR amplification and sequencing protocols is given in a previous publication (see Raupach et al. 2016b). All purified PCR products were cycle-sequenced and sequenced in both directions at contract sequencing facilities (Macrogen, Seoul, Korea, or GATC, Konstanz, Germany), using the same primers as used in PCR. Double stranded sequences were assembled and checked for mitochondrial pseudogenes (numts) analysing the presence of stop codons, frameshifts as well as double peaks in chromatograms with the Geneious version 7.0.4 program package (Biomatters, Auckland, New Zealand) (Kearse et al. 2012). For verification, BLAST searches (nBLAST, search set: others, program selection: megablast) were performed to confirm the identity of all new sequences as ground beetle sequences based on already published sequences (high identity values, very low E-values) (Zhang et al. 2000, Morgulis et al. 2008).

Comprehensive voucher information, taxonomic classifications, photos, DNA barcode sequences, primer pairs used and trace files (including their quality) are publicly accessible through the public data set "DS-BAAMA" (Dataset ID: dx.doi.org/10.5883/DS-BAAMA) on the Barcode of Life Data Systems (BOLD; www.boldsystems.org) (Ratnasingham and Hebert 2007). Finally, all new barcode data were deposited in GenBank (accession numbers: MH300683–MH300903).

DNA barcode analysis

The analysis tools of the BOLD workbench were employed to calculate the nucleotide composition of the sequences and distributions of Kimura-2-parameter distances (K2P; Kimura 1980) within and between species (align sequences: BOLD aligner; ambiguous base/gap handling: pairwise deletion). All barcode sequences became subject of the Barcode Index Number (BIN) system implemented in BOLD which clusters DNA barcodes in order to produce operational taxonomic units that closely correspond to species (Ratnasingham and Hebert 2013). A threshold of 2.2% was applied for a rough differentiation between intraspecific and interspecific distances based on Ratnasingham and Hebert (2013). It should be noted that the BIN assignments on BOLD are constantly updated as new sequences are added. Therefore, individual BINs can be split or merged in light of new data (Ratnasingham and Hebert 2013).

Furthermore, all sequences were aligned using MUSCLE (Edgar 2004) and analysed using a neighbour-joining cluster analysis (NJ; Saitou and Nei 1987) based on K2P distances with MEGA7.0.21 (Kumar et al. 2016). Non-parametric bootstrap support values were obtained by resampling and analying 1,000 replicates (Felsenstein 1985). It should be explicitly noted that this analysis is not intended to be phylogenetic. Instead of this, the shown topology represents a graphical visualization of DNA barcode divergences and putative species cluster. Finally, statistical maximum parsimony networks were constructed for species pairs with interspecific distances <2.2% with TCS 1.21 based on default settings (Clement et al. 2000) as part of the software package of PopART v.1.7 (Leigh and Bryant 2015). Such networks allow the identification of haplotype sharing between species as a consequence of recent speciation or on-going hybridization processes (e.g., Raupach et al. 2010).

Results

In total, 690 DNA barcode sequences of 47 carabid beetle species were examined. A full list of the species is presented in the supporting information (Suppl. material 1). In total, 46 species of the genus *Amara* were studied, with 41 (79%) of the 52 species documented for Germany. Five analysed species, *Amara alpina* (Paykull, 1790) (n = 3), *Amara hyperborea* Dejean, 1831 (n = 1), *Amara interstitialis* Dejean, 1828 (n = 1), *Amara spectabilis* Schaum, 1858 (n = 3), and *Amara torrida* Panzer, 1796 (n = 4), are not known from Germany. All these specimens were collected from other countries (see above). Fragment lengths ranged from 307 bp (n =14) to a full length of 657 bp. Base frequencies analysis revealed low GC-contents (average: 32%) for the barcode fragment, as it is known from insects and other arthropods. The individual mean nucleotide contents were A = 0.29, C = 0.15, G = 0.17, and T = 0.39. Intraspecific K2P distances ranged from zero to 2.18% (*Amara bifrons* (Gyllenhal, 1810)). Interspecific K2P distances had values between zero and a maximum of 10.06%.

The BIN analyses were performed on January 11th 2018. Unique BINs were revealed for 38 species (81%). Three species pairs shared a BIN: *Amara alpina* Paykull, 1790 and *Amara torrida* (Panzer, 1796) were both included in ACF5385, *Amara familiaris* (Duftschmid, 1812) and *Amara lucida* (Duftschmid, 1812) in AAC4901, and *Amara ovata* (Fabricius, 1792) and *Amara similata* (Gyllenhal, 1820) in AAJ5377. Furthermore, one BIN (ACF1000) contained three species: *Amara communis* (Panzer, 1797), *Amara convexior* Stephens, 1828, and *Amara makolskii* Roubal, 1923 (the so-called *Amara communis* complex). Interspecific distances of zero were found for *Amara alpina* and *Amara torrida* as well as for *Amara communis*, *Amara convexior* and *Amara makolskii*.

The NJ analyses based on K2P distances revealed non-overlapping clusters with bootstrap support values >90% for 33 species (70% of all studied species) with more than one studied specimen (Fig. 2). A comprehensive topology is presented in the supporting information (Suppl. material 2).

Our statistical maximum parsimony analysis revealed closely related haplotypes for *Amara ovata* (Fabricus, 1792) and *Amara similata* (Gyllenhal, 1810) (Fig. 3a). The dominant haplotypes of both species (*Amara ovata*: h1, *Amara similata*: h2) were separated by six mutational steps. An even lower number of mutational steps were found between *Amara familiaris* (Duftschmid, 1812) and *Amara lucida* (Duftschmid, 1812) (Fig. 3b): the only examined specimen of *Amara lucida* (h5) was separated from the dominant haplotype of *Amara familiaris* (h1) by two mutational steps. Furthermore, multiple haplotypes shared by more than one species were found in the *Amara communis* complex (*n* = 49; Fig. 4) and for *Amara alpina* (*n* = 3) with *Amara torrida* (*n* = 4) (Fig. 5). For the *Amara communis* complex, eight different haplotypes with two dominant ones (h1, h2) were identified. Whereas haplotype h1 was shared by 18 specimens with all three species (*Amara communis*: *n* = 6, *Amara convexior*: *n* = 2, *Amara makolskii*: *n* = 10), haplotype h2 was found exclusively in specimens of *Amara convexior* (*n* = 17). Haplotype h3, located between h1 and h2 in the network, was shared by specimens of *Amara communis* (*n* = 8) and *Amara convexior* (*n* = 1). In addition, five haplotypes represented by one specimen only (singletons) were located at the periphery of the network (*Amara communis*: h4, h5, *Amara convexior*: h8, *Amara makolskii*: h6, h7). In the case of *Amara alpina* and *Amara torrida*, the statistical maximum parsimony analysis revealed four haplotypes, with one haplotype (h2) shared by specimens of both species (*Amara alpina*: 2 specimens, *Amara torrida*: 1 specimen). This haplotype was separated by four additional steps from haplotype h1 that was restricted to specimens of *Amara torrida*. Furthermore, two singletons (h3: two additional mutational steps; h4: one additional mutational step) were connected with haplotype h1, generating a compact network that contained only a few mutational steps.

Discussion

Within the past few years, DNA-based approaches have become more and more popular for the assessment of biodiversity and identification of specimens, in particular where

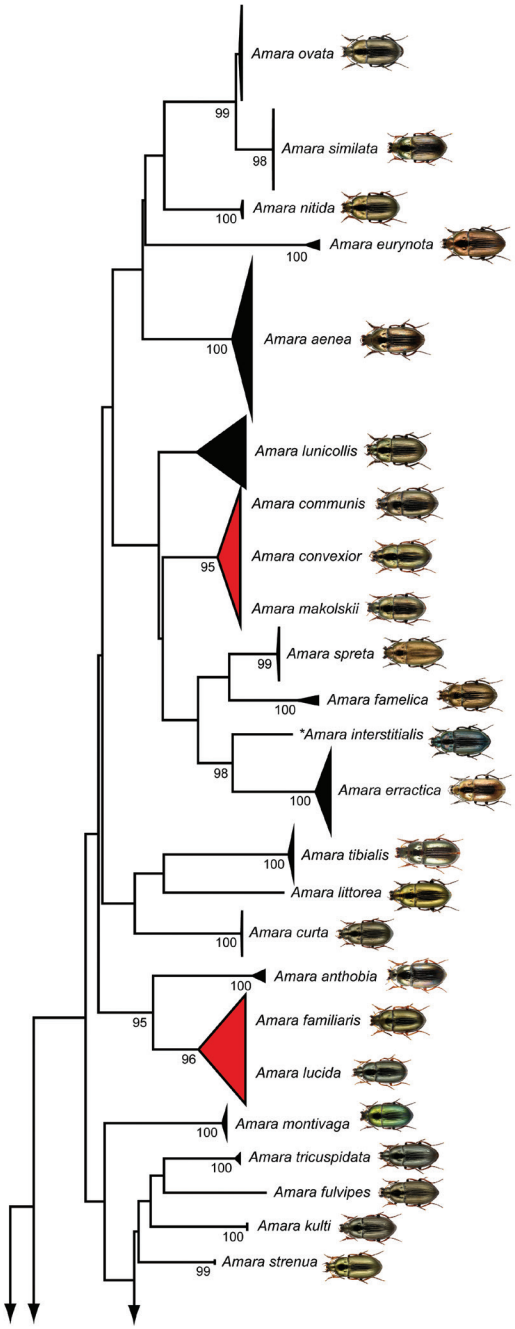

Figure 2. Neighbour-joining topology of the analysed ground beetle species based on Kimura 2-parameter distances. Triangles show the relative number of individual's sampled (height) and sequence divergence (width). Red triangles indicate species pairs with interspecific distances <2.2%. Numbers next to nodes represent non-parametric bootstrap values >90% (1,000 replicates). Asterisks indicate species not recorded in Germany. All images were obtained from www.eurocarabidae.de.

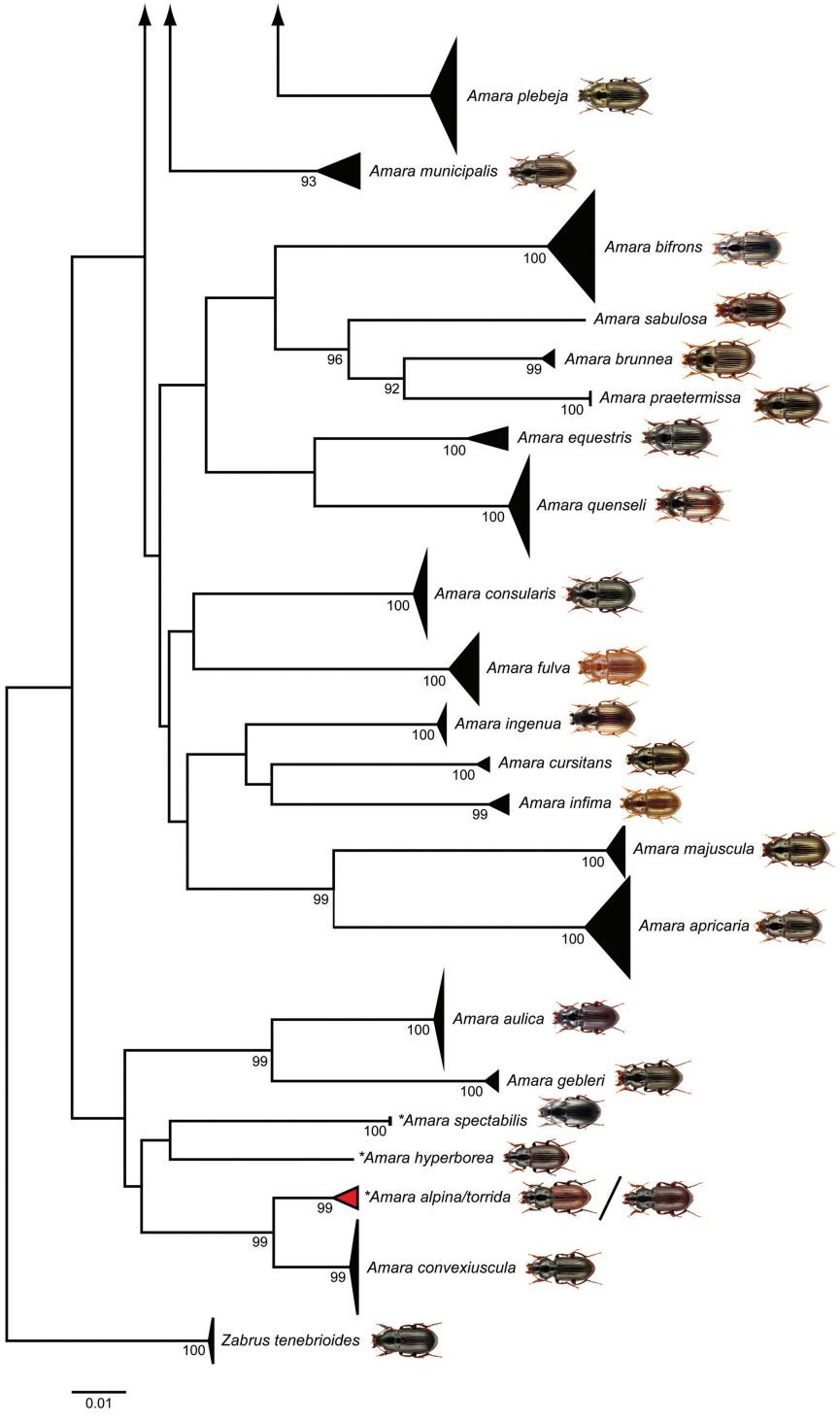

Figure 2. Continue.

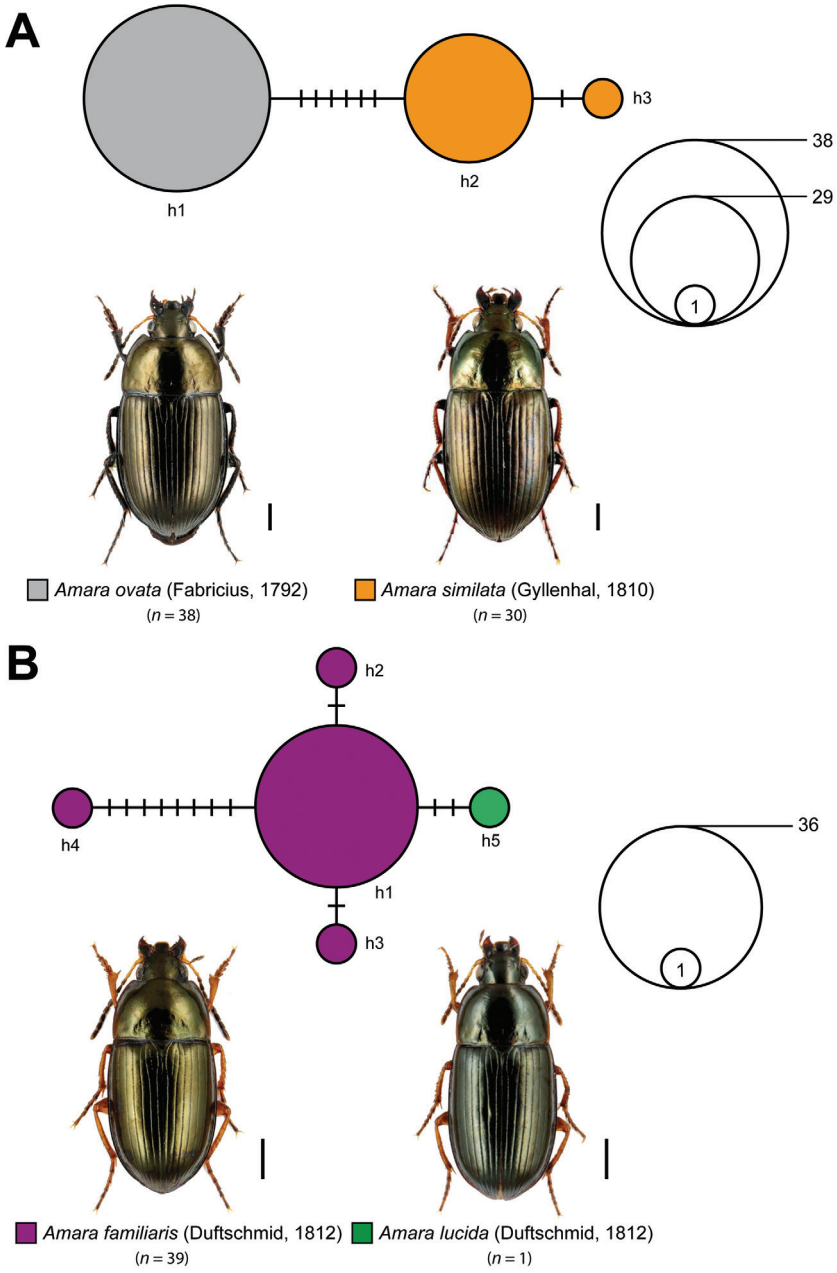

Figure 3. Maximum statistical parsimony networks of two species pairs: **A** *Amara ovata* (Fabricius, 1792) and *Amara similata* (Gyllenhal, 1810), and **B** *Amara familiaris* (Duftschmid, 1812) and *Amara lucida* (Duftschmid, 1812). Used parameters included default settings for connection steps whereas gaps were treated as fifth state. Each line represents a single mutational change whereas small black lines indicate missing haplotypes. The numbers of analysed specimens (*n*) are listed, the diameter of the circles is proportional to the number of haplotypes sampled (see given open half circles with numbers). Scale bars 1 mm. Beetle images were obtained from www.eurocarabidae.de.

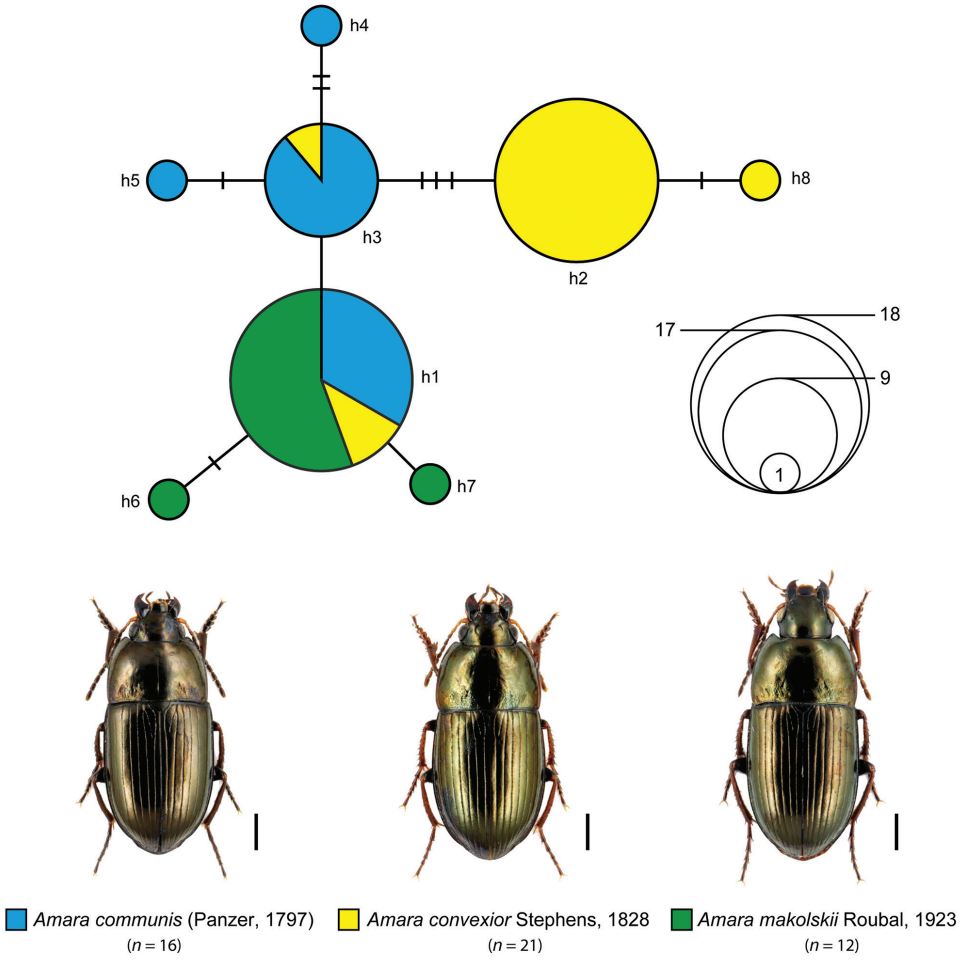

Figure 4. Maximum statistical parsimony network of the *Amara communis* complex. Used parameters included default settings for connection steps whereas gaps were treated as fifth state. Each line represents a single mutational change whereas small black lines indicate missing haplotypes. The numbers of analysed specimens (*n*) are listed, the diameter of the circles is proportional to the number of haplotypes sampled (see given open half circles with numbers). Scale bars 1 mm. Beetle images were obtained from www.eurocarabidae.de.

the traditional morphology-based identification has proved problematic (Taberlet et al. 2012). As a consequence of this development and the rise of new concepts (Hebert et al. 2003a, 2003b), the analysis of single specimens, bulk samples (metabarcoding) or environmental DNA (eDNA) will be performed routinely as part of modern species diversity assessment studies in the near future (e.g., Scheffers et al. 2012, Cristescu 2014, Kress et al. 2015). However, such studies highly rely on comprehensive on-line sequence libraries that act as references (e.g., Brandon-Mong et al. 2015, Creer et al. 2016, Staats et al. 2016). Therefore, our DNA barcode library represents an important

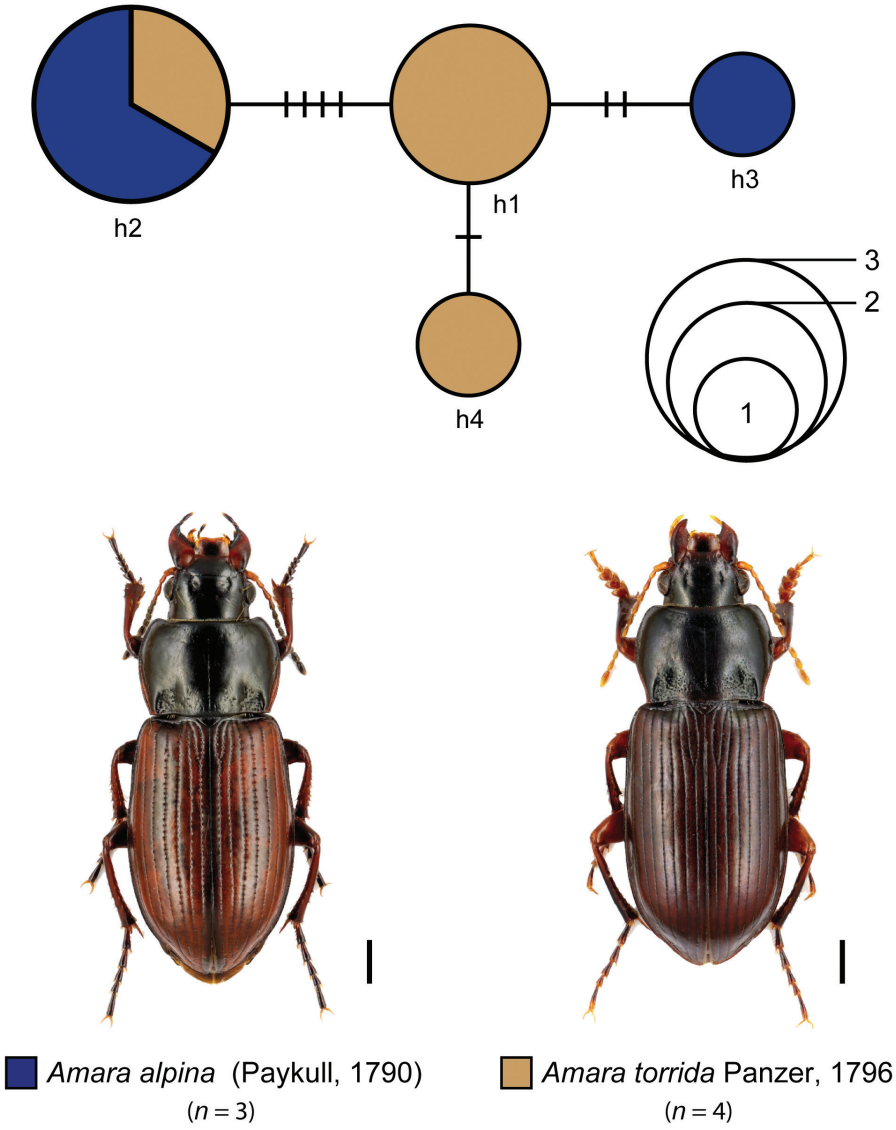

Figure 5. Maximum statistical parsimony network of *Amara alpina* (Paykull, 1790) and *Amara torrida* Panzer, 1796. Used parameters included default settings for connection steps whereas gaps were treated as fifth state. Each line represents a single mutational change whereas small black lines indicate missing haplotypes. The numbers of analysed specimens (*n*) are listed, the diameter of the circles is proportional to the number of haplotypes sampled (see given open half circles with numbers). Scale bars 1 mm. Beetle images were obtained from www.eurocarabidae.de.

step for the molecular characterization of ground beetles in Central Europe and adjacent regions. The current results demonstrate that DNA barcodes distinguish Central European species of the taxonomically challenging genus *Amara* remarkably well. Our

analysis revealed unique BINs for 38 (81%) of the 47 analysed species. The results coincide with high rates of successful species identification of previous barcoding studies on ground beetles (Raupach et al. 2010, 2011, Pentinsaari et al. 2014, Hendrich et al. 2015, Raupach et al. 2016b). In contrast to other carabid genera, e.g., *Bembidion* Latreille, 1802 (Raupach et al. 2016b) or *Calathus* Bonelli, 1810 (Hendrich et al. 2015), no evidence was found for high intraspecific distances (above 2.2%) within the analysed *Amara* species. In contrast to this, low intraspecific distances (below 2.2%) and shared haplotypes for various species pairs were revealed. Such low distances are typically indicative of a recent ancestry and/or ongoing gene flow for various species pairs (e.g., Tautz et al. 2003, Frezal and Leblois 2008, Raupach et al. 2010). We will discuss these cases in more detail.

I. *Amara ovata* (Fabricius, 1792) and *Amara similata* (Gyllenhal, 1810)

Both species are abundant and widespread members of the subgenus *Amara*, with a trans-Palearctic distribution from Europe to Eastern Siberia (e.g., Lindroth 1986, Hůrka 1996, Hieke 2006). Using morphological traits, both species are best separated on the shape of the pronotum (Hieke 1975, Lindroth 1986, Hieke 2006). Nevertheless, a close relationship of both species has been already suggested in the past (e.g., Lindroth 1986, Luff 2007). Our analysis clearly supports this view. In spite of the fact that both species have the same BIN, they form distinct clusters separated by six mutational steps (Fig. 3A). Consequently, all examined specimens can be assigned to both species without doubt. However, it should be noted that the amount of intraspecific variation of DNA barcode sequences (and mitochondrial DNA in general) can correlate with the geographical scale of sampling (e.g., Wiemers and Fiedler 2007, Bergsten et al. 2012 but see Huemer et al. 2014). For this study, all studied specimens were sampled in Europe (*Amara ovata*: 1 specimen from Belgium, 1 from Italy, 6 from Finland, 30 from Germany; *Amara similata*: 3 specimens from Finland, 27 from Germany). Only the analysis of additional beetles from other regions, e.g., Central and Eastern Asia, will show if both species can be identified across their complete distribution ranges without doubt.

II. *Amara familiaris* (Duftschmid, 1812) and *Amara lucida* (Duftschmid, 1812)

Similar to the previous species, *Amara familiaris* and *Amara lucida* are widespread species of the subgenus *Amara* with a Palearctic (*Amara familiaris*) or West Palearctic (*Amara lucida*) distribution (Hůrka 1996, Hieke 2006). From a morphological perspective, both species are very similar, being black with a greenish or brassy metallic reflection (e.g., Luff 2007). However, specimens of *Amara lucida* are somewhat smaller and a little narrower than beetles of *Amara familiaris*, but the only useful morphological traits for species identification are differences within the front angles of the pronotum

(e.g., Lindroth 1986, Hůrka 1996, Hieke 2006). Not surprisingly, the given DNA barcode data confirm the supposed closed relationship (Fig. 3B), but unfortunately only one specimen of *Amara lucida* has been examined so far. More beetles of this species should be studied in detail in the near future in order to validate if two distinct clusters exist or haplotype sharing occurs.

III. The *Amara communis* complex

Within the genus *Amara*, the *Amara communis* complex represents one of the most challenging and controversial group of species in Europe. The complex consists of four very similar and closely related species of the subgenus *Amara*: *Amara communis* (Panzer, 1797), *Amara convexior* Stephens, 1828, *Amara makolskii* Roubal, 1923, and *Amara pulpani* Kult, 1949. All species are characterized by the combination of various morphological traits including the presence of a scutellar stria, deepened and apically widened elytral striae, and the coloration of antennomere 2 and 3 (Hůrka 1996, Hůrka and Rúžičkova 1999, Paill 2016). The specific status of *Amara communis* and *Amara convexior* has been acknowledged for a long time (e.g., Hieke 2006). Both are, similar to other species of this genus, widespread and abundant species with a Palearctic (*Amara communis*) or West Palearctic (*Amara lucida*) distribution (Hůrka 1996, Hieke 2006). In contrast to this, *Amara makolsii* und *Amara pulpani* were considered as synonyms of *Amara communis* (e.g., Lindroth 1986, Hieke 2006, but see Gersdorf and Kuntze 1957, Burakowski 1967). Nevertheless, both species were accepted as valid species some years ago (Hůrka 1996, Löbl and Smetana 2017), but their distribution is still insufficiently documented (e.g., Hůrka 1996, Paill 2003, Schmidt 2004, Schäfer 2005, Gebert 2009, Müller-Kroehling 2013, Trautner et al. 2014). Not surprisingly, the DNA barcode data revealed multiple haplotype sharing between all three studied species, preventing correct species identification (Fig. 4). Unfortunately, DNA barcodes of *Amara pulpani* are currently missing and have to be generated in the future. Nevertheless, we strongly recommend a comprehensive analysis of fast evolving nuclear markers, e.g., microsatellites or SNPs, from specimens of all four species from different localities in order to evaluate if already distinct species exist or hybridization events still take place.

IV. *Amara alpina* Paykull, 1790 and *Amara torrida* (Panzer, 1796)

All data of both species were part of a previous study (Pentinsaari et al. 2014), but not discussed in detail. The two species are part of the subgenus *Curtonotus*, show a widespread circumpolar distribution, and are suggested as closely related (Lindroth 1986). In general, specimens of *Amara alpina* can be separated from *Amara torrida* by the color of the appendages and the pronotal form (Lindroth 1986). Similar to the *Amara communis* complex (see above), haplotype sharing prevents a valid discrimina-

tion of both species by the means of DNA barcoding (Fig. 5). Again, more specimens and other, especially nuclear markers, have to be studied to analyse if *Amara alpina* and *Amara torrida* still hybridize or distinct species exist.

Conclusions

Used alone or in combination with DNA metabarcoding on environmental samples (Taberlet et al. 2012), DNA barcoding is becoming a standard for basic and applied research in ecology, evolution and conservation across taxa, communities and ecosystems (Zinger and Philippe 2016). In this context, our study clearly encourages the use of DNA barcodes for the identification of ground beetles species of the taxonomically difficult genus *Amara*. However, DNA barcodes of additional eleven *Amara* species documented for Germany are currently missing. The analysis of these missing species may include other, so far undetected problematic cases. For example, *Amara chaudoiri* Schaum, 1858 and *Amara concinna* Zimmermann, 1832 are morphologically very similar species. Nevertheless, our data set and results represent another important step in building-up a comprehensive barcode library for the Carabidae in Germany and Central Europe which can be used in modern molecular biodiversity assessment studies. Despite the fact that DNA barcoding failed to deliver a valid species identification for some species in this study, it narrows the options to a pair (or in one case trio) of closely related species. Especially for the almost impossible identification of immature stages and/or females within various species of *Amara*, this is a very encouraging result.

Acknowledgments

We would like to thank Christina Blume, Claudia Etzbauer (both ZFMK, Bonn) and Jana Deppermann (DZMB, Wilhelmshaven) for their laboratory assistance. Furthermore we are very grateful to Karl-Hinrich Kielhorn (Berlin) and Frank Köhler (Bonn) for providing various specimens, and to Ortwin Bleich for giving permission to use his excellent photos of ground beetles taken from www.eurocarabidae.de. We also thank David Kavanaugh, Hongbin Liang, and Mikko Pentisaari for their helpful comments. This publication was partially financed by German Federal Ministry for Education and Research (FKZ01LI1101A, FKZ01LI1101B, FKZ03F0664A), the Land Niedersachsen and the German Science Foundation (INST427/1-1), as well as by grants from the Bavarian State Government (BFB) and the German Federal Ministry of Education and Research (GBOL2: 01LI1101B). We are grateful to the team of Paul Hebert in Guelph (Ontario, Canada) for their great support and help and in particularly to Sujeevan Ratnasingham for developing the BOLD database infrastructure and the BIN management tools. Sequencing work was partly supported by funding from the Government of Canada to Genome Canada through the Ontario Genomics Institute, whereas the Ontario Ministry of Research and Innovation and NSERC supported development of the BOLD informatics platform.

References

Aliabadian M, Beentjes KK, Roselaar CS, van Brandwijk H, Nijman V, Vonk R (2013) DNA barcoding of Dutch birds. ZooKeys 365: 25–48. https://doi.org/10.3897/zookeys.365.6287

Barco A, Raupach MJ, Laakmann S, Neumann H, Knebelsberger T (2016) Identification of North Sea molluscs with DNA barcoding. Molecular Ecology Resources 16: 288–297. https://doi.org/10.1111/1755-0998.12440

Bensasson D, Zhang D-X, Hartl DL, Hewitt GM (2001) Mitochondrial pseudogenes: Evolution`s misplaced witnesses. Trends in Ecology and Evolution 16: 314–321. https://doi.org/10.1016/S0169-5347(01)02151-6

Bergsten J, Bilton DT, Fujisawa T, Elliot M, Monagham MT, Balke M, Hendrich L, Geijer J, Herrmann J, Foster GN, Ribera I, Nilsson AN, Barraclough TG, Vogler AP (2012) The effect of geographical scale of sampling on DNA barcoding. Systematic Biology 61: 851–869. https://doi.org/10.1093/sysbio/sys037

Brandon-Mong GJ, Gan HM, Sing KW, Lee PS, Lim PE, Wilson JJ (2015) DNA metabarcoding of insects and allies: an evaluation of primers and pipelines. Bulletin of Entomological Research 105: 717–727. https://doi.org/10.1017/S0007485315000681

Burakowski B (1967) Biology, ecology and distribution of *Amara pseudocommunis* Burak. (Coleoptera, Carabidae). Annales Zoologici 24: 485–526.

Čandek K, Kuntner M (2015) DNA barcoding gap: reliable species identification over morphological and geographical scales. Molecular Ecology Resources 15: 268–277. https://doi.org/10.1111/1755-0998.12304

Clement M, Posada D, Crandall KA (2000) TCS: a computer program to estimate gene genealogies. Molecular Ecology 9: 1657–1660. https://doi.org/10.1046/j.1365-294x.2000.01020.x

Collins RA, Cruickshank RH (2013) The seven deadly sins of DNA barcoding. Molecular Ecology Resources 13: 969–975. https://doi.org/10.1111/1755-0998.12046

Costa FO, deWaard JR, Boutillier J, Ratnasingham S, Dooh RT, Hajibabaei M, Hebert PDN (2007) Biological identifications through DNA barcodes: the case of the Crustacea. Canadian Journal of Fisheries and Aquatic Sciences 64: 272–295. https://doi.org/10.1139/f07-008

Creer S, Deiner K, Frey S, Porazinska D, Taberlet P, Thomas WK, Potter C, Bik HM (2016) The ecologist`s filed guide to sequence-based identification of biodiversity. Methods in Ecology and Evolution 7: 1008–1018. https://doi.org/10.1111/2041-210X.12574

Cristescu ME (2014) From barcoding single individuals to metabarcoding biological communities: towards an integrative approach to the study of global biodiversity. Trends in Ecology and Evolution 29: 566–571. https://doi.org/10.1016/j.tree.2014.08.001

deWaard JR, Ivanova NV, Hajibabaei M, Hebert PDN (2008) Assembling DNA barcodes: analytical protocols. In: Martin C (Ed.) Methods in Molecular Biology: Environmental Genetics. Humana Press, Totowa, 275–293. https://doi.org/10.1007/978-1-59745-548-0_15

Edgar RC (2004) MUSCLE: a multiple sequence alignment method with reduced time and space complexity. BMC Bioinformatics 5: 113. https://doi.org/10.1186/1471-2105-5-113

Felsenstein J (1985) Confidence limits on phylogenies: an approach using the bootstrap. Evolution 39: 783–791. https://doi.org/10.2307/2408678

Frezal L, Leblois R (2008) Four years of DNA barcoding: Current advances and prospects. Infection, Genetics and Evolution 8: 727–736. https://doi.org/10.1016/j.meegid.2008.05.005

Gebert J (2009) Bemerkungen zum Vorkommen von *Amara (Amara) pulpani* Kult, 1949 in Deutschland – neu für Thüringen, Sachsen und Sachsen-Anhalt (Insecta: Coleoptera: Carabidae). Thüringer Faunistische Abhandlungen XIV: 169–173. [In German]

Gersdorf E, Kuntze K (1957) Bestimmungstabelle der *Amara*-Arten (Col., Car.) Deutschlands. Entomologische Blätter 53: 3–21. [In German]

Glover RH, Collins DW, Walsh K, Boonham N (2010) Assessment of loci for DNA barcoding in the genus *Thrips* (Thysanoptera: Thripidae). Molecular Ecology Resources 10: 51–59. https://doi.org/10.1111/j.1755-0998.2009.02723.x

Goldschmidt H, Toft S (1997) Variable degrees of granivory and phytophagy in insectivorous carabid beetles. Pedobiologia 41: 521–525.

Greenstone MH, Rowley DL, Heimbach U, Lundgren JG, Pfannenstiel RS, Rehner SA (2005) Barcoding generalist predators by polymerase chain reaction: carabids and spiders. Molecular Ecology 14: 3247–3266. https://doi.org/10.1111/j.1365-294X.2005.02628.x

Greenstone MH, Vandenberg NJ, Hu JH (2011) Barcode haplotype variation in North American agroecosystem lady beetles (Coleoptera: Coccinellidae). Molecular Ecology Resources 11: 629–637. https://doi.org/10.1111/j.1755-0998.2011.03007.x

Hajibabaei M, Janzen DH, Burns JM, Hallwachs W, Hebert PDN (2006) DNA barcodes distinguish species of tropical Lepidoptera. Proceedings of the National Academy of Science of the United States of America 103: 968–971. https://doi.org/10.1073/pnas.0510466103

Han T, Lee W, Lee S, Park IG, Park H (2016) Reassessment of species diversity of the subfamily Denticollinae (Coleoptera: Elateridae) through DNA barcoding. Plos One 11: e0148602. https://doi.org/10.1371/journal.pone.0148602

Hausmann A, Haszprunar G, Hebert PDN (2011) DNA barcoding the geometrid fauna of Bavaria (Lepidoptera): successes, surprises, and questions. Plos One 6: e17134. https://doi.org/10.1371/journal.pone.0017134

Hausmann A, Godfray HCJ, Huemer P, Mutanen M, Rougerie R, van Nieukerken EJ, Ratnasingham S, Hebert PDN (2013) Genetic patterns in European Geometrid moths revealed by the Barcode Index Number (BIN) System. Plos One 8: e84518. https://doi.org/10.1371/journal.pone.0084518

Haran J, Koutroumpa F, Magnoux E, Roques A, Roux G (2015) Ghost mtDNA haplotypes generated by fortuitous NUMTs can deeply disturb infra-specific genetic diversity and phylogeographic pattern. Journal of Zoological Systematics and Evolutionary Research 53: 109–115. https://doi.org/10.1111/jzs.12095

Hawlitschek O, Morinière J, Lehmann GUC, Lehmann AW, Kropf M, Dunz A, Glaw F, Detchaeron M, Schmidt S, Hausmann A, Szucsich NU, Caetano-Wyler SA, Haszprunar G (2017) DNA barcoding of crickets, katydids and grasshoppers (Orthoptera) from Central Europe with focus on Austria, Germany and Switzerland. Molecular Ecology Resources 17: 1037–1053. https://doi.org/10.1111/1755-0998.12638

Hebert PDN, Cywinska A, Ball SL, deWaard JR (2003a) Biological identifications through DNA barcodes. Proceedings of the Royal Society of London Series B: Biological Sciences 270: 313–321. https://doi.org/10.1098/rspb.2002.2218

Hebert PDN, Ratnasingham S, deWaard JR (2003b) Barcoding animal life: cytochrome *c* oxidase subunit 1 divergences among closely related species. Proceedings of the Royal Society of London Series B: Biological Sciences 270: S96-S99. https://doi.org/10.1098/rsbl.2003.0025

Hendrich L, Morinière J, Haszprunar G, Hebert PDN, Hausmann A, Köhler F, Balke M (2015) A comprehensive DNA barcode database for Central European beetles with a focus on Germany: Adding more than 3,500 identified species to BOLD. Molecular Ecology Resources 15: 795–818. https://doi.org/10.1111/1755-0998

Hieke F (1975) Beitrag zur Kenntnis der Gattung *Amara* Bon. (Coleoptera, Carabidae). Deutsche Entomologische Zeitschrift 22: 257–342. [In German]

Hieke F (1984) Revision der *Amara*-Untergattung *Leironotus* Ganglbauer, 1891 (Coleoptera, Carabidae). Mitteilungen aus dem Zoologischen Museum Berlin 60: 267–295. [In German]

Hieke F (1988) Neue Arten und neue Synonyme in der Gattung *Amara* Bonelli, 1810 (Copleoptera, Carabidae). Mitteilungen aus dem Zoologischen Museum Berlin 64: 199–268. [In German] https://doi.org/10.1002/mmnz.19970730204

Hieke F (1995) Namesverzeichnis der Gattung *Amara* Bonelli, 1810, Coleoptera, Carabidae. Schwanfelder Coleopterologische Mitteilungen (Schwanfeld), Sonderheft 2: 1–163. [In German]

Hieke (2005) Die *Amara*-Untergattung *Pseudocelia* Lutshnik, 1935 (Insecta: Coleoptera: Carabidae). Veröffentlichungen aus dem Naturkundemuseum Erfurt 24: 147–171. [In German]

Hieke F (2006) Bd. 2, Adephaga 1: Carabidae (Laufkäfer). In: Freude H, Harde KW, Lohse GA, Klausnitzer B (Eds) Die Käfer Mitteleuropas. Spektrum-Verlag, Heidelberg/Berlin, 521 pp. [In German]

Hieke F (2011) Aktueller Katalog der Gattung *Amara* Bonelli, 1810. http://www.naturkundemuseum-berlin.de/home.asp

Holland JM (2002) The Agroecology of Carabid Beetles. Intercept Limited, Andover, 356 pp.

Huemer P, Mutanen M, Sefc KM, Hebert PDN (2014) Testing DNA barcode performance in 1000 species of European Lepidoptera: Large geographic distances have small genetic impacts. Plos One 9: e115774. https://doi.org/10.1371/journal.pone.0115774

Hůrka K (1996) Carabidae of the Czech and Slovak Republics. Kabouek, Zlín, 565 pp.

Hůrka K, Růžičkova A (1999) Classification of the *Amara (Amara) communis* species aggregate based on the egg and larval stage characters (Coleoptera: Carabidae: Amarina). Acta Societatis Zoologicae Bohemicae 63: 451–461.

Hurst GDD, Jiggins FM (2005) Problems with mitochondrial DNA as marker in population, phylogeographic and phylogenetic studies: the effects of inherited symbionts. Proceedings of the Royal Society Series B: Biological Sciences 272: 1525–1534. https://doi.org/10.1098/rspb.2005.3056

Ivanova NV, deWaard JR, Hebert PDN (2006) An inexpensive, automation-friendly protocol for recovering high-quality DNA. Molecular Ecology Notes 6: 998–1002. https://doi.org/10.1111/j.1471-8286.2006.01428.x

Jordal BH, Kambestad M (2014) DNA barcoding of bark and ambrosia beetles reveals excessive NUMTs and consistent east-west divergence across Palearctic forests. Molecular Ecology Resources 14: 7–17. https://doi.org/10.1111/1755-0998.12150

Jørgensen HB, Toft S (1997) Role of granivory and insectivory in the life cycle of the carabid beetle *Amara similata*. Ecological Entomology 22: 7–15. https://doi.org/10.1046/j.1365-2311.1997.00045.x

Jung S, Duwal RK, Lee S (2011) COI barcoding of true bugs (Insecta, Heteroptera). Molecular Ecology Resources 11: 266–270. https://doi.org/10.1111/j.1755-0998.2010.02945.x

Kearse M, Moir R, Wilson A, Sone-Havas S, Cheung M, Sturrock S, Buxton S, Cooper A, Markowitz S, Duran C, Thierer T, Ashton B, Meintjes P, Drummond A (2012) Geneious Basic: an integrated and extendable desktop software platform for the organization and analysis of sequence data. Bioinformatics 15: 1647–1649. https://doi.org/10.1093/bioinformatics/bts199

Kekkonen M, Mutanen M, Kaila L, Nieminen M, Hebert PDN (2015) Delineating species with DNA barcodes: a case of taxon dependent method performances in moths. Plos One 10: e0122481. https://doi.org/10.1371/journal.pone.0122481

Kress WJ, García-Robledo C, Uriarte M, Erickson DL (2015) DNA barcodes for ecology, evolution, and conservation. Trends in Ecology & Evolution 30: 25–35. https://doi.org/10.1016/j.tree.2014.10.008

Kimura M (1980) A simple method for estimating evolutionary rates of base substitutions through comparative studies of nucleotide sequences. Journal of Molecular Evolution 16: 111–120. https://doi.org/10.1007/BF01731581

Klimeš P, Saska P (2010) Larval and adult seed consumption affected by the degree of food specialization in *Amara* (Coleoptera: Carabidae). Journal of Applied Entomology 134: 659–666. https://doi.org/10.1111/j.1439-0418.2009.01463.x

Knebelsberger T, Landi M, Neumann H, Kloppmann M, Sell A, Campbell P, Laakmann S, Raupach MJ, Carvalho G, Costa FO (2014) A reliable DNA barcode reference library for the identification of the European shelf fish fauna. Molecular Ecology Resources 14: 1060–1071. https://doi.org/10.1111/1755-0998.12238

Koivula MJ (2011) Useful model organisms, indicators, or both? Ground beetles (Coleoptera, Carabidae) reflecting environmental conditions. ZooKeys 100: 287–317. https://doi.org/10.3897/zookeys.100.1533

Koprdova S, Saska P, Soukup J (2008) The spectrum of invertebrate seed predators that contribute to the control of the rape volunteer seeds (*Brassica napus* L.). Journal of Plant Diseases and Protection 21: 261–264.

Koroiva R, Kvist S (2017) Estimating the barcoding gap in a global dataset of *cox1* sequences for Odonata: close, but no cigar. Mitochondrial DNA Part A: DNA Mapping, Sequencing, and Analysis July 28: 1–7. https://doi.org/10.1080/24701394.2017.1357709

Kotze DJ, Brandmayr P, Casale A, Dauffy-Richard E, Dekoninck W, Koivula MJ, Lövei GL, Mossakowski D, Noordijk J, Paarmann W, Pizzolotto R, Saska P, Schwerk A, Serrano J, Szyszko J, Taboada A, Turin H, Venn S, Vermeulen R, Zetto T (2011) Forty years of carabid beetle research in Europe – from taxonomy, biology, ecology and population studies to bioindication, habitat assessment and conservation. ZooKeys 100: 55–148. https://doi.org/10.3897/zookeys.100.1523

Kromp B (1989) Carabid beetle communities (Carabidae, Coleoptera) in biologically and conventionally farmed agroecosystems. Agriculture, Ecosystems and Environment 27: 241–251. https://doi.org/10.1016/0167-8809(89)90089-3

Kumar S, Stecher G, Tamura K (2016) MEGA7: Molecular Evolutionary Genetics Analysis version 7.0 for bigger datasets. Molecular Biology and Evolution 33: 1870–1874. https://doi.org/10.1093/molbev/msw054

Leigh JW, Bryant D (2015) POPART: Fullfeature software for haplotype network construction. Methods in Ecology and Evolution 6: 1110–1116. https://doi.org/10.1111/2041-210X.12410

Leite LAR (2012) Mitochondrial pseudogenes in insect DNA barcoding: differing points of view on the same issue. Biota Neotropica 12: 301–308. http://dx.doi.org/10.1590/S1676-06032012000300029

Lindroth CH (1986) The Carabidae (Coleoptera) of Fennoscandia and Denmark. Fauna Entomologica Scandinavica 15 part 2: 233–497.

Löbl I, Smetana A (2017) Catalogue of Palaearctic Coleoptera, Vol. 1, Archostemata – Myxophaga – Adephaga, Revised and Updated edition. Koninklijke Brill NV, Leiden, 1443 pp.

Lobo J, Teixeira MAL, Borges LMS, Ferreira M, Hollatz C, Gomes PT, Sousa R, Ravara A, Costa MH, Costa FO (2015) Starting a DNA barcode reference library for shallow water polychaetes from the European Atlantic coast. Molecular Ecology Resources 16: 298–313. https://doi.org/10.1111/1755-0998.12441

Lövei GL, Sunderland KD (1996) Ecology and behavior of ground beetles (Coleoptera: Carabidae). Annual Review in Entomology 41: 231–256. https://doi.org/10.1146/annurev.en.41.010196.001311

Luff ML (2007) The Carabidae (ground beetles) of Britain and Ireland (2nd edition). Handbooks for the Identification of British Insects Vol. 4 Part 2. Field Studies Council, Shrewsbury, 247 pp.

Magnacca KN, Brown MJF (2010) Mitochondrial heteroplasmy and DNA barcoding in Hawaiian *Hylaeus* (*Nesoprosopis*) bees (Hymenoptera: Colletidae). BMC Evolutionary Biology 10: 174. https://doi.org/10.1186/1471-2148-10-174

Morgulis M, Coulouris G, Rayselis Y, Madden TL, Agarwala R, Schäffer AA (2008) Database indexing for production MegaBLAST searches. Bioinformatics 24: 1757–1764. https://doi.org/10.1093/bioinformatics/btn322

Morinière J, Hendrich L, Hausmann A, Hebert PDN, Haszprunar G, Gruppe A (2014) Barcoding Fauna Bavarica: 78% of the Neuropteroida fauna barcoded! Plos One 9: e109719. https://doi.org/10.1371/journal.pone.0109719

Morinière J, Hendrich L, Balke M, Beermann AJ, König T, Hess M, Koch S, Müller R, Leese F, Hebert PDN, Hausmann A, Schubart CD, Haszprunar G (2017) A DNA barcode library for Germany`s mayflies, stoneflies and caddisflies (Ephemeroptera, Plecoptera and Trichoptera). Molecular Ecology Resources 17: 1293–1307. https://doi.org/10.1111/1755-0998.12683

Müller-Kroehling S (2013) Zum Vorkommen der bisher meist verkannten *Amara pulpani* Kult 1949 und *Amara makolskii* Roubal 1923 in Wäldern Bayerns. Angewandte Carabidologie 10: 35–40. [In German]

Oba Y, Ôhira H, Murase Y, Moriyama A, Kumazawa Y (2015) DNA barcoding of Japanese click beetles (Coleoptera, Elateridae). Plos One 10: e0116612. https://doi.org/10.1371/journal.pone.0116612

Paill W (2003) *Amara pulpani* Kult, 1949 – eine valide Art in den Alpen. Revue Suisse de Zoologie 110: 437–452. [In German]

Paill W (2016) Österreichische Erstnachweise von *Amara makolskii* Roubal, 1923 und ein Bestimmungsschlüssel der *Amara communis*-Gruppe (Coleoptera, Carabidae, Zabrini). Entomologische Blätter und Coleoptera 112: 275–286. [In German]

Park D-S, Footit RG, Maw E, Hebert PDN (2011) Barcoding bugs: DNA-based identification of the true bugs (Insecta: Hemiptera: Heteroptera). Plos One 6: e18749. https://doi.org/10.1371/journal.pone.0018749.

Pentinsaari M, Hebert PDN, Mutanen M (2014) Barcoding beetles: a regional survey of 1872 species reveals high identification success and unusually deep interspecific divergences. Plos One 9: e108651. https://doi.org/10.1371/journal.pone.0108651

Rainio J, Niemelä J (2003) Ground beetles (Coleoptera: Carabidae) as bioindicators. Biodiversity and Conservation 12: 487–506. https://doi.org/10.1023/A:1022412617568

Ratnasingham S, Hebert PDN (2007) BOLD: The Barcode of Life Data Systems. Molecular Ecology Notes 7: 355–364. https://doi.org/10.1111/j.1471-8286.2007.01678.x

Ratnasingham S, Hebert PDN (2013) A DNA-based registry for all animal species: the Barcode Index Number (BIN) system. Plos One 8: e66213. https://doi.org/10.1371/journal.pone.0066213

Raupach MJ, Astrin JJ, Hannig K, Peters MK, Stoeckle MY, Wägele JW (2010) Molecular species identifications of Central European ground beetles (Coleoptera: Carabidae) using nuclear rDNA expansion segments and DNA barcodes. Frontiers in Zoology 7: 26. https://doi.org/10.1186/1742-9994-7-26

Raupach MJ, Hannig K, Wägele JW (2011) Identification of Central European ground beetles of the genus *Bembidion* (Coleoptera: Carabidae) using DNA barcodes: a case study of selected species. Angewandte Carabidologie 9: 63–72.

Raupach M, Hendrich L, Küchler SM, Deister F, Morinière J, Gossner MM (2014) Building-up of a DNA barcode library for true bugs (Insecta: Hemiptera: Heteroptera) of Germany reveals taxonomic uncertainties and surprises. Plos One 9: e106940. https://doi.org/10.1371/journal.pone.0106940

Raupach MJ, Barco A, Steinke D, Beermann J, Laakmann S, Mohrbeck I, Neumann H, Kihara TC, Pointner K, Radulovici A, Segelken-Voigt A, Weese C, Knebelsberger T (2015) The application of DNA barcodes for the identification of marine crustaceans from the North Sea and adjacent regions. Plos One 10: e0139421. https://doi.org/10.1371/journal.pone.0139421

Raupach M, Radulovici A (2015) Looking back on a decade of barcoding crustaceans. ZooKeys 539: 53–81. https://doi.org/10.3897/zookeys.539.6530

Raupach MJ, Amann R, Wheeler QD, Roos C (2016a) The application of "-omics" technologies for the classification and identification of animals. Organisms, Diversity & Evolution 16: 1–12. https://doi.org/10.1007/s13127-015-0234-6

Raupach MJ, Hannig K, Morinière J, Hendrich L (2016b) A DNA barcode library for ground beetles (Insecta, Coleoptera, Carabidae) of Germany: The genus *Bembidion* Latreille, 1802 and allied taxa. ZooKeys 592: 121–141. https://doi.org/10.3897/zookeys.592.8316

Robinson GA, Balvin O, Schal C, Vargo EL, Booth W (2015) Extensive mitochondrial heteroplasmy in natural populations of a resurging human pest, the bed big (Hemiptera: Cimicidae). Journal of Medical Entomology 52: 734–738. https://doi.org/10.1093/jme/tjv055

Rougerie R, Lopez-Vaamonde C, Barnouin T, Delnatte J, Moulin N, Noblecourt T, Nusillard B, Parmain G, Soldati F, Bouget C (2015) PASSIFOR: A reference library of DNA barcodes for French saproxylic beetles (Insecta, Coleoptera). Biodiversity Data Journal 3: e4078. https://doi.org/10.3897/BDJ.3.e4078

Ruiter DE, Boyle EE, Zhou X (2013) DNA barcoding facilitates associations and diagnoses for Trichoptera larvae of the Churchill (Manitoba, Canada) area. BMC Ecology 13: 5. https://doi.org/10.1186/1472-6785-13-5

Saitou N, Nei M (1987) The neighbor-joining method: a new method for reconstructing phylogenetic trees. Molecular Biology and Evolution 4: 406–425.

Schäfer P (2005) Ein aktueller Nachweis von *Amara pulpani* Kult, 1949 (Col., Carabidae) aus Westfalen. Entomologische Nachrichten und Berichte 49: 226–227. [In German]

Scheffers BR, Joppa LN, Pimm SL, Laurance WF (2012) What we know and don't know about Earth's missing biodiversity. Trends in Ecology & Evolution 27: 501–510. https://doi.org/10.1016/j.tree.2012.05.008

Schmidt J (2004) *Amara pulpani* Kult, 1949 und *Amara nitida* Sturm, 1825 (Col., Carabidae) kommen auch an der deutschen Ostseeküste vor. Entomologische Nachrichten und Berichte 48: 43–45. [In German]

Schmidt S, Schmid-Egger C, Morinière J, Haszprunar G, Hebert PDN (2015) DNA barcoding largely supports 250 years of classical taxonomy: identifications for Central European bees (Hymenoptera, Apoidea *partim*). Molecular Ecology Resources 15: 985–1000. https://doi.org/10.1111/1755-0998

Smith MA, Fisher BL (2009) Invasions, DNA barcodes, and rapid biodiversity assessment using the ants of Mauritius. Frontiers in Zoology 6: 31. https://doi.org/10.1186/1742-9994-6-31

Smith MA, Bertrand C, Crosby K, Eveleigh ES, Fernandez-Triana J, Fisher BL, Gibbs J, Hajibabaei M, Hallwachs W, Hind K, Hrcek J, Huang D-W, Janda M, Janzen DH, Li Y, Miller SE, Packer L, Quicke D, Ratnasingham S, Rodriguez J, Rougerie R, Shaw MR, Sheffield C, Stahlhut JK, Steinke D, Whitfield J, Wood M, Zhou X (2012) *Wolbachia* and DNA barcoding insects: Patterns, potential, and problems. Plos One 7: e36514. https://doi.org/10.1371/journal.pone.0036514

Smith MA, Fernández-Triana JL, Eveleigh E, Gómez J, Guclu C, Hallwachs W, Hebert PDN, Hrcek J, Huber JT, Janzen D, Mason PG, Miller S, Quicke DLJ, Rodriguez JJ, Rougerie R, Shaw MR, Várkonyi G, Ward DF, Whitfield JB, Zaldívar-Riverón A (2013) DNA barcoding and the taxonomy of Microgastrinae wasps (Hymenoptera, Braconidae): impacts after 8 years and nearly 20 000 sequences. Molecular Ecology Resources 13: 168–176. https://doi.org/10.1111/1755-0998.12038

Staats M, Arulandhu AJ, Gravendeel B, Horst-Jensen A, Scholtens I, Peelen T, Prins TW, Kok E (2016) Advances in DNA metabarcoding for food and wildlife forensic species identification. Analytical and Bioanalytical Chemistry 408: 4615–4630. https://doi.org/10.1007/s00216-016-9595-8

Taberlet P, Coissac E, Pompanon F, Brochmann C, Willerslev E (2012) Towards next-generation biodiversity assessment using DNA metabarcoding. Molecular Ecology 21: 2045–2050. https://doi.org/10.1111/j.1365-294X.2012.05470.x

Tautz D, Arctander P, Minelli A, Thomas RH, Vogler AP (2003) A plea for DNA taxonomy. Trends in Ecology and Evolution 18: 70–74. https://doi.org/10.1016/S0169-5347(02)00041-1

Thomas CFG, Parkinson L, Griffiths GJK, Fernandez Garcia A, Marshall EJP (2001) Aggregation and temporal stability of carabid beetle distributions in field and hedgerow habitats. Journal of Applied Ecology 38: 100–116. https://doi.org/10.1046/j.1365-2664.2001.00574.x

Trautner J, Fritze M-A, Hannig K, Kaiser M (2014) Distribution Atlas of Ground Beetles in Germany. Books on Demand, Norderstedt, 348 pp.

Werren JH, Baldo L, Clark ME (2008) *Wolbachia*: master manipulators of invertebrate biology. Nature Reviews 6: 741–751. https://doi.org/10.1038/nrmicro1969

Wiemers M, Fiedler K (2007) Does the DNA barcoding gap exist? – a case study in blue butterflies (Lepidoptera: Lycaenidae). Frontiers in Zoology 4: 8. https://doi.org/10.1186/1742-9994-4-8

Will KW, Rubinoff D (2004) Myth of the molecule: DNA barcodes for species cannot replace morphology for identification and classification. Cladistics 20: 47–55. https://doi.org/10.1111/j.1096-0031.2003.00008.x

Woodcock TS, Boyle EE, Roughley RE, Kevan PG, Labbee RN, Smith ABT, Goulet H, Steinke D, Adamowicz SJ (2013) The diversity and biogeography of the Coleoptera of Churchill: insights from DNA barcoding. BMC Ecology 13: 40. https://doi.org/10.1186/1472-6785-13-40

Zhang Z, Schwartz S, Wagner L, Miller W (2000) A greedy algorithm for aligning DNA sequences. Journal of Computational Biology 7: 203–214. https://doi.org/10.1089/10665270050081478

Zhou X, Adamowicz SJ, Jacobus LM, deWalt RE, Hebert PDN (2009) Towards a comprehensive barcode library for arctic life – Ephemeroptera, Plecoptera, and Trichoptera of Churchill, Manitoba, Canada. Frontiers in Zoology 6: 30. https://doi.org/10.1186/1742-9994-6-30

Zhou X, Robinson JL, Geraci CJ, Parker CR, Flint Jr OS, Etnier DA, Ruiter D, DeWalt RE, Jacobus LM, Hebert PDN (2011) Accelerated construction of a regional DNA-barcode reference library: caddisflies (Trichoptera) in the Great Smoky Mountains National Park. Journal of the North American Benthological Society 30: 131–162. http://dx.doi.org/10.1899/10-010.1

Zinger L, Philippe H (2016) Coalescing molecular evolution and DNA barcoding. Molecular Ecology 25: 1908–1910. https://doi.org/10.1111/mec.13639

Supplementary material 1

Barcode analysis using the BOLD workbench

Authors: Michael J. Raupach, Karsten Hannig, Jérôme Morinière, Lars Hendrich

Data type: Data table.

Explanation note: Molecular distances based on the Kimura 2-parameter model of the analysed specimens of the studied species of the genera *Amara* and *Zabrus*. Divergence values were calculated for all studied sequences, using the Nearest Neighbour Summary implemented in the Barcode Gap Analysis tool provided by the Barcode of Life Data System (BOLD). Align sequencing option: BOLD aligner (amino acid based HMM), ambiguous base/gap handling: pairwise deletion. ISD = intraspecific distance. BINs are based on the barcode analysis from 15-01-2018. Asterisks indicate species not recorded from Germany. Species pairs with interspecific distances <2.2% are marked in bold.

Link: https://doi.org/10.3897/zookeys.@@.24169.suppl1

Supplementary material 2

Neighbour-joining topology

Authors: Michael J. Raupach, Karsten Hannig, Jérôme Morinière, Lars Hendrich

Data type: Neighbour-joining topology.

Explanation note: Neighbour-joining phylogram of all analysed ground beetle specimen based on Kimura 2-parameter distances. Individuals are classified using ID numbers from BOLD and species name. Numbers next to nodes represent non-parametric bootstrap values (1,000 replicates, in %).

Link: https://doi.org/10.3897/zookeys.@@.24169.suppl2

ZooKeys 759: 81–97 (2018)
doi: 10.3897/zookeys.759.15149
http://zookeys.pensoft.net

RESEARCH ARTICLE

A peer-reviewed open-access journal
ZooKeys
Launched to accelerate biodiversity research

Mapping the expansion of coyotes (*Canis latrans*) across North and Central America

James W. Hody[1], Roland Kays[1,2]

1 *North Carolina State University, Department of Forestry and Environmental Resources, 2800 Faucette Drive, Raleigh, NC, USA 27607* **2** *North Carolina Museum of Natural Sciences, Nature Research Center, 9 West Jones Street, Raleigh, NC, USA 27601*

Corresponding author: *Roland Kays* (rwkays@ncsu.edu)

Academic editor: *E. Eizirik* | Received 21 July 2017 | Accepted 30 March 2018 | Published 22 May 2018

http://zoobank.org/2D6125FB-10FA-435F-A431-A4B3ECE78836

Citation: Hody JW, Kays R (2018) Mapping the expansion of coyotes (*Canis latrans*) across North and Central America. ZooKeys 759: 81–97. https://doi.org/10.3897/zookeys.759.15149

Abstract

The geographic distribution of coyotes (*Canis latrans*) has dramatically expanded since 1900, spreading across much of North America in a period when most other mammal species have been declining. Although this considerable expansion has been well documented at the state/provincial scale, continent-wide descriptions of coyote spread have portrayed conflicting distributions for coyotes prior to the 1900s, with popularly referenced anecdotal accounts showing them restricted to the great plains, and more obscure, but data-rich accounts suggesting they ranged across the arid west. To provide a scientifically credible map of the coyote's historical range (10,000–300 BP) and describe their range expansion from 1900 to 2016, we synthesized archaeological and fossil records, museum specimens, peer-reviewed reports, and records from wildlife management agencies. Museum specimens confirm that coyotes have been present in the arid west and California throughout the Holocene, well before European colonization. Their range in the late 1800s was undistinguishable from earlier periods, and matched the distribution of non-forest habitat in the region. Coyote expansion began around 1900 as they moved north into taiga forests, east into deciduous forests, west into costal temperate rain forests, and south into tropical rainforests. Forest fragmentation and the extirpation of larger predators probably enabled these expansions. In addition, hybridization with wolves (*C. lupus*, *C. lycaon*, and/or *C. rufus*) and/or domestic dogs has been documented in the east, and suspected in the south. Our detailed account of the original range of coyotes and their subsequent expansion provides the core description of a large scale ecological experiment that can help us better understand the predator-prey interactions, as well as evolution through hybridization.

Keywords
coyote, *Canis latrans*, range expansion, museum records, FAUNMAP, VertNet, historical ecology, Holocene

Introduction

During the past century, coyotes have undergone a dramatic range expansion across much of North and Central America. Previously restricted to the western two-thirds of North America, the species now occurs across most of the continent, from the Atlantic to the Pacific seaboard and from Alaska to Panama (Macdonald and Sillero-Zubiri 2004). Despite widespread management as a pest species (Andelt 1987, Knowlton et al. 1999), coyotes have nevertheless expanded their geographic range by an estimated 40% since the 1950s, at least twice as much any other North American carnivore during the same time period (Laliberte and Ripple 2004).

Various interacting factors are thought to have contributed to coyotes' rapid expansion in North America. First, extirpation of apex predators likely helped coyotes expand by reducing predation risk and allowing coyotes to expand their niche to larger prey. Specifically, the extirpation of wolves (*C. lupus*, *C. rufus*, and/or *C. lycaon*) and cougar (*Puma concolor*) across most of eastern North America, and the decline of cougar and jaguar (*Panthera onca*) in Central America probably set the stage for coyote colonization (Bekoff and Gese 2003, Berger and Gese 2007, Cove et al. 2012, Méndez-Carvajal and Moreno 2014). Second, conversion of once-forested landscapes to agricultural landscapes in eastern North America and Central America likely facilitated coyote expansion by creating suitable coyote habitat in areas that were previously unsuitable (Vaughan 1983, Parker 1995, Macdonald and Sillero-Zubiri 2004). The expansion of coyotes into western Canada and Alaska has been attributed to the creation of new human settlements during gold rushes in the late 1880s (Gier 1975, Moore and Parker 1992), although this explanation has not been critically tested. Additionally, hybridization of coyotes with wolves and domestic dogs in eastern North America introduced new genotypes that may have promoted colonization and survival in eastern habitats (Kays et al. 2010, VonHoldt et al. 2011, Thornton and Murray 2014). Coyotes expanding into the southeastern United States likewise bear evidence of introgression from dogs (Adams et al. 2003). There is currently no evidence of coyote hybridization with dogs or wolves in the northwestern flank of their expansion, but coyotes moving into Central America are suspected to be hybridizing with dogs based on morphological characters (Cove et al. 2012, Hody 2016).

This ongoing range expansion poses an excellent case study in community ecology and acclimation or adaptation in the Anthropocene, and also presents a new challenge for conservation, as the ecological implications of spreading coyotes are still largely unknown. Coyotes may represent a new top predator in eastern North America and other parts of the continent, with cascading effects on predator communities and disease dynamics (Gompper 2002, Levi et al. 2012). Likewise, the recent arrival of coyotes in Panama may position them to colonize South America, with unknown implications for tropical ecosystems (Hidalgo-Mihart et al. 2004, Méndez-Carvajal and Moreno 2014,

Hody 2016). Rigorously testing the causes and consequences of coyote range expansion requires an accurate historical context for where the species previously occurred. However, current accounts of coyote distribution suffer from two major problems.

First, the historic distribution of coyotes prior to the westward expansion of European settlers in the 1800s has recently been confused in the literature. This confusion is largely due to misinterpretation of a figure from Moore and Parker (1992) and Parker (1995). In these publications, the authors provide a general depiction of historical coyote ranges before and after European colonization of North America. In contrast to the authors' detailed written descriptions of subsequent coyote range expansion in eastern North America, these continent-wide maps were conceptual illustrations of an existing historical narrative and did not assess actual coyote occurrence data. More accurate coyote range maps have been published in the past (e.g., Young and Jackson 1951, Nowak 1978, 1979), but the Parker (1995) map has recently been reproduced as accurate description of coyote range expansion in the scientific and popular literature (e.g. Levy 2012).

In this popular narrative, coyotes were restricted to true prairie ecosystems prior to European settlement (Figure 1), bounded between the Mississippi River and the Rocky Mountains from southern Canada to central Mexico (Moore and Parker 1992, Parker 1995). The extirpation of wolves and land conversion by Europeans then presumably allowed a westward expansion of coyotes in the late 1800s, followed by a series of eastern expansions during the 1900s (Moore and Parker 1992, Parker 1995, Levy 2012).

However, range maps based on physical evidence (Nowak 1978, 1979), historical accounts, and coyote specimens in California suggests a wider western distribution. Grinnell et al. (1937) indicated that coyotes occurred in California well before European settlement, with the exception of a few heavily forested counties along the northern California seacoast, which coyotes colonized during the early 1900s. Numerous accounts by Native Americans and early European colonists confirm the presence of coyotes in California, as do zooarchaeological remains (e.g., Young and Jackson 1951 and references therein). Moreover, the genetic structure of Californian coyote populations suggest that they occurred in the area well before European colonization (Sacks et al. 2004), contradicting the hypothesis of a recent westward expansion.

Additionally, the original northern and southern range limits of coyotes remain uncertain in both narratives (Nowak 1978, Moore and Parker 1992). In Alaska and northern Canada, authors have debated whether coyotes historically occurred in low densities, arrived during the 1880s, or arrived during the 1900s (Nowak 1978, Parker 1995, MacDonald and Cook 2009). The original southern extent of coyote range has been similarly controversial. Fossil evidence confirms that coyotes were present in the Yucatán Peninsula and northwestern Costa Rica during the Pleistocene (Lucas et al. 1997, Arroyo-Cabrales and Alvarez 2003), but their southern distribution after late-Pleistocene climatic changes is less clear. In their seminal work on coyote ecology, Young and Jackson (1951) suggested that coyotes only recently colonized Central America, although the written accounts of coyote-like canids in the 1500s and late 1800s provide anecdotal evidence otherwise (Monge-Nájera and Morera Brenes 1987, Hidalgo-Mihart et al. 2004). Pre-Columbian coyote remains have also been found

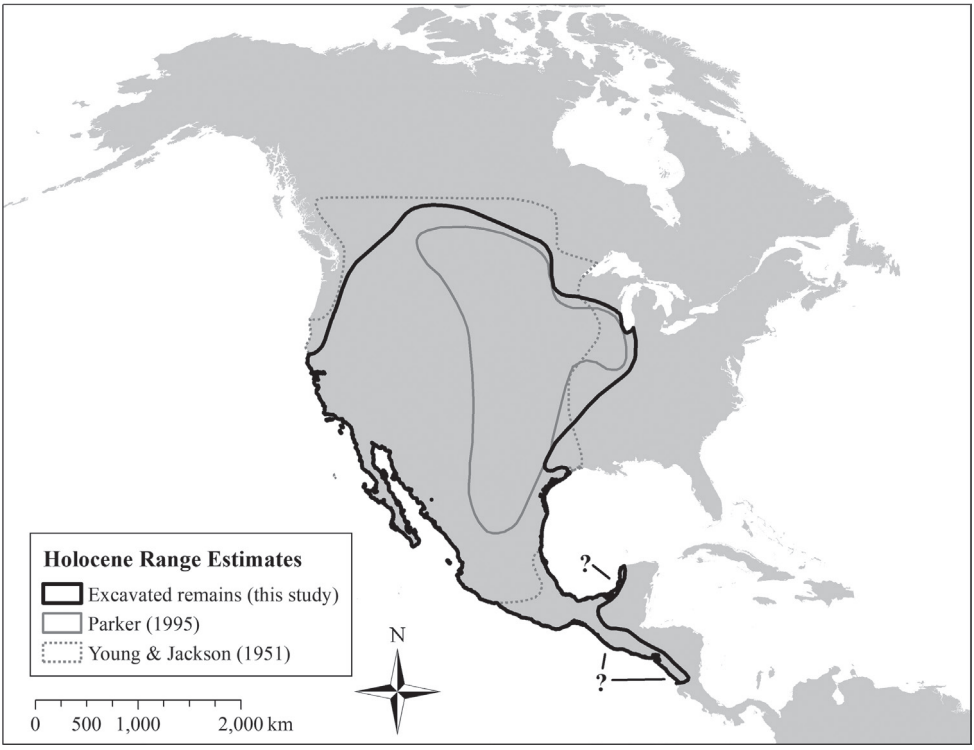

Figure 1. Comparison of Holocene coyote range maps, pre-expansion. Fossil and zooarchaeological remains suggest that coyotes were distributed throughout western North America prior to European colonization, contrary to widely-cited accounts (e.g., Parker 1995).

in at least two sites in the Yucatán Peninsula, lending credibility to this hypothesis (Hidalgo-Mihart et al. 2004). Overall, the historical distribution of coyotes during the Holocene remains poorly characterized and warrants reexamination.

A second problem with existing large-scale accounts of coyote range is that the recent expansion of coyotes has been coarsely described, without clear spatiotemporal detail. Maps are typically offered without citing reference material, and with few, widely scattered time intervals. Consolidating and improving continent-wide descriptions of coyote range expansion would facilitate testing hypotheses about their effects on newly colonized ecosystems.

Fortunately, coyotes are well represented in museum collections, having been hunted extensively due to their abundance and widespread reputation as a nuisance species. Furthermore, coyotes are also well represented in the fossil and zooarchaeological record, allowing inferences about their distribution several thousand years ago. We compiled museum records from recent biological surveys, fossil and zooarchaeological collections, peer-reviewed literature, and management agency reports to characterize the historical distribution of coyotes prior to European settlement and catalogue their expansion decade-by-decade from 1900 to 2016.

Materials and methods

We compiled coyote occurrences from two data repositories: VertNet (Constable et al. 2010) and the Quaternary Faunal Mapping Project, FAUNMAP (Graham and Lundelius 2010). These repositories allow ecological inferences at two different time-scales. FAUNMAP documents fossil and zooarchaeological coyote remains (hereafter, "excavated remains") throughout the Quaternary period, providing occurrence records across deep time scales. Conversely, VertNet documents coyote specimens collected during biological surveys of live animals (e.g., skins, skeletons, taxidermy animals, tissue samples; hereafter, "preserved specimens") and allows inferences about the distribution of coyotes from the mid-1800s through the present. Both data sources provide spatially and temporally referenced coyote occurrences across North America, collectively documenting their distribution over the past 10,000 years.

For our query in FAUNMAP, we searched for excavated remains of coyotes (*Canis latrans*) from the Holocene epoch (10,000-0 years before present, BP). Taxonomically modern coyotes (*C. latrans*) also occurred in the late Pleistocene, but biomes and faunal assemblages present in North America at the time drastically differed from those of the Holocene (Van Valkenburgh and Hertel 1993, Williams et al. 2004), with measurable effects on the ecological niche of the coyote itself (Meachen and Samuels 2012, Meachen et al. 2014, Pardi and Smith 2016). We therefore focus on their Holocene distribution, considering their Pleistocene range a separate but closely related topic.

Our query in VertNet considered preserved specimens of coyotes (*Canis latrans*), coydogs (*C. latrans* × *familiaris*), and coywolves (*C. latrans* × *lycaon*/*lupus*/*rufus*) that were collected during 1850–2016. We restricted our query to records that included information about the year and location where the specimen was collected. For quality control reasons, we only considered specimens that included georeferenced point coordinates or enough locality information to reference the data to a specific county. Coyote records from Mexico collected between 1850–1899 were retained as an exception to this rule, because more precise data were not available. In these cases, we allowed records that were referenced to at least a state-level.

In addition to these specimen records, we also compiled first-occurrence records and fossil records of coyotes from peer-reviewed literature and reports by state wildlife management agencies (references listed in Suppl. material 1). For first-occurrence records, we favored observations that were associated with either physical specimens (e.g. from hunters and trappers) or archived photographs (e.g., from camera traps) wherever possible, although we also considered other reputable first-hand accounts in areas where data were sparse. These records proved particularly valuable in defining the expansion of coyotes in Central America and the southeastern United States. For fossil and zooarchaeological records, we searched peer-reviewed reports of excavated coyote remains from Mexico and Central America, dated to 10,000–300 years BP. These records supplement FAUNMAP, the spatial coverage of which is limited to the United States and Canada. Since fewer records of excavated remains are available for this region, it is more difficult to clearly define the southernmost historical limit of

coyotes. However, these records provide some indication of the Holocene distribution of coyotes in Central America. Other types of data (e.g., Native American folklore, narrative accounts of European settlers) might further elucidate the historical range of coyotes. However, we restricted our inferences in this study to physical specimens, scientific literature, and management agency records, which can be more readily referenced to a specific spatial location and time interval. All the raw coyote occurrence data are available through Data Dryad (http://doi:10.5061/dryad.1qp358p).

We used these datasets to create two maps. First, we sought to clarify the Holocene distribution of coyotes before large-scale settlement by Europeans using FAUNMAP and a subset of the VertNet data (collected 1850–1899). We also identify which FAUNMAP records had a known minimum age >300 BP to permit stronger inference. Second, we used data from VertNet, peer-reviewed literature, and state management agencies to develop a highly detailed map of 20th century coyote range expansion at 10-year intervals. In both cases, we approximated range boundaries for each historical period (Holocene, 1900, 1910, etc.) by manually constructing polygons around occurrence records from the corresponding time interval.

During the 20th century, coyotes were occasionally brought into areas by hunters and trappers prior to natural expansion into the area (Parker 1995). These introductions produced isolated coyote records ahead of the colonizing front, but coyote populations in these areas usually did not persist (Fener et al. 2005, Kays et al. 2010). To avoid including these populations in our analysis, we excluded extreme spatial outliers from our distribution map (e.g., an isolated record might be omitted if it occurred in an area with known historical introductions and no neighboring records occurred within 500 km for many years).

In the Holocene figure, we also displayed coarse approximations of potential forest cover based on Ramankutty and Foley (2010). We included this layer to visually illustrate the spatial distribution of historical coyote specimens in relation to dominant land cover types. We defined potential forest cover as areas where tropical, temperate, or boreal forests would have occurred in the area based on large-scale estimates by Ramankutty and Foley (2010). We caution that the historical extent of forest cover in North and Central America contracted and expanded considerably prior to European contact due to the agriculture activities, settlement building, and land burning practices of Pre-Columbian civilizations (Denevan 1992, Kimmerer and Lake 2001, Cook et al. 2012). Thus, potential forest cover should not be interpreted as a literal, static depiction of American land cover throughout the Holocene. Instead, it should be interpreted as a general index for areas where forest cover frequently or intermittently occurred over several thousand years.

Results

Our query in FAUNMAP yielded 347 records from the United States and Canada with specific data on the minimum and maximum age of the coyote remains. These were distributed between the Pacific Ocean and the Mississippi River, with the exception of two spatial outliers occurring in New Brunswick, Canada and Florida, USA

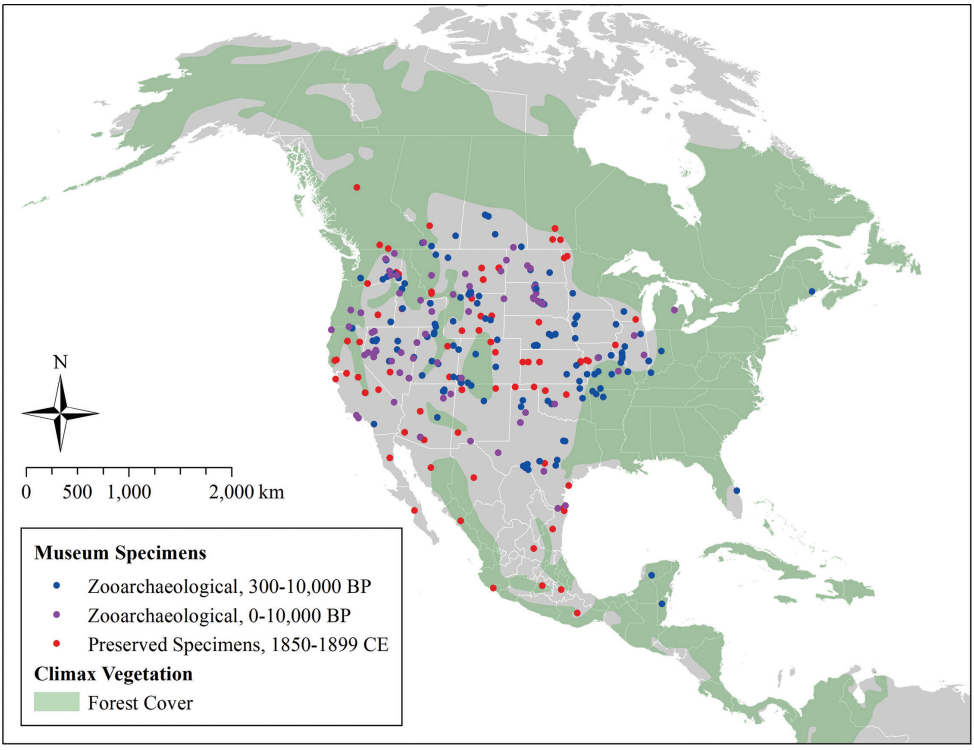

Figure 2. Historical distribution of coyotes from 10,000 years before present (BP) to 1899. Zooarchaeological (FAUNMAP) records document the distribution of coyotes during the Holocene (0–10,000 BP).

(Figure 2). It is possible that these two records reflect a more widespread eastern distribution of coyotes in the Holocene. However, we find it more likely that they reflect misidentified remains of related *Canis* sp.

Our query in VertNet yielded 12,319 records of coyotes and coyote hybrids from North and Central America, providing specimen-vouchered coyote occurrences from 1850-2016. Among these records, 4,949 were already georeferenced, and an additional 3,523 records had sufficient locality information to reference the data to individual counties or corresponding political units. An additional 3,747 records could only be referenced to the state- or province-level. We retained such occurrence records for Mexico to address the dearth of available data prior to 1900, but omitted these records elsewhere due to the availability of higher-quality county-level data. Only 100 records had no useable locality information.

Holocene distribution (10,000 BP–1899)

The spatial distribution of coyote specimens from the late 1800s was similar to the distribution of coyote remains older than 300 BP. Specifically, coyotes extended east to

Mississippi and Ohio Rivers and west through California and the arid west (Figure 2). These data indicate that that coyotes' range in the late-1800s reflected a longstanding geographic distribution that formed well before the 1700s, not a recent westward expansion. This contradicts widely-cited descriptions of the historical distribution of coyotes (Figure 1), which suggest that California and the Rocky Mountains as areas that were colonized by coyotes as recently as the 19th and 20th centuries (Moore and Parker 1992, Parker 1995, Levy 2012). Instead, the historical distribution of coyotes matches areas where non-forested habitats (e.g., grassland, prairie, desert) dominate the climax vegetation, more closely corresponding to earlier range descriptions by Nowak (1978, 1979, 2002) and Young and Jackson (1951). The Holocene distribution of coyotes in Mesoamerica remains unclear due to the relatively small number of published historical specimens available from this area.

Contemporary expansion (1900–2016)

Combining museum records and regional coyote literature, we created a detailed continent-wide description of coyote range expansion at 10 year intervals (Figure 3). This map consolidates previous efforts and corrects popular misconceptions about the magnitude of coyotes' expansion in the west. Additionally, it provides the first account of coyote range expansion at this level of spatial and temporal detail. We offer this as a starting point for future discussions and encourage further improvements to this map wherever local data might become available. Additional research is needed in some areas, particularly Central America and the Mid-Atlantic United States, where historical records are sparse.

Discussion

We compiled coyote occurrences from past biological surveys, fossils, zooarchaeological records, and existing literature to document the historical distribution of coyotes throughout the Holocene and reconstruct decade-by-decade range expansion during 1900–2016. Our findings indicate that coyotes historically occupied a larger area of North America than generally suggested in recent literature, more closely matching the historical range presented by Young and Jackson (1951) and Nowak (1978, 1979) than Parker (1995) (Figure 1). Our results closely resemble the written range description by Nowak (1979), which assesses coyotes as having "a wide distribution, primarily in the western half of the continent" prior to European contact, with unknown range limits but extending "at least as far east as southern Wisconsin, northwestern Indiana, western Arkansas, and central Texas."

The distribution of excavated coyote remains 10,000–300 BP matches the distribution of preserved coyote specimens collected between 1850 and 1899 almost identically, suggesting that the geographic range of coyotes in the late 1800s had already been

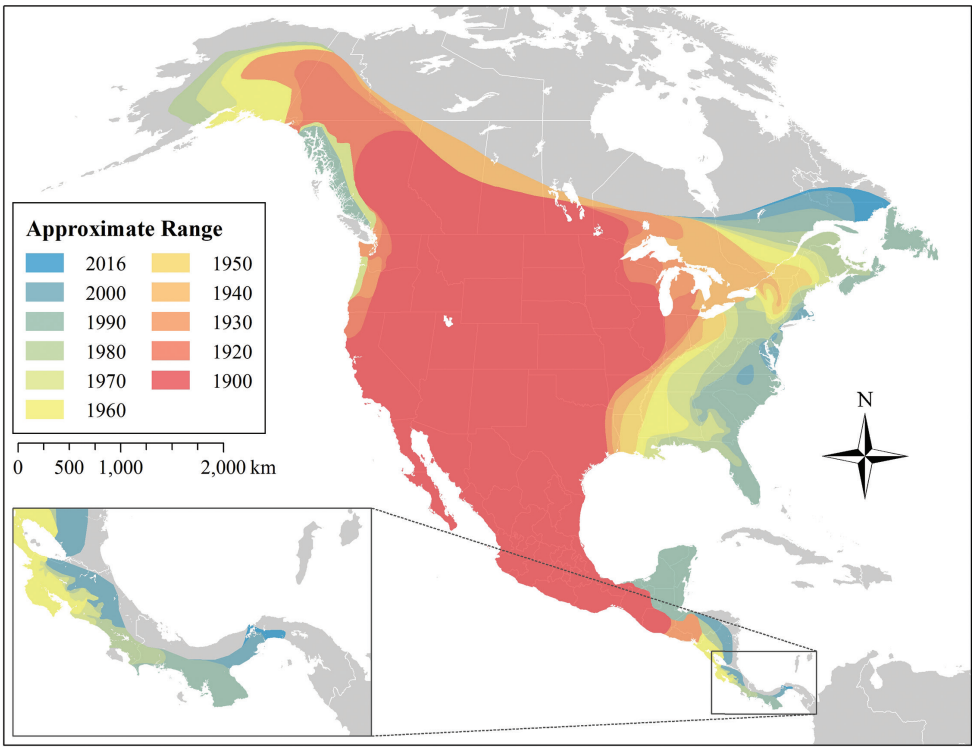

Figure 3. Coyote range expansion by decade, 1900–2016. Ranges are based on occurrence of museum specimens, peer-reviewed literature with associated specimens or photographs, and reports from state wildlife management agencies. The distribution of coyotes between the Yucatán Peninsula and Nicaragua is coarsely depicted due to the paucity of available data, representing the earliest confirmed occurrence. All referenced materials are listed in Suppl. material 1.

established prior to the 1700s. This same spatial pattern emerged when FAUNMAP data were subdivided in other ways, suggesting that this was not an artifact of how we defined our time intervals. Importantly, Holocene coyote remains ≥4,000 BP showed the same general pattern presented in Figure 2, confirming the presence of coyotes as far east as Arkansas and central Texas, as far south as the Yucatán Peninsula, and as far west as California. These records predate the rise of North and Central American civilizations with large permanent settlements (e.g., Olmec, Aztec, Mayan, Mississippian) (Kuiper 2010), suggesting that coyotes were widely distributed throughout the Holocene independent of large-scale land use change by Pre-Columbian civilizations.

Excavated coyote remains and 19th century museum records occurred throughout most non-forested habitats in North America. These specimen records show that coyotes occurred in the Rocky Mountains and Arid West throughout the Holocene, contradicting the proposed western expansion of coyotes during the late-1800s (Parker 1995), although there was a smaller expansion into forests of the Pacific Northwest in the early 1900s.

The distribution of excavated remains includes four notable outliers, warranting further discussion: one in southern Florida, one in New Brunswick, and two on the Yucatán Peninsula. Although we consider the New Brunswick sample questionable, the Florida and Yucatán specimens might reflect historical range dynamics of coyotes. The Florida record is dated to the early Holocene, but its estimated range age overlaps with the late Pleistocene as well. Coyote fossils from this geological epoch have been documented across the Florida peninsula (Graham and Lundelius 2010), which was previously dominated by grassland ecosystems (Feranec and MacFadden 2000, Feranec 2004). This record likely reflects coyote occurrence in the late Pleistocene, or misidentified red wolf remains from the early Holocene. Alternatively, it might indicate that coyotes briefly persisted in the savannah habitats of southern Florida after forest habitats arose elsewhere in eastern North America. The New Brunswick record is much younger, referring to mandibles found in a Native American shell midden from the year 830 ± 65 BP. While this is possible that these remains represent an extreme eastern distribution of coyotes in the past (Stewart 1976), we suspect that they may be misidentified remains from domestic dogs, which were also found on site and appear in similar deposits from New England (Ingraham 2011).

The two Yucatán specimens, both noted by Hidalgo-Mihart et al. (2004), suggest a historical presence of coyotes in parts of Central America, and possible range expansion associated with Mayan land use and deforestation. The westerly record is dated to the early Holocene (Arroyo-Cabrales and Alvarez 2003), suggesting a longstanding presence of coyotes in the area (Hidalgo-Mihart et al. 2004). This record occurs near relatively open habitat along the western coast of the Yucatán Peninsula (Ramankutty and Foley 2010), possibly facilitating their historical presence there. The eastern record is much younger, associated with Postclassic Mayan ruins in Belize (Emery 1999), and may indicate that coyotes existed in areas deforested by the Maya civilization (Hidalgo-Mihart et al. 2004). Interestingly, written accounts noted by Monge-Nájera and Morera Brenes (1987) and Hidalgo-Mihart et al. (2004) spatially coincide with areas that most heavily cultivated and deforested prior to European contact (Cook et al. 2012).

We cannot definitively assess the Holocene southern limit of coyotes due to paucity of data in Central America. However, we generally agree with Hidalgo-Mihart et al. (2004) that coyotes may have existed in naturally occurring open habitats and Pre-Columbian agricultural areas of Central America prior to the 1500s based on available records, contrasting earlier descriptions (Young and Jackson 1951). We hypothesize that the southern distribution of coyotes might have fluctuated during the Holocene, with populations extending eastward across the Yucatán Peninsula and southward along the Pacific coast of Central America in periods when barriers of forested habitat were broken, either naturally or by agricultural activities of Mesoamerican civilizations. Additional research is needed to clarify their historical distribution of coyotes south of Mexico, but all available evidence suggests that this species was restricted to habitats north of the Nicoya Peninsula in northwestern Costa Rica until the mid-1900s (Vaughan 1983).

Our map of coyote records from 1900-2016 shows how and when coyotes expanded their range into forested biomes. Agriculture was widespread in these previously forested

regions by 1900, so this more open, fragmented landscape presumably aided their expansion, although Kays et al. (2008) note that eastern coyotes now occur in large forested wilderness, and thus are not reliant on open habitats. Our map also reflects the relatively rapid colonization of the northeast in comparison with the southeast, which Kays et al. (2010) suggested was due to higher levels of wolf introgression allowing a more rapid evolution of larger body size. More recently, VonHoldt et al. (2016) showed that wolf genes associated with body size have been positively selected for in eastern coyotes, and rapidly spread throughout the eastern population. Coyotes now occur through eastern North America, and are now expanding to isolated islands with recent sightings in the Florida Keys (Greene and Gore 2013) and Long Island, New York (Weckel et al. 2015).

Although coyote range expansion into eastern Canada has been well studied (Crête and Desrosiers 1995, Crête et al. 2001, Patterson and Messier 2003, Chubbs and Phillips 2005), historical reasons for the northward expansion of coyotes into western Canada and Alaska described in the literature remain sparse. This early northwestern expansion is generally attributed to land clearing and refuse left by settlers during the gold rushes of the late 1800s (Gier 1975, Moore and Parker 1992). This explanation appears chronologically appropriate, but it is doubtful that these disturbances alone would provide coyotes with enough momentum to establish resident populations in western Canada and further colonize southeastern Alaska in the 1900s. Interestingly, coyotes have now established at least one breeding population in the Taiga Shield ecozone, near Yellowknife, Northwest Territories (Cluff 2006). It is unclear whether this population extends into undeveloped areas, or if it is restricted to disturbed habitats (Cluff 2006).

Likewise, coyote expansion southward across Central America is also not well studied. Coyotes rapidly expanded into deforested habitats in eastern Panama (Méndez-Carvajal and Moreno 2014, Hody 2016), and the dense forests of the Darién now represent the last major barrier between coyote populations and South American savannah ecosystems (Hidalgo-Mihart et al. 2004, Méndez-Carvajal and Moreno 2014). However, this barrier may be more permeable than previously thought, especially along the coastlines, raising concerns that coyotes might reach South America in the near future (Hody 2016). If coyotes reach South America, it is likely that the grassland and agricultural habitats in Colombia and Venezuela could support viable populations, unless competition with native carnivores restricts them. Observations in eastern Panama suggests that road construction and agricultural development might facilitate coyote range expansion in previously forested tropical landscapes (Méndez-Carvajal and Moreno 2014, Hody 2016), but we find it improbable that coyotes would expand into intact parts of the Amazon rainforest. Conversely, we speculate that the open habitats of the Andes might offer suitable coyote habitat in such a scenario, and allow further expansion around the Amazon. Regardless of its extent, coyote colonization of South America would be an event of profound ecological significance; barring direct introductions by humans, expansion of a North American predator into South American ecosystems has not been observed since the Great American Biotic Interchange 3 million years ago (Wallace 1876, Simpson 1980, Marshall et al. 1982, Leigh et al. 2014), and its potential effects on native wildlife is entirely unknown.

Conclusion

The expansion of coyotes across the American continent offers a natural experimental system for assessing ecological questions related to their roles as predators, and evolutionary questions related to their hybridization with dogs and wolves. By collecting and mapping all historical and fossil records of coyotes we were able to correct old misconceptions of their original range, and more precisely map and date their recent expansions. We hope these maps will provide useful context for future research into the ecology and evolution of this incredibly adaptive carnivore.

References

Adams JR, Leonard JA, Waits LP (2003) Widespread occurrence of a domestic dog mitochondrial DNA haplotype in southeastern US coyotes. Molecular Ecology 12(2): 541–546. https://doi.org/10.1046/j.1365-294X.2003.01708.x

Andelt WF (1987) Coyote predation. In: Novak M (Ed.) Wild furbearer management and conservation in North America. Ontario Ministry of Natural Resources, Toronto, 128–140.

Arroyo-Cabrales J, Alvarez T (2003) A preliminary report of the late Quaternary mammal fauna from Loltún Cave, Yucatán, México. In: Schubert BW, Mead J., Graham RW (Eds) Ice Age cave faunas of North America. Indiana University Press, Bloomington, 262–272.

Bekoff M, Gese EM (2003) Coyote (*Canis latrans*). In: Feldhamer B, Thompson C, Chapman JA (Eds) Wild mammals of North America: Biology, management, and conservation. Johns Hopkins University Press, Baltimore, 467–481.

Berger KM, Gese EM (2007) Does interference competition with wolves limit the distribution and abundance of coyotes? Journal of Animal Ecology 76: 1075–1085. https://doi.org/10.1111/j.1365-2656.2007.01287.x

Bermúdez SEC (2013) Ticks (Acari: Ixodidae, Argasidae) of coyotes in Panama. Systematic and Applied Acarology 18(2): 112–115. https://doi.org/10.11158/saa.18.2.2

Chubbs TE, Phillips FR (2005) Evidence of range expansion of eastern coyotes, *Canis latrans*, in Labrador. Canadian Field-Naturalist 119: 381–384. https://doi.org/10.22621/cfn.v119i3.149

Cluff HD (2006) Extension of Coyote, *Canis latrans*, breeding range in the Northwest Territories, Canada. Canadian Field-Naturalist 120: 67–70. https://doi.org/10.22621/cfn.v120i1.248

Constable H, Guralnick R, Wieczorek J, Spencer C, Peterson AT, Bart H, Bates J, Cotter G, Hanken J, Moritz C, Simmons N, Trueb L (2010) VertNet: A new model for biodiversity data sharing. PLoS Biology 8: e1000309. https://doi.org/10.1371/journal.pbio.1000309

Cook BI, Anchukaitis KJ, Kaplan JO, Puma MJ, Kelley M, Gueyffier D (2012) Pre-Columbian deforestation as an amplifier of drought in Mesoamerica. Geophysical Research Letters 39: 2–6. https://doi.org/10.1029/2012GL052565

Cove MV, Pardo VLE, Spínola RM, Jackson VL, Sáenz JC (2012) Coyote *Canis latrans* (Carnivora: Canidae) Range extension in northeastern Costa Rica: Possible explanations and consequences. Latin American Journal of Conservation 3: 82–86.

Crête M, Desrosiers A (1995) Range expansion of coyotes, *Canis latrans*, threatens a remnant herd of caribou, *Rangifer tarandus*, in southeastern Québec. Canadian Field-Naturalist 109: 227–235.

Crête M, Ouellet J-P, Tremblay J-P, Arsenault R (2001) Suitability of the forest landscape for coyotes in norteastern North America and its implications for coexistence with other carnivores. Ecoscience 8: 311–319. https://doi.org/10.1080/11956860.2001.11682658

Denevan WM (1992) The pristine myth: The landscape of the Americas in 1492. Annals of the Association of American Geographers 82: 369–385. https://doi.org/10.1111/j.1467-8306.1992.tb01965.x

Emery KF (1999) Continuity and variability in Postclassic and colonial animal use at Lamanai and Tipu, Belize. In: White CD (Ed.) Reconstructing ancient Maya diet. University of Utah Press, Salt Lake City, 61–82.

Fener HM, Ginsberg JR, Sanderson EW, Gompper ME (2005) Chronology of range expansion of the Coyote, *Canis latrans*, in New York. Canadian Field-Naturalist 119: 1–5. https://doi.org/10.22621/cfn.v119i1.74

Feranec RS (2004) Geographic variation in the diet of hypsodont herbivores from the Rancholabrean of Florida. Palaeogeography, Palaeoclimatology, Palaeoecology 207: 359–369. https://doi.org/10.1016/S0031-0182(04)00047-1

Feranec RS, MacFadden BJ (2000) Evolution of the grazing niche in Pleistocene mammals from Florida: Evidence from stable isotopes. Palaeogeography, Palaeoclimatology, Palaeoecology 162: 155–169. https://doi.org/10.1016/S0031-0182(00)00110-3

Georges S (1976) A range extension of the coyote in Quebec. Canadian Field-Naturalist 90: 78–79.

Gier HT (1975) Ecology and social behavior of the coyote. In: Fox MW (Ed.) The wild canids. Von Nostrand Reinhold, New York, NY, USA, 247–262.

Gompper ME (2002) Top carnivores in the suburbs? Ecological by colonization issues raised by colonization of north-eastern North America by coyotes. BioScience 52: 185–190. https://doi.org/10.1641/0006-3568(2002)052[0185:TCITSE]2.0.CO;2

Graham RW, Lundelius EL (2010) FAUNMAP II: New data for North America with a temporal extension for the Blancan, Irvingtonian and early Rancholabrean. FAUNMAP II Database, version 1.0. http://www.ucmp.berkeley.edu/neomap/use.html [July 29, 2016]

Greene DU, Gore JA (2013) Coyote (*Canis latrans*) in the Florida Keys. Florida Field Naturalist 41: 126–129.

Grinnell J, Dixon JS, Linsdale JM (1937) Fur-bearing mammals of California: Their natural history, systematic status and relations to man. University of California Press, Berkeley, 777 pp.

Hidalgo-Mihart MG, Cantú-Salazar L, González-Romero A, López-González CA (2004) Historical and present distribution of coyote (*Canis latrans*) in Mexico and Central America. Journal of Biogeography 31: 2025–2038. https://doi.org/10.1111/j.1365-2699.2004.01163.x

Hidalgo-Mihart MG, Contreras-Moreno FM, Pérez-Solano LA, Hernández-Lara C (2013) Primeros registros de coyote (*Canis latrans*) en Campeche, México. Revista Mexicana de Biodiversidad 84: 1012–1017. https://doi.org/10.7550/rmb.33108

Hill EP, Sumner PW, Wooding JB (1987) Human influences on range expansion of coyotes in the southeast. Wildlife Society Bulletin 15(4): 521–524.

Hody JW (2016) Canid collision - Range expansion by coyotes (*Canis latrans*) and crab-eating foxes (*Cerdocyon thous*) in Panama and interpretation of camera trap data. MS thesis, Raleigh, USA: North Carolina State University. https://repository.lib.ncsu.edu/handle/1840.20/33317

Ingraham RC (2011) Specialized taphonomies in an eastern Maine shell midden: Faunal analysis of Site 62-8, Holmes Point West, Machias, Maine. MS thesis, Orono, USA: University of Maine. http://digitalcommons.library.umaine.edu/etd/1615

Kays R, Curtis A, Kirchman JJ (2010) Rapid adaptive evolution of northeastern coyotes via hybridization with wolves. Biology Letters 6: 89–93. https://doi.org/10.1098/rsbl.2009.0575

Kays RW, Gompper ME, Ray JC (2008) Landscape ecology of eastern coyotes based on large-scale estimates of abundance. Ecological Applications 18: 1014–1027. https://doi.org/10.1890/07-0298.1

Kimmerer RW, Lake FK (2001) The role of indigenous burning in land management. Journal of Forestry 99(11): 36–41.

Knowlton FF, Gese EM, Jaeger MM (1999) Coyote depredation control: An interface between biology and management. Journal of Range Management 52: 398–412. https://doi.org/10.2307/4003773

Kuiper K (2010) Pre-Columbian America: Empires of the New World. Britannica Educational Publishing, New York, 194 pp.

Laliberte AS, Ripple WJ (2004) Range contractions of North American carnivores and ungulates. BioScience 54: 123–138. https://doi.org/10.1641/0006-3568(2004)054[0123:RCONAC]2.0.CO;2

Leigh EG, O'Dea A, Vermeij GJ (2014) Historical biogeography of the Isthmus of Panama. Biological Reviews 89: 148–172. https://doi.org/10.1111/brv.12048

Levi T, Kilpatrick AM, Mangel M, Wilmers CC (2012) Deer, predators, and the emergence of Lyme disease. Proceedings of the National Academy of Sciences 109: 10942–10947. https://doi.org/10.1073/pnas.1204536109/-/DCSupplemental.www.pnas.org/cgi/doi/10.1073/pnas.1204536109

Levy S (2012) Rise of the coyote: The new top dog. Nature 485: 296–297. https://doi.org/10.1038/485296a

Lucas SG, Alvarado GE, Vega E (1997) The Pleistocene mammals of Costa Rica. Journal of Vertebrate Paleontology 17: 413–427. https://doi.org/10.1080/02724634.1997.10010985

Macdonald DW, Sillero-Zubiri C (2004) The biology and conservation of wild canids. Oxford University Press Inc., New York, 450 pp. https://doi.org/10.1093/acprof:oso/9780198515562.001.0001

MacDonald SO, Cook JA (2009) Recent mammals of Alaska. University of Alaska Press, Fairbanks, 387 pp.

Marshall LG, Webb SD, Sepkoski JJ, Raup DM (1982) Mammalian evolution and the Great American Interchange. Science 215: 1351–1357. https://doi.org/10.1126/science.215.4538.1351

Meachen JA, Janowicz AC, Avery JE, Sadleir RW (2014) Ecological changes in coyotes (*Canis latrans*) in response to the Ice Age megafaunal extinctions. PLoS ONE 9: e116041. https://doi.org/10.1371/journal.pone.0116041

Meachen JA, Samuels JX (2012) Evolution in coyotes (*Canis latrans*) in response to the megafaunal extinctions. Proceedings of the National Academy of Sciences 109: 4191–4196. https://doi.org/10.1073/pnas.1113788109

Méndez-Carvajal P, Moreno R (2014) Mammalia, Carnivora, Canidae, *Canis latrans* (Say, 1823): Actual distribution in Panama. Check List 10: 376–379. https://doi.org/10.15560/10.2.376

Monge-Nájera J, Morera Brenes B (1987) Why is the coyote (*Canis latrans*) expanding its range? A critique of the deforestation hypothesis. Revista de Biología Tropical 35: 169–171.

Moore GC, Parker GR (1992) Colonization by the eastern coyote (*Canis latrans*). In: Boer AH (Ed.) Ecology and management of the eastern coyote. Wildlife Research Unit, University of New Brunswick, Fredericton, 23–38.

Nowak RM (1978) Evolution and taxonomy of coyotes and related *Canis*. In: Bekoff M (Ed.) Coyotes: Biology, behavior, and management. Academic Press, Inc., New York, 3–16.

Nowak RM (1979) North American Quaternary Canis. Museum of Natural History, University of Kansas, Lawrence, 154 pp.

Nowak RM (2002) The original status of wolves in eastern North America. Southeastern Naturalist 1(2): 95–130. https://doi.org/10.1656/1528-7092(2002)001[0095:TOSOWI]2.0.CO;2

Pardi MI, Smith FA (2016) Biotic responses of canids to the terminal Pleistocene megafauna extinction. Ecography 39: 141–151. https://doi.org/10.1111/ecog.01596

Parker G (1995) Colonization. In: Eastern coyote: the story of its success. Nimbus Publishing, Halifax, 16–35.

Patterson BR, Messier F (2003) Age and condition of deer killed by coyotes in Nova Scotia. Canadian Journal of Zoology 81: 1894–1898. https://doi.org/10.1139/z03-189

Peña-Mondragón JL, Castillo Álvarez A, Benítez-Malvido J (2014) Primer registro de coyote (*Canis latrans*) en la región de La Selva Lacandona, Chiapas, México. Acta Zoológica Mexicana 30(3): 696–700.

Platt SG, Miller BW, Miller CM (1998) First record of the coyote (*Canis latrans*) in Belize. Vida Silvestre Neotropical 7: 139–140.

Ramankutty N, Foley JA (2010) ISLSCP II Potential Natural Vegetation Cover. In: Hall FG, Collatz G, Meeson B, Los S, Brown de Colstoun E, Landis D (Eds) ISLSCP Initiative II Collection. Oak Ridge National Laboratory Distributed Active Archive Center, Oak Ridge, Tennessee, USA. https://doi.org/10.3334/ORNLDAAC/961

Sacks BN, Brown SK, Ernest HB (2004) Population structure of California coyotes corresponds to habitat-specific breaks and illuminates species history. Molecular Ecology 13: 1265–1275. https://doi.org/10.1111/j.1365-294X.2004.02110.x

Simpson GG (1980) Splendid isolation: The curious history of South American mammals. Yale University Press, New Haven, 266 pp.

Sosa-Escalante J, Hernández S, Segovia A, Sánchez-Cordero V (1997) First record of the coyote, *Canis latrans*, in the Yucatan Peninsula, Mexico. Southwestern Naturalist 42(4): 494–495.

Stewart FL (1976) Coyote in New Brunswick during prehistoric times. Nature Canada 5: 27. https://doi.org/10.1017/CBO9781107415324.004

Thornton DH, Murray DL (2014) Influence of hybridization on niche shifts in expanding coyote populations. Diversity and Distributions 20: 1355–1364. https://doi.org/10.1111/ddi.12253

Van Valkenburgh B, Hertel F (1993) Tough times at La Brea: Tooth breakage in large carnivores of the late Pleistocene. Science 261: 456–459. https://doi.org/10.1126/science.261.5120.456

Vaughan C (1983) Coyote range expansion in Costa Rica and Panama. Brenesia 21: 27–32.

vonHoldt BM, Kays R, Pollinger JP, Wayne RK (2016) Admixture mapping identifies introgressed genomic regions in North American canids. Molecular Ecology 25: 2443–2453. https://doi.org/10.1111/mec.13667

vonHoldt BM, Pollinger JP, Earl DA, Knowles JC, Boyko AR, Parker H, Geffen E, Pilot M, Jedrzejewski W, Jedrzejewska B, Sidorovich V, Greco C, Randi E, Musiani M, Kays R, Bustamante CD, Ostrander EA, Novembre J, Wayne RK (2011) A genome-wide perspective on the evolutionary history of enigmatic wolf-like canids. Genome Research 21: 1294–1305. https://doi.org/10.1101/gr.116301.110

Wallace AR (1876) The geographical distribution of animals: With a study of the relations of living and extinct faunas as elucidating the past changes of the earth's surface.

Weckel M, Bogan DA, Burke RL, Nagy C, Siemer WF, Green T (2015) Coyotes go "bridge and tunnel": A narrow opportunity to study the socio-ecological impacts of coyote range expansion on Long Island, NY pre- and post-arrival. Cities and the Environment 8: 1–28.

Weeks JL, Tori GM, Shieldcastle MC (1990) Coyotes (*Canis latrans*) in Ohio. Ohio Journal of Science 90(5): 142–145.

Williams JW, Shuman BN, Webb III T, Bartlein PJ, Leduc PL (2004) Late-Quaternary vegetation dynamics in North America: Scaling from taxa to biomes. Ecological Monographs 74: 309–334. https://doi.org/10.1890/02-4045

Young SP, Jackson HHT (1951) The clever coyote. University of Nebraska Press, Lincoln, 411 pp.

Supplementary material 1

Detailed list of references and data sources

Authors: James W. Hody, Roland Kays

Data type: Reference data

Explanation note: List of references used to determine historical extent and regional first-occurrences of coyotes (*Canis latrans*) in North and Central America.

Link: https://doi.org/10.3897/zookeys.759.15149.suppl1

Supplementary material 2

Coyote range expansion, 1900–2016

Authors: James W. Hody, Roland Kays

Data type: Geospatial data (shapefile)

Link: https://doi.org/10.3897/zookeys.759.15149.suppl2

ZooKeys 759: 99–116 (2018)
doi: 10.3897/zookeys.759.24742
http://zookeys.pensoft.net

RESEARCH ARTICLE

A peer-reviewed open-access journal
ZooKeys
Launched to accelerate biodiversity research

Anomaloglossus meansi sp. n., a new Pantepui species of the *Anomaloglossus beebei* group (Anura, Aromobatidae)

Philippe J.R. Kok[1], Michaël P.J. Nicolaï[2], Amy Lathrop[3], Ross D. MacCulloch[3]

1 *Amphibian Evolution Lab, Department of Biology, Vrije Universiteit Brussel, Pleinlaan 2, B-1050 Brussels, Belgium* **2** *Department of Biology, Vrije Universiteit Brussel, Pleinlaan 2, B-1050 Brussels, Belgium* **3** *Centre for Biodiversity and Conservation Biology, Royal Ontario Museum, 100 Queen's Park, Toronto, Ontario M5S 2C6, Canada*

Corresponding author: *Philippe J. R. Kok* (philippe.kok@vub.be)

Academic editor: *A. Crottini* | Received 28 February 2018 | Accepted 9 April 2018 | Published 22 May 2018

http://zoobank.org/F536AF25-E792-4C99-B4D6-FA4B76FDA45D

Citation: Kok PJR, Nicolaï MPJ, Lathrop A, MacCulloch RD (2018) *Anomaloglossus meansi* sp. n., a new Pantepui species of the *Anomaloglossus beebei* group (Anura, Aromobatidae). ZooKeys 759: 99–116. https://doi.org/10.3897/zookeys.759.24742

Abstract

Recent extinctions and drastic population declines have been documented in the Guiana Shield endemic frog genus *Anomaloglossus*, hence the importance to resolve its alpha-taxonomy. Based on molecular phylogenies, the literature has long reported the occurrence of an undescribed species in the Pakaraima Mountains of Guyana in the Pantepui region. We here describe this new taxon and demonstrate that in addition to divergence at the molecular level the new species differs from congeners by a unique combination of morphological characters, notably a small size (maximum SVL in males 18.86 mm, maximum SVL in females 21.26 mm), Finger I = Finger II when fingers adpressed, Finger III swollen in breeding males, fringes on fingers absent, toes basally webbed but lacking fringes, in life presence of a thin dorsolateral stripe from tip of snout to tip of urostyle, and a black throat in preserved males (immaculate cream in females). Virtually nothing is known about the ecology of the new species. We suggest the new species to be considered as Data Deficient according to IUCN standards.

Keywords

Aromobatidae, diversity, Guiana Shield, Guyana, Pakaraima Mountains

Introduction

In their influential work about bird diversification in the Venezuelan highlands, Mayr and Phelps (1967) coined the term "Pantepui" to describe the high-elevation life zones of the Guiana Shield highlands in north-eastern South America. Pantepui is best known for its numerous isolated vertical-sided sandstone table-top mountains, the iconic Lost World's tepuis, and huge tepuian massifs, last erosional remnants of a vast ancient plateau (see Kok 2013 for details). The number of phylogenetic lineages restricted to Pantepui is remarkable given the relatively reduced size of that bioregion. Pantepui seems to act as a reservoir of endemism at the species level, but also at the genus level and, to a lesser extent, at the family level (see Kok 2013 for summary). Various biogeographical hypotheses have been proposed to explain the origin and drivers of diversification of tepui-summit species/populations (Mayr and Phelps 1967, see Kok 2013 for a summary). Recent phylogeographic studies based on non-flying vertebrates (e.g. Kok et al. 2012, 2017, 2018a, b, Leite et al. 2015, Lehmberg et al. 2018) suggested a complex historical biogeography involving the synergy of long distance dispersals, vicariance and habitat shifts.

Vertical isolation makes tepui ecosystems particularly sensitive to global warming (see Rull and Vegas-Vilarrúbia 2006, Nogué et al. 2009). Because of their remoteness and the difficulties to access most tepuis and tepuian massifs, sampling in the area has been historically low, hindering the pressing need to evaluate the taxonomic status and accurate distribution of Pantepui endemic species. The situation is particularly critical in some groups in which recent extinctions or drastic population declines have been documented, such as in the Guiana Shield endemic frog genus *Anomaloglossus* (e.g. Fouquet et al. 2015, 2018). The genus currently comprises 28 species (Grant et al. 2017, Fouquet et al. 2018), and likely originated in the Pantepui region (area sensu Kok 2013), where several endemics with restricted distributions are reported; more widespread species are found in the lowlands of the eastern Guiana Shield (Vacher et al. 2017). The *beebei* species group (sensu Grant et al. 2017) is restricted to the eastern Pantepui region of Venezuela and Guyana and currently contains six species, one of them still undescribed (Figure 1). That unnamed species has previously been reported in the literature as *Anomaloglossus* sp. Ayanganna (Grant et al. 2006, 2017), *Anomaloglossus* cf. *praderioi* (Kok 2010) and as *Anomaloglossus* sp. B (Kok et al. 2012) and was recovered sister to *A. praderioi* (La Marca, 1997) by Grant et al. (2006, 2017) and Kok et al. (2012). The new taxon was first collected in October 2000 by AL and RDM during an expedition to Mount Ayanganna in Guyana, then found on the Wokomung Massif, Guyana, in July 2003 by D. Bruce Means and in October 2004 by AL and RDM. There is no additional report of the species since then. Although its status as an undescribed species has never been disputed, no formal description has yet been proposed. It is our aim to resolve the issue and describe this new species based on the eleven collected specimens currently available.

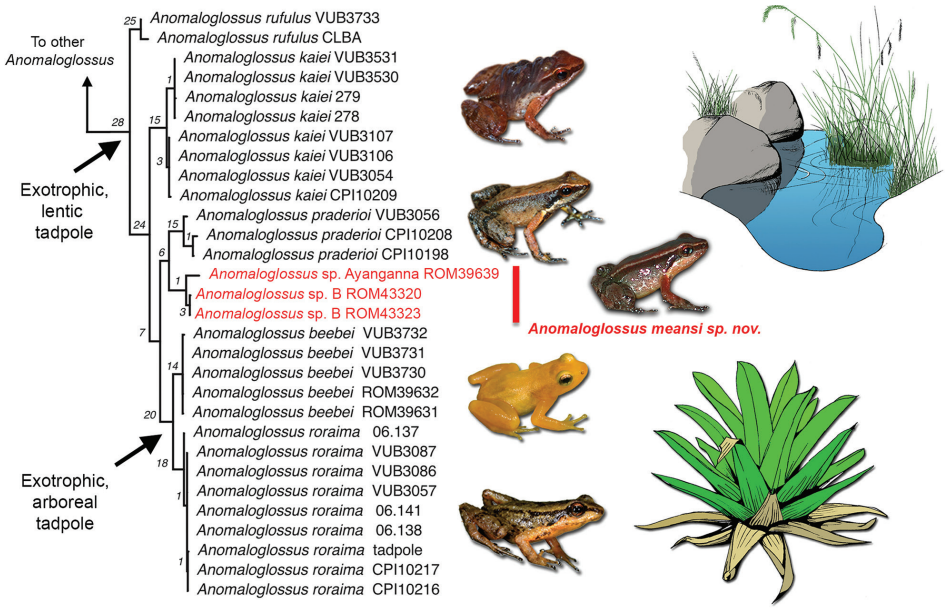

Figure 1. Optimal relationships of the *Anomaloglossus beebei* group (modified from Grant et al. 2017). Numbers at nodes are Goodman-Bremer values. The new species is highlighted in red. *Anomaloglossus* photos are by PJRK, except *A. meansi*, which is by D. Bruce Means. Drawings by Kim Roelants.

Materials and methods

Nomenclature

Taxonomy and terminology follow Grant et al. (2006, 2017). The description format is adapted from the most recent species (re)descriptions in the genus (e.g., Kok et al. 2006, Myers and Donnelly 2008, Kok 2010, Kok et al. 2010, Fouquet et al. 2015, 2018).

Fieldwork and deposition of specimens

Collecting activities took place on Mount Ayanganna and the Wokomung Massif, west-central Guyana (Figure 2). These two mountains, located in the southern Pakaraima range, are the easternmost high tepuis in the Guiana Shield. Ayanganna and Wokomung are 37 km apart, and some anuran species occur on both mountains (e.g. in the genus *Stefania*, MacCulloch et al. 2006), although the degree of species overlap is not yet fully known.

Specimens were collected by hand and euthanized by immersion in a solution of MS 222 (ROM specimens) or by immersion in 20% isopropanol (CPI specimen). Tissue (a piece of liver or thigh muscle) was removed from most specimens immediately after euthanasia and preserved in 95–100% ethanol for later molecular analyses.

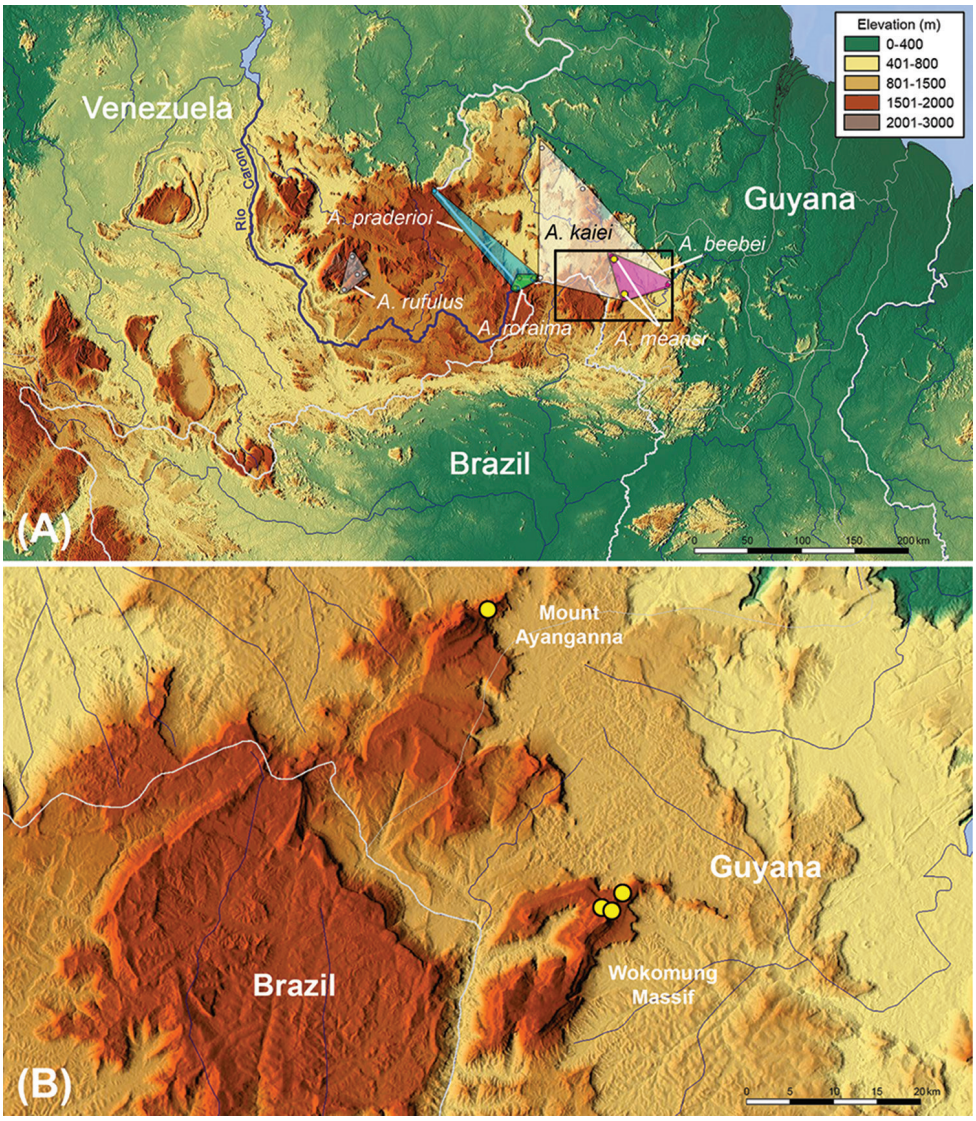

Figure 2. Occurrence map of the *Anomaloglossus* species belonging to the *beebei* group (coloured convex polygons); distribution of *A. meansi* sp. n. is depicted by yellow dots. **A** map of the Eastern Pantepui District; black rectangle is enlarged in **B**. **B** localities of occurrence of *Anomaloglossus meansi* sp. n. based on museum specimens.

Whole individuals were fixed in 10% formalin and later transferred to 70% ethanol for permanent storage. Type specimens have been deposited in the collections of the Royal Ontario Museum, Canada (ROM) and the Coastal Plains Institute and Land Conservancy, USA (CPI); tissue samples were deposited in the Amphibian Evolution Lab, Biology Department, Vrije Universiteit Brussel (VUB) and ROM. Coordinates and elevations were acquired using Global Positioning System units and referenced to map datum WGS84.

Morphology

All morphometric data were taken from the preserved specimens by the same person (MPJN), to the nearest 0.01 mm, under a Leica stereo dissecting microscope using an electronic digital caliper. Colour pattern in life was taken from field notes and colour photographs. Sex and maturity were determined by the presence/absence of vocal slit(s) and by dissection. Comparisons of external character states are based both on original descriptions and examination of museum specimens (see Appendix for comparative material examined). Abbreviations for measurements are as follows:

SVL	snout-vent length
HW	head width, at level of angle of jaws
HL	head length, from angle of jaw to tip of snout
IOD	inter orbital distance
EN	eye to naris distance, from anterior edge of eye to centre of naris
SL	snout length, from anterior edge of eye to tip of snout
TSL	tip of snout length, from centre of naris to tip of snout
IND	internarial distance, the distance between the centres of nares
EL	eye horizontal length
TYM	tympanum horizontal length
HAND I–IV	relative lengths of fingers, from the proximal edge of the palmar tubercle to the tip of each finger
WFD	width of disc on Finger III
FAL	forearm length, from elbow joint to proximal edge of metacarpal tubercle
THL	thigh length, from vent opening to flexed knee
TIL	tibia length, from knee to heel
TAL	tarsus length, from heel to proximal edge of outer metatarsal tubercle
FL	foot length, from proximal edge of inner metatarsal tubercle to tip of Toe IV
WTD	width of disc on Toe IV

Taxonomy

***Anomaloglossus meansi* sp. n.**
http://zoobank.org/84C73332-67F9-4412-8140-CF70F1FB419C
Figures 3–4; Table 1

Anomaloglossus sp. Ayanganna Grant et al. 2006: 120–121, 2017: S66.
Anomaloglossus cf. *praderioi* Kok 2010: 66.
Anomaloglossus sp. B Kok et al. 2012: supplementary information.

Holotype. ROM 43896, adult male from the vicinity of Camp 2 on the Wokomung Massif, Potaro-Siparuni District, Guyana (05°06.5833'N; 059°49.2667'W), 1234 m elevation, collected by A. Lathrop and R. James on 30 October 2004.

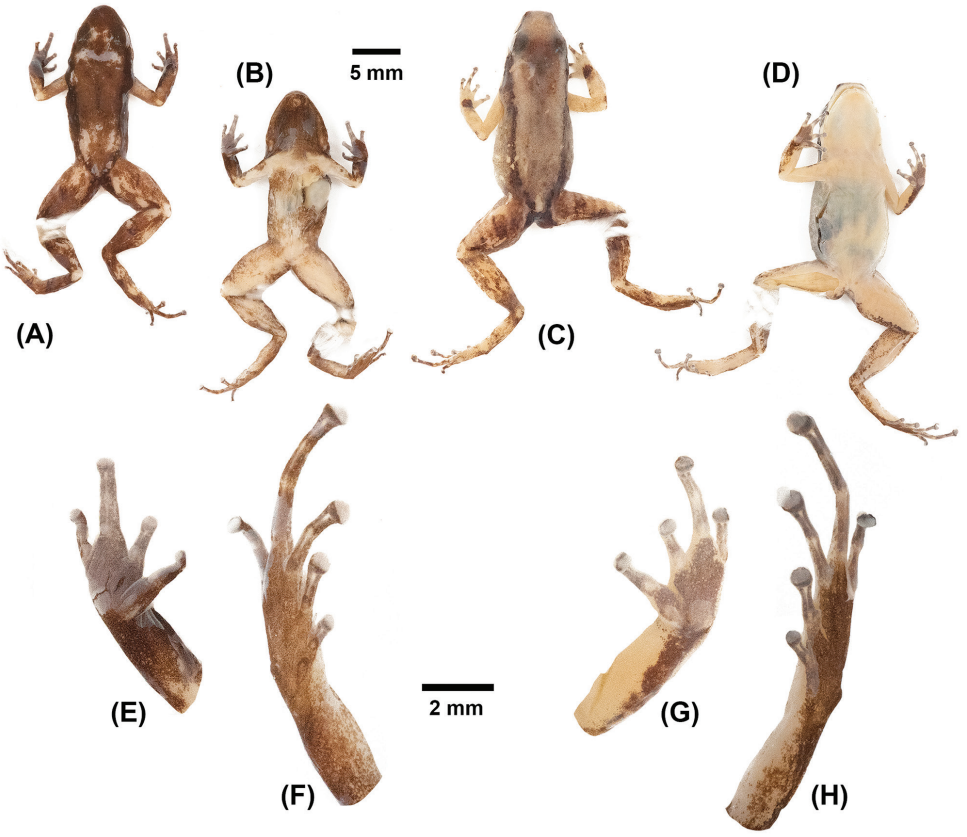

Figure 3. *Anomaloglossus meansi* sp. n. in preservative. **A** male holotype ROM 43896, dorsal view **B** male holotype ROM 43896, ventral view **C** female paratype ROM 43323, dorsal view **D** female paratype ROM 43323, ventral view **E** male holotype ROM 43896, ventral view of right hand **F** male holotype ROM 43896, ventral view of right foot **G** female paratype ROM 43323, ventral view of left hand **H** female paratype ROM 43323, ventral view of left foot.

Paratypes (n = 10). An adult male (ROM 39639) from the northeast plateau of Mount Ayanganna, Cuyuni-Mazaruni District, Guyana (05°24.1'N; 059°57.4'W), 1490 m elevation, collected by R. D. MacCulloch, A. Lathrop and C. Cox on 26 October 2000; four adult females (ROM 43320, ROM 43329, ROM 43331, ROM 43332) from the vicinity of Camp 2 on the Wokomung Massif, Potaro-Siparuni District, Guyana (05°06.5833'N; 059°49.2667'W), 1234 m elevation, collected by A. Lathrop, R. D. MacCulloch and S. Khan between 26–31 October 2004; one adult female (ROM 43323) from the vicinity of Camp 3 on the Wokomung Massif, Potaro-Siparuni District, Guyana (05°05.65'N; 059°50.5833'W), 1411 m elevation, collected by A. Lathrop, R. D. MacCulloch and S. Khan on 3 November 2004; one juvenile (ROM 43322) from the vicinity of Camp 2 on the Wokomung Massif, Potaro-Siparuni District, Guyana (05°06.5833'N; 059°49.2667'W), 1234 m elevation, collected by C. Alban on 26 October 2004; two juveniles (ROM 43324, ROM 43325) from the vicinity of

Table 1. Morphometric measurements (in mm) of the type series of *Anomaloglossus meansi* sp. n. Abbreviations are defined in the text. Means ± SD are followed by the range in parentheses.

Character	Male (n = 3)	Female (n = 5)	Juvenile (n = 3)
SVL	18.53±0.35 (18.15–18.86)	19.15±1.48 (17.66–21.26)	12.72±2.13 (10.69–14.94)
HW	5.89±0.09 (2.19–2.73)	6.11±0.24 (5.81–6.31)	4.28±0.60 (1.48–1.78)
IOD	2.39±0.30 (2.19–2.73)	2.41±0.20 (2.17–2.72)	1.61±0.15 (1.48–1.78)
HL	5.56±0.31 (5.32–5.91)	5.48±0.28 (5.13–5.81)	3.79±0.60 (3.13–4.29)
EN	1.63±0.04 (1.60–1.68)	1.68±0.11 (1.48–1.75)	1.17±0.26 (0.96–1.41)
SL	2.79±0.02 (2.77–2.82)	2.81±0.17 (2.56–3.00)	2.05±0.30 (1.76–2.36)
EL	2.37±0.17 (2.17–2.48)	2.36±0.13 (2.22–2.51)	1.83±0.13 (1.73–1.89)
TYM	1.08±0.04 (1.03–1.12)	1.06±0.14 (0.86–1.24)	0.69±0.15 (0.58–0.86)
IND	2.44±0.05 (2.39–2.48)	2.60±0.16 (2.37–2.82)	1.83±0.24 (1.59–2.07)
TSL	1.24±0.10 (1.15–1.35)	1.41±0.10 (1.29–1.53)	0.87±0.17 (0.74–1.06)
HAND I	3.12±0.20 (2.96–3.35)	3.25±0.13 (3.10–3.45)	1.89±0.70 (3.10–2.69)
HAND II	3.13±0.06 (3.07–3.2)	3.30±0.14 (3.07–3.45)	2.34±0.39 (2.06–2.78)
HANDIII	4.68±0.10 (4.26–4.44)	4.84±0.19 (4.17–4.66)	3.04±0.46 (2.76–3.57)
HAND IV	3.10±0.10 (3.00–3.2)	3.14±0.12 (2.93–3.22)	2.15±0.31 (1.84–2.46)
WFD	0.57±0.07 (0.52–0.65)	0.55±0.06 (0.52–0.65)	0.43±0.06 (0.37–0.47)
FAL	4.27±0.40 (3.81–4.56	4.41±0.41 (3.97–5.04)	2.54±0.84 (1.94–3.51)
THL	8.29±0.42 (7.80–8.54)	8.85±0.28 (8.52–9.18)	5.37±1.07 (4.61–6.60)
TIL	8.45±0.33 (8.07–8.66)	9.09±0.35 (8.61–9.48)	6.13±1.13 (5.12–7.35)
TAL	4.47±0.21 (4.26–4.68)	4.56±0.38 (4.05–5.02)	3.04±0.73 (2.50–3.86)
FL	7.2±0.38 (7.07–7.45)	7.86±0.38 (7.53–8.48)	4.89±1.27 (3.82–6.29)
WTD	0.72±0.06 (0.67–0.78)	0.68±0.06 (0.61–0.76)	0.43±0.03 (0.42–0.46)

Camp 2 on the Wokomung Massif, Potaro-Siparuni District, Guyana (05°06.5833'N; 059°49.2667'W), 1234 m elevation, collected by A. Lathrop, R. D. MacCulloch and S. Khan between 28–31 October 2004; and one adult male (CPI11000) from Falls Camp on the Wokomung Massif, Potaro-Siparuni District, Guyana (05°05.4333'N; 059°50.2833'W), ca. 1371 m elevation, collected by D. Bruce Means on 24 July 2003.

Diagnosis. The following characteristics pertain to preserved specimens unless otherwise noted. A medium-sized *Anomaloglossus* differing from other species in the genus by the following combination of characters: (1) mean SVL in males 18.53 mm (18.15–18.86 mm, n = 3), mean SVL in females 19.15 mm (17.66–21.26, n = 5); (2) skin on dorsum shagreened, venter smooth; (3) tympanic annulus visible anteroventrally; (4) Fingers I and II subequal in length, FI = FII when fingers adpressed; (5) tip of Finger IV not surpassing the base of the distal subarticular tubercle on Finger III when fingers adpressed; (6) distal subarticular tubercle on Finger III and IV present; (7) Finger III swollen in males (conspicuous pre- and postaxial swelling in breeding males); (8) fringes on fingers absent; (9) toes basally webbed, fringes on toes absent; (10) tarsal keel well defined, slightly tubercle-like and weakly curved at proximal end; (11) black arm gland absent, glandular supracarpal pad present in both sexes (larger and more glandular in males); (12) cloacal tubercles absent; (13) pale paracloacal mark present; (14) in life, thin dorsolateral stripe present, from tip of snout to tip of urostyle

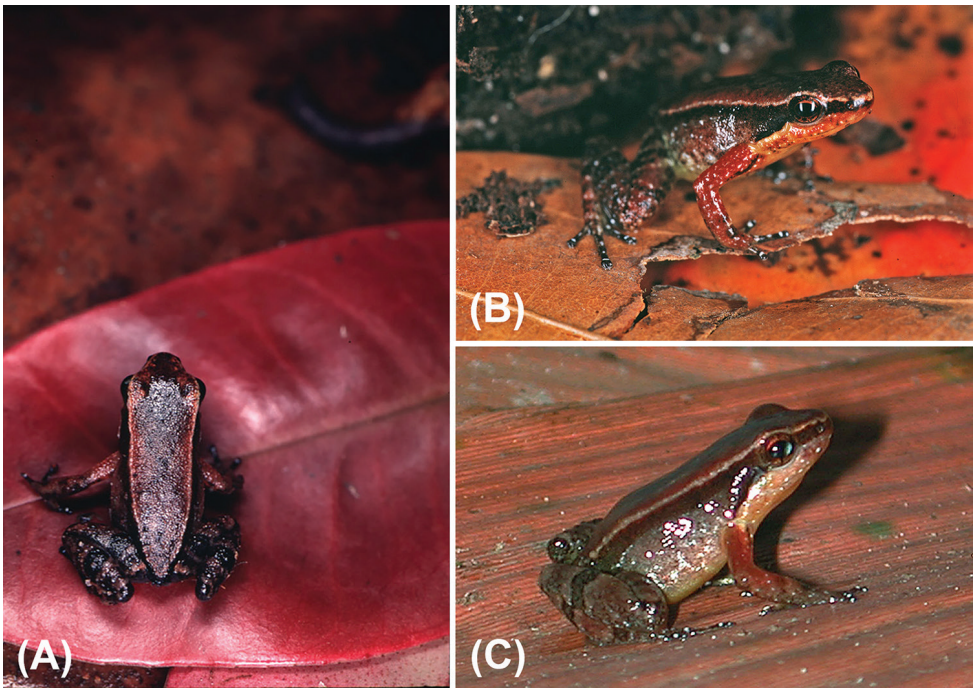

Figure 4. *Anomaloglossus meansi* sp. n. in life. **A** female paratype ROM 43332, dorsal view **B** female paratype ROM 43329, dorsolateral view **C** male paratype CPI 11000, dorsolateral view. Photographs (**A, B**) by AL; photograph (**C**) courtesy D. Bruce Means.

(not visible, or only barely distinguishable in preservative); (15) ventrolateral stripe absent, but presence of irregular white blotches on the lower flank; (16) oblique lateral stripe absent; (17) sexual dichromatism in throat colour pattern: throat heavily pigmented with melanophores in males (dark brown to black in life), immaculate cream in females (yellowish-orange in life); (18) sexual dichromatism in ventral colour pattern: belly pigmented with melanophores in males, immaculate cream in females; (19) in life, iris metallic reddish bronze with fine dark brown reticulation; (20) large intestine extensively pigmented; (21) testes cream, unpigmented; (22) mature oocytes partly pigmented; (23) median lingual process small, longer than wide, tapered; (24) maxillary teeth present, small.

Comparisons. *Anomaloglossus meansi* sp. n. can mainly be distinguished from the four described species belonging to the *degranvillei* group [sensu Vacher et al. 2017 and Fouquet et al. 2018, i.e. *A. blanci* Fouquet, Vacher, Courtois, Villette, Reizine, Gaucher, Jairam, Ouboter & Kok, 2018, *A. degranvillei* (Lescure, 1975), *A. dewynteri* Fouquet, Vacher, Courtois, Villette, Reizine, Gaucher, Jairam, Ouboter & Kok, 2018 and *A. surinamensis* Ouboter & Jairam, 2012; characters in parentheses] by having FI = FII when fingers adpressed (FI > FII), the tympanic annulus anteroventrally conspicuous (inconspicuous), and a conspicuous thin dorsolateral stripe from tip of snout to tip of urostyle (absent or inconspicuous).

Anomaloglossus meansi sp. n. can mainly be distinguished from the four described species belonging to the *stepheni* group [sensu Vacher et al. 2017, i.e. *A. apiau* Fouquet, Souza, Nunes, Kok, Curcio, Carvalho, Grant & Rodrigues, 2015, *A. baeobatrachus* (Boistel & de Massary, 1999), *A. leopardus* Ouboter & Jairam, 2012 and *A. stepheni* (Martins, 1989); characters in parentheses] in lacking an oblique lateral stripe (present, even if short and discontinuous in *A. apiau*), and in having a conspicuous thin dorsolateral stripe from tip of snout to tip of urostyle (absent).

Anomaloglossus meansi sp. n. can mainly be distinguished from the three described species belonging to the *megacephalus* group [sensu Grant et al. 2017, i.e. *A. megacephalus* Kok, MacCulloch, Lathrop, Willaert & Bossuyt, 2010, *A. verbeeksnyderorum* Barrio-Amorós, Santos & Jovanovic, 2010, *A. wothuja* (Barrio-Amorós, Fuentes-Ramos & Rivas-Fuenmayor, 2004); characters in parentheses] in having only basal toe webbing (moderate to extensive), in lacking an oblique lateral stripe (present, even if short and/or discontinuous), and in having a conspicuous thin dorsolateral stripe from tip of snout to tip of urostyle (absent).

Compared to the other five species belonging to the *beebei* group [sensu Grant et al. 2017, i.e. *A. beebei* (Noble, 1923), *A. kaiei* (Kok, Sambhu, Roopsind, Lenglet & Bourne, 2006), *A. praderioi*, *A. roraima* (La Marca, 1997) and *A. rufulus* (Gorzula, 1990)], *A. meansi* sp. n. can easily be distinguished from *A. beebei* by its larger size in males (maximum SVL 18.86 mm in *A. meansi* [n = 3,] versus maximum SVL 16.80 mm [n=18] in *A. beebei*), smooth ventral skin (granular in *A. beebei*), basal toe webbing (moderate in *A. beebei*), and in having a conspicuous thin dorsolateral stripe from tip of snout to tip of urostyle (absent or originating from the posterior corner of eye); from *A. kaiei* in having a conspicuous thin dorsolateral stripe from tip of snout to tip of urostyle (originating from the posterior corner of eye in *A. kaiei*) and a black throat in preserved males (greyish, never black in *A. kaiei*); from *A. roraima* by its larger size in females (maximum SVL 21.26 mm in *A. meansi* [n = 3,] versus maximum SVL 19.30 mm [n = 18] in *A. roraima*), smooth ventral skin (granular in *A. roraima*), and in having a conspicuous thin dorsolateral stripe from tip of snout to tip of urostyle (when present originating from the anterior or posterior corner of eye in *A. roraima*); from *A. rufulus* in having a conspicuous thin dorsolateral stripe from tip of snout to tip of urostyle (absent in *A. rufulus*) and the posterior part of belly unmarked (heavily marbled in *A. rufulus*). *Anomaloglossus meansi* sp. n. is most similar to *A. praderioi* with which it shares a conspicuous thin dorsolateral stripe from tip of snout to tip of urostyle but is immediately distinguished by its smaller size in males (maximum SVL 18.86 mm in *A. meansi* [n = 3,] versus maximum SVL 22.40 mm [n = 11] in *A. praderioi*), the absence of fringes on toes (extensive in *A. praderioi*), Finger III with pre- and postaxial swelling in breeding males (preaxial swelling only in *A. praderioi*), less toe webbing (compare Figure 3 with figure 2 in Kok 2010), and the lack of black spots on chest and lower flanks in males (present in *A. praderioi*).

Compared to the remainder 12 *Anomaloglossus* species not yet assigned to any group [*A. ayarzaguenai* (La Marca, 1997), *A. breweri* (Barrio-Amorós, 2006), *A. guanayensis* (La Marca, 1997), *A. moffetti* Barrio-Amorós & Brewer-Carías, 2008, *A. murisipanensis*

(La Marca, 1997), *A. parimae* (La Marca, 1997), *A. parkerae* (Meinhardt & Parmelee, 1996), *A. shrevei* (Rivero, 1961), *A. tamacuarensis* (Myers & Donnelly, 1997), *A. tepequem* Fouquet, Souza, Nunes, Kok, Curcio, Carvalho, Grant & Rodrigues, 2015, *A. tepuyensis* (La Marca, 1997) and *A. triunfo* (Barrio-Amorós, Fuentes-Ramos & Rivas-Fuenmayor, 2004); characters in parentheses], *A. meansi* sp. n. mainly differs in having only basal toe webbing (moderate to extensive), and in having a conspicuous thin dorsolateral stripe from tip of snout to tip of urostyle (absent).

Description of the holotype. Adult male (ROM 43896; Figure 3), 18.58 mm SVL, in suboptimal state of preservation (extensive ventral incisions, dorsal skin locally damaged); body robust; head as wide as long, HL 99.7% of HW, HW 32% of SVL; dorsal skin shagreened; ventral skin smooth; snout moderately long, SL 47% of HL, 128% of EL, round in dorsal view, protruding in lateral view, extending past lower jaw; nares located close to tip of snout, directed posterolaterally, visible from front, barely visible in dorsal and ventral views, EN 28% of HL, 77% of ED, EN 60% of SL, TSL 49% of SL; posterior rim of naris bordered posteriorly by an inconspicuous crescent-shaped ridge; IND 40% of HW; canthus rostralis rounded; loreal region concave; IOD 104% of EL, longer than upper eyelid; postrictal tubercles low and inconspicuous; tympanic membrane inconspicuous, round, concealed posterodorsally by a diffuse supratympanic swelling; tympanic annulus visible anteroventrally, TYM 52 % of EL; choanae small, circular, located anterolaterally. Maxillary teeth present, small. Tongue longer than wide, free posteriorly, with rounded margin, small median lingual process longer than wide, tapered. Vocal slits bilateral, large, extending from edge of tongue to angle of jaw.

Forelimb swollen, robust, 94% of FAL. Ulnar fold absent, metacarpal ridge absent; swollen, glandular supracarpal pad present, heavily pigmented with melanophores; hand moderate in size, 24% of SVL, 75% of HW; relative length of fingers III>II=I=IV; pre- and postaxial swelling on third finger (i.e. Finger III swollen); fingers without fringes; tip of Finger IV not reaching distal subarticular tubercle on Finger III when fingers adpressed; finger discs expanded, wider than long, about 1.4 times width of digit; width of disc on Finger III 0.52 mm; palmar tubercle large, egg shaped, 0.72 mm (larger than Finger III disc), thenar tubercle smaller, elliptical; one or two round to ovoid subarticular tubercles (one each on Fingers I and II, two each on Fingers III and IV, with distal tubercle on Finger IV less conspicuous).

Hind limb robust, moderately long, with heel of adpressed leg reaching posterior corner of eye; skin granular with no cloacal tubercles discernible (but this could be an artefact of preservation); TL 46% of SVL, heels not in contact when hind limbs are flexed at right angle to sagittal plane of body; FL 38% of SVL; relative length of adpressed toes IV>III>V>II>I; Toe I very short, its tip barely reaching the base of subarticular tubercle of Toe II when adpressed; toe discs larger than width of toes; disc on Toe I only slightly larger than width of digit; width of disc on Toe IV 0.67 mm; toes basally webbed, lateral fringes absent; one to three round to ovoid subarticular tubercles (one each on Toes I and II, two each on Toes III and V, and three on Toe IV, with distal tubercle on Toe IV the smallest and least conspicuous). Inner metatarsal tubercle protuberant elliptical**,** 0.47 mm in length, outer metatarsal tubercle round, protuber-

ant, pigmented, 0.35 mm in diameter. No medial metatarsal tubercle discernible. Tarsal keel slightly tubercle-like and weakly curved at proximal end, extending distally to preaxial edge of Toe I. Metatarsal fold not visible.

Colour of holotype in life. Dorsal ground colour chestnut brown with a short black middorsal line between shoulders. A black line from snout tip through eye, extending dorsolaterally to groin. A narrow pale brown dorsolateral stripe above this line, blending into the chestnut dorsal ground colour. Upper surface of limbs light brown proximally, becoming dark brown distally. Flanks reddish brown with yellow spots on lower flanks. Venter pale brown with dark brown mottling, throat very dark brown to black. Underside of limbs orange-red, changing to dark reddish brown on distal forearms.

Colour of holotype in preservative. After more than 13 years in preservative, dorsal ground colour became dark chestnut brown with a short middorsal black longitudinal line in the scapular region. No other dorsal marking present. Dorsal surface of arms varies from light brown proximally to dark brown, purplish-black towards the granular supracarpal pads. Dorsal surface of legs light brown with darker brown markings. Flanks dark brown to purplish-black with pale spots on lower flanks. Narrow pale brown dorsolateral stripes indistinguishable from dorsal ground colour, although the black dorsolateral stripe remains visible. Throat black, heavily pigmented with melanophores; belly cream, pigmented with melanophores (less densely distributed than on throat). Pale paracloacal marks are visible. Palms dark brown, soles medium brown (Figure 3).

Measurements of holotype (in mm). SVL = 18.58; HL = 5.91; HW = 5.93; IOD = 2.26; EN = 1.68; SL = 2.77; TSL = 1.35; EL = 2.16; TYM = 1.12; IND = 2.39; HAND I = 3.06; HAND II = 3.2; HAND III = 4.44; HAND IV = 3.09; WFD = 0.52; FAL = 3.81; THL = 7.80; TIL = 8.61; TAL = 4.48; FL = 7.08; WTD = 0.67.

Sexual dimorphism and variation within the type series. Males are usually smaller than females, 18.15–18.86 mm SVL (n = 3) versus 17.66–21.26 mm SVL (n = 5) in females, with Finger III distinctly swollen in breeding males (Figure 3). Supracarpal pads are less extended and less glandular in females and juveniles than in males. Colouration is sexually dichromatic; throat heavily pigmented black in males (immaculate yellowish-orange in females), and belly yellowish-orange pigmented with melanophores in males (immaculate yellowish-orange in females) (Figure 3). Venter immaculate in juveniles, although small pigmented areas on throat may occur (presumably in juvenile males).

Morphometric variation is summarized in Table 1, illustrations of a male and a female paratype in life are in Figure 4. Snout in dorsal and ventral views varies from round to truncate (the latter more particularly in females, see Figure 3).

There is substantial variation in colour among preserved individuals, obviously due to preservation artefact (CPI11000 for instance is much lighter than all other individuals). Lower lip pigmented in all male and juvenile individuals, but only in three out of five females. The interorbital region is usually darker than the dorsal ground colour. A short middorsal dark brown/black longitudinal line usually present in the scapular region. One female (ROM 43329) has a diffuse diamond shape marking on the anterior dorsum. Upper surface of arms and legs is cream to dark brown, with darker markings

Figure 5. Habitat of *Anomaloglossus meansi* sp. n. on the Wokomung Massif **A** photograph (looking NE) of the highest part of the massif; the plateau in the centre of the photo is the tallest part of the entire Wokomung Massif **B** cloud forest at about 1385 m elevation, habitat of *Anomaloglossus meansi* sp. n. Photographs courtesy D. Bruce Means.

on legs. Palms and soles are light to dark brown. Flanks vary from cream to very dark purplish brown.

Distribution and natural history. The only localities documented for the new species are depicted in Figure 2. Specimens were collected in cloud forest (Figure 5), on the ground or low vegetation. Most were collected after nightfall, although one adult and one juvenile were collected during daylight. Specimens were collected on mountain flanks, not summits; at 1490 m on Ayanganna, and at 1234 m, 1371 m and 1411 m on Wokomung. The majority of specimens (eight) were collected at 1234 m on Wokomung. Fewer were collected at higher elevations; only one each at 1490 m on Ayanganna, 1371 m and 1411 m on Wokomung. This may have been because of habitat differences; high-canopy open forest at lower elevation and dense, low-canopy vegetation at higher elevations (see Discussion).

Etymology. It is a great pleasure to name this new species after our friend and colleague D. Bruce Means, indefatigable explorer of the "islands in the sky", and who collected one specimen of the new species and contributed with photographs and data. Thanks to his extensive fieldwork, Bruce Means greatly contributed to our understanding of the distribution, ecology, and taxonomy of Pantepui amphibians and reptiles. The specific epithet should be treated as a noun in the genitive case.

Phylogenetic relationships. The new species was recovered sister to *Anomaloglossus praderioi* by Grant et al. (2006, 2017) and Kok et al. (2012) (see Figure 1). Uncorrected *p* distance in the "barcoding" fragment of the 16S rRNA gene [Vences et al. (2005); based on the sequences used in Grant et al. (2017) and calculated in PAUP 4.0a161 (Swofford 2002)] is 4.3-4.8% between *Anomaloglossus praderioi* and *A. meansi*

sp. n. Genetic divergence between populations of *A. praderioi* from the slopes of Roraima-tepui and Maringma-tepui is 0.2%, whereas divergence between populations of *A. meansi* sp. n. from Mount Ayanganna and the Wokomung Massif is 0.9–1.0%.

Conservation status. *Anomaloglossus meansi* sp. n. is only known from four localities and the 11 specimens used in the description. Virtually nothing is known about its ecology, breeding behaviour and population density. Given the uncertainty on its population status we suggest *Anomaloglossus meansi* sp. n. to be listed as Data Deficient according to the IUCN Red List category guidelines (2014).

Discussion. Although Ayanganna and Wokomung are close neighbours, the habitats on their slopes are not exactly similar. The slopes of Ayanganna are a series of relatively flat poorly drained plateaus alternating with steeper slopes. Collecting activities were concentrated on the plateaus, where the vegetation consists of dense, low-canopy high-tepui forest, with a dense understory of woody shrubs and large terrestrial bromeliads (MacCulloch and Lathrop 2009).

The slopes of Wokomung have no large flat plateaus. Habitat at the collecting sites consists of well-drained slopes covered in lower montane cloud forest with some epiphytes and medium density understory, including scattered terrestrial bromeliads. Streams were common on the slopes (MacCulloch et al. 2006). The majority of specimens were found in this habitat, and this may indicate that *Anomaloglossus meansi* sp. n. prefers this to other habitat types; or is a reflection of collecting effort in these habitats.

Species in the *Anomaloglossus beebei* group are currently only known from east of the Rio Caroní, in the Eastern Pantepui District. *Anomaloglossus rufulus* is restricted to the highlands of the eastern part of the Chimantá Massif in Venezuela, whereas *A. kaiei* has a rather large distribution in the uplands of the Pakaraima Mountains of Guyana (Figure 2). The sister species *A. roraima* and *A. beebei* are allopatric, *A. roraima* being restricted to the highlands of the eastern tip of the Eastern Tepui Chain, whereas *A. beebei* is reported further to the east in the uplands of Kaieteur National Park, the Wokomung Massif and Mount Ayanganna (Figure 2). A similar spatial distribution is detected in the sister species *A. praderioi* and *A. meansi* sp. n., which are also allopatric, with *A. praderioi* reported from the uplands of the Eastern Tepui Chain, whereas *A. meansi* sp. n. is only known further to the east in the uplands of Mount Wokomung and Mount Ayanganna.

As mentioned above, virtually nothing is known about the ecology of *A. meansi* sp. n. Based on its phylogenetic position it is likely this species has an exotrophic, lentic tadpole (Figure 1). Comprehensive ecological data are crucial for the assessment of species conservation status, but these assessments are known for a few species only in the Pantepui region and there is a high risk that population declines remain unnoticed in such remote areas.

Two additional phylogenetically distinct species of *Anomaloglossus* remain to be described in the *megacephalus* group (see Grant et al. 2017; the authors, in progress), but several locally restricted *Anomaloglossus* species probably await discovery (Vacher et al. 2017).

Acknowledgments

PJRK is supported by a postdoctoral fellowship from the Fonds voor Wetenschappelijk Onderzoek Vlaanderen (FWO12A7617N). AL and RDM were supported by grants from the Royal Ontario Museum Governors and Department of Natural History. Permission to conduct this study in indigenous lands in the Pakaraima Mountains of Guyana was granted by the Guyanese Ministry of Amerindian Affairs. Research and export permits were issued by the Guyana Environmental Protection Agency. We thank the following curators and collection managers for their assistance and access to collections under their care: F.J. Bisbal, E. Camargo, R. Rivero, J. Sánchez (Museo de la Estación Biología de Rancho Grande, Maracay, Venezuela; EBRG), E. La Marca (Universidad de los Andes, Departamento de Geografía, Mérida, Venezuela; ULABG), M. Salazar (Universidad Central de Venezuela, Museo de Biología, Caracas, Venezuela; MBUCV), and J.C. Señaris (Museo de Historia Natural La Salle, Caracas, Venezuela; MHNLS). K. Roelants (Vrije Universiteit Brussel, Belgium) kindly drew the figures used in Figure 1. We also thank A. Fouquet (Laboratoire Écologie, évolution, interactions des systèmes amazoniens, Université de Guyane, Cayenne, French Guiana) and E. La Marca (ULABG) for constructive comments on an earlier version of this manuscript.

References

Barrio-Amorós CL (2006) A new dendrobatid frog (Anura: Dendrobatidae: *Colostethus*) from Aprada tepui, southern Venezuela. Zootaxa 1110: 59–68.

Barrio-Amorós CL, Santos JC, Jovanovic O (2010) A new dendrobatid frog (Anura: Dendrobatidae: *Anomaloglossus*) from the Orinoquian rainforest, southern Venezuela. Zootaxa 2413: 37–50.

Barrio-Amorós CL, Fuentes-Ramos O, Rivas-Fuenmayor GA (2004) Two new species of *Colostethus* (Anura: Dendrobatidae) from the Venezuelan Guayana. Salamandra 40: 183–200.

Barrio-Amorós CL, Brewer-Carías C (2008) Herpetological results of the 2002 expedition to Sarisariñama, a tepui in Venezuelan Guayana, with the description of five new species. Zootaxa 1942: 1–68.

Boistel R, de Massary J-C (1999) Les amphibiens vénéneux de la famille des dendrobatidés. Le Courrier de la Nature 176: 34–39.

Fouquet A, Souza SM, Nunes PMS, Kok PJR, Curcio FF, de Carvalho CM, Grant T, Rodrigues MT (2015) Two new endangered species of *Anomaloglossus* (Anura: Aromobatidae) from Roraima State, northern Brazil. Zootaxa 3926: 191–210. https://doi.org/10.11646/zootaxa.3926.2.2

Fouquet A, Vacher J-P, Courtois E, Villette B, Reizine H, Gaucher P, Jairam R, Ouboter P, Kok PJR (2018) On the brink of extinction: two new species of *Anomaloglossus* from French Guiana and amended definition of *Anomaloglossus degranvillei* and *A. surinamensis* (Anura: Aromobatidae). Zootaxa 4379: 001–023. https://doi.org/10.11646/zootaxa.4379.1.1

Gorzula SJ (1990 "1988") Una nueva especie de *Dendrobates* (Amphibia: Dendrobatidae) del Macizo del Chimantá, Estado Bolívar, Venezuela. Memoria. Sociedad de Ciencias Naturales La Salle 48: 143–149.

Grant T, Frost DR, Caldwell JP, Gagliardo R, Haddad CF, Kok PJR, Means DB, Noonan BP, Schargel WE, Wheeler WC (2006) Phylogenetic systematics of dart-poison frogs and their relatives (Amphibia: Athesphatanura: Dendrobatidae). Bulletin of the American Museum of Natural History 299: 1–262. https://doi.org/10.1206/0003-0090(2006)299[1:PSODFA]2.0.CO;2

Grant T, Rada M, Anganoy-Criollo M, Batista A, Dias PE, Jeckel AM, Machado DJ, Rueda-Almonacid JV (2017) Phylogenetic systematics of dart-poison frogs and their relatives revisited (Anura: Dendrobatoidea). South American Journal of Herpetology 12 (Special Issue 1): S1–S90. https://doi.org/10.2994/SAJH-D-17-00017.1

IUCN Standards and Petitions Subcommittee (2014) Guidelines for Using the IUCN Red List Categories and Criteria. Version 11. Prepared by the Standards and Petitions Subcommittee. http://www.iucnredlist.org/documents/ RedListGuidelines.pdf

Kok PJR (2010) A redescription of *Anomaloglossus praderioi* (La Marca, 1998) (Anura: Aromobatidae: Anomaloglossinae), with description of its tadpole and call. Papéis Avulsos de Zoologia 50: 51–68.

Kok PJR (2013) Islands in the Sky: Species Diversity, Evolutionary History, and Patterns of Endemism of the Pantepui Herpetofauna. PhD thesis, Leiden, The Netherlands: Leiden University.

Kok PJR, Sambhu H, Roopsind I, Lenglet GL, Bourne GR (2006) A new species of *Colostethus* (Anura: Dendrobatidae) with maternal care from Kaieteur National Park, Guyana. Zootaxa 1238: 35–61.

Kok PJR, MacCulloch RD, Lathrop A, Willaert B, Bossuyt F (2010) A new species of *Anomaloglossus* (Anura: Aromobatidae) from the Pakaraima Mountains of Guyana. Zootaxa 2660: 18–32.

Kok PJR, MacCulloch RD, Means DB, Roelants K, Van Bocxlaer I, Bossuyt F (2012) Low genetic diversity in tepui summit vertebrates. Current Biology 22(15): R589–R590. https://doi.org/10.1016/j.cub.2012.06.034

Kok PJR, Russo VG, Ratz S, Means DB, MacCulloch RD, Lathrop A, Aubret F, Bossuyt F (2017) Evolution in the South American 'Lost World': insights from multilocus phylogeography of stefanias (Anura, Hemiphractidae, *Stefania*). Journal of Biogeography 44(1): 170–181. https://doi.org/10.1111/jbi.12860

Kok PJR, Ratz S, MacCulloch RD, Lathrop A, Dezfoulian R, Aubret F, Means DB (2018a) Historical biogeography of the palaeoendemic toad genus *Oreophrynella* (Amphibia: Bufonidae) sheds a new light on the origin of the Pantepui endemic terrestrial biota. Journal of Biogeography 45(1): 26–36. https://doi.org/10.1111/jbi.13093

Kok PJR, Bittenbinder MA, van den Berg JK, Marques-Souza S, Sales Nunes PM, Laking AE, Teixeira Jr M, Fouquet A, Means DB, MacCulloch RD, Rodrigues MT (2018b) Integrative taxonomy of the gymnophthalmid lizard *Neusticurus rudis* Boulenger, 1900 identifies a new species in the eastern Pantepui region, north-eastern South America, Journal of Natural History 52: 1029–1066. https://doi.org/10.1080/00222933.2018.1439541

La Marca E (1997 "1996") Ranas del genero *Colostethus* (Amphibia: Anura: Dendrobatidae) de la Guayana Venezolana con la descripción de siete especies nuevas. Publicaciones de la Asociación de Amigos de Doñana 9: 1–64.

Lehmberg ES, Elbassiouny AA, Bloom DD, Lopez-Fernandez H, Crampton WGR, Lovejoy NR (2018) Fish biogeography in the "Lost World" of the Guiana Shield: Phylogeography of the weakly electric knifefish *Gymnotus carapo* (Teleostei: Gymnotidae). Journal of Biogeography. https://doi.org/10.1111/jbi.13177

Leite YLR, Kok PJR, Weksler M (2015) Evolutionary affinities of the "Lost World" mouse suggest a late Pliocene connection between the Guiana and Brazilian shields. Journal of Biogeography 42: 706–715. https://doi.org/10.1111/jbi.12461

Lescure J (1975) Contribution à l'étude des amphibiens de Guyane Française. III. Une nouvelle espèce de *Colostethus* (Dendrobatidae): *Colostethus degranvillei* n. sp. Bulletin du Museum National d'Histoire Naturelle, Série 3, Zoologie 293: 413–420.

MacCulloch RD, Lathrop A (2009) Herpetofauna of Mount Ayanganna, Guyana. Results of the Royal Ontario Museum Ayanganna Expedition 2000. Royal Ontario Museum Science Contributions 4: 1–36.

MacCulloch RD, Lathrop A, Khan SZ (2006) Exceptional diversity of *Stefania* (Anura: Cryptobatrachidae) II: six species from Mount Wokomung, Guyana. Phyllomedusa 5: 31–41. https://doi.org/10.11606/issn.2316-9079.v5i1p31-41

Martins M (1989) Nova espécie de *Colostethus* da Amazónia central (Amphibia: Dendrobatidae). Revista Brasileira de Biologia 49: 1009–1012.

Mayr E, Phelps WS (1967) The origin of the bird fauna of the south Venezuelan highlands. Bulletin of the American Museum of Natural History 136: 269–328.

Meinhardt DJ, Parmelee JR (1996) A new species of *Colostethus* (Anura: Dendrobatidae) from Venezuela. Herpetologica 52: 70–77.

Myers CW, Donnelly MA (1997) A tepui herpetofauna on a granitic mountain (Tamacuari) in the borderland between Venezuela and Brazil: Report from the Phipps Tapirapecó Expedition. American Museum Novitates 3213: 1–71.

Myers CW, Donnelly MA (2008) The summit herpetofauna of Auyantepui, Venezuela: report from the Robert G. Goelet American Museum-Terramar Expedition. Bulletin of the American Museum of Natural History 308: 1–147. https://doi.org/10.1206/308.1

Noble GK (1923) New batrachians from the Tropical Research Station British Guiana. Zoologica 3: 289–299.

Nogué S, Rull V, Vegas-Vilarrúbia T (2009) Modeling biodiversity loss by global warming on Pantepui, northern South America: projected upward migration and potential habitat loss. Climatic Change 94: 77–85. https://doi.org/10.1007/s10584-009-9554-x

Ouboter PE, Jairam R (2012) Amphibians of Suriname. Brill, Leiden, 376 pp.

Rivero JA (1961) Salientia of Venezuela. Bulletin of the Museum of Comparative Zoology 126: 1–207.

Rull V, Vegas-Vilarrúbia T (2006) Unexpected biodiversity loss under global warming in the neotropical Guayana Highlands. Global Change Biology 12: 1–9. https://doi.org/10.1111/j.1365-2486.2005.001080.x

Swofford DL (2002) PAUP*. Phylogenetic Analysis Using Parsimony (*and Other Methods). Version 4. Sinauer Associates, Sunderland, Massachusetts.

Vacher J-P, Kok PJR, Rodrigues MT, Dias Lima J, Lorenzini A, Martinez Q, Fallet M, Courtois EA, Blanc M, Gaucher P, Dewynter M, Jairam R, Ouboter P, Thébaud C, Fouquet A (2017) Cryptic diversity in Amazonian frogs: integrative taxonomy of the genus *Anomaloglossus* (Amphibia: Anura: Aromobatidae) reveals a unique case of diversification within the Guiana Shield. Molecular Phylogenetics and Evolution 112: 158–173. https://doi.org/10.1016/j.ympev.2017.04.017

Vences M, Thomas M, van der Meijden A, Chiari Y, Vieites DR (2005) Comparative performance of the 16S rRNA gene in DNA barcoding of amphibians. Frontiers in Zoology 2: 5. https://doi.org/10.1186/1742-9994-2-5

Appendix 1

Comparative material examined

Anomaloglossus ayarzaguenai: Venezuela, Estado Bolívar, Cerro Jaua, MHNLS 12949 (holotype), MHNLS 12950–51 (2 paratypes).

Anomaloglossus beebei: Guyana, Potaro-Siparuni District, Kaieteur National Park, IRSNB 13721–26, 13728–53, ULABG 6817 (ex IRSNB 13727).

Anomaloglossus breweri: Venezuela, Estado Bolívar, Aprada-tepui, Cueva del Fantasma, MHNLS 17044 (holotype), MHNLS 17045–46 (2 paratypes).

Anomaloglossus guanayensis: Venezuela, Estado Bolívar, Serranía de Guanay, MHNLS 10708 (holotype), MHNLS 10712–10714 (3 paratypes), 10716–10717 (2 paratypes), 10724–10725 (2 paratypes).

Anomaloglossus kaiei: Guyana, Potaro-Siparuni District, Kaieteur National Park, IRSNB 1938 (holotype), IRSNB 1939–64 (26 paratypes), IRSNB 14420–57, ROM 42999; Cuyuni-Mazaruni District, Wayalayeng, IRSNB 14922–24, Maringma-tepui, IRSNB 14925–31, Mount Wokomung, ROM 43321, ROM 43327, ROM 43330, ROM 43333.

Anomaloglossus megacephalus: Guyana, Cuyuni-Mazaruni District, Maringma-tepui, IRSNB 1986 (holotype), Mount Ayanganna, ROM 39637–38 (2 paratypes).

Anomaloglossus moffetti: Venezuela, Estado Bolívar, Sarisariñama-tepui, EBRG 4645 (holotype), EBRG 4646–51 (6 paratypes).

Anomaloglossus murisipanensis: Venezuela, Estado Bolívar, Murisipán-tepui, MHNLS 11385 (holotype).

Anomaloglossus parimae: Venezuela, Estado Amazonas, Cerro Delgado Chalbaud, ULABG 4221 (holotype), ULABG 4212–20 (9 paratypes), ULABG 4222–26 (5 paratypes).

Anomaloglossus parkerae: Venezuela, Estado Bolívar, Sierra de Lema, Salto El Danto, MHNLS 2901, MHNLS 11088–89.

Anomaloglossus praderioi: Guyana, Cuyuni-Mazaruni District, Maringma-tepui, IRSNB 11403–13; Venezuela, Estado Bolívar, Mount Roraima ULABG 4196 (holotype), MHNLS 11272 (paratype), Sierra de Lema, EBRG 5569.

Anomaloglossus roraima: Guyana, Cuyuni-Mazaruni District, Wei-Assipu-tepui, IRSNB 15851, IRSNB 15865, IRSNB 15904–11, Maringma-tepui, IRSNB 15864, IRSNB 15883–901; Venezuela, Estado Bolívar, Mount Roraima, ULABG 4197 (holotype).

Anomaloglossus rufulus: Venezuela, Estado Bolívar, Amari-tepui, Chimantá Massif, MHNLS 10361 (holotype).

Anomaloglossus tamacuarensis: Venezuela, Estado Amazonas, Sierra Tapirapecó, north base of Pico Tamacuari, MBUCV 6430–33 (4 paratypes).

Anomaloglossus tepuyensis: Venezuela, Estado Bolívar, Auyán-tepui, ULABG 2557 (holotype).

Anomaloglossus triunfo: Venezuela, Estado Bolívar, Cerro Santa Rosa, Serranía del Supamo, EBRG 4756 (holotype), EBRG 4757–59 (3 paratypes).

Anomaloglossus verbeeksnyderorum: Venezuela, Estado Amazonas, Tobogán de la Selva, Municipio Atures, MHNLS 19649 (holotype).

Anomaloglossus wothuja: Venezuela, Estado Amazonas, base of Cerro Sipapo, Tobogán del Cuao, EBRG 6689 (holotype).

ZooKeys 759: 117–136 (2018)
doi: 10.3897/zookeys.759.24810
http://zookeys.pensoft.net

DATA PAPER

A peer-reviewed open-access journal
ZooKeys
Launched to accelerate biodiversity research

The inland water macro-invertebrate occurrences in Flanders, Belgium

Rudy Vannevel[1], Dimitri Brosens[2], Ward De Cooman[1], Wim Gabriels[1], Frank Lavens[1], Joost Mertens[1], Bart Vervaeke[1]

1 *Flanders Environment Agency (VMM), Dr. De Moorstraat 24-26, B-9300 Aalst, Belgium* **2** *Research Institute for Nature and Forest (INBO), Havenlaan 88 bus 73, B-1000 Brussels, Belgium*

Corresponding authors: *Bart Vervaeke* (b.vervaeke@vmm.be); *Ward De Cooman* (w.decooman@vmm.be); *Rudy Vannevel* (r.vannevel@vmm.be)

Academic editor: *P. Stoev* | Received 8 March 2018 | Accepted 24 April 2018 | Published 22 May 2018

http://zoobank.org/B74A09F1-799D-4820-8CE9-E8F727BBDE1F

Citation: Vannevel R, Brosens D, De Cooman W, Gabriels W, Lavens F, Mertens J, Vervaeke B (2018) The inland water macro-invertebrate occurrences in Flanders, Belgium. ZooKeys 759: 117–136. https://doi.org/10.3897/zookeys.759.24810

Abstract

The Flanders Environment Agency (VMM) has been performing biological water quality assessments on inland waters in Flanders (Belgium) since 1989 and sediment quality assessments since 2000. The water quality monitoring network is a combined physico-chemical and biological network, the biological component focusing on macro-invertebrates. The sediment monitoring programme produces biological data to assess the sediment quality. Both monitoring programmes aim to provide index values, applying a similar conceptual methodology based on the presence of macro-invertebrates. The biological data obtained from both monitoring networks are consolidated in the VMM macro-invertebrates database and include identifications at family and genus level of the freshwater phyla Coelenterata, Platyhelminthes, Annelida, Mollusca, and Arthropoda. This paper discusses the content of this database, and the dataset published thereof: 282,309 records of 210 observed taxa from 4,140 monitoring sites located on 657 different water bodies, collected during 22,663 events. This paper provides some background information on the methodology, temporal and spatial coverage, and taxonomy, and describes the content of the dataset. The data are distributed as open data under the Creative Commons CC-BY license.

Keywords

Biotic indices, Flanders Environment Agency (VMM), macro-invertebrates, sediments, water quality

Origin and context of the observations

Biotic indices and monitoring networks

The macro-invertebrates dataset contains data on the occurrence of macro-invertebrates in inland water bodies, obtained from water and sediment quality assessments. The objective of the assessments is to provide biotic index values. Biotic indices are based on two properties: the number of taxa indicating the biodiversity, and the sensitivity of organisms (of a selected number of taxa) to (mainly organic) pollution. Biotic indices based on macro-invertebrates complement the physico-chemical water quality and are commonly considered as pollution indicators (hence they are called water quality indices), although they also partially reflect overall habitat conditions. Higher biotic index values tend to reflect the general water body or habitat status; lower values indicate the water quality conditions, of which the oxygen level prevails. Since biotic indices are intended for quick and practical use, numbers of organisms are estimated and the identification level is restricted.

The biological water-quality monitoring programme based on macro-invertebrates was initiated by Belgian national legislation in 1987. It was further developed in the 1990s by the Flemish authorities responsible for water quality control of surface waters, to meet regional environmental legislation. After 2000, it was redirected in support of the Water Framework Directive (WFD, 2000/60 EC). The water quality monitoring network is developed by the Flanders Environment Agency (VMM, https://www.vmm.be/) and its preceding Flemish water authorities involved in wastewater and sanitation to assess the quality status of water bodies in Flanders. The quality is assessed by means of biotic indices: the Belgian Biotic Index (BBI) (De Pauw and Vanhooren 1983; De Pauw and Vannevel 1991; NBN 1984) and the Multimetric Macroinvertebrate Index Flanders (MMIF) (Gabriels et al. 2010). These indices aim to assess water quality of (mainly impacted) public waters on an annual or multi-annual basis in different water types of both freshwater and brackish aquatic systems. Related biological quality elements include diatoms, macrophytes, and fish.

The sediments quality-monitoring network was developed in 2000 to support decision-making on the dredging of waterways. Between 1992 and 2000, sediment monitoring was part of research programmes of which the results are also included in the dataset. The macro-invertebrates are one element of the Sediment Quality index, completing information on sediments quantity and substrate composition. The methodology is described by De Deckere et al. (2000), De Pauw et al. (2000), and De Pauw and Heylen (2001), and deals with sediment characterization by means of the TRIAD approach (AMINAL 1998). This threefold approach combines a biological, ecotoxicological and physical-chemical component.

The VMM water quality database contains data on occurrence, abundance, habitat conditions, pollutants, quality indices, and sampling conditions. Iconographic material is available, but not included in the published dataset. Regular sampling at a regional scale is ongoing since 1989. The database is modelled according to the field protocol

and identification list published by De Pauw and Vannevel (1991), the forms being regularly updated and adapted by VMM's monitoring staff. The database was designed and developed in 2000 to allow automated calculation of biotic index values. Biotic indices are used to produce statistics and maps on ecological water quality: the BBI (range: 0–10) was used for VMM's annual reports from 1990 onwards and replaced by the MMIF (range: 0–1) in 2011. The MMIF allows the calculation of Ecological Quality Ratios (EQRs) as required by the EU Water Framework Directive (2000/60/EC), along with other biological and physico-chemical quality elements. Annual VMM reports are available online (http://www.vmm.be/publicaties).

The data elements of the VMM sediment quality database are similar to those of the water quality database. Iconographic material is also available, although not publicly accessible. Regular sampling at a regional scale started in 2000, with the database being modelled according to the field protocol and identification list published by De Deckere et al. (2000). The database was designed and developed in 2000 to allow automated calculation of the Biotic Sediment Index (BSI; range: 0–10) values, in order to produce statistics and maps on sediments water quality. Annual sediment reports are published from 2000 onwards (in Dutch) and are available online (http://www.vmm.be/publicaties).

In total, the dataset covers the period between 1989 and 2016, and contains 282,309 records of 210 observed taxa from 22,663 samples of 4,140 monitoring sites located on 657 different water bodies.

Spatial and temporal coverage

Belgium is located in the centre of Western Europe and its surface area reaches 30,528 km². Of the three administrative regions, Flanders is situated in the northern part and covers an area of 13,522 km² (which is 44.29 % of the Belgian territory), roughly situated at 51° latitude and 4° longitude. Flanders has a temperate maritime climate that is strongly influenced by the North Sea and the Atlantic Ocean. Average precipitation in Belgium is 852 mm during the period 1981–2010, with the highest value (1089 mm) in 2001 and the lowest value (640 mm) in 1989. Mean temperature between 1981 and 2010 is 10.5 °C. Population density in Flanders is 462 inhabitants/km² in 2010, which makes it one of the most densely populated areas in Europe.

The three major rivers in Flanders are the Yser, Scheldt, and Meuse (Fig. 1). All discharge into the North Sea, but only the river Yser and a few canals drain directly into the sea within the Flemish territory. According to the WFD, the river Yser and Scheldt basins are part of the Scheldt River Basin District that also includes parts of France and the Netherlands. In a similar way, the Meuse River Basin District covers parts of Belgium, France, Luxemburg, Germany, and the Netherlands. Within the Belgian territory, both river basin districts are subdivided into so-called subunits according to the regions (Flanders, Wallonia, and the Brussels Capital Region). As such, the dataset covers the Scheldt-Flanders (BESCHELDE-VL) and the Meuse-Flanders

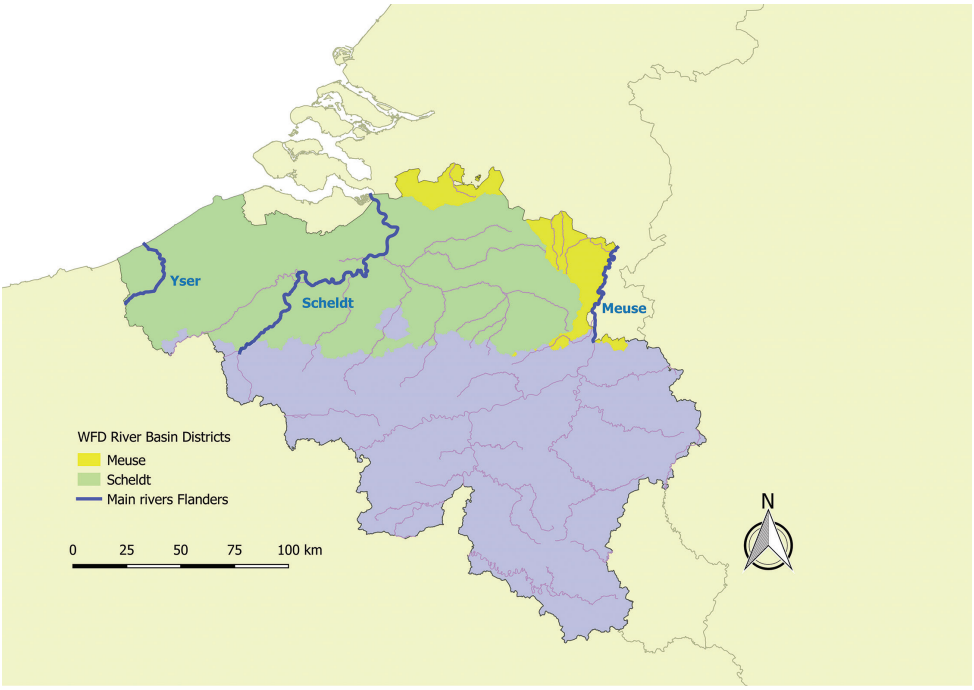

Figure 1. Location of the region of Flanders in Belgium, its main rivers (Yser, Scheldt, Meuse) and the subunits of the WFD river basin districts.

(BEMAAS-VL) subunits. The WFD basin structure is based on clusters of 11 Flemish river basins delineated in the early 1990s.

Bounding box for covered area and period:

– Flanders:
  - 50.68 to 51.51 N; 2.54 to 5.92 E (DD)
– Temporal coverage:
  - Surface water quality: 1989-03-15 – 2016-11-30
  - Sediment quality: 2000-07-12 – 2016-08-02

Water quality monitoring network and methodology

The water quality network (Fig. 2) comprises surface water bodies of all types: flowing and standing waters (including rivers, streams, canals, inner city waters); navigable and non-navigable waterways and watercourses; natural, heavily modified and artificial water courses and lakes; freshwater and transitional water bodies. See VMM (2009) for a description of the typological classification of the Flemish water bodies.

Since 1989, over 4,106 locations in estuaries, rivers, streams, canals, and standing waters have been sampled by the VMM. Over the years, and in particular after the

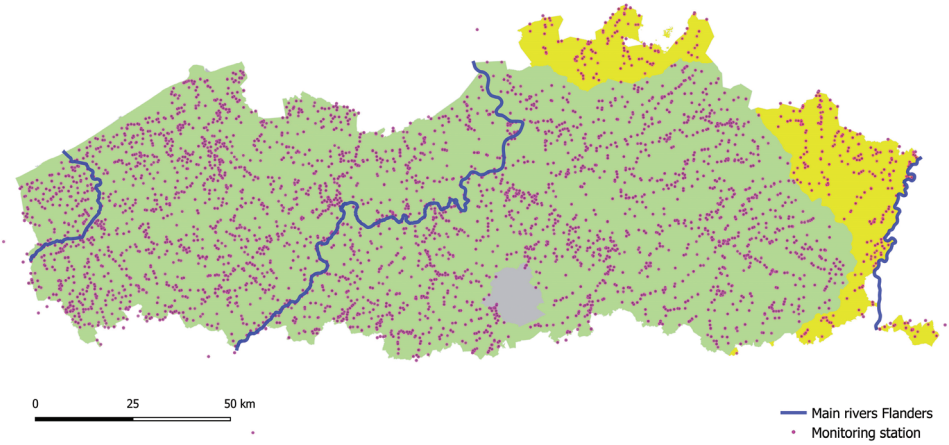

Figure 2. The VMM monitoring network for surface water quality assessments.

implementation of the Water Framework Directive in 2000, this network gradually evolved towards a set of about 500 potential monitoring stations, of which a core set of 39 are frequently monitored for macro-invertebrates. Monitoring efforts are highest between 1992 and 2005 (Fig. 3). Five monitoring stations are located in France and 17 in the Netherlands. Biological sampling is accompanied by general physico-chemical field measurements.

Since the monitoring strategy aims to assess water quality for decision-making, most sampling stations are located on pollution-impacted water bodies. Those water bodies include head streams, tributaries, and canals or waterways, as well as locations up- and downstream from significant pollution sources (e.g. industrial plants, wastewater treatment plants). Monitoring sites on smaller water bodies have been selected for specific impact assessments, e.g. eutrophication from farming. Occasionally, smaller investigations, often on request, resulted in the monitoring of protected areas, upper stream areas, oxbows, gravel pits, or ponds. The monitoring strategy has changed since the beginning of the 1990s, moving from a vast and dense network to a rather restricted core set of stations designed to meet European reporting obligations, in particular the WFD.

The monitoring process includes sampling and field observations (noted on a field protocol), treatment of the sample in the laboratory (sieving and sorting out organisms by handpicking), identification of the organisms, and derivation of the biotic index value from an index table. The procedure for sampling macro-invertebrates in surface waters is described by De Pauw and Vanhooren (1983) and NBN (1984) for handnet sampling (kicking method), and by De Pauw et al. (1986) for using artificial substrates. The sampling method was applied as follows: handnet (87%), artificial substrates (13%), unknown (less than 1%). Field observations, including in situ physico-chemical measurements, are noted on a field protocol. The methods for sampling and sample treatment are standardised and certified; additional information

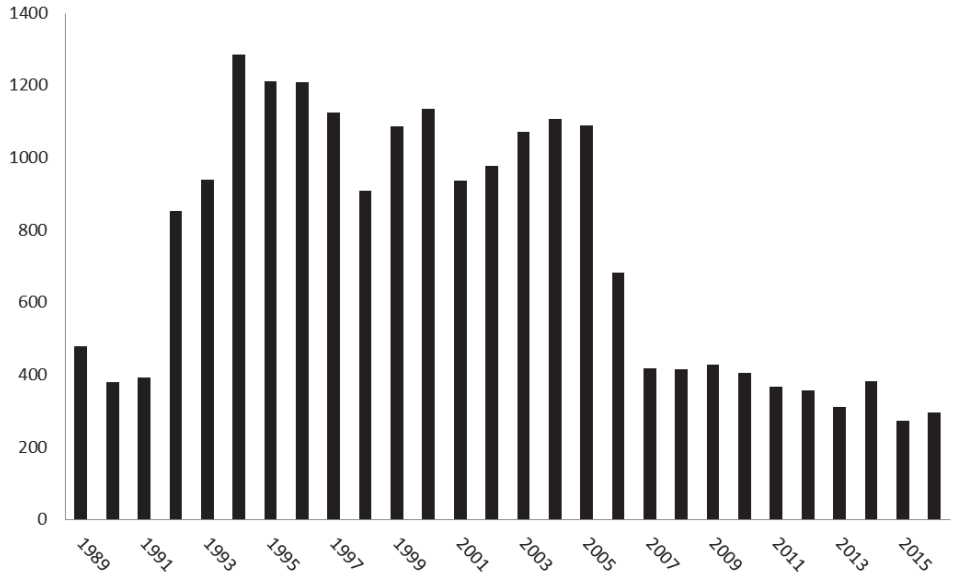

Figure 3. Sampling effort of the water quality network (number of samples per year).

can be obtained by contacting the corresponding authors. Relevant field information is included in the reported database, partially aggregated in the Darwin Core term 'dwc:dynamicProperties'. The geographic coordinates in the dataset indicate the precise location of the station on the river stretch sampled ('dwc:locationID'). However, as the sampling method prescribes the sampling of different microhabitats at the location and over a length of several metres, the co-ordinates are indicative of a stretch up to about 10 metres.

Overall, the water quality database covers two river basin district subunits, 19 water body types, 656 water bodies located in Flanders, 4,106 monitoring stations (of which 22 are located outside the Belgian territory), 20,545 samples, 208 taxa, and 267,648 taxonomic identifications.

Sediment quality monitoring network and methodology

Sediment quality monitoring stations (Fig. 4) include mainly headwaters and navigable waterways for the purpose of dredging to secure shipment. Other sites are located on water bodies subject to sanitation. As such, sediment monitoring sites are located on rivers, canals and docks, including tidal rivers and locations in industrialised harbour areas.

Since 1992, over 805 locations in estuaries, rivers, and canals have been monitored by the VMM. According to the increase of knowledge and management requirements, this network gradually evolved towards a core set of about 300 monitoring stations,

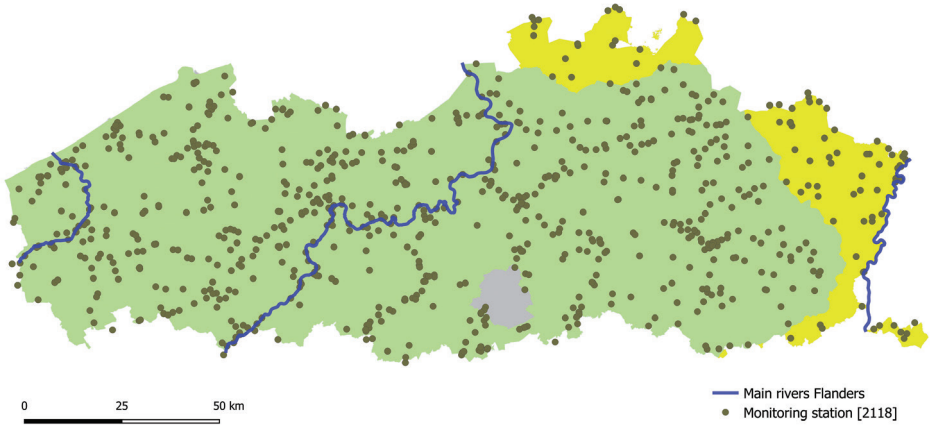

Figure 4. The VMM monitoring network for sediment quality assessments.

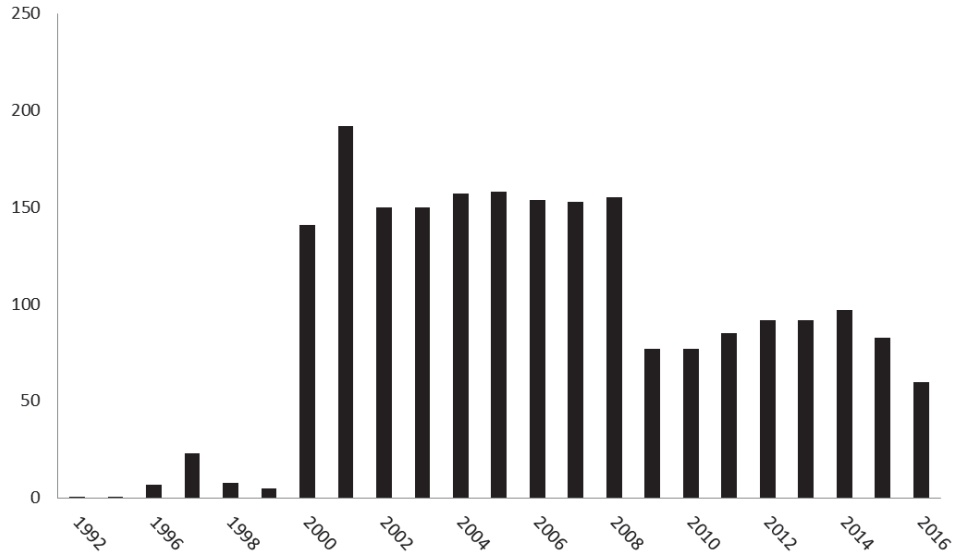

Figure 5. Sampling effort of the sediment quality network (number of samples per year).

monitored with a sexennial frequency. Monitoring efforts are highest between 2000 and 2008 (Fig. 5). Two monitoring stations are located in France and nine in the Netherlands.

The process of sediment monitoring is similar to water quality monitoring, but some different practices are applied. The procedure for sampling macro-invertebrates in sediments is described in a compendium for sampling and analysis, produced by the Flemish ministry for nature and environment (AMINAL 1998). Prescribed sampling methods include core and grab samplers. The sampling methods were applied as follows: grab sampler (90%), core sampler (10%), or unknown (less than 1%). Field

observations are noted on a field protocol. The methods for sampling and sample treatment are standardised and certified; additional information can be obtained by contacting the corresponding authors. Relevant field information is included in the reported database, partially aggregated in 'dwc:dynamicProperties'. The geographic co-ordinates in the dataset indicate the precise location of the station on the river stretch investigated ('dwc:locationID'). However, as the sampling method prescribes subsampling, the co-ordinates are indicative of a stretch up to about 50 metres.

Overall, the water sediment database covers 2 river basin district subunits, 19 water body types, 405 water bodies located in Flanders, 805 monitoring stations (of which 11 are located outside the Belgian territory), 2,118 samples, 150 taxa, and 14,661 taxonomic identifications.

Quality Control

The following comments regarding quality control apply to both the water and the sediment quality network. Field protocols and identification lists were used to allow comparable observations between networks and samplers. Field observations are highly objective in this way, although differences resulting from personal interpretation may still occur. However, content slightly changed over the years since a number of protocol versions with new and adapted data elements have been produced. The same applies to taxonomic identification. In this respect, it is advised to consult also the expert publications based on the VMM dataset (see reference list: 'Publications based on this dataset'). Differences with present taxonomic nomenclature can be experienced and, for this reason, distortion of biotic index values is avoided as much as possible by using a 'fixed' nomenclature. Be aware that a large number of people have contributed to the taxonomic identification over the years, which has unavoidably led to errors (misidentification, inclusion of terrestrial specimen, etc.). In this respect, the identifications of, for instance, Aeolosomatidae may require further examination. For taxonomic verification of sample material, experts should contact the Royal Belgian Institute of Natural Sciences (RBINS, Brussels) (http://collections.naturalsciences.be/) where the VMM macro-invertebrate samples are stored. RBINS identifiers (coded KBIN-IG: xxxxx) apply to all VMM samples of a single year.

Additional information

The water quality and sediment networks are part of a broader monitoring programme, using the same monitoring locations. Additional information is available on other biological (including macrophytes and diatoms), habitat (hydromorphology, water level, and flow) and physico-chemical quality elements, according to the requirements of the European Commission (Water Framework Directive and other environmental legislation), European authorities (European Environment Agency), and other reporting obligations. Detailed information about these programmes can be obtained by con-

tacting the authors. As far as the spatial data are aligned with the INSPIRE directive (2007/2/EC), the monitoring site identifier can be used to search related data. In the other cases, VMM (info@vmm.be) can be consulted. At the time of publication, no taxonomic data of this dataset have been reported to international authorities.

Taxonomy

Taxonomic coverage

Taxonomic information is restricted to a selected set of macro-invertebrate taxa, with identification limited to the taxonomic level required and needed to calculate biotic index values. For that purpose, taxa are listed in a protocol on which identifications are ticked off. The same identification lists apply to both the water and the sediment quality networks. It is mandatory to use the VMM identification lists to calculate biotic index values.

Taxonomic identification levels range from order to genus level and is the same for both the water quality and sediment methodology:

- For water quality monitoring, taxonomic groups and identification levels are defined by De Pauw and Vanhooren (1983) as follows: Platyhelminthes: genus; Oligochaeta: family; Hirudinea: genus; Mollusca: genus; Crustacea: family; Plecoptera: genus; Ephemeroptera: genus; Trichoptera: family; Odonata: genus; Megaloptera: genus; Hemiptera: genus; Coleoptera: family; Diptera: family, except Chironomidae (two groups: Chironomidae *forma* thummi-plumosus and Chironomidae *forma* non-thummi-plumosus); Hydracarina (presence).
- For sediment monitoring, taxonomic groups and identification levels are defined by De Pauw and Heylen (2001): Platyhelminthes: genus; Oligochaeta: (presence); Hirudinea: genus; Mollusca: genus; Crustacea: family; Plecoptera: genus; Ephemeroptera: genus; Trichoptera: family; Odonata: genus; Megaloptera: genus; Hemiptera: genus; Coleoptera: family; Diptera: family, except Chironomidae (two groups: Chironomidae *forma* thummi-plumosus, Chironomidae *forma* non-thummi-plumosus); Hydracarina (presence).

The identification list by De Pauw and Vannevel (1991) applied to the water quality network in the 1990s includes 220 taxa. At present, the VMM identification list contains 229 taxa reported from Flemish standing waters and watercourses. Differences in numbers of taxa are a result of:

- taxonomic classification, in particular the splitting of some genera of molluscs. As an example, the splitting of the genus *Physa* into the genera *Physa* and *Physella* is only clear from 2005 onwards;

– the inclusion of alien species (Gabriels et al. 2005), e.g. *Corbicula,* Ampharetidae (including *Hypania invalida*);
– the addition of freshwater-brackish species, mainly crustaceans, but also occasional records of Ampharetidae (including *Hypania invalida*).

In preparation of the dataset for inland water, a number of records have been included or excluded, which resulted in the publication of 226 taxa. These changes relate to:

– Included: brackish-marine taxa: Panopeidae, Varunidae (Crustacea), Sabellidae (Polychaeta), *Rangia* (Mollusca);
– Included, but not systematically recorded taxa: Nemathelminthes, Coelenterata (including *Hydra*), Hydracarina, Cladocera (including *Daphnia*), Ostracoda, Copepoda;
– Excluded: marine taxa: Veneroida (Mollusca);
– Excluded: non-macro-invertebrates (e.g. fish species);
– Excluded: occasionally recorded non-target taxa: Porifera, Bryozoa, Nemertea, Collembola.

A particular case concerns the chironomids, of which two 'forms' occur (thummi-plumosus and non-thummi-plumosus), referring to the presence of external respiratory tubes at low oxygen conditions. This distinction is of importance for calculating the biotic index. They are denoted in 'dwc:taxonRemarks' by Chironomidae thummi-plumosus and Chironomidae non-thummi-plumosus.

It is worth mentioning that a few scientists used the VMM samples for in-depth taxonomic research on species occurrence and distribution, with identification beyond the level indicated (see reference list: publications based on this dataset). Expert data are not included in the reported datasets. An example of such a continued study on VMM sample material is Boets et al. (2016) on alien macroinvertebrates in Flanders, with identification up to species level. These data are also available on GBIF: http://www.gbif.org/dataset/3c428404-893c-44da-bb4a-6c19d8fb676a. Unfortunately, due to the different design of the studies, the occurrence records of both datasets are not unambiguously connectable.

Taxonomic ranks

The following list contains the taxonomic classification of macro-invertebrates that have been recorded, that are present, or that are expected to occur in Belgium. According to the VMM identification list, 245 taxa are selected. Out of this number, 210 taxa have been observed between 1989 and 2016. Some taxa (indicated with *) have been recorded in the past or are expected to occur in Belgium, but do not appear in the dataset. One reason is that, due to geographical differences, some taxa of Odonata, Ephemeroptera, and Plecoptera in particular are considered less common in Flanders. On the other hand, the dataset also includes some non-target taxa. Single-species taxa

occurring within the investigated area are indicated by adding the species name, although the dataset only contains the genus name. The occurrence of single-species taxa was checked against the Dutch register of species (Nederlands Soortenregister, http://www.nederlandsesoorten.nl/).

Kingdom: Animalia
Phylum: Coelenterata, **Class:** Hydrozoa
Species: *Hydra sp., Craspedacusta sowerbii*, Cordylophora caspia**
Phylum: Platyhelminthes, **Class:** Turbellaria, **Order:** Rhabdocoela
Genus: *Mesostoma*
Phylum: Platyhelminthes, **Class:** Turbellaria, **Order:** Seriata
Family: Planariidae, **Genera/species**: *Crenobia alpina*, *Phagocata vitta**, *Planaria torva*, *Polycelis*
Family: Dugesiidae, **Genus**: *Dugesia*
Family: Dendrocoelidae, **Genera/species**: *Bdellocephala punctata*, *Dendrocoelum*
Phylum: Nematoda
Phylum: Nematomorpha
Genus: *Gordius**
Phylum: Annelida, **Class:** Oligochaeta
Families: Aeolosomatidae, Branchiobdellidae, Enchytraeidae, Haplotaxidae, Lumbricidae, Lumbriculidae, Naididae, Tubificidae
Phylum: Annelida, **Class:** Polychaeta
Families: Ampharetidae, Sabellidae
Phylum: Annelida, **Class:** Hirudinea
Family: Piscicolidae, **Genera**: *Cystobranchus*, *Piscicola*
Family: Glossiphoniidae, **Genera/species**: *Glossiphonia*, *Helobdella*, *Hemiclepsis marginata*, *Placobdella* (syn. *Haementeria*) *costata*, *Theromyzon tessulatum*
Family: Hirudidae, **Genera/species**: *Haemopis*, *Hirudo medicinalis**
Family: Erpobdellidae, **Genera**: *Dina*, *Erpobdella*, *Trocheta*
Phylum: Mollusca, **Class:** Gastropoda
Family: Neritidae, **Genus**: *Theodoxus*
Family: Viviparidae, **Genus**: *Viviparus*
Family: Valvatidae, **Genus**: *Valvata*
Family: Bithyniidae, **Genus**: *Bithynia*
Family: Hydrobiidae, **Genera/species**: *Avenionia**, *Bythinella*, *Lithoglyphus naticoides*, *Marstoniopsis scholtzi*, *Potamopyrgus antipodarum*, *Pseudamnicola confusa*
Family: Physidae, **Genera/species** : *Aplexa hypnorum*, *Physa*, *Physella*
Family: Lymnaeidae, **Genera/species** : *Lymnaea*, *Myxas glutinosa*
Family: Planorbidae, **Genera/species**: *Anisus*, *Armiger crista*, *Bathyomphalus contortus*, *Gyraulus*, *Hippeutis complanatus*, *Menetus dilatatus*, *Planorbarius corneus*, *Planorbis*, *Segmentina nitida*
Family: Ancylidae, **Genera/species** : *Ancylus fluviatilis*, *Ferrissia*
Family: Acroloxidae, **Species**: *Acroloxus lacustris*

Phylum: Mollusca, **Class:** Bivalvia
Family: Margaritiferidae, **Species**: *Margaritifera margaritifera**
Family: Unionidae, **Genera**: *Anodonta*, *Pseudanodonta*, *Unio*
Family: Dreissenidae, **Genera**: *Dreissena*, *Mytilopsis*
Family: Sphaeriidae, **Genera**: *Sphaerium*, *Pisidium*
Family: Cyrenidae, **Genus**: *Corbicula*
Family: Mactridae, **Genus**: *Rangia*
Phylum: Arthropoda, **Class:** Arachnida, **Order:** Aranea
Species: *Argyroneta aquatica**
Phylum: Arthropoda, **Class:** Arachnida, **Order:** Actinedida (syn. Hydracarina)
Phylum: Arthropoda, **Subphylum:** Crustacea, **Class:** Branchiopoda, **Order:** Anostraca, Notostraca, Conchostraca
Families/species: Chirocephalidae*, Leptestheriidae: *Leptestheria dahalacensis**, Limnadiidae: *Limnadia lenticularis**, Triopsidae*
Phylum: Arthropoda, **Subphylum:** Crustacea, **Class:** Branchiopoda, **Order:** Cladocera
Families: Daphniidae a.o.
Phylum: Arthropoda, **Subphylum:** Crustacea, **Class:** Ostracoda
Phylum: Arthropoda, **Subphylum:** Crustacea, **Class:** Maxillopoda, **Subclass:** Copepoda
Phylum: Arthropoda, **Subphylum:** Crustacea, **Class:** Maxillopoda, **Subclass:** Branchiura
Families: Argulidae: *Argulus*
Phylum: Arthropoda, **Subphylum:** Crustacea, **Class:** Malacostraca, **Orders:** Mysidacea, Amphipoda, Isopoda, Decapoda
Families: Asellidae, Astacidae, Atyidae: *Atyaephyra desmaresti*, Cambaridae, Corophiidae: *Corophium curvispinum*, Crangonyctidae, Gammaridae, Janiridae, Mysidae, Palaemonidae, Panopeidae, Sphaeromatidae, Talitridae, Tanaidae, Varunidae: *Eriocheir sinensis*
Phylum: Arthropoda, **Class:** Insecta, **Order:** Ephemeroptera
Family: Siphlonuridae, **Genera**: *Isonychia**, *Metreletus*, *Siphlonurus**
Family: Baetidae, **Genera**: *Baetis*, *Centroptilum*, *Cloeon*, *Procloeon*
Family: Oligoneuriidae, **Genus**: *Oligoneuriella**
Family: Heptageniidae, **Genera**: *Ecdyonurus*, *Epeorus**, *Heptagenia*, *Rhitrogena**
Family: Leptophlebiidae, **Genera**: *Habroleptoides**, *Habrophlebia*, *Leptophlebia*, *Paraleptophlebia*
Family: Ephemerellidae, **Genus**: *Ephemerella*
Family: Potamanthidae, **Species**: *Potamanthus luteus**
Family: Ephemeridae, **Genus**: *Ephemera*
Family: Polymitarcidae, **Species**: *Ephoron virgo**
Family: Caenidae, **Genera/species**: *Brachycercus harisella*, *Caenis*
Phylum: Arthropoda, **Class:** Insecta, **Order:** Odonata
Family: Calopterygidae, **Genus**: *Calopteryx*
Family: Lestidae, **Genera**: *Lestes*, *Sympecma*
Family: Platycnemidae, **Species**: *Platycnemis pennipes*

Family: Coenagrionidae, **Genera/species**: *Cercion lindeni*, *Ceriagrion tenellum*, *Coenagrion*, *Enallagma cyathigerum*, *Erythromma*, *Ischnura*, *Nehalennia speciosa*, *Pyrrhosoma nymphula*
Family: Aeshnidae, **Genera/species**: *Aeshna*, *Anax*, *Brachytron pratense*
Family: Gomphidae, **Genera**: *Gomphus*, *Onychogomphus*, *Ophiogomphus**
Family: Cordulegasteridae, **Species**: *Cordulegaster boltonii*
Family: Corduliidae, **Genera/species**: *Cordulia aenea*, *Epitheca bimaculate**, *Oxygastra curtisii**, *Somatochlora*
Family: Libellulidae, **Genera**: *Crocothemis erythrea*, *Leucorrhinia*, *Libellula*, *Orthetrum*, *Sympetrum*
Phylum: Arthropoda, **Class:** Insecta, **Order:** Plecoptera
Family: Taeniopterygidae, **Genera**: *Brachyptera**, *Rhabdiopteryx**, *Taeniopteryx*
Family: Nemouridae, **Genera**: *Amphinemura**, *Nemura*, *Nemurella*, *Protonemura*
Family: Capniidae, **Genus**: *Capnia**
Family: Leuctridae, **Genus**: *Leuctra*
Family: Perlidae, **Genera**: *Dinocras**, *Marthamea**, *Perla*
Family: Perlodidae, **Genera**: *Isogenus**, *Isoperla*, *Perlodes**
Family: Chloroperlidae, **Genus**: *Chloroperla**
Phylum: Arthropoda, **Class:** Insecta, **Order:** Hemiptera
Family: Mesoveliidae, **Species**: *Mesovelia furcata*
Family: Hydrometridae, **Genera**: *Hydrometra*
Family: Hebridae, **Genus**: *Hebrus,*
Family: Veliidae, **Genera**: *Microvelia, Velia*
Family: Gerridae, **Genus**: *Gerris*
Family: Naucoridae, **Species**: *Ilyocoris cimicoides*, *Naucoris maculatus*
Family: Aphelocheiridae, **Species**: *Aphelocheirus aestivalis*
Family: Nepidae, **Species**: *Nepa cinerea*, *Ranatra linearis*
Family: Pleidae, **Species**: *Plea minutissima*
Family: Notonectidae, **Genus**: *Notonecta*
Family: Corixidae, **Genera**: *Arctocorisa*, *Callicorixa*, *Corixa*, *Cymatia*, *Glaenocorisa*, *Hesperocorixa*, *Micronecta*, *Paracorixa*, *Sigara*
Phylum: Arthropoda, **Class:** Insecta, **Order:** Neuroptera
Families: Sisyridae, Osmylidae
Genera: *Sisyrus**, *Osmylus**
Phylum: Arthropoda, **Class:** Insecta, **Order:** Megaloptera
Families: Sialidae
Genus: *Sialis*
Phylum: Arthropoda, **Class:** Insecta, **Order:** Coleoptera
Families/species: Dryopidae, Dytiscidae, Elminthidae, Georissidae: *Georissus crenulatus**, Gyrinidae, Haliplidae, Hydraenidae, Hydrophilidae, Hygrobiidae: *Hygrobia hermanni*, Noteridae, Psephenidae: *Eubria palustris*, Scirtidae
Phylum: Arthropoda, **Class:** Insecta, **Order:** Trichoptera

Families: Beraeidae, Brachycentridae, Ecnomidae, Glossosomatidae, Goeridae, Hydropsychidae, Hydroptilidae, Lepidostomatidae, Leptoceridae, Limnephilidae, Molannidae, Odontoceridae, Philopotamidae, Phryganeidae, Polycentropodidae, Psychomyidae, Rhyacophilidae, Sericostomatidae

Phylum: Arthropoda, **Class:** Insecta, **Order:** Lepidoptera

Genera/species: *Acentropus niveus**, *Cataclysta**, *Nymphula**, *Parapoynx**

Phylum: Arthropoda, **Class:** Insecta, **Order:** Diptera

Families: Athericidae, Blephariceridae*, Ceratopogonidae, Chaoboridae, Chironomidae (formae *thummi-plumosus* and *non-thummi-plumosus*), Culicidae, Cylindrotomidae, Dixidae, Dolichopodidae, Empididae, Ephydridae, Limoniidae, Muscidae, Psychodidae, Ptychoderidae, Rhagionidae, Scatophagidae, Sciomyzidae, Simulidae, Stratiomyidae, Syrphidae-*Eristalinae*, Tabanidae, Thaumaleidae, Tipulidae.

Dataset

Dataset specifications

The occurrence dataset is available at:
IPT: https://data.inbo.be/ipt/resource?r=vmm-macroinvertebrates-events
GBIF: https://www.gbif.org/dataset/5ca32e22-1f1b-4478-ba7f-1916c4e88d67

Recommended citation to the dataset:
VMM, INBO (2018). Inland water macro-invertebrate occurrences in Flanders, Belgium. Flanders Environment Agency (VMM). Sampling_event Dataset https://doi.org/10.15468/4cvbka accessed via GBIF.org.

Specifications:
- Object name: *Inland water macro-invertebrate occurrences in Flanders, Belgium*
- Character encoding: UTF-8
- Format name: Darwin Core Archive format
- Format version: 1.8
- Distribution: https://ipt.inbo.be/archive.do?r=vmm-macroinvertebrates-events
- First Publication date of data: 2018-01-17
- Language: English
- Licenses of use: https://creativecommons.org/licenses/by/4.0/legalcode
- Metadata language: English
- Date of metadata creation: 2018-02-01
- Hierarchy level: Dataset

Dataset description

The occurrence data from the VMM macro-invertebrate database are extracted, standardised and published as a single sample-based dataset in Darwin Core Archives format. The dataset contains data on the surface water quality and the sediment quality networks of inland waters, since the data of both networks refer to the same locations, habitat specifications and taxonomic lists. Within the limits of the sampling procedure, sampling requires a maximum effort to obtain organisms, without guaranteeing taxonomic completeness of the whole biocoenosis. Verification of the origin of the data is possible on the basis of 'dwc:habitat', referring to 'water body' in the case of the water quality network and to 'sediment' in the case of the sediment quality network.

Sampling stations have a unique code referring to a single location, but represent one or several quality elements. The VMM station code links to other biological (diatoms, macrophytes) and physico-chemical monitoring programmes. Only physico-chemical field observations are included in the GBIF dataset in 'dwc:dynamic properties'.

Concept and methodology of the Belgian Biotic Index (BBI) and the Biotic Sediment Index (BSI) are comparable. BBI, MMIF and BSI values are reported under Darwin Core extension 'dwc:MeasurementOrFact'. At the time of publication, MeasurementOrFact data could not be obtained through the Global Biodiversity Information Facility (GBIF, https://www.gbif.org/), but can be downloaded via the Integrated Publishing Toolkit (IPT) link https://ipt.inbo.be/resource?r=vmm-macroinvertebrates-events.

The data are standardised to Darwin Core (Wieczorek et al. 2012) with a custom SQL view on the original VMM database and then published making use of the GBIF Integrated Publishing Toolkit (Robertson et al. 2014) instance at the INBO (http://data.inbo.be/ipt). The following list includes some of the Darwin Core terms (DCs) (http://rs.tdwg.org/dwc/terms/) used in the dataset, with additional details on the dataset content:

- language: en (English)
- license: CC_BY_4.0
- rightsholder: Flanders Environment Agency
- eventID: notation "monitoring site code : sample number". Note: an event stands for a single sample taken at a particular time and location
- OccurrenceID: unique identifier; notation "BEVL_VMM_serial number of macro-invertebrate (mainv) observation". BEVL: Belgium – Vlaanderen; VMM: institution acronym
- recordedBy: name of sampler(s)
- waterBody: notation "River basin ; Name(s) of the water body(-ies) ; Water body code". River basins: Scheldt river basin, Meuse river basin
- habitat: notation "Water body type code ; Water body type name ; Physical compartment". The typology is according to the EU Water Framework Directive. 'Physical compartment' distinguishes between Water body and Sediment
- datasetID: DOI10.15468/4cvbka

- institutionCode: VMM (Vlaamse Milieumaatschappij - Flanders Environment Agency)
- datasetName: Inland water macroinvertebrate occurrences in Flanders, Belgium
- basisOfRecord: human observation
- individualCount: number of individual in the sample according to following classes: A = 1, B = 2-10, C = 11-50, D = 51-100, E = 101-1000, F = ≥1001
- dynamicProperties:
  - Substrate composition: Sand, Clay-loam, Silt, Gravel-boulders, Peat, Concrete
  - Substrate condition: No remarks, Leaves & branches, Oily substances, Solid waste, Plastics, Biological life
  - Pool-riffle pattern: high, present, weak, absent, permanently absent
  - Sinuosity: high, present, weak, absent, permanently absent
  - Current: stagnant, running
  - Structure Left (river bank): strengthened, natural, dug
  - Structure Right (river bank): strengthened, natural, dug
  - Flow: Standing/slow, Moderate, Fast
  - Water Colour: No remarks, Clearly green, Clearly brown, Clearly red, Clearly grey, Clearly black, Clearly other
  - Odour: No remarks, Phenol, Manure, Fuel, H2S, Sewer gases, Chlorine, Detergents, Sludge, Other
  - Tidal flow: Rising tide, Slack period, Lowering tide
  - Water surface condition: No visual pollution, Plant cuttings / plants, Dead fish, Oil, Floating waste, Algal foam, Duckweed, Surfactant foam, Tar, Other
  - Water column condition: No visual pollution, Algal bloom, Daphnia bloom, Methane production, Flocs, Filamentous algae, Sphaerotilus, Other
  - Pollution: No visual pollution, Domestic discharges, Industrial discharges, Direct agricultural discharges, Diffuse agricultural pollution, Cyanobacteria biofilm, Unknown
- measurementID: notation “monitoring site code : sample number : parameter code”. Parameter codes are according to EEA (European Environment Agency) codes and biotic index acronyms (BBI: Belgian Biotic Index, BSI: Belgian Sediment Index, MMIF: Multi-metric Macro-invertebrate Index Flanders)
- measurementType: name of the physico-chemical parameter or biological indicator
- measurementValue: figure of the physico-chemical analysis or biotic index value
- measurementUnit: unit of the physico-chemical analysis; biotic indices are unitless
- eventDate: notation “yyyy-mm-dd”
- samplingProtocol: refers to written procedures of sampling by hand net (pond net) or artificial substrates (in the case of water body monitoring), or by grab or core sampler (in the case of sediment monitoring)
- eventRemarks: “Previous weather conditions / Current weather conditions: No remarks, Heavy rainfall, Very sunny”
- scientificName: see taxonomic list
- kingdom: Animalia

- taxonRank: phylum, order, family, genus, species
- nomenclaturalCode: ICZN
- taxonRemarks: only applies to the distinction between Chironomidae *thummi-plumosus* and Chironomidae *non-thummi-plumosus*
- locationID: monitoring site code
- countryCode: BE (Belgium), FR (France), NL (the Netherlands)
- publishingCountry: BE
- continent: Europe
- municipality: name of community
- decimalLatitude: latitude of the sampling site
- decimalLongitude: longitude of the sampling site
- geodeticDatum: WGS84
- verbatimLatitude: Lambert72
- verbatimLongitude: Lambert72
- verbatimCoordinateSystem: Belgian Lambert72

Acknowledgements

The authors want to thank the reviewers of this paper, Pieter Boets, Nora Escribano, and Yasen Mutafchiev, for their thorough reading and valuable comments. Also thanks to Robert Mesibov for the technical evaluation of the dataset.

This dataset was published as part of SAFRED (Saving Freshwater Biodiversity Data), a project led by Aaike De Wever (Royal Belgian Institute of Natural Sciences, RBINS) and technically supported by Dimitri Brosens (Research Institute for Nature and Forest, INBO; Belgian Biodiversity Platform, BBPf).

The following people provided content to the VMM macro-invertebrates database by setting up monitoring programmes, sampling, and/or identifying organisms since 1989 (water quality network) or 2000 (sediment network) (VMM, otherwise mentioned): Klaas Annys, Jos Beyens, Pauwel Bogaert, Chris Booghs, Eric Coenen, Stef Cools, Nancy Cooreman, Stefaan De Bruycker, Daniël Danckaert, Ward De Cooman, Kenneth Crombez, Maarten De Jonge, Jan Deketele, Jolien Deloof, Philippe De Maesschalck, Johan De Meirsman, Erwin De Meyer, Jan De Pril, Mieke Denys, Veronique Denys, Peggy De Roover, Dieter De Simpelaere, Peter De Smedt, Sandra De Smedt, Lieven De Temmerman, Annick De Winter, Kris De Wit, Jurgen Dewolf, Andy Dufoer, Raf Elst, Rhais Fauvarque, Wim Gabriels, Erik Ghyselbrecht, Bram Haspeslagh, Frank Higgs, Melchior Jacobs, Erik Jansen, Anne Mie Jansseune, Philippe Kimpe, Valerie Knaepen, Saskia Lammens, Hendrik Lankers, Frank Lavens, Cornelis Luyken, Henk Maeckelberghe, Koen Maertens, Christophe Maes, Dominique Maeyaert, Geert Meganck, Bie Mertens, Joost Mertens, Jaak Moens, Ludovicus Meyvis, Philippe Michiels, Laurent Neuville, Sabine Oomsels, Robrecht Pillen, Dorien Quicke, Dolf Ringelé, Raf Ryckeboer, Katrin Saelen, Patrick Salembier, Saskia Scheers, Hugo Sijmons, Annick Stickens, Philippe Stouten, Katrien Strobbe, Tom Tytgat, Agnes Van Aelst, Freddy Van Baekel, Denise Van Baelen,

Hildegard Van Campenhout, Gunter Vandenbroeck, Luc Van Den Broeck, Bart Vandepoel, Erwin Van Den Dries, Madeleine Vandeput, Evelien Van De Vyver, Christiane Van der Auwera, Isabelle Vanhoutte, Rudy Vannevel, Greet Van Opstal, Johan Verbruggen, Martin Verdievel, Bart Verhaeghe (VMW), Bart Vervaeke, Jos Verstappen, Thierry Warmoes, Leslie Weerbrouck, Karline Wittevrongel (SVW).

References

References cited in this paper

AMINAL (1998) Handboek voor de karakterisatie van de bodems van de Vlaamse waterlopen, volgens de Triade. Ministerie van de Vlaamse Gemeenschap, Departement leefmilieu en infrastructuur, Administratie Milieu-, Natuur-, Land-, en Waterbeheer, Brussels, 110 pp. [In Dutch, unpublished]

De Deckere E, De Cooman W, Florus M, Devroede-Vanderlinden M-P (Ed) (2000) Handboek voor de karakterisatie van de bodems van de Vlaamse waterlopen, volgens triade. Ministerie van de Vlaamse Gemeenschap, 112 pp. [In Dutch]

De Pauw N, Beyst B, Heylen S (2000) Development of a biological assessment method for river sediments in Flanders, Belgium. Verhandlungen des Internationalen Verein Limnologie 27: 2703–2708. https://doi.org/10.1080/03680770.1998.11898158

De Pauw N, Heylen S (2001) Biotic index for sediment quality assessment of watercourses in Flanders, Belgium. Aquatic Ecology 35: 121–133. https://doi.org/10.1023/A:1011478427152

De Pauw N, Roels D, Fontoura AP (1986) Use of artificial substrates for standardized sampling of macroinvertebrates in the assessment of water quality by the Belgian Biotic Index. Hydrobiologia 133: 237–258. https://doi.org/10.1007/BF00005595

De Pauw N, Vanhooren G (1983) Method for the biological quality assessment of watercourses in Belgium. Hydrobiologia 100: 153–168. https://doi.org/10.1007/BF00027428

De Pauw N, Vannevel R (1991) Macro-invertebraten en waterkwaliteit. Stichting Leefmilieu, Antwerpen, 316 pp. [In Dutch]

Gabriels W, Goethals PLM, De Pauw N (2005) Implications of taxonomic modifications and alien species on biological water quality assessment as exemplified by the Belgian Biotic Index method. Hydrobiologia 542: 137–150. https://doi.org/10.1007/s10750-004-1452-7

Gabriels W, Lock K, De Pauw N, Goethals PLM (2010) Multimetric Macroinvertebrate Index Flanders (MMIF) for biological assessment of rivers and lakes in Flanders (Belgium). Limnologica 40: 199–207. https://doi.org/10.1016/j.limno.2009.10.001

NBN (1984) Qualité biologique des cours d'eau – Determination de l'indice biotique se basant sur les macro-invertébrés aquatiques. / Biologische kwaliteit van de waterlopen – Bepaling van de biotische index steunende op aquatische macro-invertebraten. Norme Belge – Belgische Norm NBN T92-402. Belgisch Instituut voor normalisatie – Institut Belge de Normalisation, 11 pp. [In Dutch and French]

VMM (2009) Biological assessment of the natural, heavily modified and artificial surface water bodies in Flanders according to the European Water Framework Directive. Vlaamse Milieumaatschappij (VMM), Aalst, Belgium. December 2009, 80 pp.

Robertson T, Döring M, Guralnick R, Bloom D, Wieczorek J et al. (2014) The GBIF Integrated Publishing Toolkit: Facilitating the Efficient Publishing of Biodiversity Data on the Internet. PLoS ONE 9(8): e102623. doi: 10.1371/journal.pone.0102623

Wieczorek J, Bloom D, Guralnick R, Blum S, Döring M et al. (2012) Darwin Core: An Evolving Community-Developed Biodiversity Data Standard. PLoS ONE 7(1): e29715. https://doi.org/10.1371/journal.pone.0029715

Publications based on this dataset

Boets P (2013) Impact assessment of alien macroinvertebrates in Flanders (Belgium). PhD thesis, Gent, Belgium: Ghent University, 209 pp.

Boets P, Brosens D, Lock K, Adriaens T, Aelterman B, Mertens J, Goethals PLM (2016) Alien macroinvertebrates in Flanders (Belgium). Aquatic Invasions 11(2): 131–144. http://dx.doi.org/10.3391/ai.2016.11.2.03

Boets P, Lock K, Goethals PLM (2010) First record of Synurella ambulans (Müller, 1846) (Amphipoda: Crangonyctidae) in Belgium. Belgian Journal of Zoology 140(2): 244–245.

Boets P, Lock K, Goethals PLM (2011) Using long-term monitoring to investigate the changes in species composition in the harbour of Ghent (Belgium). Hydrobiologia 663: 155–166. https://doi.org/10.1007/s10750-010-0567-2

Boets P, Lock K, Tempelman D, van Haaren T, Platvoet D, Goethals PLM (2012) First occurrence of the Ponto-Caspian amphipod Echinogammarus trichiatus (Martynov, 1932) (Crustacea: Gammaridae) in Belgium. Bioinvasion Records 1(2): 115–120.

Boets P, Lock K, Adriaens T, Mouton A, Goethals PLM (2012) Distribution of crayfish (Decapoda, Astacoidea) in Flanders (Belgium): an update. Belgian Journal of Zoology 142(1): 86–92. https://doi.org/10.3391/bir.2012.1.2.06

Boets P, Lock K, Adriaens T, Goethals P (2014) Exotische macroinvertebraten in Vlaanderen - Verspreiding en impact op inheemse waterfauna. Natuur.focus 13(1): 22–30. [In Dutch]

De Somere P (2008) Datagebaseerde verspreidingsmodellen voor macro-invertebraten in Vlaamse riviersedimenten / Data driven species distribution models for macroinvertebrates in Flemish river sediments. MSc thesis, Gent, Belgium: Universiteit Gent, 54 pp.

Gabriels W (2007) Multimetric assessment of freshwater macroinvertebrate communities in Flanders, Belgium. PhD thesis, Gent, Belgium: Ghent University, 207 pp.

Gabriels W, Goethals PLM, De Pauw N (2005) Implications of taxonomic modifications and alien species on biological water quality assessment as exemplified by the Belgian Biotic Index method. Hydrobiologia 542: 137–150. https://doi.org/10.1007/s10750-004-1452-7

Gabriels W, Lock K, De Pauw N, Goethals PLM (2010) Multimetric Macroinvertebrate Index Flanders (MMIF) for biological assessment of rivers and lakes in Flanders (Belgium). Limnologica 40: 199–207. https://doi.org/10.1016/j.limno.2009.10.001

Goethals PLM (2005) Data Driven Development of Predictive Ecological Models for Benthic Macroinvertebrates in Rivers - Gegevensgebaseerde Ontwikkeling van Predictieve Ecologische Modellen voor Benthische Macro-invertebraten in Rivieren. PhD thesis Gent, Belgium: Universiteit Gent, 378 pp.

Goethals P, Gabriels W, Dedecker A, De Cooman W, De Pauw N (2006) Analyse van relaties tussen sedimentkarakteristieken en macroinvertebratengemeenschappen a.d.h.v. data mining technieken. Tijdschrift Water (2006), 4 pp. [In Dutch]

Lock K (2013) First records of trickle midges in Flanders (Diptera: Thaumaleidae). Bulletin de la Société royale belge d'Entomologie/Bulletin van de Koninklijke Belgische Vereniging voor Entomologie 149: 160–162.

Lock K, Adriaens T, Goethals P (2014) Effect of water quality on blackflies (Diptera: Simuliidae) in Flanders (Belgium). Limnologica 44: 58–65. https://doi.org/10.1016/j.limno.2013.08.001

Lock K, Dekoninck W, Adriaens T, Goethals PLM (2012) Distribution and ecology of mosquito larvae (Diptera: Culicidae) in Flanders (Belgium). Belgian Journal of Zoology 142(2): 138–142.

Lock K, Dekoninck W, Van De Meutter F, Goethals PLM (2012) Effect of water quality on waterbugs (Hemiptera: Gerromorpha & Nepomorpha) in Flanders (Belgium): results from a large-scale field survey. Annales de Limnologie - International Journal of Limnology 49: 121–128. https://doi.org/10.1051/limn/2013047

Lock K, Goethals PLM (2008) Distribution and ecology of the stoneflies (Plecoptera) of Flanders (Belgium). Annales de Limnologie - International Journal of Limnology 44(3): 203– 213. https://doi.org/10.1051/limn:2008005

Lock K, Goethals PLM (2011) Distribution and ecology of the mayflies (Ephemeroptera) of Flanders (Belgium). Annales de Limnologie - International Journal of Limnology 47: 159–165. https://doi.org/10.1051/limn/2011011

Lock K, Goethals PLM (2012) Distribution and ecology of the caddisflies (Trichoptera) of Flanders (Belgium). Annales de Limnologie - International Journal of Limnology 48: 31–37. https://doi.org/10.1051/limn/2011056

Lock K, Goethals PLM (2014) Predicting the occurrence of stoneflies (Plecoptera) on the basis of water characteristics, river morphology and land use. Journal of Hydroinformatics 16(4): 812–821. https://doi.org/10.2166/hydro.2013.188

Lock K, Van Haaren T, Tempelman D, Chérot F, Adriaens T (2013) Distribution and ecology of soldier fly larvae captured in Flemish surface waters (Diptera : Stratiomyidae). Bulletin de la Société royale belge d'Entomologie/Bulletin van de Koninklijke Belgische Vereniging voor Entomologie 149: 150–159.

Messiaen M, Lock K, Gabriels W, Vercauteren T, Wouters K, Boets P, Goethals PLM (2010) Alien macrocrustaceans in freshwater ecosystems in the eastern part of Flanders (Belgium). Belgian Journal of Zoology 140(1): 30–39.

ZooKeys 759: 137–147 (2018)
doi: 10.3897/zookeys.759.21627
http://zookeys.pensoft.net

RESEARCH ARTICLE

A peer-reviewed open-access journal
ZooKeys
Launched to accelerate biodiversity research

Notes on some toad bugs from China (Hemiptera, Heteroptera, Gelastocoridae)

Tong-Yin Xie[1,2], Guo-Qing Liu[3]

1 *College of Agriculture, Northeast Agricultural University, Harbin 150030, China* **2** *Key Laboratory of Soybean Biology, in Chinese Ministry of Education, Northeast Agricultural University, Harbin 150030, China* **3** *Institute of Entomology, Nankai University, Tianjin, 300071, China*

Corresponding author: *Guo-Qing Liu* (liugq@nankai.edu.cn)

Academic editor: *J. Zahniser* | Received 14 October 2017 | Accepted 19 April 2018 | Published 22 May 2018

http://zoobank.org/8D9F73B2-5FF8-4B05-B88A-B87E4BE7B267

Citation: Xie T-Y, Liu G-Q (2018) Notes on some toad bugs from China (Hemiptera, Heteroptera, Gelastocoridae). ZooKeys 759: 137–147. https://doi.org/10.3897/zookeys.759.21627

Abstract

The three species of *Nerthra* Say, 1832 (Hemiptera: Heteroptera: Gelastocoridae) occurring in China are reviewed. Dorsal habitus photographs of the two species, *Nerthra asiatica* (Horváth, 1892) and *Nerthra indica* (Atkinson, 1889), are provided, accompanied by illustrations of male genitalic structures and female ventral aspect of posterior abdominal segments. The male of *Nerthra asiatica* is recorded and reviewed for the first time.

Keywords

Hemiptera, Gelastocoridae, *Nerthra*, China

Introduction

Toad bugs (Gelastocoridae) are a remarkable group of aquatic bugs (Nepomorpha) which are derived from aquatic ancestors and have become secondarily terrestrial (Hebsgaard et al. 2004). Gelastocoridae contains three recent genera and approximately 103 species distributed worldwide, but much more prevalent in the tropics (Polhemus 1995). It is divided into two subfamilies, Gelastocorinae and Nerthrinae. Recent Gelastocorinae (two genera) are reported in only in America, from southern Canada

to north Argentina (Štys and Jansson 1988; Chen et al. 2005), but there is one fossil species, *Gelastocoris curiosus* Poinar & Brown, 2016 described from Burmese amber (Poinar and Brown 2016). The Nerthrinae includes one fossil genus, *Cratonerthra* Martins-Neto, 2005 with two species (Ruf et al. 2005), and one recent genus, *Nerthra* Say, 1832, currently including 92 valid recent species, of which nine species occur in south-eastern Asia west of Wallace line, and three species present in China (Kment and Jindra 2008, Xie and Liu 2013, Faúndez and Ashworth 2015).

Material and methods

The male genitalia were examined in glycerol and illustrated using a Zeiss Discovery V8 microscope. All measurements are given in millimetres (see Table 1). The digital photographs of specimens (Fig. 1A–D) were taken with a Zeiss Discovery V20 camera. All the studied specimens are deposited in the Institute of Entomology, Nankai University (NKUM), Tianjin, China.

Systematics

***Nerthra asiatica* (Horváth, 1892)**
Figs 1A, B; 2A–G

Mononyx asiaticus Horváth, 1892: 136.
Mononyx grossus Montandon, 1899: 395 (syn. Kiritshenko 1926: 226); Distant 1906: 16; Oshanin 1909: 956; Oshanin 1912: 89; Kiritshenko 1926: 226; Wu 1935: 559.
Nerthra asiatica: Todd 1955: 349; Todd 1957: 154; Nieser and Chen 1992: 5; Polhemus 1995: 24; Thirumalai 1998: 192; Bal and Basu 2003: 542; Kment and Jindra 2008: 191; Xie and Liu 2013: 6.

Material examined. CHINA: Sichuan Province: 1♂, Mount Emei [峨眉山], 29.58N, 103.41E, 24. IV. 1962, Bai-juan CHEN leg.; 1♀, Ya'an [雅安], 29.98N, 103.01E, 4. VII. 1963, alt. 600–900m, Jiang XIONG leg.; **Hubei Province:** 1♀, Wufeng Tujia Autonomous County [五峰土家族自治县], 30.20N, 110.67E, 10. VII. 1999, alt. 1000m, Chuan-ren LI leg.; 1♂, National Natural Reserve of Xingdou Mountain [星斗山国家级自然保护区], 30.14N, 109.00E, 30. VII. 1999, alt. 840–900m, Chuan-ren LI leg.; **Xizang (Tibet) Autonomous Region:** 1♀, Mêdog county [墨脱县], 29.33N, 95.34E, alt. 800m, VIII. 1984, Tan HE leg.

Redescription. Body large size for the genus. Body dorsally brown with scutellum slightly darker than rest (Fig. 1A–B). Ventral surface dark brown, the bases of the middle and hind legs with a few patches of yellowish brown.

*Head***.** Apical tubercle absent, lateral and superapical tubercles small, irregular in shape, not sharply pointed.

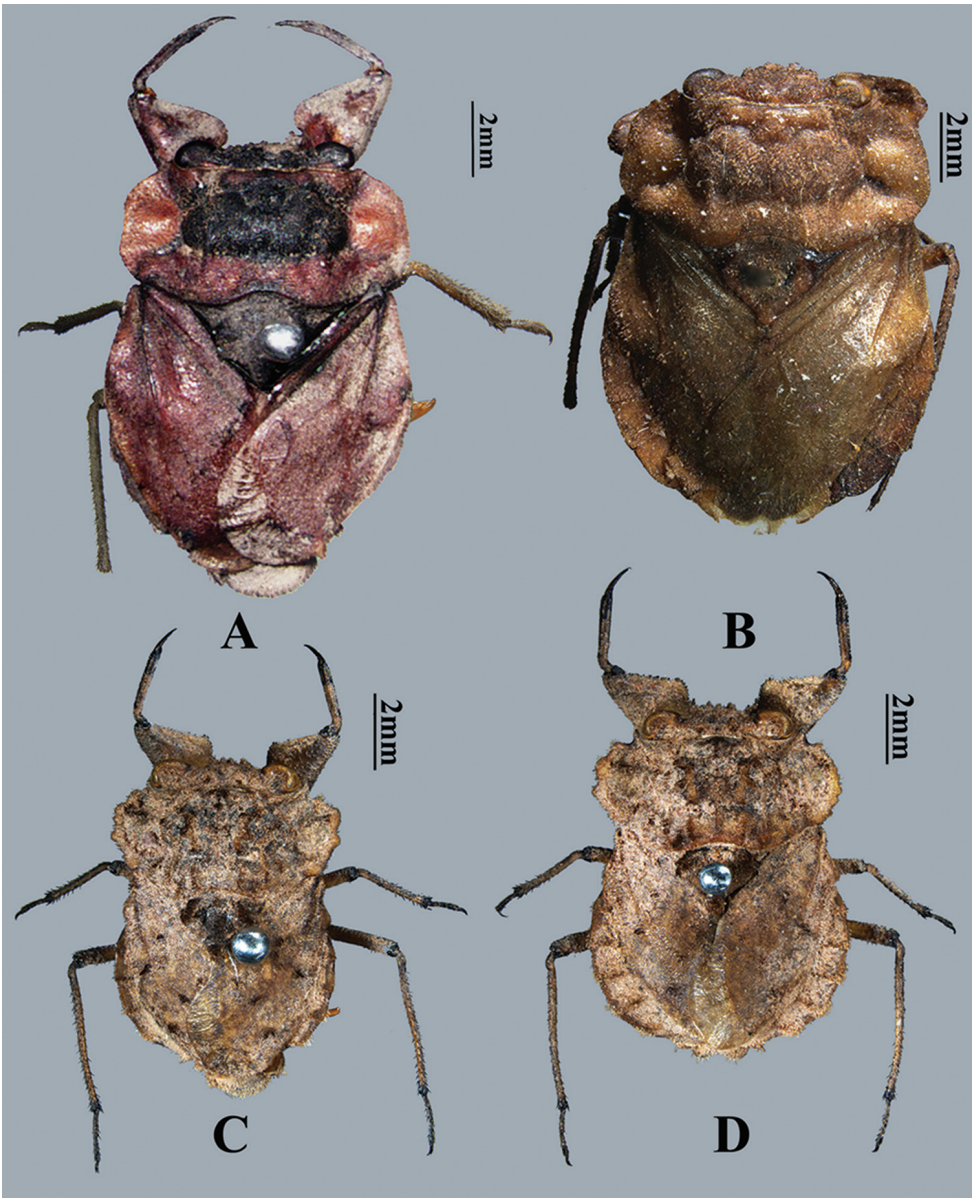

Figure 1. Dorsal habitus of *Nerthra* spp. **A** *N. asiatica* (Horváth) (♂) **B** *N. asiatica* (♀) **C** *N. indica* (Atkinson) (♂) **D** *N. indica* (♀).

Thorax. Pronotum widest at transverse furrow, a little narrower than abdomen; lateral margins of pronotum parallel or nearly so, anterior and posterior margin weakly sinuate; surface coarsely granulate. Scutellum elevated, apex slightly lobed, with tumescences at the middle of the lateral margins. Hemelytra not extending to the end of the abdomen, membrane well developed; embolium with the basal half of the lateral

Table 1. Measurements of *Nerthra* species.

Species and sex	Range	Body length	Body width	Head length	Head width	Pronotum length	Pronotum width
Nerthra asiatica							
Male (*N* = 1)		12.3	8.2	0.8	4.8	3.3	7.2
Female (*N* = 4)	min	11.6	8.1	0.9	4.6	0.9	7.7
	max	12.3	8.9	1.2	4.8	1.3	8.2
	average	11.8	8.5	1.1	4.7	1.2	8.0
Nerthra indica							
Male (*N* = 31)	min	8.7	5.9	0.4	3.9	2.3	6.1
	max	9.2	6.3	0.6	4.2	2.7	6.5
	average	9.0	6.1	0.5	4.0	2.6	6.3
Female (*N* = 48)	min	9.6	6.6	0.4	3.9	2.4	6.7
	max	10.3	7.8	1.1	4.5	3.1	7.8
	average	9.9	7.3	0.7	4.3	2.9	7.5
*Nerthra macrothorax**							
Male	min	7.9	6.0	–	–	–	5.9
	max	–	–	–	–	–	–
	average	–	–	–	–	–	–
Female	min	9.2	6.7	–	–	–	6.8
	max	10.6	8.2	–	–	–	8.2
	average	9.9	7.45	–	–	–	7.5

* these measurements are from Polhemus and Polhemus 2012 and Todd 1955.

margin nearly straight, not expanded laterally at middle. Connexivum greatly expanded laterally in females. Bristles short or moderately long, clavate, slightly curved, bristles in rows and clumps on hemelytra and in clumps on scutellum and pronotum.

Abdomen. Abdominal V-IV sternites of male mostly asymmetrical, ninth sternite rather oval, wider than long, not as long as eighth sternite; seventh sternite sternite about half as long as eighth sternite; fifth sternite very short medially (Fig. 2E). In female, abdomen nearly symmetrical. Lobes of ovipositor slightly projecting posteriorly; posterior margin of last visible abdominal sternite triangularly emarginate (Fig. 2F).

Distribution. China (Sichuan Province, Hubei Province, Xizang (Tibet) Autonomous Region), India (Todd 1955, Kment and Jindra 2008).

Remarks. This is the first time the male has been described. In the shape of the pronotum it would seem to be closely related to *N. spissa* (Distant, 1911), but the right paramere (Fig. 2C–D) of these two species is different. *Nerthra spissa* has a rather large male clasper for the size of the insect, nearly straight, cylindrical, abruptly narrowed to point at apex, twisted, and the aedeagal furrow obliquely crossing the basal half of clasper. This species differs from *N. indica* (Atkinson, 1889) by the its larger body size and the shapes of the tubercles of the head, the lateral margin of the pronotum, the hind wing (Fig. 2G), and the structures of male and female genitalia.

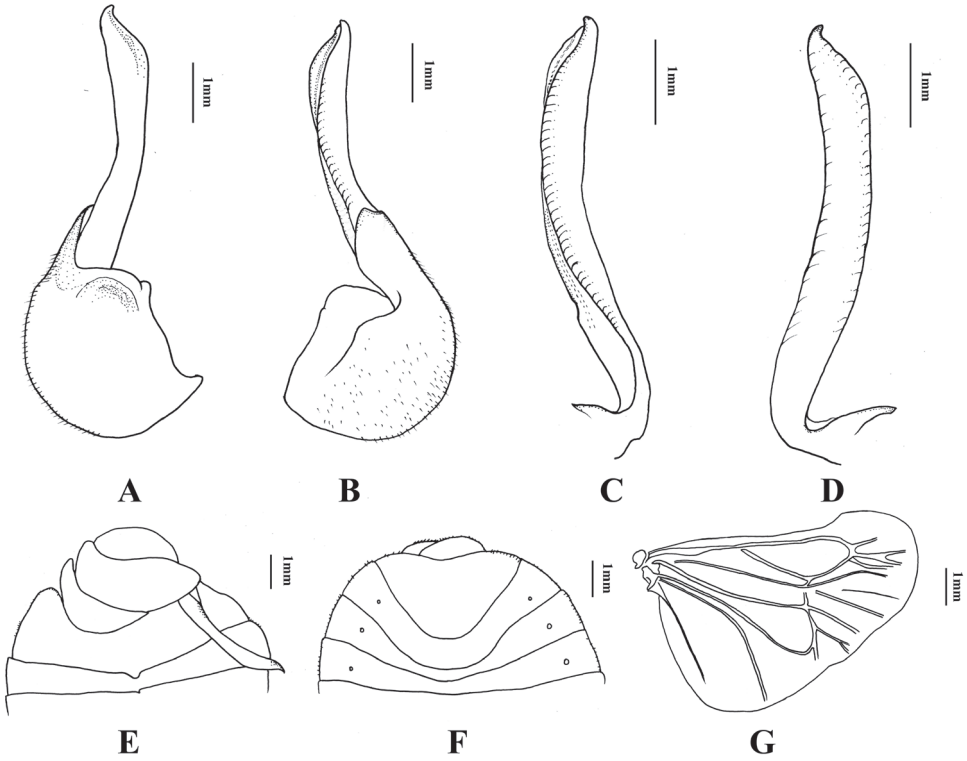

Figure 2. *Nerthra asiatica* (Horváth). **A–B** Genital capsule in different views **C–D** Right paramere in different views **E** Ventral view of posterior abdominal segments of male **F** Female subgenital plate **G** hind wing.

The holotype is a female from China: Flumen Poi-ho (G. N. Potanin)' [= Sichuan, Gar Qu (= Pai Ho River)] (Kiritshenko 1926; Todd 1955; Polhemus 1995). The paratype of *Mononyx grossus* Montandon in the Francis Huntington Snow Entomological Collection at the University of Kansas was labelled 'Thibet (Mou-Pin)' [= Sichuan, Ya'an (= Mou-ping country)] (Todd 1955). This species found in Mêdog county is reported from Xizang (Tibet) Autonomous Region for the first time.

Nerthra indica (Atkinson, 1889)

Figs 1C, D; 3A–G

Mononyx indicus Atkinson, 1889: 345; Montandon 1899: 394; Distant 1906: 15; Maxwell-Lefroy 1909: 709; Paiva 1919: 372.
Mononyx projectus Distant, 1911: 310 (syn. Todd 1955: 405).
Mononyx turgidulus Distant, 1911: 311 (syn. Todd 1961: 94).
Nerthra turgidula: Todd 1955: 406; Bal and Basu 2003: 542.

Nerthra indica: Todd 1955: 405; Todd 1961: 93; Nieser 1977: 298; Todd 1977: 216; Lansbury 1988: 189; Nieser and Chen 1992: 5; Bal and Basu 2003: 542; Kment and Jindra 2008:, 195; Xie and Liu 2013: 6.
Nerthra arunachalensis Thirumalai, 1998: 190; syn. Kment and Jindra 2008: 195.

Material examined. CHINA: Jiangxi Province: 1♂, Jinggang Mountain [井冈山], 26.75N, 114.29E, 27. VII. 2002, Wan-liang ZHANG & Jian-hua DING leg.; **Fujian Province: 1**♀, ChongAn [崇安], 27.75N, 118.03E, VI. 1982, Qiang HE leg.; 1♂, Jianning Country [建宁县](26.83N, 116.84E), 26. IX. 2002; Wan-liang ZHANG leg.; 1♂, 2♀, Natural reserve of Jiangshi [将石自然保护区], 27.12N, 117.26E, 13. VIII. 2011, Zhen YE leg.; **Guangxi Zhuang Autonomous Region:** 1♂, Longsheng country [龙胜县], 25.80N, 110.01E, 14. VI. 1963, Si-kong LIU leg.; 1♀, Yao Autonomous County of Jinxiu[金秀瑶族自治县], 24.13N, 110.19E, 23. IX. 1981, Collector unknown; 1♀, Shengtang Mountain of Jinxiu[金秀圣堂山], 24.96N, 110.12E, alt. 900m, 18. V. 1999, Fu-sheng HUANG leg.; 1♂, 1♀, Defu of Napo country[那坡德孚], 23.39N, 105.83E, alt. 1350m, 21. VI. 2000, Jian YAO leg.; 1♀, Beidou of Napo country[那坡北斗], 23.04N, 105.93E, alt. 550m, 22. VI. 2000, Jian YAO leg.; 1♀, Jingxi Diding Autonomous Region[靖西底定自治区], 23.09N, 105.99E, alt. 1000–1700m, 23. VI. 2000, Jian YAO leg.; 1♂, Tiantang mountain of Rong country[玉林市容县黎村天堂山], 22.58N, 110.73E, alt. 730–740m, 17. VIII. 2009, Bo CAI & Ke-long JIAO leg.; **Guizhou Province:** 1♂, 7♀, Maolan National Nature Reserve[茂兰国家级自然保护区], 23.43N, 103.02E, 30. VII. 2013, Tong-yin XIE & Fu-xia HE leg.; **Yunnan Province:** 1♀, Pingbian Miao Autonomous county[屏边苗族自治县], 22.98N, 103.68E, alt. 1500m, 28. V. 1996, Wen-jun BU leg.; 1♂, 1♀, Mengkuan river of Mengla country[勐腊县勐仑镇勐宽河], 21.45N, 101.56E, 18.VIII.2010, Jing WANG leg.; 15♂, 24♀, Menglun town of Mengla country[勐腊县勐仑镇], 21.94N, 101.25E, alt. 534m, 4. VIII. 2010, Kai DANG leg.; 1♀, Nangun river of Cangyuan country[沧源县班洪乡南滚河保护区], 23.29N, 99.10E, alt. 534m, 6. V. 2011; Zhen YE leg.; **Xizang (Tibet) Autonomous Region:** 1♂, Mêdog county[墨脱县], 29.33N, 95.34E, alt. 1100m, VIII. 1984, Tan HE leg. 2♂, Mêdog county suburb[墨脱城郊], 29.30N, 95.36E, alt. 1100m, 15. VIII. 2003, Huai-jun XUE & Xin-pu WANG leg.; 1♂, 2♀, Beibeng town of Mêdog county[墨脱背崩县城], 29.24N, 95.18E, alt. 780–1100m, 13. VIII. 2003, Huai-jun XUE & Xin-pu WANG leg.; 1♀, Mêdog county-108K[墨脱县城-108K], 29.33N, 95.33E, alt. 880–1100m, 16. VIII. 2003, Huai-jun XUE & Xin-pu WANG leg..

Redescription. Body middle sized for the genus. Body dorsally brown, with variable yellowish or other marking, often obscured by muddy crust. Scutellum slightly darker than rest of dorsal surface (Fig. 1C–D). Body sculpture, outlines of the pronotum, hemelytra and abdomen very variable.

Head. Apex of head with four tubercles, one at the apex is not visible in the dorsal view, the others sometimes rather indistinct (Fig. 1C–D).

Thorax. The lateral margins of the pronotum markedly asymmetrical, pronotum about as wide at anterior third as at the level of the transverse furrow. Scutellum el-

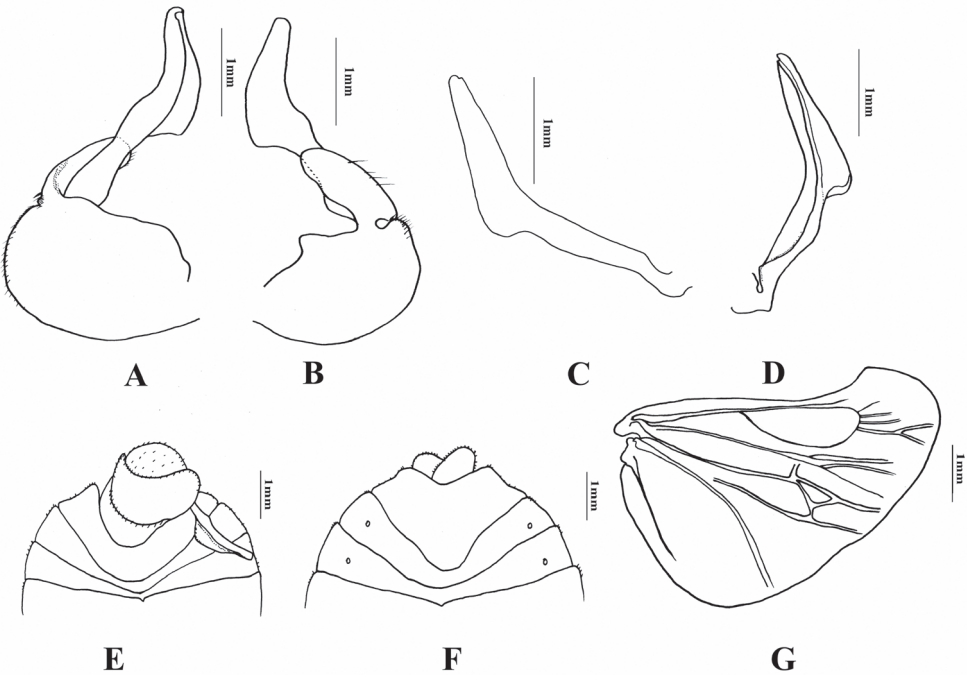

Figure 3. *Nerthra indica* (Atkinson). **A–B** Genital capsule in different views **C–D** Right paramere in different views **E** Ventral view of posterior abdominal segments of male **F** Female subgenital plate **G** hind wing.

evated, tumescent laterally and at apex, with curved ridge paralleling sinuosity of posterior margin of pronotum. The outline of the ovipositor was the same and the ventral submarginal tumescences on the last visible abdominal sternite absent. Hemelytra not quite reaching end of abdomen in the females, membrane well developed; embolium narrow at base, dilated before middle, anterior portion and apex of dilation more or less rounded. Ventral surface and the apex of the fore, middle, and hind legs dark brown.

Abdomen. Abdomen greatly expanded laterally in females. Bristles mostly short and clavate, groups of long black bristles on basal tumescences and median part of pronotum. Abdominal sternites of male mostly asymmetrical, but nearly symmetrical in female. Lobes of ovipositor asymmetrical slightly lobed and projecting posteriorly. Ninth sternite wider than long, not as long as eighth sternite; seventh sternite sternite about half as long as eighth sternite; fifth sternite very short medially. Right paramere swollen apically and stick out at middle.

Remarks. Body shape most closely related to *N. lobata* (Montandon, 1899) from which it may be separated by the male genitalia shape (Fig. 3A–D), the smaller ovipositor lobes which are less projecting, and the lack of lateral submarginal tumescences of the last visible abdominal sternite in the females.

Distribution. China (Jiangxi, Fujian, Guangxi Zhuang Autonomous Region, Sichuan, Guizhou, Yunnan, Xizang (Tibet) Autonomous Region), India, Nepal, Vietnam, Laos (Todd 1955; Kment and Jindra 2008).

***Nerthra macrothorax* (Montrouzier, 1855)**

Galgulus macrothorax Montrouzier, 1855: 110.
Scylaecus macrothorax: Stål 1861: 201.
Peltopterus macrothorax: Stål 1863: 408; Montandon 1899: 779; Kirkaldy 1906: 150; Esaki 1928: 75; Sonan 1934: 21; Hoffmann 1941: 44; Miyamoto 1953: 35, Miyamoto 1954: 28.
Nerthra macrothorax: Todd 1955: 414; Todd 1957: 157; Todd 1959: 63; Todd 1960: 172; Todd 1961, 93; Polhemus 1995: 24; Chen et al. 2005: 47; Nieser and Chen 2005: 308; Kment and Jindra 2008: 203; Polhemus and Polhemus 2012: 357, Xie and Liu 2013: 6; Sano 2016: 31.

Description (from Todd 1955). Body light brown, front of head provided with five large, rounded tubercles, four of which are flatted on top and densely covered with short clavate bristles; ocelli absent. Pronotum greatly expanded laterally; lateral margins converging anteriorly, subparallel for posterior half; posterior angle projecting obliquely posterolateral, rather pointed; posterior margin with five concavities.

Scutellum rather small, apex narrowed, basal portion depressed, inclining to apex which is the most elevated part. Hemelytra entirely coriaceous, fused together, extending slightly beyond end of abdomen, large longitudinal carinae present; base of embolium greatly expanded laterally. Connexivum broadly expanded laterally in both sexes. Entire body covered with short, broadly clavate bristles, bristles pale and especially dense on pronotum and on the elevations of the head.

Abdominal sternites of female nearly symmetrical except for posterior margin of last sternite, which is slightly emarginated, but with apex slightly convex just below the lobes of the ovipositor, the latter somewhat rounded and the left one overlapping the right. Abdominal sternites of male rather small, last visible abdominal sternite wider than long, nearly twice as long as seventh sternite, which has the right side elongate, spatulate.

Clasper of male rather sickle-shaped, but nearly straight, very slightly enlarged at apex then tapering to a blunt point.

Notes. During the daytime this species hides in wet mud or sand, or under stones or plant debris (Chen et al. 2005). Nieser and Chen (2005) observed these toad bugs burrowing in the sand on a beach in the south of Taiwan. In view of its inability to fly, its wide distribution is attributed to dispersion by drift on plant debris (Todd 1960). The authors have not seen this species, and distribution data for this species was collected from the published literature.

Distribution. China (Taiwan), Japan, Philippines, Malaysia, Indonesia, Australia (Kment and Jindra 2008).

Acknowlegements

We would like to express our sincere thanks to Dávid Rédei (Nankai University) for providing references and Petr Kment (National Museum, Kunratice) for critically reading the

manuscript and providing important suggestions. This study is supported by the "Young Talents" Project of Northeast Agricultural University (No. 16QC04), the Natural Science Foundation of Heilongjiang Province, China (No. C2017017) and Key Laboratory of Soybean Biology, in Chinese Ministry of Education, Northeast Agricultural University (SB16B01).

References

Atkinson ET (1889) New or little known Indian Rhynchota. Journal of the Asiatic Society Bengal 57(1888): 333–345.

Bal A, Basu RC (2003) Insecta: Hemiptera: water-bugs. In: Fauna of Sikkim (Part 2). Zoological Survey of India. State Fauna Series, 541–557.

Chen PP, Nieser N, Zettel H (2005) The aquatic and semi-aquatic bugs (Heteroptera: Nepomorpha & Gerromorpha) of Malesia. Fauna Malesiana Handbooks 5, Brill, Leiden/Boston, 546 pp.

Distant WL (1906) Rhynchota. Vol. III. (Heteroptera Homoptera). In: Bingham CT (Eds) The fauna of British India including Ceylon and Burma. Taylor & Francis, London, 13–51.

Distant WL (1911) Rhynchota. Vol. V. Heteroptera: Appendix. In: Shipley AE, Marshall GAK (Eds) The fauna of British India including Ceylon and Burma. Taylor & Francis, London, 310–312.

Esaki T (1928) Aquatic and semiaquatic Heteroptera. In: Karin SK, Miller SE (Eds) Insects of Samoa and other Samoan terrestrial Arthropoda. Part II. Hemiptera, Fasc. 2. British Museum (Natural History), London, 67–80.

Faúndez EI, Ashworth AC (2015) Notas sobre la familia Gelastocoridae (Hemiptera: Heteroptera) en el extremo sur de Chile, con descripción de un subgénero y especie nuevos. Anales Instituto Patagonia 43: 69–74. https://doi.org/10.4067/S0718-686X2015000200005

Hebsgaard M, Andersen NM, Damgaard J (2004) Phylogeny of the true water bugs (Nepomorpha: Hemiptera-Heteroptera) based on 16S and 28S rDNA and morphology. Systematic Entomology 29(4): 488–508. https://doi.org/10.1111/j.0307-6970.2004.00254.x

Hoffmann WE (1933) A preliminary list of the aquatic and semi-aquatic Hemiptera of China, Chosen (Korea), and Indo-China. Lingnan Science Journal 12(Supplement): 243–258.

Hoffmann WE (1941) Catalogue of aquatic Hemiptera of China, Indo-China, Formosa, and Korea. Lingnan Science Journal 20(1): 1–78.

Horváth G (1892) Hemiptera nonnulla nova Asiatica. Természetrajzi Füzetek 15: 134–137.

Kirkaldy GW (1906) List of the genera of the pagiopodous Hemiptera-Heteroptera, with their type species, from 1758 to 1904 (and also of the aquatic and semi-aquatic Trochalopoda). Transactions of the American Entomological Society 32: 117–156.

Kiritshenko AN (1926) Beiträge zur Kenntnis palaearktischer Hemipteren. Konowia 5: 218–226.

Kiritshenko AN (1930) Nauchnye rezul'taty Entomologicheskikh ekspeditsiy Zoologicheskogo Muzeya v Ussuriyskiy kray. IV. Hemiptera cryptocerata. (Résultate scientifiques des Expéditions entomologiques du Musée Zoologique dans la région d'Oussouri. IV. Hemiptera cryptocerata). Ezhegodnik Zoologicheskogo Muzeya Akademii Nauk SSSR 431–440. [In Russian, Latin diagnoses of new species and French title]

Kment P, Jindra Z (2008) Review of the family Gelastocoridae (Heteroptera: Nepomorpha) of south-eastern Asia. In: Grozeva S, Simov N (Eds) Advances in Heteroptera research. Festschrift in Honour of 80th Anniversary of Michail Josifov, 189–213.

Lansbury I (1988) Gelastocoridae (Hem.-Het.) in the Hope Entomological Collections, University Museum, Oxford. Entomologist's Monthly Magazine 124: 243–250.

Maxwell-Lefroy H (1909) Indian Insect Life. Thacker, Spink & Co., Calcutta/Simla, 786 pp.

Miyamoto S (1953) Tokara expedition. Nymph 2: 33–41. [In Japanese]

Miyamoto S (1954) Collecting records from Tokara Islands. Shin Konchû 7(1): 28–34. [In Japanese]

Montandon AL (1899) Hemiptera Cryptocerata. S. fam. Mononychinae. Notes et descriptions d'espèces nouvelles, 2-éme partie. Buletinul Societatii de Sciinte din Bucuresti-Româna 8: 774–780.

Montrouzier P (1855) Essai sur la faune de l'île de Woodlark ou Moiou. Annales de la Société Linnéenne de Lyon 7(2): 1–114.

Nieser N (1977) Gelastocoridae in the Zoologisches Museum der Humboldt-Universität zu Berlin (Heteroptera). Deutsche Entomologische Zeitschrift (N. F.) 24: 293–303.

Nieser N, Chen PP (1992) Notes on Gelastocoridae and Ochteridae (Heteroptera) with the description of five new species. Storkia 1: 2–13.

Nieser N, Chen PP (2005) The water bugs (Hemiptera: Nepomorpha and Gerromorpha) of Vanuatu. Tijdschrift voor Entomologie 148: 307–327. https://doi.org/10.1163/22119434-900000173

Oshanin B (1909) Verzeichnis des Palaearktischen Hemipteren mit besonderer Brücksichtigung ihrer Verteilung im Russischen Reiche. I. Band. Heteroptera. III. Lieferung. Ende des Bandes. Ezhegodnik Zoologicheskago Muzeya Imperatorskoy Akademii Nauk 14 (Prilozhenie): 587–1087.

Oshanin B (1912) Katalog der paläarktischen Hemipteren (Heteroptera, Homoptera Auchenorrhynchaund Psylloidea). R. Friedländer & Sohn, Berlin, 187 pp. https://doi.org/10.5962/bhl.title.13940

Paiva CA (1919) Rhynchota from the Garo Hills, Assam. Records of the Indian Museum 16: 349–377. https://doi.org/10.5962/bhl.part.25927

Poinar JrG, Brown AE (2016) Toad bugs (Hemiptera: Gelastocoridae) in Myanmar amber. Cretaceous Research 63: 39–44. doi: http://dx.doi.org/10.1016/j.cretres.2016.02.013

Polhemus DA, Polhemus JT (2012) Guide to the aquatic Heteroptera of Singapore and Peninsular Malaysia. IX. Infraorder Nepomorpha, families Ochteridae and Gelastocoridae. The Raffles Bulletin of Zoology 60: 343–359.

Polhemus JT (1995) Family Gelastocoridae Kirkaldy, 1897 - toad bugs. In: Aukema B, Rieger Ch (Eds) Catalogue of the Heteroptera of the Palaearctic Region. Vol. 1. Enticocephalomorpha, Dipsocoromorpha, Nepomorpha, Gerromorpha and Leptopodomorpha. The Netherlands Entomological Society, Amsterdam, 23–25.

Ruf ML, Goodwyn PP, Martins-Neto RG (2005) New Heteroptera (Insecta) from the Santana Formation, Lower Cretaceous (Northeastern Brazil), with description of a new family and new taxa of Naucoridae and Gelastocoridae. Gaea 1: 68–74.

Sano S (2016) New localities of *Nerthra macrothorax* (Heteroptera, Gelastocoridae) from Miyako and Ikema Islands, the Ryukyus, Japan. Rostria 59: 31–33.

Sonan J (1934) On *Peltopterus macrothorax* (Montrouzier). Transactions of the Natural History Society of Formosa 24: 21–22. [In Japanese]

Stål C (1861) Nova methodus familias quasdam Hemipterorum disponendi. Öfversigt af Kungliga Vetenskapsakademiens Förhandlingar 18(4): 195–212.

Stål C (1863) Verzeichniss der Mononychiden. Berliner Entomologische Zeitschrift 7: 405–408. https://doi.org/10.1002/mmnd.47918630308

Štys P, Jansson A (1988) Check-list of recent family-group and genus-group names of Nepomorpha (Heteroptera) of the world. Acta Entomologica Fennica 40: 1–44.

Thirumalai G (1998) The genus *Nerthra* (Say) from India with a description of a new species from Arunachal Pradesh, North Eastern India (Gelastocoridae: Hemiptera: Insecta). Records of the Zoological Survey of India 96(1997): 189–193.

Todd EL (1955) A taxonomic revision of the family Gelastocoridae (Hemiptera). University of Kansas Science Bulletin 37: 277–475. https://doi.org/10.5962/bhl.part.1590

Todd EL (1957) Five new species of Gelastocoridae with comments on other species (Hemiptera). Proceedings of the Entomological Society of Washington 59: 145–162.

Todd EL (1959) The Gelastocoridae of Melanesia. Nova Guinea, New Series 10: 61–95.

Todd EL (1960) Notes on *Nerthra macrothorax* (Montrouzier) (Hemiptera: Gelastocoridae). Proceedings of the Entomological Society of Washington 62: 116.

Todd EL (1961) Notes on some toad bugs (Hemiptera: Gelastocoridae) from India. Proceedings of the Biological Society of Washington 74: 93–94.

Todd EL (1977) Distributional and nomenclatural notes on some Gelastocoridae in the collection of the Bernice P. Bishop Museum (Hemiptera). Proceedings of the Biological Society of Washington 90: 214–217.

Wu ChF (1935) Family Gelastocoridae. In: Wu ChF (Ed.) Catalogus Insectorum Sinensium. Volume II. Fan Memorial Institute of Biology, Peiping, 559 pp.

Xie TY, Liu GQ (2013) Catalogue of Nepomorpha (Hemiptera: Heteroptera) from China (I). Science paper online 1–18. http://www.paper.edu.cn/releasepaper/content/201305–98